

COASTAL REGION OF NORTHERN ALASKA

Guidebook to Permafrost and Related Features

edited by M. Torre Jorgenson

Guidebook 10



Published by



STATE OF ALASKA
DEPARTMENT OF NATURAL RESOURCES
DIVISION OF GEOLOGICAL & GEOPHYSICAL SURVEYS
2011

COASTAL REGION OF NORTHERN ALASKA

Guidebook to Permafrost and Related Features

edited by M. Torre Jorgenson

With contributions by M. Torre Jorgenson, ABR Inc., Environmental Research & Services; H. Jesse Walker, Louisiana State University; Jerry Brown, Woods Hole Oceanographic Institution; Ken Hinkel, University of Cincinnati; Yuri Shur, University of Alaska Fairbanks; Tom Osterkamp, University of Alaska Fairbanks; Chien-Lu Ping, University of Alaska Fairbanks; Mikhail Kanevskiy, University of Alaska Fairbanks; Wendy Eisner, University of Cincinnati; Caryn Rea, ConocoPhillips Alaska, Inc.; Anne Jensen, Ukpeagvik Iñupiat Corporation, UIC Science, Barrow, AK; Owen Mason, GeoArch Alaska; Leanne Lestak, University of Colorado–Boulder, INSTAAR

Division of Geological & Geophysical Surveys

Guidebook 10

Prepared for
Ninth International Conference on Permafrost
June 29 – July 3, 2008
University of Alaska Fairbanks
Torre Jorgenson, Trip Leader

COVER PHOTOS:

Top: *Collapsing blocks along an extremely ice-rich portion of the Beaufort Sea coast near Pitt Point.*

Middle: *The main facilities for the Alpine Oil Field situated on the Colville River Delta.*

Bottom: *Abundant waterbird habitat on the coastal plain is associated with development of ice-wedge polygons (foreground) and thermokarst lakes (background).*



STATE OF ALASKA
Sean Parnell, *Governor*

DEPARTMENT OF NATURAL RESOURCES
Daniel S. Sullivan, *Commissioner*

DIVISION OF GEOLOGICAL & GEOPHYSICAL SURVEYS
Robert F. Swenson, *State Geologist and Director*

Publications produced by the Division of Geological & Geophysical Surveys (DGGS) are available for free download from the DGGS website (www.dggs.alaska.gov). Publications on hard-copy or digital media can be examined or purchased in the Fairbanks DGGS office:

Alaska Division of Geological & Geophysical Surveys
3354 College Rd., Fairbanks, Alaska 99709-3707
Phone: (907) 451-5020 Fax (907) 451-5050
dggspubs@alaska.gov
www.dggs.alaska.gov

Alaska State Library
State Office Building, 8th Floor
333 Willoughby Avenue
Juneau, Alaska 99811-0571

Alaska Resource Library & Information
Services (ARLIS)
3150 C Street, Suite 100
Anchorage, Alaska 99503

Elmer E. Rasmuson Library
University of Alaska Fairbanks
Fairbanks, Alaska 99775-1005

University of Alaska Anchorage Library
3211 Providence Drive
Anchorage, Alaska 99508

This publication released by the Division of Geological & Geophysical Surveys was produced and printed in Fairbanks, Alaska, at a cost of \$19.00 per copy. Publication is authorized by Alaska Statute 41, which charges the division “to determine the potential of Alaskan land for production of metals, minerals, fuels, and geothermal resources; the location and supplies of groundwater and construction materials; the potential geologic hazards to buildings, roads, bridges, and other installations and structures; and shall conduct such other surveys and investigations as will advance knowledge of the geology of Alaska.”

CONTENTS

PART 1: ENVIRONMENT OF THE BEAUFORT COASTAL PLAIN.....	1
Overview.....	1
Climate.....	1
Geology.....	4
Geomorphology and Surficial Geology.....	6
Marine.....	8
Glaciomarine.....	8
Fluvial and Glaciofluvial.....	9
Eolian.....	10
Lacustrine Processes and Drained-Lake Basins.....	10
Permafrost.....	11
Factors Affecting Permafrost Development.....	11
Thermal Regime.....	16
Active-Layer Dynamics.....	18
Ground Ice.....	19
Response of Permafrost to Climate Change and Disturbance.....	24
Patterned Ground.....	27
Soils.....	29
Vegetation.....	29
Oceanography and Sea Ice.....	35
Coastal Dynamics.....	36
Coastline Types.....	36
Coastal Erosion.....	39
PART 2: OIL DEVELOPMENT.....	41
History of Oil Development.....	41
Sequence of Oilfield Development.....	45
Environmental Impacts and Mitigation.....	46
Oil Exploration.....	49
Facility Planning.....	49
Construction and Operation.....	49
PART 3: TOUR OF PRUDHOE BAY AND KUPARUK OILFIELDS.....	51
Overview.....	51
Stop 1: Deadhorse Facilities.....	53
Stop 2: Oil Operations at Drill Site 12.....	54
Stop 3: Dust Impacts.....	55
Stop 4: Buried Pipeline Trenching Trials.....	55
Stop 5: Riverbank Exposure Along Sagavanirktok River.....	59
Stop 6: Pump Station 1.....	60
Stop 7: Impoundment at Drill Site 7.....	63
Stop 8: Oil Spill Cleanup and Restoration Near GC2.....	64
Stop 9: Betty Pingo.....	66
Stop 10: Ice-Wedge Degradation.....	68
Stop 11: Tundra Frost Scars.....	69
Stop 12: Kuparuk Operations Center.....	70
Stop 13: Rehabilitation of Gravel Washouts at Culverts.....	71
Stop 14: Land Rehabilitation at Mine Site D.....	74

Stop 15: Oil Spill Cleanup and Restoration near Drill Site 2U.....	75
Stop 16: Drained-Lake Basin at CPF-3.....	78
Stop 17: Buried Reserve Pit at Drill-Site 3O	79
Stop 18: Land Rehabilitation after Gravel Removal.....	80
Stop 19: Oliktok Point, Arctic Ocean, and Salt-Killed Tundra	81

PART 4: TOUR OF THE COLVILLE RIVER DELTA.....85

Overview.....	85
Stop 1: Nuiqsut.....	93
Stop 2: Beaded Drainage.....	98
Stop 3: Drained Lake and Ice-Cored Mounds.....	98
Stop 4: Pingo in Drained Lake	100
Stop 5: The Gubik Formation.....	101
Stop 6: Degrading Ice Wedges	105
Stop 7: Putu Channel.....	106
Stop 8: A Tapped Lake, an Eroding Pingo and Thaw Lakes.....	110
Stop 9: Peat Banks, Ice Wedges, and Polygons	112
Stop 10: A Point Bar and Stabilized Portion of the Gubik Formation	115
Stop 11: Tapped Lake and Lake Degradation	117
Stop 12: Floodplain Development	117
Stop 13: Drill Site CD-4.....	119
Stop 14. Slough Entrance, Willow Vegetation, and Turf-House Site.....	119
Stop 15: Sand Dune and Turf-House Site	120
Stop 16: Lake Nanuk.....	121
Stop 17: Low Tundra Surface	125
Stop 18: Niglik (The Woods Camp).....	126
Stop 19: Sand Bar and Harrison Bay	129
Stop 20: Alpine Oilfield	131
Stop 21: Colville Pipeline Crossing	132
Stop 22: Colville Mine Site.....	134

PART 5: TOUR OF BARROW.....137

Overview.....	137
Stop 1: Downtown Barrow.....	141
Stop 2: Changes Along the Chukchi Coastline	142
Stop 3: Ray Expedition for the First International Polar Year	144
Stop 4: Barrow Research Facilities	145
Stop 5: Barrow Environmental Observatory and Early Research.....	146
Stop 6: International Biological Programme Studies.....	151
Stop 7: Buried Ice Wedges and Ice-Wedge Degradation	153
Stop 8: Cake Eater Road Snow Fence.....	158
Stop 9: Biocomplexity Site and Monitoring the Urban Heat Island	159
Stop 10: Frost Mounds at Footprint Lake	162
Stop 11: Barrow Gas Fields	163
Stop 12: Dry Lake Drainage	165
Stop 13: UIC Material Site and NSB Solid Waste Disposal	165
Stop 14: Birnirk Archaeological Site	165

Stop 15: Elson Lagoon Near Brant Point.....	166
Stop 16: Elson Lagoon Near Tekegakrok Point.....	169
Stop 17: Barrow Spit and the Nuvuk Archaeological Site.....	170

ACKNOWLEDGMENTS.....	172
REFERENCES.....	173

FIGURES

Figure 1. Landsat image of the Beaufort Coastal Plain.....	2
2. Graph showing mean annual temperatures, wind speeds, and mean daily wind speeds for Barrow and Kaktovik.....	3
3. Graph showing thawing-degree-day sums for Kuparuk from 1983 to 2002.....	3
4. Figure showing cross-section of the generalized geologic stratigraphy of the central North Slope.....	4
5. Figure showing generalized stratigraphic column of geologic formations of the central Beaufort Coastal Plain.....	5
6. Map showing surficial geology of the central and western Beaufort Coastal Plain.....	6
7. Photographs of bank exposures of the dominant surficial deposits on the Beaufort Coastal Plain, including coastal plain, glacio-marine, inactive eolian sand, active eolian sand, thaw lake, and tidal flat deposits.....	7
8. Photographs of bank exposures of the dominant surficial deposits on the Beaufort Coastal Plain, including inactive floodplain overbank, beach ridge, and lagoon deposits.....	9
9. Airphotos of lakes and basins in various stages of development on the coastal plain just west of the Colville River Delta.....	12
10. Photos showing characteristic shorelines of lakes, including a thermokarst lake with a collapsing undercut bank, a non-thermokarst lake with slumping bank that meets a wave-cut bench at waterline, a secondary thermokarst lake eroding into the ice-rich center of a basin, and an infilling pond with limnic sediments in the adjacent tundra soil.....	13
11. Map showing distribution of permafrost zones and ice wedges in relation to mean annual freezing-degree days.....	13
12. Diagram showing stratigraphy of soil and ice morphology in fine-grained, ice-rich permafrost.....	14
13. Diagram of the distribution of permafrost in relation to surface terrain.....	14
14. Illustration showing mechanisms of syngenetic and epigenetic permafrost formation.....	15
15. Illustration of temperature profiles from deep boreholes across the Beaufort Coastal Plain showing the depth of permafrost.....	15
16. Illustration of typical permafrost temperature profile in northern Alaska.....	16
17. Figure showing time series of permafrost temperatures at various depths at West Dock in Prudhoe Bay.....	16
18. Figure showing time series of permafrost temperatures from 1951 to 2003 in a deep borehole at Barrow.....	17
19. Figure showing a temperature profile from a deep borehole beneath a lake near Barrow.....	17
20. Figure showing temperature profiles from deep boreholes in relation to the shoreline of Elson Lagoon near Barrow.....	18

21. Figure showing maximum active-layer thicknesses at eight Circumarctic Active Layer Monitoring (CALM) sites on the Beaufort Coastal Plain	18
22. Figure showing maximum active-layer thicknesses at the West Dock and Franklin Bluffs near Prudhoe Bay from 1987 to 2002	19
23. Photo showing big ice wedges in glaciomarine deposits at Point McLeod, Beaufort Sea coast	20
24. Diagram of ice-wedge formation	20
25. Photos showing that groundwater moving along the top of the permafrost or through wedge ice can create cavities in the wedge ice.....	21
26. Photo showing the Leffingwell Pingo near the Kadleroshilik River.....	22
27. Photos showing main segregated ice structures typical for the coastal region of northern Alaska.....	22
28. Illustration showing cryogenic structures in glaciomarine sediments along Harrison Bay near Cape Halkett.....	23
29. Figure showing volume of ground ice by ice structure, lithofacies, and terrain unit.....	23
30. Photos of a variety of thermokarst landforms, including thermokarst lake, collapse blocks undercut by thermoerosional niches, thermokarst pit, mixed pits and polygons, polygonal trough network that creates high-centered polygons, retrogressive thaw slump, beaded stream, and thermokarst gullies	25
31. Airphotos from 1982 and 2001 showing extensive permafrost degradation over that period	26
32. Diagram illustrating the degradation and stabilization of ice wedges.....	26
33. Photos of ice aggradation and degradation in permafrost creating a variety of surface patterns, including nonpatterned ground, disjunct polygon rims, low-relief low-centered polygons, high-relief low-centered polygons, low-relief high-centered polygons, and high-relief high-centered polygons	27
34. Illustration showing successional stages in the formation of frost scars and earth hummocks	28
35. Photos of common soil types of the Beaufort Coastal Plain.....	30
36. Map of ecotypes in the central–western Alaska Beaufort Coastal Plain.....	31
37. Photo of lowland, lacustrine, and coastal ecosystems of the Beaufort Coastal Plain	33
38. Photo of riverine and upland of the Beaufort Coastal Plain.....	34
39. Figure showing mean monthly sea level at Prudhoe Bay, 1994–2006.....	35
40. Photos showing flooding at Barrow caused by large storm surges in October 1963 and October 2002	35
41. Figure showing extent of sea ice during summer months of 2007 compared to fall minimum extents in 1980, 1990, 2000, and 2007.....	36
42. Map of coastline types.....	37
43. Photos of differing shoreline profiles	38
44. Figure showing representative nearshore bathymetry of the Colville Delta, Beaufort Lagoon, and Elson Lagoon along the Beaufort Sea coast.....	39
45. Figure showing erosion rates in relation to coastline type and shoreline soil texture.....	39
46. Map showing distribution of oil reserves and oilfields in the central Beaufort Coastal Plain	41
47. Maps showing historical development of oil facilities from 1977 to 1999 on the central Beaufort Coastal Plain.....	43
48. Map showing extent of oil-related facilities in 2003.....	44

49. Figure showing changes in acreage of oilfield facilities from 1977 to 2001	45
50. Photos showing decreasing sizes of production and exploratory well pads.....	47
51. Landsat image of the Prudhoe Bay oilfield	51
52. Diagram of oilfield facilities in Prudhoe Bay illustrating the flow of crude oil from a drill site to Pump Station 1.....	52
53. Photos showing aerial views of a drill site with a drill rig and a central processing facility with large flare pits for venting uncontrollable pressure surges.....	53
54. Figure showing annual throughput of crude oil in the Trans-Alaska Pipeline System since 1977	53
55. Airphoto of oilfield support services at Deadhorse showing dense development of facilities.....	54
56. Airphoto of Drill Site 12 showing a typical layout of a drill site developed according to the design and engineering techniques used during the 1970s.....	55
57. Airphoto showing ice-wedge degradation caused by heavy dust loads along heavily traveled roads in areas of dense development.....	56
58. Photos showing degrading ice wedges caused by dust from a road in Deadhorse	56
59. Airphoto of berms left over from trenching trials that evaluated five methods for burying a cold gas pipeline.....	57
60. Figure showing layout of the trenching trials at Material Site 3 for evaluating the feasibility and costs of various techniques for creating a trench for a buried gas pipeline.....	57
61. Photo showing a chain-trenching machine and the traditional method of trenching using charges to loosen the frozen soil and a backhoe to remove the spoil.....	58
62. Photos showing trenches created in 2003 by four trenching techniques and subsequently backfilled with ice-rich spoil material	58
63. Airphoto of riverbanks along the Sagavanirktok River near Deadhorse.....	59
64. Photos of a soil exposure along the bank of the Sagavanirktok River	59
65. Airphoto of Pump Station 1, the start of the Trans-Alaska Pipeline	60
66. Illustration showing layout of the facilities at Pump Station 1	61
67. Photo showing drag-reducing agent that is injected into the pipeline to reduce friction, increase throughput, and reduce the number of turbines needed to push the oil	61
68. Diagram of the Trans-Alaska Pipeline System showing the special designs needed for cold climates, permafrost terrain, and seismically active conditions.....	62
69. Photos of the beginning of the Trans-Alaska Pipeline System at Milepost 0 and of the zigzag construction of the pipeline design to allow thermal expansion and contraction	62
70. Diagrams of a check valve (with valve clapper) and gate valve used by the TAPS to control oil movement.....	63
71. Airphoto of an impoundment caused by parallel gravel roads near Drill Site 7	63
72. Airphoto of the GC2 oil spill site after cleanup and ecological restoration.....	64
73. Photos showing techniques used to clean up a crude oil spill near GC2 in Prudhoe Bay and to restore tundra vegetation damaged by the oil and the cleanup.....	65
74. Photos showing regrowth of tundra sod chunks that were spread during the winter, and hand transplanting of live tundra sod mats during the summer to help restore the tundra damaged by the oil spill and cleanup at the GC2 oil spill	66
75. Airphoto of the Betty Pingo	67

76. Map showing distribution of 766 steep-sided pingos and broad-based mounds within the Beechey Point Quadrangle encompassing the Prudhoe Bay and Kuparuk oilfields	67
77. Photo of Prudhoe Pingo.....	68
78. Maps of topography and thaw depths extrapolated from the 100-m- (330-ft-) spaced measurements from the Circumarctic Active Layer Monitoring grid at Betty Pingo	68
79. A comparison of airphotos from 1988 and 2004 revealing extensive degradation of ice wedges on coastal plain deposits adjacent to the Kuparuk River.....	69
80. Airphoto of frost boils.....	69
81. Photos showing an aerial view of abundant frost boils on coastal plain deposits in the Kuparuk oilfield, and a ground view of active frost boils near Galbraith Lake.....	70
82. Landsat image (circa 2000) of the Kuparuk oilfield.....	71
83. Airphoto of the main operations center in the Kuparuk oilfield.....	72
84. Diagram of the processing stream for produced oil at a central processing facility	72
85. Airphoto of the location of a gravel washout downstream of the main spine road near the Kuparuk operations center.....	73
86. Photos showing problems associated with culverts and gravel deposition on tundra.....	73
87. Airphoto of Mine Site D after completion of rehabilitation activities	74
88. Photos showing Mine Site D in the Kuparuk oilfield, the site of wide-ranging rehabilitation studies.....	75
89. Airphoto of the location near Drill Site 2U of the oil spill that occurred in 1989	76
90. Photos showing the cleanup of oil spill site after initial flushing in fall 1989 and mechanical scraping in winter 1990	77
91. Figures showing changes in the concentrations of Total Petroleum Hydrocarbons (TPH) and percent of total live cover from 1989 to 1999 at a crude oil spill near Drill Site 2U.....	77
92. Airphoto of a young, ice-poor, drained-lake basin surrounding a large pond, and an old, ice-rich lake basin with many small ponds	78
93. Airphoto of Drill Site 3O, which was developed in the mid-1980s.....	79
94. Airphoto of Drill Site 3R showing the thin, polygonized gravel fill remaining after removal of the short gravel road going directly to the drill site	80
95. Illustration showing cross-sectional profile of elevations of the ground surface and permafrost table across a former gravel road at Drill Site 3R	80
96. Photos showing the remaining gravel fill after most of the fill had been removed from an abandoned entrance road to Drill Site 3R	81
97. Airphoto of Oliktok Point on the northern end of the Kuparuk oilfield.....	82
98. Map of the network of Distant Early Warning (DEW) stations built across the North American Arctic.....	82
99. Photos showing coastal meadows that occupy a thin band of salt-affected habitats along the Beaufort Sea coast.....	83
100. Landsat image of Colville River Delta showing the location of the tour stops described in the guidebook	86
101. Map of geomorphic units on the Colville River Delta and adjacent terrain.....	87
102. Photo of flooding during spring breakup on the Colville River Delta, showing the persistence of ice in the deep part of the distributary channels.....	87

103. Graph showing volume and date of annual peak discharge at the head of the Colville River Delta, 1992–2007	88
104. Photos showing sedimentation during spring break that deposits thick layers of mud	88
105. Photos showing depositional environments of the Colville River Delta.....	89
106. Diagram of the evolution of soil stratigraphy and ice morphology during floodplain development on the Colville River Delta.....	91
107. Photos showing aerial views of development of ice-wedge polygons associated with nonpatterned, disjunct, low-density, and high-density polygons, Colville River Delta.....	91
108. Map of changes in the landscape of the Colville River Delta from 1955 to 1992 due to channel erosion, deposition, and lake drainage	93
109. Airphoto of the Native village of Nuiqsut, situated on a high west bank of the Niglik channel of the Colville River.....	94
110. Photo of Inupiat camp at the site of the future Nuiqsut village.....	95
111. Photo of Nuiqsut village in 1982.....	95
112. Photo of Nuiqsut schoolhouse on pilings.....	96
113. Photo of house pad under construction	96
114. Photo showing runway construction	96
115. Photo showing the Nivakti dredging gravel from the bottom of the Nechelik Channel near Nuiqsut in 1982	97
116. Illustration showing survey of runway location prior to fill.....	97
117. Photo of buried gas pipeline in Nuiqsut installed in 2006	97
118. Airphoto of a beaded stream just south of Nuiqsut.....	98
119. Airphoto of a young drained-lake basin on coastal-plain deposits adjacent to the Colville River Delta, near Nuiqsut.....	99
120. Topographic profile of a drained-lake basin on the coastal plain west of the Colville Delta.....	99
121. Photos of ice-cored mounds typically formed only in young drained-lake basins	100
122. Photo of a small pingo formed in the center of a recently drained lake basin	100
123. Airphoto of the riverbank below Nuiqsut that provides a large exposure of the coastal plain deposits associated with the Gubik Formation.....	101
124. Photos showing a thermo-erosional niche in the Gubik Formation and the differential deposition of sediments in a niche	101
125. Photo showing blocks of permafrost in the Gubik that have collapsed along the weak lineaments of ice wedges.....	102
126. Illustration showing Nuiqsut Gubik erosion, 1948–2004	102
127. Photo showing an exposed ice wedge in the exposed coastal plain deposits.....	103
128. Photograph showing an exposure of coastal plain deposits that reveals the complex, disrupted stratigraphy of the interbedded peat and slightly pebbly loamy sands.....	104
129. Photo showing gravel and boulders on the beach at the base of a Gubik exposure.....	104
130. Airphoto of small waterbodies in the depressions formed by the thawing of ice wedges	105
131. Photos showing a dry trough and gully formed by melting ice wedges.....	105
132. Photo showing cottongrass tussocks (<i>Eriophorum vaginatum</i>) on tundra surface	106
133. Airphoto of the Putu Channel, which connects the Nechelik Channel with the main east channel.....	106

134. Diagram of flow reversal in Putu Channel	107
135. Airphoto of Putu ponds, which formed in swales between sand dunes	107
136. Photo of Putu Pond, showing vegetation types and a rare rainbow	108
137. General map showing Putu Pond in relation to the muddy riverbar on Putu Channel.....	108
138. Graph showing active-layer development at Putu Pond under different surface conditions	108
139. Photo of ground squirrels ('parka squirrels') on the sand dunes.....	109
140. Photo of interbedded peat and sand in an eolian sand deposit near west Putu Channel	109
141. Airphoto of a tapped lake that had developed in an abandoned river channel.....	110
142. Photo of a pingo formed in the middle of a tapped lake now being eroded by the Nechelik Channel.....	110
143. Photo of river ice that was deposited into a tapped lake by overbank flooding during spring breakup	111
144. Photo of ice floes with willow debris stranded at the pingo site	111
145. Airphoto of a large point bar near Nuiqsut, showing the pattern of successional development from a barren riverbar to an abandoned delta floodplain deposit with deep, low-centered polygons	112
146. Photo of an exposure of thick organic accumulations associated with an abandoned floodplain deposit along the Nechelik Channel.....	112
147. Photo of a 3-m- (9.8-ft-) wide ice wedge	113
148. Photo of a deep, low-centered polygon on an abandoned floodplain deposit after it was drained by development of gullies formed along melting ice wedges	113
149. Photo showing the progressively melting ice wedge in ice-rich abandoned floodplain deposits, leading to gully development	114
150. Photo showing extreme undercutting of a peat/sand bank on the Nechelik Channel	114
151. Photo showing the contrast between river and lake erosion of ice-wedge polygons	115
152. Photo showing the first point bar downstream of the Gubik Bluff near Nuiqsut.....	115
153. Photo showing the bank transition from the ancient coastal plain of the Gubik Formation to the floodplain of the Colville River Delta	116
154. Photo of the north end of Nuiqsut Gubik showing the transition from the coastal plain deposits to a small dune ridge and on to an inactive delta floodplain deposit	116
155. Airphoto of a tapped lake illustrating various degrees of fill.....	117
156. Airphoto showing a toposequence from the river to the highest floodplain step.....	118
157. Figure showing the toposequence across the floodplain illustrating changes in geomorphic units, soils, and vegetation as the delta develops over time.....	118
158. Airphoto showing the initial stages of construction of the CD-4 drill site, which was recently added to the two earlier drill sites at the Alpine oil field.....	119
159. Airphoto of a slough off the Nechelik Channel with two tapped lakes	120
160. Photo of sand dune near the entrance to Nanuk Lake with snowdrift lasting late in the season.....	121
161. Airphoto of the drained-lake basin, or 'tapped lake,' of the former Nanuk Lake	121
162. Illustration showing Nanuk Lake entrance channel and scour hole.....	122
163. Photo showing Nanuk Lake during flooding in 1971	122
164. The expansion of the entrance/exit to Nanuk Lake between 1948 and 2004.....	123

165. Illustration of Nanuk Lake showing the division that results from selective deposition during flooding.....	123
166. Photo of lakebed with footprints of brown bear, caribou, geese, and Inupiat.....	124
167. Photo showing artifacts being eroded into the river at Nanuk Lake entrance.....	124
168. Photo of Drill Site CD-2 of the Alpine oil field initially completed in 2000 with an oil boom across mouth of Nanuk Lake.....	124
169. Airphoto of Drill Site CD-2 and the site of a proposed bridge crossing of the Nechelik Channel to provide access from Alpine to satellite fields in the NPRA.....	125
170. Photo of riverbank showing typical erosion.....	125
171. Graph showing erosion rates on the low tundra at the proposed bridge crossing.....	126
172. Photo showing low tundra with low-relief high-centered polygons and high-relief, low-centered polygons caused by ice-wedge expansion.....	126
173. Airphoto of the tidal flats at the mouth of the Nechelik Channel.....	127
174. Erosion at the ‘trade fair’ area at Niglik, which later became the site of Woods camp	127
175. Photo of Niglik, or the Woods camp, at the mouth of the Nechelik Channel	127
176. Photo of caribou in the river.....	128
177. Photos of permafrost cellars commonly used to keep fish and game frozen through the summer	128
178. Photo of Nannie Woods preparing white fish for drying, and hanging white fish (‘pepsi’).....	128
179. Figure showing profile from Nechelik Channel to Harrison Bay across the Niglik sand bar.....	129
180. Photo of low sand dune on mudflat vegetated with dune grass.....	129
181. Photos showing brackish coastal meadow with salt-tolerant sedges and grasses and salt-killed tundra inundated by storm surges.....	129
182. Photo showing detrital peat eroded upriver and trapped on a sand bar during waning floods.....	130
183. Photo of large spruce log, which originated from the boreal forest up the MacKenzie River.....	130
184. Photo of sea ice—when there was more of it.....	130
185. Airphoto of the Alpine oilfield in the central portion of the delta.....	131
186. Photo from the air of the central production facility in the Alpine oilfield, showing the intense concentration of drilling and production facility on one pad	132
187. Airphoto of the buried pipeline crossing on the east bank of the Colville River.....	132
188. Cross-sectional profile of the buried pipeline crossing showing surficial deposits, soil temperature isotherms, and the pipe alignment.....	133
189. Photos of winter construction at the horizontal directional drilling (HDD) construction site, showing the drilling of a pilot hole and later insertion of the welded pipe into the drill hole	134
190. Aerial view of the HDD terminus on the east bank of the Colville River, showing the vertical thermo-siphons and emergence of the pipelines from the Alpine oilfield.....	134
191. Airphoto of the mine site on the east bank of the main channel, where gravel was excavated for the Alpine oilfield	135
192. Aerial view of the second phase of gravel mining at the mine site.....	135
193. Illustration showing the Barrow landscape, Barrow Environmental Observatory, and tour stops	138
194. Graph showing climatic records since 1941.....	139

195. Graph of a stratigraphic section of the coastal landscape, showing idealized stratigraphy and radiocarbon ages of various features	139
196. Photo of thaw lakes and drained-lake basins, which are dominant features of the coastal plain.....	139
197. Aerial views of young, medium, old, and ancient drained-lake basins in various stages of development, based on vegetation and surface patterns related to ice aggradation	140
198. Illustration showing the differences in mean total organic carbon pools within the top 1 m (3.3 ft) among four different ages of drained-lake basins	140
199. Illustration showing drained-lake basins predominantly oriented nearly north–south, while the lakes show more variation in orientation	141
200. Aerial views of downtown Barrow fronting the Chukchi Sea	141
201. Aerial photos of view south of Barrow along the Chukchi coast.....	142
202. Aerial photos showing analysis of coastal erosion from 1948 to 1997 along a broader stretch of Chukchi coast.....	142
203. Illustrations showing coastal changes for seven periods between 1948 and 2002.....	143
204. Photo showing the research station in 1883	144
205. Photo showing the research station of the 1881–1883 Ray Expedition that collected the measurements for the first International Polar Year	144
206. Aerial view of the Naval Arctic Research Laboratory (NARL) camp	145
207. Aerial view of the ARL–NARL and airstrip on the gravel spit.....	145
208. Aerial view of the northern section of the Barrow Environmental Laboratory (BEO) and coastal plain landscape, showing the prevalence of drained-lake basins and an ancient beach ridge	146
209. Photo showing a soil trench exposing a cross-section of frost boils	147
210. Illustration of a cross-section of the coastal landscape showing the relationship of tundra soils to landscape position	147
211. Cross-section of the coastal plain, showing changes in topography and salt concentrations at depth	148
212. Illustration of toposequence across the coastal landscape, showing changes in micro-relief, thaw depths, soil morphology, moisture content, gravel content, and particle size distribution	149
213. Graph showing mean thaw depths during the 1960s measured by U.S. Army Corps of Engineers Cold Regions Research and Engineering Laboratory (CRREL), compared to more recent thaw depths measured under the auspices of the Circumarctic Active Layer Monitoring program	150
214. Graph showing annual permafrost temperatures for 1950s and 2000s at Special 2 site	150
215. Map of the many study sites of the International Biome Program.....	151
216. Aerial photo showing oblique view of the main International Biome Program tundra biome sites in the early 1970s	151
217. Photos showing Tundra Biome Site 4 transect for measuring soil and vegetation characteristics established in 1973 and resurveyed in 2000.....	152
218. Graph comparing thaw depths in 1973 and 2000 in relationship to microsites associated with low-centered polygons	152
219. Map of the headwater erosion of knickpoints along Footprint Creek	153
220. Drawing of ice-wedge stratigraphy and radiocarbon ages of the surficial deposits from the buried ice-wedge tunnel	154
221. Diagram of the permafrost tunnel excavated in the 1960s and radiocarbon ages.....	154

222. Photos showing views of the horizontal tunnel, pebbly sand loam at the east end of the tunnel, and extremely ice-rich segregated ice above the ice wedge.....	155
223. Figure showing permafrost stratigraphy illustrating ground-ice morphology and ice contents of the shaft to the buried ice-wedge tunnel	156
224. Photo of the older terrain near the permafrost tunnel, which has very large ice wedges; degradation of the ice wedges is creating small ponds	157
225. A time series of airphotos of the buried ice-wedge site, showing extensive degradation of ice wedges that has been increasing over time	157
226. A close-up view of a pond that has been enlarged and subsequently colonized by aquatic sedges from 1948 to 1997	158
227. Photos of snow fences used to reduce the amount of drifting snow that accumulates in Barrow; melting of the high drifts creates large ponds during summer.....	158
228. Graph showing snowdrifts created by the snow fence	159
229. Graph showing soil temperatures at varying distances upwind and downwind of the snow fence	160
230. Figure showing that heat of building and other human activity has contributed to a measurable warming of the city environment relative to the more distant areas in the Barrow region.....	161
231. Graph showing the increase in air temperatures in Barrow relative to the use of natural gas for heating.....	161
232. Airphoto and satellite image of Footprint and Dry lakes	162
233. Photos showing frost mounds, small ice-cored mounds, that are common in young drained-lake basins	162
234. Graph of soil stratigraphy of cores obtained from nine frost mounds, showing the relationship of thick surface organics, massive ice in the mound core, and the morphology of segregated ice below the massive ice	163
235. Map of Barrow gas fields	164
236. Map of the Barrow spit showing the location of the Birnirk village sites, along with radiocarbon ages for numerous locations along the spit	165
237. Map of monitoring segments A–D at the Elson Lagoon key site for the circumpolar Arctic Coastal Dynamics program and bathymetric profiles of Elson Lagoon.....	166
238. Cross-section of Elson Lagoon illustrating water and soil temperatures and salinity.....	167
239. Thermal profiles under Elson Lagoon	168
240. Photos showing soil exposures from an old drained-lake basin with organic-rich limnic sediments, and an old, remnant surface with highly deformed organic masses within a slightly pebbly loamy sand.....	168
241. Views of erosion along Elson Lagoon, illustrating the abundance of ground ice and the collapse of blocks along an ice wedge	169
242. Changes in the coastline at Section D from 2003 to 2007, obtained by continuous ground survey along the top of the bluff with a differential GPS	169
243. Changes in coastline along Section D from 1948 to 2005	170
244. 1953 view of the bluff at the Nuvuk site at the tip of Point Barrow	171
245. Photo of a harpoon head excavated from the Nuvuk site. The harpoon has two vestigial barbs, an incised triangle above the line hole, and incised lines running from the base of the blade slot to the base of the harpoon head	172

DEDICATION

Ernest deKoven Leffingwell



Ernest deKoven Leffingwell was a polar explorer, geologist, surveyor, and a pioneer in permafrost science in North America. He was born January 13, 1875, in Knoxville, Illinois. He was educated at the Racine Grammar School at Trinity College and later attended the University of Chicago, where he earned three degrees in geology: a B.A., an M.A., and a Ph.D. In 1895, he taught science at St Albans School in Knoxville. He first became a polar explorer when he worked as the chief scientist for the Baldwin–Ziegler Polar Expedition, which unsuccessfully attempted to reach the North Pole from Franz Josef Land in 1901. In 1903 he became Superintendent and Professor of Geology at St. Albans. During the Spanish–American War he served as a seaman on the U.S.S. Oregon.

During the Baldwin–Ziegler Polar Expedition, Leffingwell met Ejnar Mikkelsen, a Danish adventurer and Arctic expert. Together they envisioned a scientific expedition to investigate rumors of land to the north of Alaska's Arctic coast, and to complete the mapping of the little-known land in the region. With the backing of \$5,000 from John D. Rockefeller, the pair organized the Anglo-American Polar Expedition. Along with physician Dr. G.P. Howe, naturalist Ejnar Ditlevsen, and four sailors, they set sail on the Duchess of Bedford from Victoria, British Columbia, in 1906. By the end of the summer the explorers had journeyed as far as Flaxman Island. The boat, however, became locked in the ice and the explorers wintered on Flaxman Island. When spring came they found that their small schooner had been too badly damaged by the ice to be seaworthy. Mikkelsen journeyed overland to Valdez with a team of sled dogs, while all of the others except Leffingwell were picked up by a passing whaling ship.

From 1906 through 1914, Leffingwell spent nine summers and six winters on the coast between Point Barrow and Herschel Island. With the aid of Eskimo helpers he made 31 trips by dogsled, on foot, and by small boat, covering 7,240 km (4,500 mi) during 30 months away from his base camp. After the initial funding was spent, his work was largely self funded. The winter of 1913–1914 was Leffingwell's last on Flaxman Island.

In the spring of 1914 he left the Arctic for Washington, D.C., never to return. With minimal support from the U.S. Geological Survey, he spent a year and a half writing a professional paper on his investigations (Leffingwell, 1919). It was a monumental work of pioneering geology, permafrost science, ethnography, and coastal observations, leaving a record of his many notable accomplishments. He created the first accurate map of a 240-km (150-mi) section of Alaska's coastline, documented the position of 1,500 soundings and the extent of the Continental Shelf, and named many of the landmarks in the area. Leffingwell studied the Sadlerochit Mountains and related geology; the formation extends under much of the coastal plain and is one of the main reservoirs in the oil fields in northern Alaska. He was the first to scientifically describe permafrost and the nature of ground ice and develop a fundamental explanation of ice-wedge formation. Documentation of oil seeps in Leffingwell's 1919 report led to the designation in 1923 of the Naval Petroleum Reserve 4 (later renamed National Petroleum Reserve–Alaska [NPRA]). The Leffingwell Camp Site, on a remote barrier island off Alaska, was declared a National Historic Landmark in 1978.



COASTAL REGION OF NORTHERN ALASKA

GUIDEBOOK TO PERMAFROST AND RELATED FEATURES

edited by Torre Jorgenson¹

With contributions by Jerry Brown, Wendy Eisner, Ken Hinkel, Anne Jensen, M. Torre Jorgenson, Mikhail Kanevskiy, Leanne Lestak, Owen Mason, Tom Osterkamp, Chien-Lu Ping, Caryn Rea, Yuri Shur, and H. Jesse Walker

PART 1: ENVIRONMENT OF THE BEAUFORT COASTAL PLAIN

by Torre Jorgenson¹, Yuri Shur², Tom Osterkamp³, Chien-Lu Ping⁴, and Mikhail Kanevskiy²

OVERVIEW

The Arctic Coastal Plain of northern Alaska and the adjacent Yukon, or more appropriately called the Beaufort Coastal Plain within a circum-arctic context, is the northernmost portion of the United States and is America's connection to the Arctic. It is the largest contiguous region of wetlands within the Arctic (Circumpolar Arctic Vegetation Mapping [CAVM] Team, 2003), in large part due to the continuous presence of permafrost beneath the surface. The land is dominated by lakes and ponds, sedge and grass marshes, and wet sedge tundra that remains frozen for most of the year but bursts into plant and animal activity during a short summer. Migratory birds from all parts of the world converge on this region to breed, nest, and raise young. It is also a place where many global forces have been converging. First, it was a pathway for the spread of the Inuit culture eastward across arctic North America. In modern times, whalers followed bowhead whales into the pack ice, military contractors constructed the network of Distant Early Warning radar stations bringing the first large-scale development to the region, and oil companies developed one of the largest industrial complexes on the planet. These natural and human dimensions of the arctic environment are all forced to deal with permafrost, whether it be its effects on soil properties and ecological productivity or the engineering constraints on infrastructure developments.

This guidebook was developed in celebration of the Ninth International Conference on Permafrost held in Fairbanks in 2008, which brought together scientists and engineers from permafrost regions around the world to share their expertise at a time when permafrost is increasingly threatened by climate change. The guidebook is organized into five parts. In Part 1, we provide an overview of the coastal-plain environment with special emphasis on permafrost and its consequences to ecological and human development

(fig. 1). Part 2 provides an overview of oil development in the region that has been the main driver of societal and economic changes. In the remaining three parts, the guidebook focuses on providing detailed descriptions of four stops in the Prudhoe Bay and Kuparuk oilfields, the Colville River delta, and the Barrow region that illustrate prominent permafrost-related phenomena and human adaptation to the permafrost environment.

CLIMATE

The climate is characterized by 8- to 9-month-long winters and persistent winds. Mean annual air temperatures are similar across the coast from Barrow (-12.3°C [9.9°F]) to Prudhoe Bay (-11.3°C [11.7°F]) and Barter Island (-12.4°C [9.7°F]) (U.S. Weather Service data). The 10-year running mean of the long-term record (1921–2005) at Barrow, however, reveals a relatively warm period during the late 1930s to early 1940s, gradual cooling until the early 1970s, and rapid warming after 1976 (fig. 2). Most of this warming is due to warmer winters, whereas, summer temperatures have shown little warming (Osterkamp, 2003). Summer temperatures of particular interest, however, are the unusually warm summers of 1989 and 1998, as expressed by thawing-degree-days sums, which is the sum of mean daily temperatures through the summer season (fig. 3).

Precipitation is extremely low and the area would be considered a desert if not for permafrost preventing the subsurface drainage of water. Mean annual precipitation is ~200 mm (7.9 in) per year, most of which falls as snow and is redistributed by strong winds. August receives the highest monthly precipitation. Seasonal snow cover begins in September–October and extends until May–June. Average snow depth on the coastal plain from January through April in Barrow is 25 cm (9.8 in). The amounts probably are underestimated, however, due to the difficulty of measuring blowing snow.

¹ABR Inc., Environmental Research & Services, P.O. Box 80410, Fairbanks, Alaska 99708-0410; currently employed by Alaska Ecoscience, 2332 Cordes Way, Fairbanks, Alaska, 99709; ecoscience@alaska.net

²Professor, Department of Civil & Environmental Engineering, University of Alaska Fairbanks, P.O. Box 755900, Fairbanks, Alaska 99775-5900

³Professor Emeritus, Geophysical Institute, University of Alaska, P.O. Box 757320, Fairbanks, Alaska 99775-7320

⁴Professor, Palmer Research Center, University of Alaska Fairbanks, 533 E. Fireweed, Palmer, Alaska 99645-6629

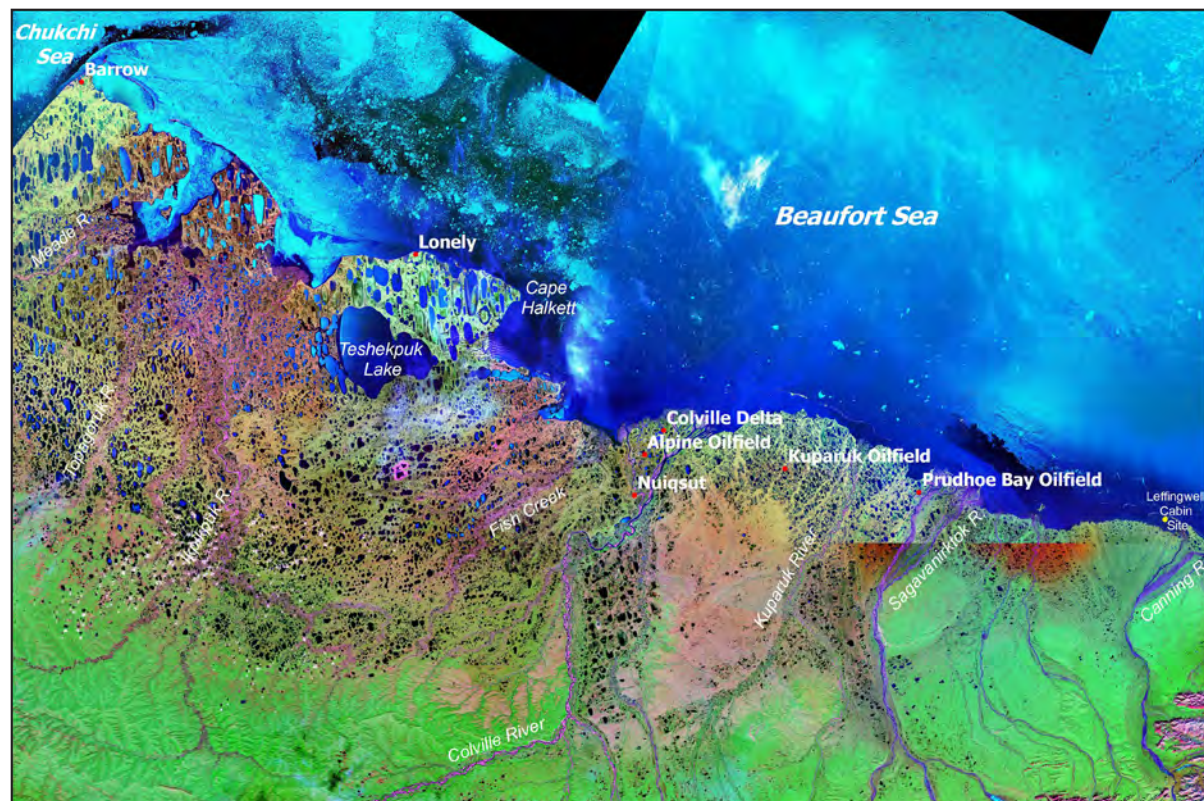


Figure 1. Landsat image of the Beaufort Coastal Plain.

Mean annual wind speeds are slightly higher at Barrow (5.7 m/s [18.7 ft/s]) than Barter Island (4.8 m/s [15.7 ft/s]) (U.S. Weather Service data), although the frequency of strong winds is higher at Barter Island (Brower and others, 1988) (fig. 2). When comparing the frequency of strong winds (>22 knots, 11 m/s, [36 ft/s]) in October, the frequency of strong winds at Barter Island (14 percent) is more than double than that at Barrow (6 percent) (Brower and others, 1988). For Barrow, the frequency of high-wind events decreased during the 1950s through the 1970s, and have increased through the 1980s and 1990s (Brown and others, 2003; Lynch and others, 2003; Lynch and others, 2004). This analysis is problematic, however, because the instruments were moved to a higher, 10-m (33-ft) tower at the airport in 1986 (Papineau, 2004). Peak wind speeds for Barrow and Kaktovik occur during the winter months and storms during June and July are relatively rare (fig. 2). Storm frequency increases through the summer and peaks in October at a time when open water is at its greatest extent (Atkinson, 2005). For the period 1973 to 2003, storm events have been predominantly from the east (68 percent) as compared to the west (32 percent) (Papineau, 2004). On a circumpolar basis, storms along the Beaufort coast have the lowest mean maximum speed and power of any sector (Atkinson, 2005).

Extreme storm events are of particular concern for coastal erosion. At Barrow, major storms (mean daily wind speeds >14 m/s [>46 ft/s]) during the open water season (July–October) since 1950 have occurred on August 24, 1950; October 4, 1954; October 3, 1963; September 20, 1986; October 24, 1990; October 11, 1993; October 29–30, 1993; October 8, 1995; October 24, 1998; October 5–6, 1999; and August 10, 2000 (fig. 2). The most notable of these are the 1950 (19 m/s [62 ft/s] daily mean), 1954 (14 m/s [46 ft/s]), 1963 (17 m/s [56 ft/s]), 1986 (22 m/s [72 ft/s]) from Papineau [2004] using data from the Climate Monitoring and Diagnostics Laboratory at Barrow), and 2000 (17 m/s [56 ft/s]) storms (NOAA data for other years). Storms at Kaktovik, however, are not synchronous with those at Barrow. At Kaktovik, major summer storms (mean daily wind speeds >15 m/s [>49 ft/s]) between 1974 and 1985 occurred in September 24–25, 1974; October 24–25, 1974; October 30, 1974; October 28, 1975; October 7–8, 1978; October 3, 1979; October 20, 1982; September 29–30, 1984; September 16–17, 1985; and October 18, 1985. The most notable of these are the storms of 1975 (17 m/s [56 ft/s] daily mean), 1982 (20 m/s [66 ft/s]), and 1985 (17 m/s [56 ft/s]). Another large storm on September 13, 1970, centered on the central and eastern Beaufort Sea coast, reportedly

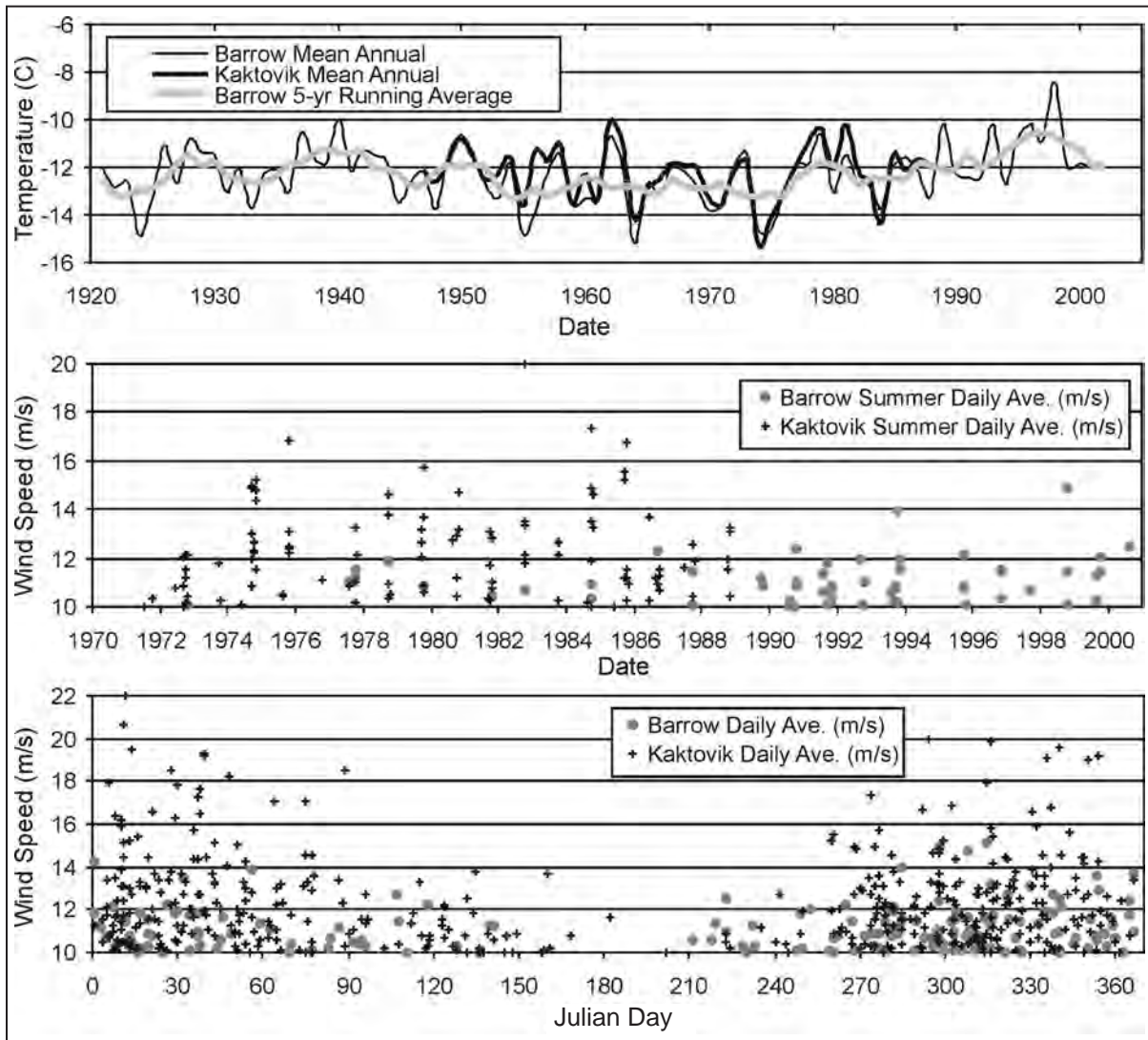


Figure 2. Mean annual temperatures (top), storm wind speeds (middle), and mean daily wind speeds (bottom) for Barrow (1921–2001) and Kaktovik (1948–1988).

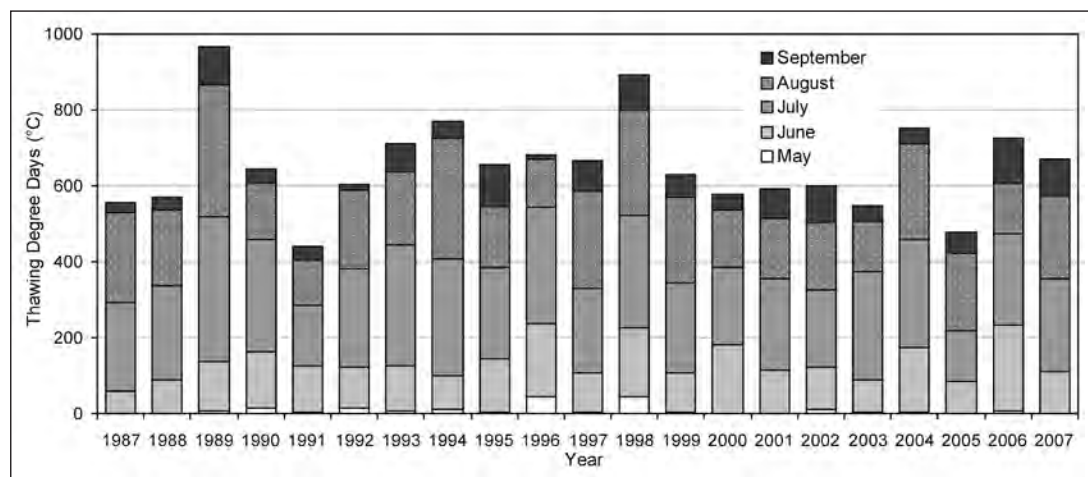


Figure 3. Thawing-degree-day sums for Kuparuk from 1983 to 2002.

had gusts up to 36 m/s (118 ft/s) and caused extensive flooding from Cape Halkett to Tuktoyaktuk, Canada (Reimnitz and Maurer, 1979; Solomon, 2005). Historical accounts of storms along the Canada's Beaufort Sea coast indicate strong storms in that region also occurred in 1919, 1928, 1944 (equivalent to the 1970 storm), and 1955 (Solomon, 2005).

The easterly storms typically develop when there is high pressure over the Beaufort Sea and low pressure over Alaska or the Bering Sea (Papineau, 2004). In contrast, westerly storms arise from several synoptic patterns, including (1) high pressure over Alaska, far east Siberia and the Chukchi Sea, (2) low pressure over the Arctic Ocean, and (3) low pressure systems that develop over the north Pacific and move north into the Arctic via the Bering Strait or from the Gulf of Alaska and then across Alaska into the Beaufort Sea (Papineau, 2004).

GEOLOGY

The rocks of northern Alaska depict a diverse geologic history of the Brooks Range and adjacent North Slope, which represent deposits that once belonged to the North American craton, passive margin sediments, rift-related sediments, pelagic sediments, volcanoclastics, and foreland-basin deposits (Moore and others, 1994). Together they comprise the broad composite terrane termed the Arctic Alaska Terrane, a transitional sequence of sedimentary rocks ranging in age from Precambrian

to Cenozoic. The terrane is subdivided into two major geologic structures—the Colville Basin and the North Slope Subterrane (fig. 4). The Colville Basin overlies the North Slope Subterrane and is a foreland basin of Cretaceous–Tertiary age that filled with sediments shed from the rising Brooks Range. Accumulations of Mississippian to Quaternary lithologies underlying the coastal plain have formed a ~10-km- (~6-mi-) thick wedge of limestone, shale, and sandstone deposited in marine, deltaic, and fluvial environments (Gryc, 1988; Moore and others, 1994; Bird and Houseknecht, 2002a). The Colville Basin is bounded on the north by the Barrow Arch, which may have been formed by subduction-related buoying. The Barrow Arch holds the hydrocarbon reservoir for the supergiant Prudhoe Bay oilfield. Rocks in the south part of the Colville Basin are gently folded, showing that Brooks Range deformation was actively stepping northward as recently as late Cretaceous time. In the northeast, thrust faulting, folding, and erosion have brought pre-Cretaceous Colville Basin rocks to the surface. The North Slope Subterrane is comprised of Cretaceous and older rocks underlying the Colville Basin and much of the Brooks Range, where it is exposed in isolated areas. Compression of the Arctic Alaska plate during mid-Cretaceous time was produced by the combined forces of terrane accretion at the southern margin of the Arctic Alaska Plate and rift-zone expansion in the marine basin bordering the plate to the north. The resulting deformation formed the

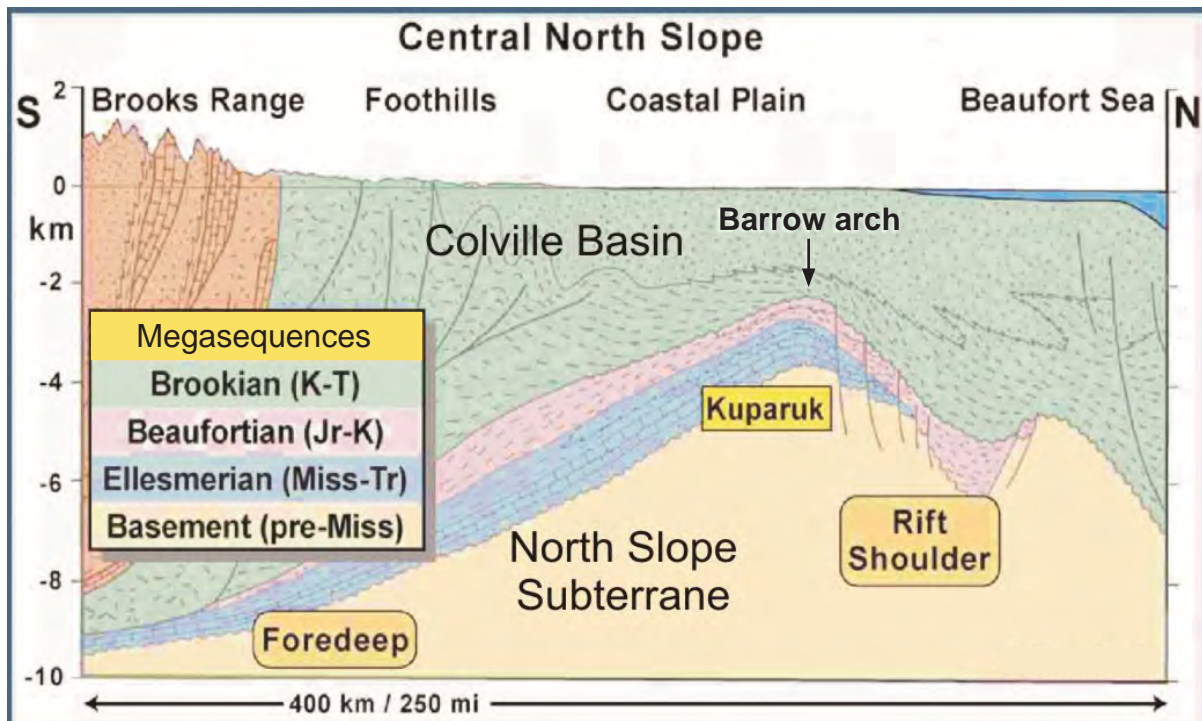


Figure 4. Cross-section of the generalized geologic stratigraphy of the central North Slope (courtesy of D. Houseknecht).

Brooks Range thrust-fault belt and the foreland Colville River Basin and Barrow Arch (Moore and others, 1994). Modern seismic activity and deformation of Quaternary sediments are evidence of the continuation of the Brooks Range orogeny. The North Slope, however, has not had a major earthquake since a magnitude 5.3 event in 1968.

Oil exploration on the North Slope has historically targeted the proven accumulations of oil associated with the Ellesmerian sequence at the crest of the Barrow Arch (Bird and Houseknecht, 2002a; Bureau of Land Management, 2004) (fig. 5). Oil development at Prudhoe Bay focused on the Shublik, Sadlerochit, Lisburne, and Endicott group and formation of the Ellesmerian sequence. Later development of the Kuparuk oilfield targeted the Kingak Shale (fig. 5). Recent discovery of

a major oil play in the previously unrecognized Jurassic sandstone reservoir has expanded exploration interests to members of the Beaufortian Sequence.

The Prudhoe Bay oilfield originally had estimated total reserves of 23 billion barrels (bbl) of oil, and it has already produced ~15 billion bbls of oil over the past 30 years (National Research Council, 2003). New estimates of potential oil reserves by the USGS suggest that between 5.9 and 13.2 billion bbls of oil are technically recoverable in National Petroleum Reserve–Alaska (NPR), with ~80 percent of that occurring in the northern third of NPR (Bird and Houseknecht, 2002b). By comparison, a 1998 USGS assessment of oil and gas resources in the Arctic National Wildlife Refuge (ANWR) estimated that between 4.3 and 11.8 billion

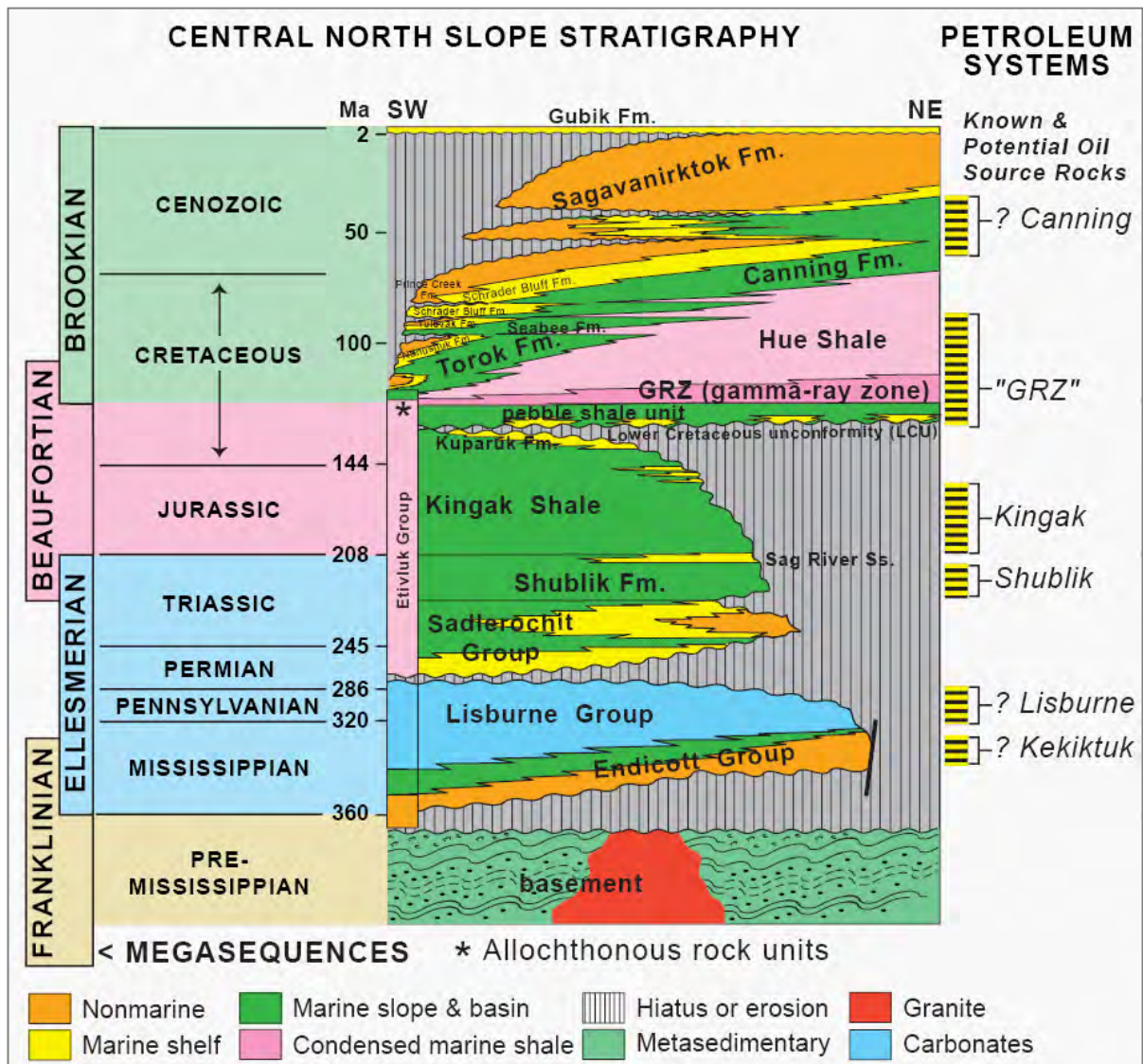


Figure 5. Generalized stratigraphic column of geologic formations of the central Beaufort Coastal Plain (from Garrity and others, 2005).

bbls of oil are technically recoverable in the so-called '1002 Area' (Bird and Houseknecht, 1998). Most of the economically recoverable oil lies to the west of the Marsh Creek Anticline in the undeformed region closest to the areas of current oil development in Prudhoe Bay. Oil accumulations in the NPRA and ANWR are estimated to be of moderate sizes, ~30–250 million bbls each, significantly smaller than those found in currently developed Prudhoe Bay.

GEOMORPHOLOGY AND SURFICIAL GEOLOGY

Terrestrial deposits of the coastal plain are derived from upland watersheds, glacial outwash during periods of deglaciation, and marine transgressions during warmer interglacial periods (Rawlinson, 1993). Coastal plain sediments consist of nearshore marine, glaciomarine, alluvial/deltaic, and eolian deposits of Holocene to mid-Quaternary ages (figs. 6 and 7). Together they are referred to as the Gubik Formation (Dinter, 1985), although the initial concept of the Gubik was limited to a complex interbedded sequence of unconsolidated marine sand and silty clay with a minor component of alluvial

deposits (Black, 1964). The nearshore marine sediments have been attributed to series of marine transgressions (Carter and others, 1986; Rawlinson, 1993). Lacustrine processes also greatly modify coastal-plain deposits by reworking and sorting surficial deposits, melting ground ice, and creating large, oriented lake basins. Draining of lakes along the coast and rising sea levels have created large embayments, particularly along the Cape Simpson and Cape Halkett coasts. Numerous large rivers traverse the coastal plain and deposit fine-grained sediments at the coast. The largest river, the Colville, drains 60,000 km² (23,166 mi²) and has a delta of 666 km² (257 mi²) (Walker, 1976).

The surficial geology and geomorphology of the coastal plain have been extensively studied since the pioneering work of Schrader (1904), who descended the Colville River and traveled along the coast to Cape Lisburne, and Leffingwell (1919), who documented the geology and geomorphology of much of the Beaufort Coast. A remarkable synthesis of the patterns and processes of the surficial deposits of the coastal plain was developed by Rawlinson (1993), based on his own extensive field studies and the reports of others. Most of the following descriptions are summarized from

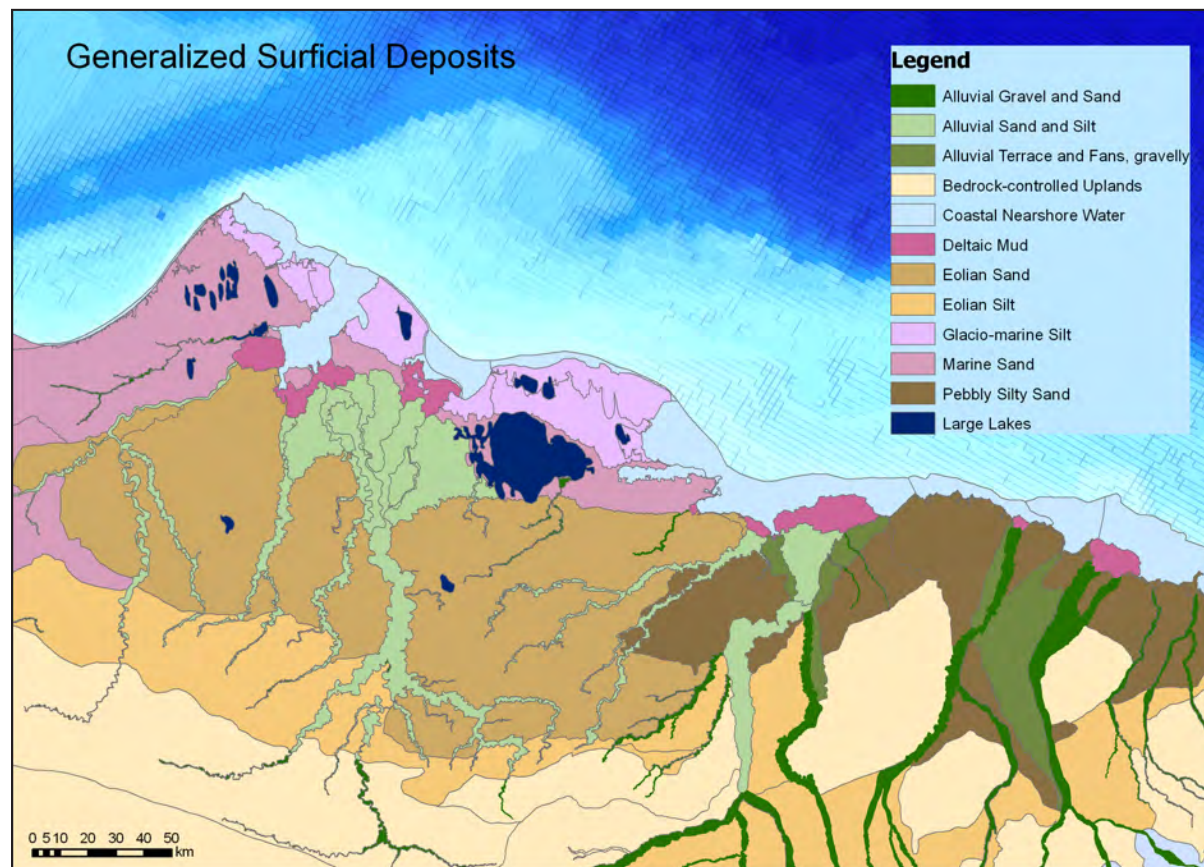


Figure 6. Surficial geology map of the central and western Beaufort Coastal Plain.

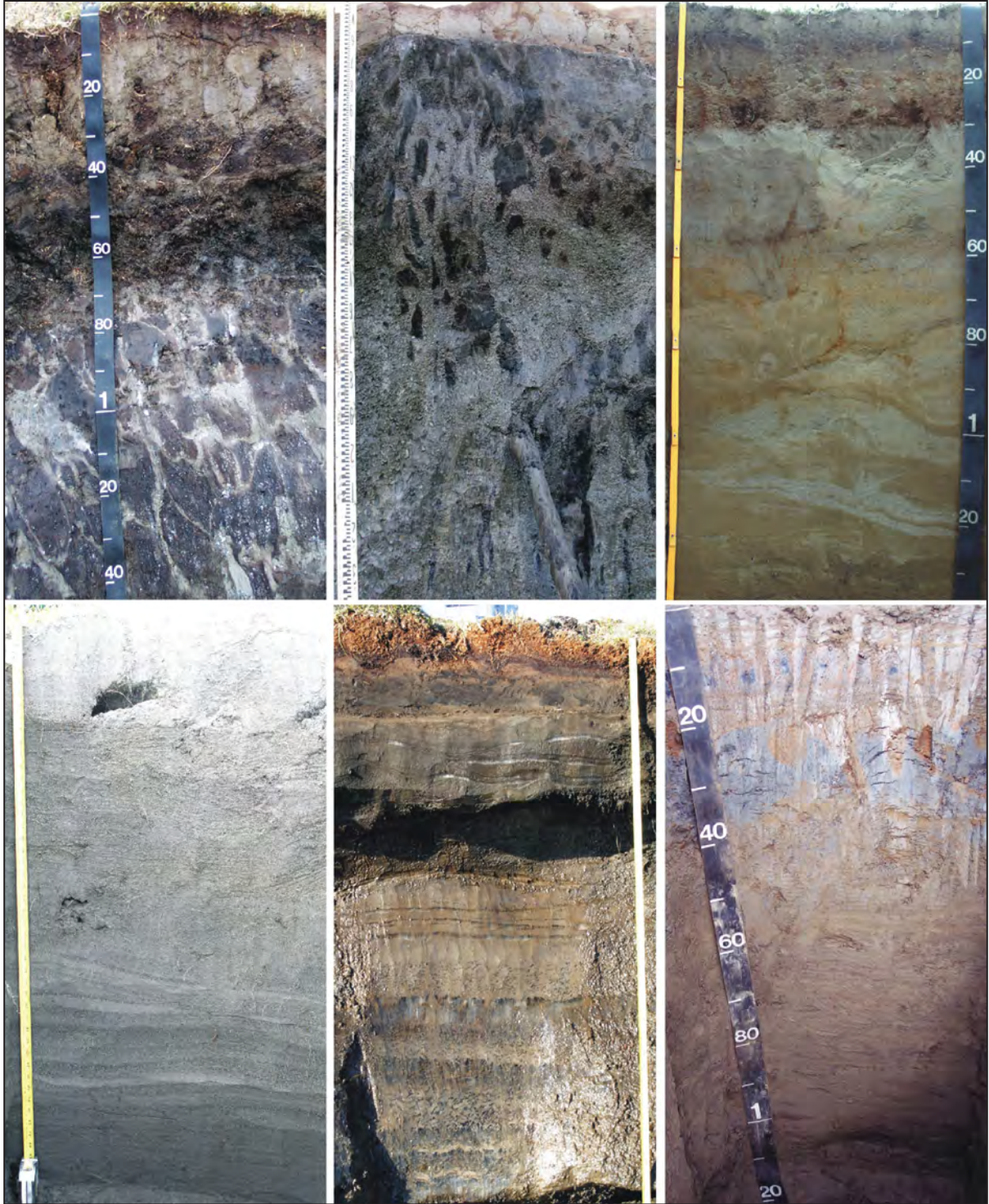


Figure 7. Photographs of bank exposures of the dominant surficial deposits on the Beaufort Coastal Plain, including (clockwise from upper left) coastal plain (Beechey Sand), glacio-marine, inactive eolian sand, tidal flat, thaw lake, and active eolian sand (photos by T. Jorgenson).

his work, although some of the important field studies are referenced in conjunction with the descriptions of specific surficial deposits below. Note that radiocarbon dates presented in this guidebook present the values of the original reports, although in many instances it is not clear whether they are radiocarbon age (specified as RC year BP) or calibrated calendar years (specified as cal year BP or cal ka BP).

MARINE

Modern coastal deposits include beach deposits, sand dunes, tidal flats, organic-rich salt marshes, barrier islands, and lagoonal sediments (Short, 1973; Wiseman and others, 1973; Barnes and others, 1977; Lewellen, 1977; Harper, 1978; Naidu and others, 1984; Reimnitz and others, 1988; and Jorgenson and Brown, 2005). These have mostly been deposited during the last 5,000 years when sea level approached within a few meters of current levels.

During at least four, and perhaps as many as six, periods in the last 3.5 million years, there has been periodic warming of the arctic climate during interglacial events that has led to high sea-level stands and marine transgressions. The transgressions left distinctive marine deposits or wave-cut benches across much of the coastal plain (O'Sullivan, 1961; Hopkins, 1967; Carter and Galloway, 1982; Brigham, 1983; Carter and others, 1986; Kaufman and others, 1990; Dinter and others, 1990; Rawlinson, 1993). The Colvillian and the younger Bigbendian transgressions (2.48 to 3.5 million years ago) are associated with prominent terraces east of the Colville River. The Fishcreekian transgression, variously estimated to have occurred 1.87 to 2.48 million years ago (Carter and others, 1986) or 1 to 1.5 million years ago (Kaufman and others, 1990), may be represented by Terrace C east of the Colville River. The Pelukian transgression, which probably occurred 120 to 130 thousand years ago, reportedly produced shoreline features and sediments at elevations up to 10 m (33 ft) above present sea level. The ridge of beach sand and gravel that runs from Barrow to Harrison Bay is attributed to this transgression (Carter and Robinson, 1981). The last major transgression, the Simpsonian, represents a high sea-level stand of up to 7 m (23 ft) that occurred about 75 thousand years ago. The Flaxman Member of the Gubik Formation is attributed to this transgression and is found discontinuously along much of the Beaufort Sea coast. The Flaxman Member, which consists mostly of clayey silt and silty sand, is notable for the exotic erratic clasts that probably were transported by icebergs from the Canadian Archipelago (MacCarthy, 1958; Rodeick, 1979; Hopkins, 1982).

Along the northern portion of the NPRA is an extensive area of marine sand, which Carter and Galloway (1985) interpreted to have been deposited

by more than one marine transgression. The deposits consist of fine to medium sand containing pebbles and fine granules of chert and minor beds of clayey sand, sandy silt, and thin lenses of organic matter. They are massive to poorly stratified and organic masses are highly contorted by ice-wedge formation. The deposits are thought to be associated with shallow nearshore water, barrier islands, bars, and spits.

Marine beach deposits are found along modern and former shorelines (Hopkins and Hartz, 1978; Carter and Galloway, 1985). The deposits typically are narrow, but can be quite extensive laterally. They consist chiefly of stratified coarse to fine sand, granule, and pebble gravel. Marine shells are common as well as organic horizons and driftwood. Occasional erratic boulders up to 1 m (3.3 ft) have been reported. Actively forming beaches have deep active layers up to 2 m (6.6 ft), in contrast to the abandoned inland beach ridges, where permafrost generally is within 0.5 m (1.6 ft) of the surface.

Lagoons fringe most of the coast and are protected by barrier islands and remnants of the coastal plain (Naidu and Mowatt, 1975; Hopkins and Hartz, 1978; Naidu and others, 1984). Barrier islands predominate and are composed solely of gravelly-sandy deposits and formed by littoral currents. In contrast, the remnant islands have thick peat deposits and tundra vegetation, and presumably represent cutoff or detached portions of the former coastal plain. Most of the barrier islands are part of five prominent island chains associated with sediment input from large rivers. These include: (1) islands extending westward from the Sagavanirktok River delta that form the Simpson Lagoon; (2) islands extending westward from the Canning River delta that form the Stefansson Sound; (3) islands fronting the coast from the Hulahula to the Jago River deltas that form Barter Lagoon; (4) islands fronting the coast in front of the Aichilik and Kongakut River deltas that form the Beaufort Lagoon; and (5) islands extending eastward from the Point Barrow barrier spit that form the Elson Lagoon. Lagoons formed behind these island chains extend 30–70 km (18–44 mi) in length, and their widths vary significantly, depending on the locations of the individual barrier islands. The lagoons typically have maximum depths of 3–4 m (9.8–13.1 ft). At Simpson Lagoon, stratigraphic evidence indicates that Simpson Lagoon resulted from a combination of processes, including coalescence of laterally growing coastal lakes and their subsequent drowning by the post glacial rising sea level (Naidu and others, 1984). A radiocarbon date of a peat deposit at the base of a core suggests that the lagoon was part of a coastal plain about 4.5 RC ka BP (Naidu and others, 1984).

GLCIOMARINE

Glaciomarine deposits are found discontinuously along much of the coast (fig. 8), and are identified by the clayey silt and silty sand deposits that have abundant erratic clasts of dolomite, diabase, pyroxenite, granite, and quartzite. The most prominent deposit is the Flaxman Member of the Gubik Formation, which has been associated with the Simpsonian transgression (Hopkins, 1982; Rawlinson, 1993). It occurs at elevations up to 7 m (23 ft) above current sea level. The erratic clasts are thought to have been derived from the breakup of an ice sheet in the Canadian arctic and rafted in on icebergs (MacCarthy, 1958; Roedick, 1979; Hopkins, 1982). The marine sands along the coast of the NPRA (Williams and others, 1977; Carter and Galloway, 1985) also have sparse exotic clasts indicative of glaciomarine origin (Ping and others, 2008). Thermoluminescence dates for sediments range from 53 to 81 ka and cluster between 71 and 76 ka.

Coastal deposits in northern NPRA also appear to be of glaciomarine origin, although they have been described by Carter and Galloway (1985) as marine sand and silts. In the Cape Halkett area, they consist of a few meters of glaciomarine silt, clayey silt, and silty sand that bear erratic stones of Canadian provenance. Black (1983) suggests a glacial origin for some fine-grained material in the bluff at nearby McLeod Point. The remains of Pacific

marine mammals have been found, including ribbon seal, and gray whale (Repenning, 1983). Along the southern margin of the glaciomarine silt is a large beach ridge that extends from Harrison Bay to Barrow. Slightly inland is an extensive area of marine sand (Williams and others, 1977; Carter and Galloway, 1985).

FLUVIAL AND GLACIOFLUVIAL

Major rivers draining the coastal plain into the Beaufort Sea include, from east to west, the Kongakut, Jago, Hulahula, Canning, Sagavanirktok, Kuparuk, Colville, Fish Creek, Ikpikpuk, Topagoruk, and Meade Rivers. Of these, the Colville is by far the largest, draining 29 percent of the North Slope. The characteristics of these rivers range from those with substantial mountain watersheds and gravelly floodplains (Kongakut, Canning, and Sagavanirktok rivers) to those with sandy floodplains that are limited to the coastal plain (Jago, Fish Creek, Ikpikpuk, and Meade rivers). The eastern rivers typically end in large, gravelly outwash fans, and the western rivers end in broad, muddy deltas.

Floodplain deposits have been differentiated into coarse channel and fine-grained overbank deposits, and whether they are active, inactive, and abandoned according to the frequency of flooding (Cannon and Mortenson, 1982; Rawlinson, 1993; Jorgenson and others, 1996). Active channels are regularly flooded,

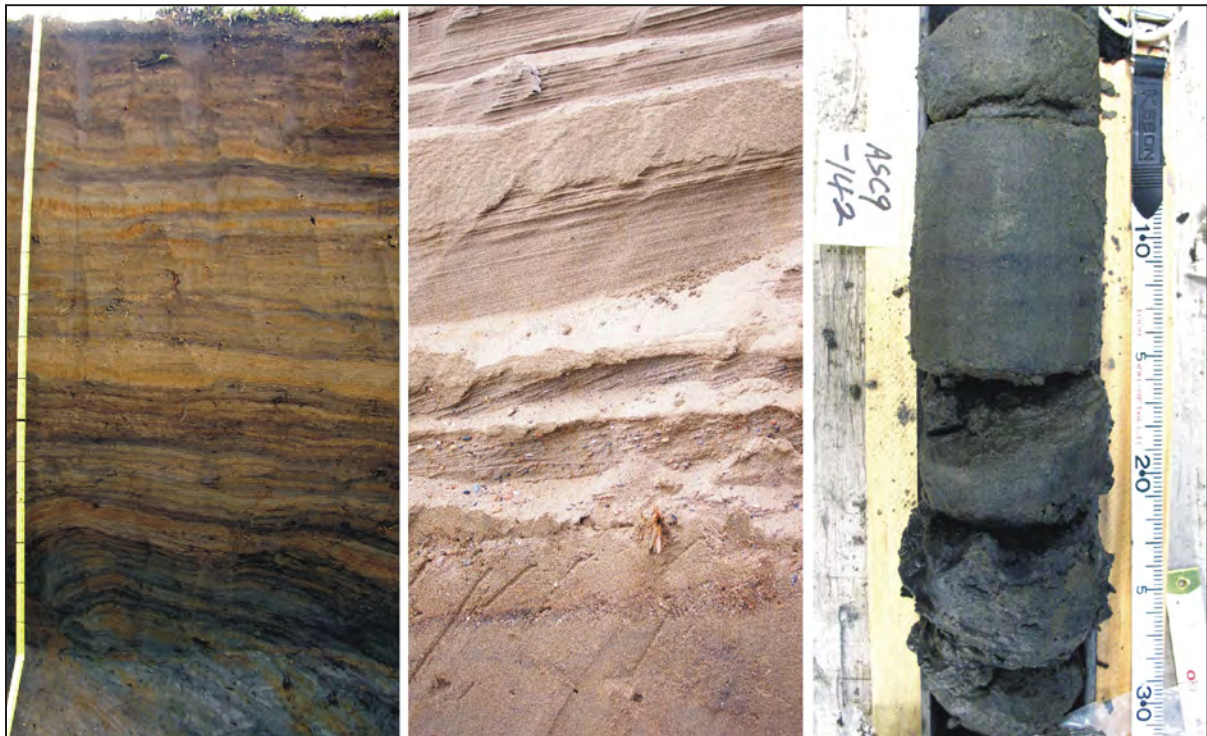


Figure 8. Photographs of bank exposures of the dominant surficial deposits on the Beaufort Coastal Plain, including (from left to right) inactive floodplain overbank, beach ridge, and lagoon deposits (photos by T. Jorgenson, C.-L. Ping, and M. Kanveskiy).

scoured, and unvegetated, whereas inactive channels are flooded only during high-water events and usually are vegetated. Active overbank deposits are flooded almost every year, have interbedded, laminar silts and sand, are well drained, and support vigorous willow vegetation. Inactive overbank deposits are flooded every 5–25 years and have interbedded organic and silt layers (fig. 8). Abandoned overbank deposits are flooded so infrequently that flooding has little effect on soils and vegetation. The surface is covered with thick peat with few to no mineral layers.

Fluvial terraces above the modern floodplain are found along most modern river valleys and were probably formed over a long period during the Pleistocene (Carter and Galloway, 1985). Fluvial terraces occur on both sides of the Colville River (Rawlinson, 1993). Fossil spruce logs have been found at several localities, indicating the deposits were formed during warmer, interglacial intervals (Carter and Galloway, 1982).

Glaciofluvial outwash deposits are abundant on the coastal plain eastward from the Colville River, where the mountains are closer and the rivers extend out of glaciated valleys (Rawlinson, 1993; Reimnitz and Wolf, 1998). The gravel deposits have complex depositional environments associated with both glacial and interglacial events. The deeper, older deposits, termed the Ugnuravik gravel by Rawlinson (1993), are exposed in the gravel pits in the Kuparuk area and are thought to extend from the Sagavanirktok to the Canning River. Fluvial and glaciofluvial deposition of these sediments represents a long period of erosion from the Brooks Range. Younger deposits between the Kuparuk and Sagavanirktok rivers, termed the Put alluvium, appear to be associated with fluvial processes during warm interglacial events, as indicated by wood, and younger outwash associated with late Wisconsinan glaciation in the Brooks Range.

EOLIAN

Wind-blown deposits are widespread across the coastal plain as sand sheets, sand dunes, and loess blankets. Particularly notable are the enormous sand sea in the central NPRA (Carter, 1981) and the widespread thick loess deposit that blankets much of the lower foothills across the regions (Carter, 1988). Smaller active dune systems are common along point- and lateral-bars of major rivers and deltas (Walker, 1976). The eolian sand is thought to have originated during four main intervals (Carter and others, 1984). The most recent period occurred 8 to 11 ka BP, the second period 11 to 13.5 ka BP, the third period 13.5 to 36 ka BP, and the earliest period started during the early Wisconsinan and ended 36 ka BP. Many of the sand deposits are mantled with a thin blanket of eolian silt and stabilized by surface organic horizons.

Active sand dunes are common downwind from active sandbars of river channels (Walker, 1973; Jorgenson and others, 1997b). They can be barren or colonized by early successional willows, grasses, and legume forbs. The dunes show no soil development and lack surface organic horizons (fig. 7).

A distinctive, slightly pebbly sand sheet is widespread between the Colville and Kuparuk Rivers, in isolated regions between the Kuparuk and Sagavanirktok rivers, and abundant again between the Sagavanirktok and Canning rivers. The deposit, termed the Beechey sand, has been interpreted by Rawlinson (1993) to be of eolian origin, but the genesis remains problematic because it has trace amounts of gravel with clasts up to 10 cm (4 in) in size, is slightly saline, lacks bedding structures, and is devoid of organic material or macrofossils. Texture varies from predominantly silt loam to loamy sand, but can include up to 5 percent gravel. The gravel, which is polished and usually faceted on one end, is thought to have been introduced into the sand from underlying deposits by frost-related processes (Rawlinson, 1993). Based on thermoluminescence dating of basal samples, Rawlinson (1993), concluded the deposits were of middle to late Wisconsinan age, with a maximum age of about 26 RC ka BP.

LACUSTRINE PROCESSES AND DRAINED-LAKE BASINS

The oriented lakes of the Arctic Coastal Plain of Alaska and Canada have long fascinated scientists because of their importance to ecological processes (Hobbie, 1984) and permafrost dynamics (Hopkins, 1949; Sellman and others, 1975), their striking pattern and orientation (Cabot, 1947; Black and Barksdale, 1949; Livingstone, 1954; Côté and Burn, 2002; Hinkel and others, 2005), widespread occurrence (Frohn and others, 2005), apparent cyclic development (Cabot, 1947; Britton, 1957), and uncertainty about their origins (Carson, 1968). Although a thermokarst origin for the majority of lakes has been postulated frequently, the specific mechanisms of ice aggradation, degradation, and lake orientation remain controversial.

A ‘thaw-lake cycle’ to explain the repeating and overlapping pattern of thermokarst lakes and basins was first proposed by Cabot (1947) based on interpretation of lake patterns evident on aerial photographs. Britton (1957) soon articulated a more complete process that involved: (1) initial flooding of basins; (2) lake expansion and coalescence through lateral mechanical erosion and thawing accompanied by material sorting; (3) drainage; (4) ice-wedge development in drained basins; and (5) secondary development of thaw ponds from ice-wedge degradation. Everett (1980) conceptualized the most complete cycle beginning with an ice-rich raised surface that included: (1) climate change or surface disturbance

that initiates permafrost degradation; (2) degradation of ice wedges and development of small thaw ponds; (3) expansion of the thaw pond by surface and subsurface thawing; (4) expansion into large lakes by bank erosion and subsurface thawing accompanied by material sorting; (5) partial or complete drainage by stream capture or breaching; (6) and re-establishment of ice-wedges and surface polygon patterns. Finally, Billings and Peterson (1980) described a 'thaw-lake cycle' with 10 stages similar to Everett's but emphasized the role of ice-wedge aggradation and degradation within basins.

Recent analysis by Jorgenson and others (2006) indicates that lake evolution is much more complex and less cyclic than theorized by previous investigations. In the area they studied in the eastern NPRA, there was insufficient ground ice in the oldest terrain to form thaw lakes, the aggradation of ice in the margins of drained-lake basins was insufficient to heave the surface up to near original topographic conditions, and the process occurs at too slow a rate for a 'thaw-lake cycle' to have developed during the Holocene. On the basis of topographic profiles, stratigraphic analysis, radiocarbon dating, and photogrammetric analysis, they developed an alternative conceptual model of lake and basin development to explain the patterns and process for the extensive sand sheets underlying most of the coastal plain. Developmental stages include: (1) initial flooding of depressions to form primary lakes during the early Holocene; (2) lateral erosion, with sorting and redistribution of sediments; (3) lake drainage as the stream network expands; (4) differential ice aggradation in silty centers and sandy margins; (5) formation of secondary thaw lakes in the heaved centers of ice-rich basins and infilling of ponds along the low margins; and (6) basin stabilization (fig. 9).

True thermokarst lakes in northern Alaska are found predominantly in areas with thick silt deposits, such as the narrow coastal plain extending from Barrow to Cape Halkett, which is underlain by glaciomarine silts and clays and the Colville River Delta (Jorgenson and others, 1998). Near Barrow, the silty soils can have volumetric ice contents greater than 80 percent (Brown, 1968). Small thaw lakes are located on the distal, higher portions of abandoned floodplains with thick, silty overbank deposits (Jorgenson and others, 2003c) and are particularly abundant near the lower Ikpikpuk River. Deep thaw lakes formed in massive ice in late Pleistocene loess deposits are common in the lower Brooks Foothills (Carter, 1988). In addition, extensive areas of thermokarst are present on the Seward Peninsula (Hopkins, 1949; Kidd, 1990) and Siberian lowlands, which have thick accumulations of Pleistocene massive ice. A thermokarst origin for lakes is evident by the collapsing margin of the lake that extends well below water line and the bank typically is cut by

a thermoerosional niche (fig. 10). In contrast, a non-thermokarst origin is indicated by a debris-covered bank that ends on a wave-cut bench at water line. Although there can be some settlement (0.1–0.5 m [0.4–20 in]) of the eroding shoreline as it thaws, the settlement is not sufficient to cause the basin in which the water is impounded.

Other types of lakes are formed by fluvial and deltaic processes. Riverine lakes are common along large, meandering river floodplains on the coastal plain, and to a lesser extent on braided floodplains in the foothills. The lakes are oriented along the sinuous channels of the riverbed and shapes are not affected by wind erosion. Older floodplains with riverine lakes formed by channel scouring, however, can also have a minor number of thaw lakes developed on narrow, abandoned floodplain deposits. Delta lakes are found on all the deltas along the Beaufort Sea coast and range from freshwater in the upper deltas to saline along the outer tidal flats. On the outer delta, lakes and ponds can form in depressions and impoundments of the tidal flats and abandoned channels.

PERMAFROST

FACTORS AFFECTING PERMAFROST DEVELOPMENT

Perennially frozen ground (permafrost) is a unique characteristic of polar regions and high mountains that is fundamental to geomorphic processes and ecological development in tundra and boreal forests. Permafrost-affected regions cover about 23 percent of the exposed land in the northern hemisphere and its stability is particularly important to the fate of ecosystems and human development in the circum-arctic region. Permafrost distribution in the northern hemisphere is divided into four zones based on the extent of land underlain by permafrost (Brown and others, 1997): continuous (>90 percent area with permafrost), discontinuous (50–90 percent), sporadic (10–50 percent), and isolated (>0–10 percent). These zones are closely related to mean annual air temperatures (MAAT), with approximate temperatures of -6°C (21.2°F), -6° to -2°C (21.2°–28.4°F), -2° to 0°C (28.4°–32°F), and 0° to 2°C (32°–35.6°F), respectively. The Beaufort Coastal Plain is within the zone of continuous permafrost (fig. 11).

Permafrost is defined as earth material having a temperature below 0°C for two or more years, although most permafrost is hundreds to tens of thousands of years old. Due to the freezing temperatures in permafrost, water is maintained in a solid state (ice). Some unfrozen water may be present, however, depending on temperature and the effects of soil texture and salinity on lowering the freezing point of water. The upper horizons of soil with permafrost reflect seasonal climatic variations by developing a seasonally thawed

layer above the permafrost table (surface), termed the active layer (fig. 12). In places where permafrost is thawing from above, such as below a deep lake, a talik (perennially unfrozen zone) may develop above the permafrost, or around a zone where groundwater has penetrated (fig. 13).

Permafrost properties depend on the geologic origin of the soil, cryogenic origin, and development over time (Johnston, 1981). Permafrost can form in two ways. Epigenetic permafrost forms when the soil slowly freezes downward after sediment deposition has ended. At the depth of initial permafrost formation

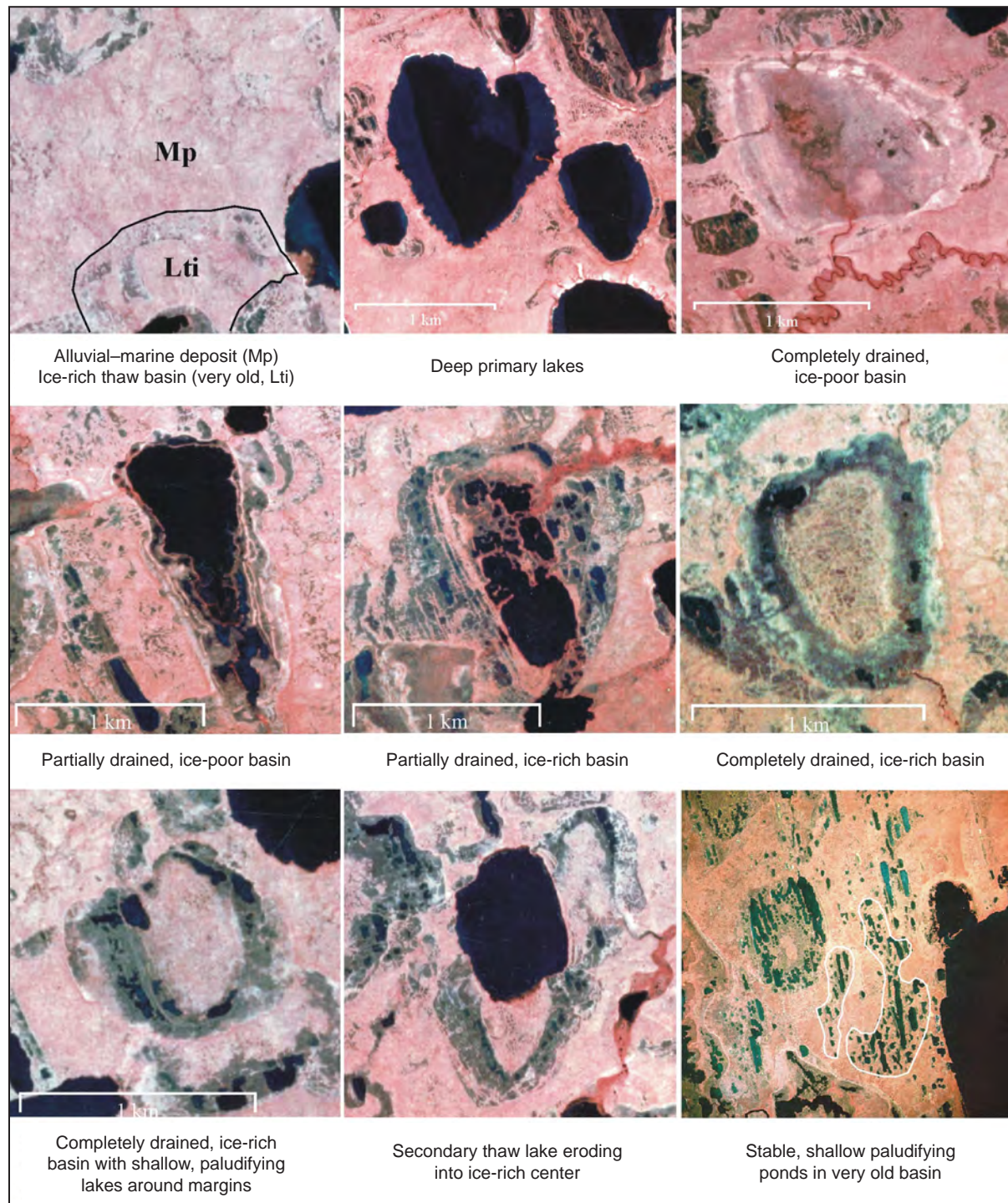


Figure 9. Airphotos of lakes and basins in various stages of development on the coastal plain just west of the Colville River Delta.



Figure 10. Characteristic shorelines of lakes, including (upper left) a thermokarst lake with a collapsing undercut bank, (upper right) a non-thermokarst lake with slumping bank that meets a wave-cut bench at waterline, (lower left) a secondary thermokarst lake eroding into the ice-rich center of a basin, and (lower right) an infilling pond with limnic sediments in the adjacent tundra soil (photos by T. Jorgenson).

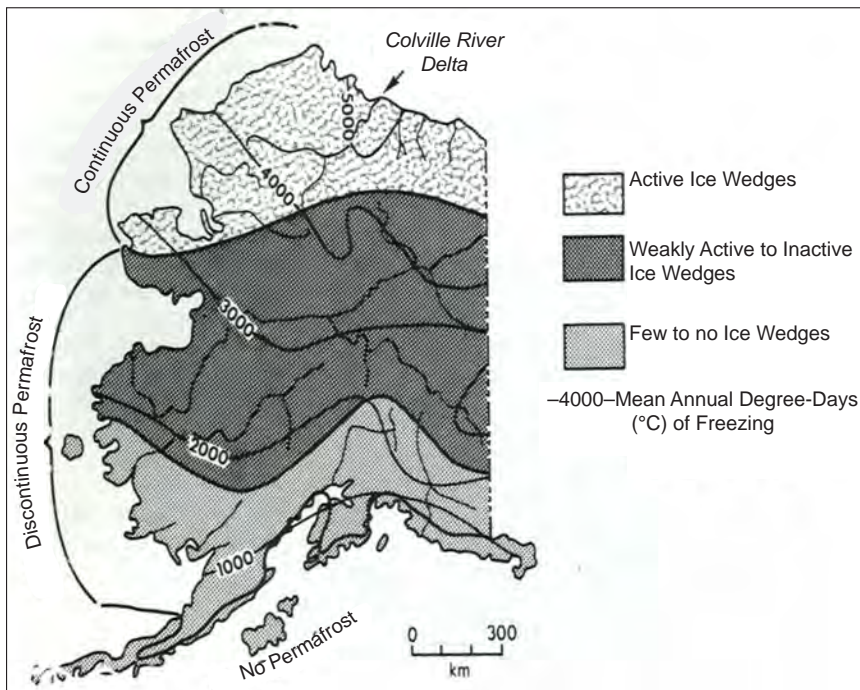


Figure 11. Distribution of permafrost zones and ice wedges in relation to mean annual freezing-degree days (adapted from Péwé, 1975).

below the active layer (typically 1–1.5 m [3.3–4.9 ft]), the permafrost slowly freezes downward into unfrozen material, although there is some minor upward freezing as the active layer thins in response to changes in surface vegetation and soil (Kanevskiy and others, 2008). In contrast, syngenetic permafrost is formed simultaneously with sediment deposition. Consequently, two surfaces are moving upward: the ground surface of the accumulating sediment and peat, and the permafrost surface at the bottom of the readjusting active layer. Epigenetic and syngenetic permafrost also can develop concurrently

in newly exposed sediments with continuing sediment accumulation as frost penetrates downward from the permafrost base, while syngenetic permafrost grows upward into the accumulating sediments (fig. 14).

Permafrost thickness generally is 200–400 m (650–1,300 ft) thick over most of the coastal plain, although a thickness of 650 m (2,130 ft) has been measured at Prudhoe Bay (Gold and Lachenbruch, 1973) (fig. 15). Gold and Lachenbruch (1973) suggested that permafrost was first formed on the coastal plain during the first glacial episode of the early Pleistocene and has existed continuously since.

Figure 12. Diagram of stratigraphy of soil and ice morphology in fine-grained, ice-rich permafrost, illustrating (A) active layer, (B) transient layer, (C) intermediate layer with ataxitic ice formed during decrease of the active layer depth with accumulation of organic matter on the soil surface, (D) deeper permafrost with lenticular ice, (E) young ice wedge developed in the intermediate layer, and (F) old ice wedge formed during an earlier period. Symbol 1 shows the thickness of the organic layer; symbol 2 marks the top of the permafrost table; and symbol 3 represents maximum thaw depth during a cool summer (illustration by M. Kanevskiy).

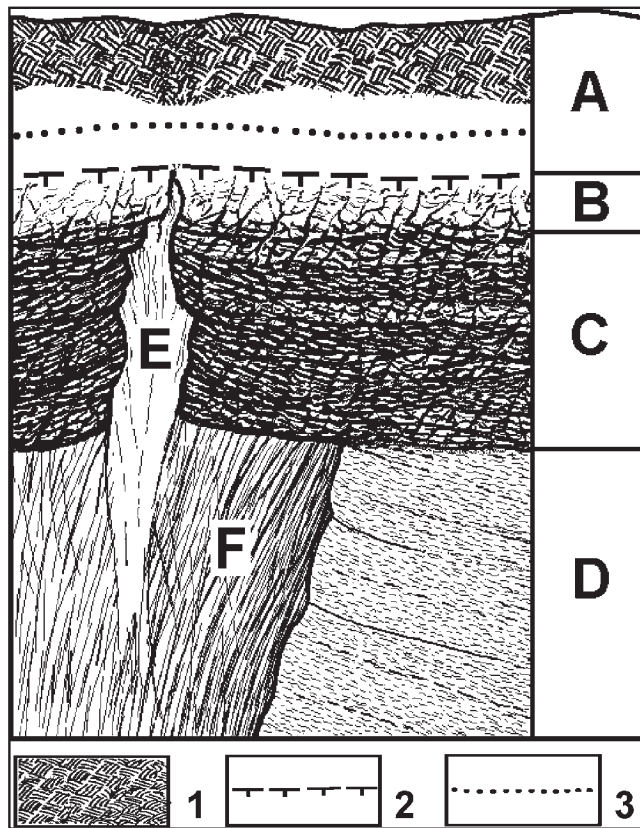


Figure 13. Diagram of the distribution of permafrost in relation to surface terrain (from Ferrians and others, 1969). Note the unfrozen zone (talik) underneath a shallow lake, the absence of permafrost below a large deep lake, and the absence of permafrost under deep ocean water.

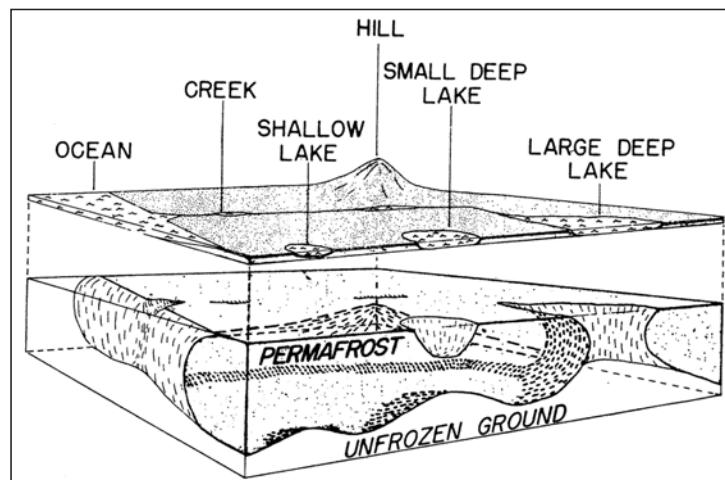


Figure 14. Mechanisms of (A) syngenetic (Popov, 1967) and (B) epigenetic permafrost formation (Kanevskiy and others, 2008).

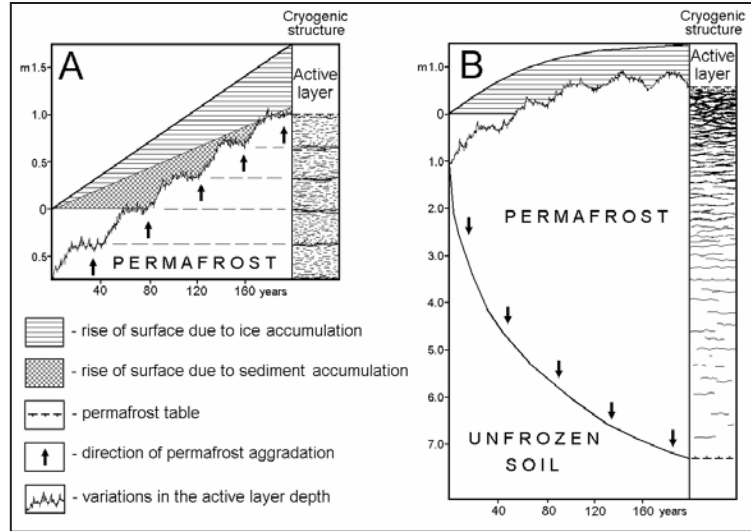
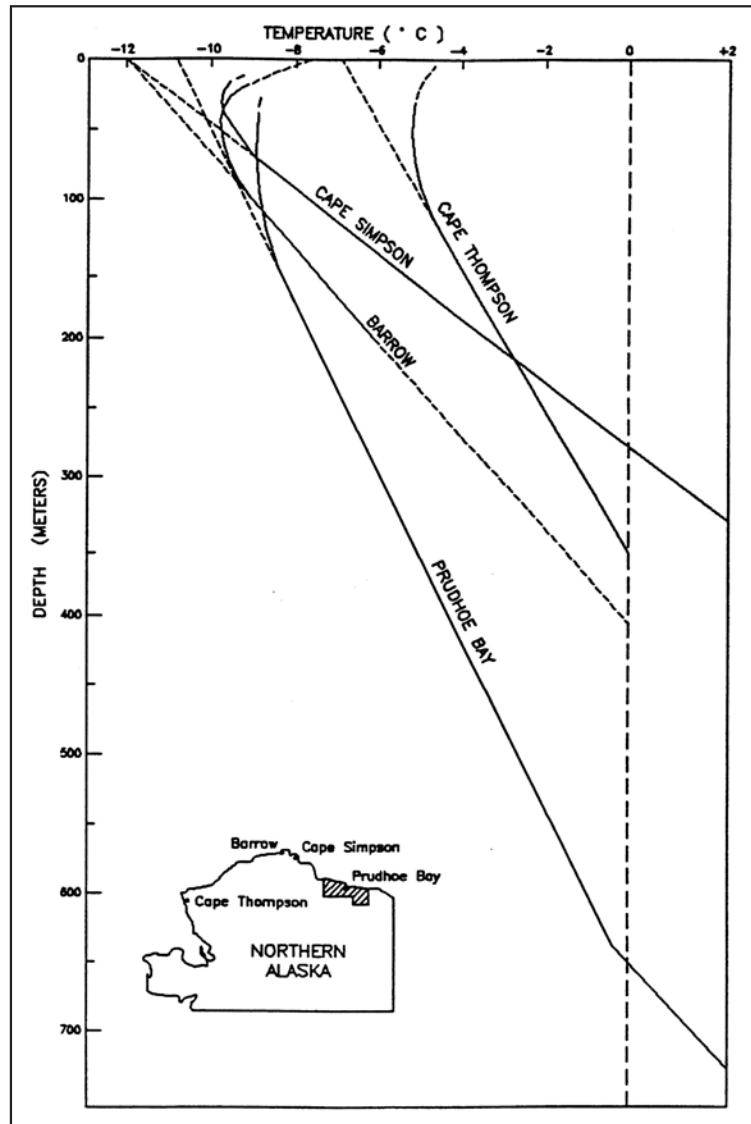


Figure 15. Temperature profiles from deep boreholes across the Beaufort Coastal Plain showing the depth of permafrost (Lachenbruch and others, 1962).



THERMAL REGIME

Temperature profiles obtained from deep boreholes provide a record of air temperature changes over a long period because of the delayed response of temperature changes at great depths (Lachenbruch and Marshall, 1986; Osterkamp, 2003) (fig. 16). Long-term measurements made by research groups from the U.S. Geological Survey (Lachenbruch and others, 1988) and University of Alaska Fairbanks (Romanovsky and others, 2002; Osterkamp, 2005) allow development of a general scenario of permafrost and active-layer conditions for northern Alaska. Although the general scenario represents permafrost and active-layer conditions, there are known exceptions and, since data are sparse, there are likely other exceptions to be found.

Air temperatures in northern Alaska increased from the late 1800s until about 1940, and decreased into the late 1970s, increased sharply and then changed little to the end of the century, as indicated by the temperature profiles (Lachenbruch and others, 1982; Clow and Urban, 2002; Osterkamp and Romanovsky, 1996; Osterkamp, 2007). Permafrost warming was coincident with the increase in air temperatures in Alaska after the Little Ice Age but appears to have started later. This warming extended from Cape Thompson, north to Barrow, and east to Barter Island (Lachenbruch and Marshall, 1986; Osterkamp and Jorgenson, 2005). The magnitude of the warming was typically 2 to 4°C (4–7°F) with less warming to the south and east (fig. 15).

During the fourth quarter of the 20th century, permafrost temperatures warmed across northern Alaska from Barrow to the Alaska–Canada border coincident with a statewide increase in air temperatures that began in 1977 (Osterkamp, 2007; fig. 17). From Prudhoe Bay, the warming extended south through the Brooks Range. The magnitude of the warming at the surface of the permafrost (through 2003) averaged 3°C (5°F) west of

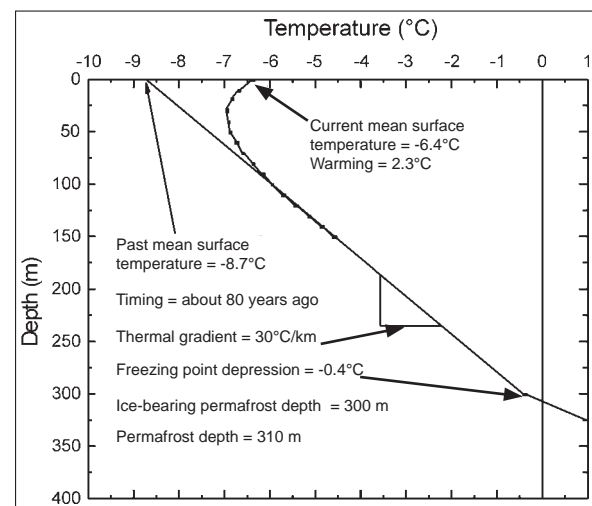


Figure 16. Typical permafrost temperature profile in northern Alaska (provided by T. Osterkamp). Timing of the warming is determined from the penetration depth of the curvature. Seasonal effects are not shown.

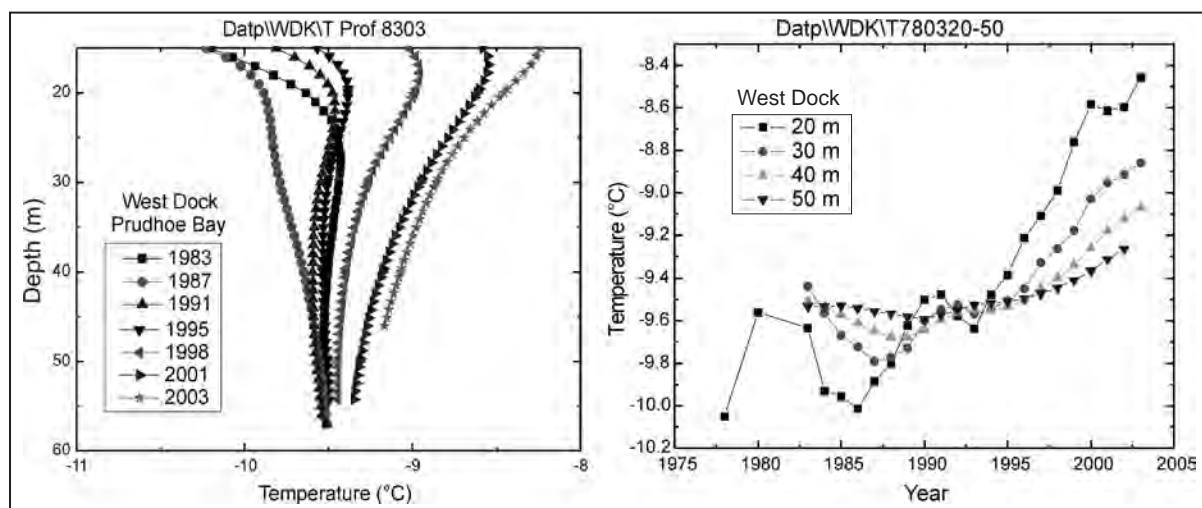


Figure 17. Time series of permafrost temperatures at various depths at West Dock in Prudhoe Bay (left). The profiles show permafrost warming during the late 1970s and early 1980s, cooling in the mid 1980s, and warming since then. The time series of temperatures at specific depths at the same site is provided at right. Note that seasonal variations are suppressed and that the zero annual amplitude is not well defined while temperatures are changing rapidly (illustration by T. Osterkamp).

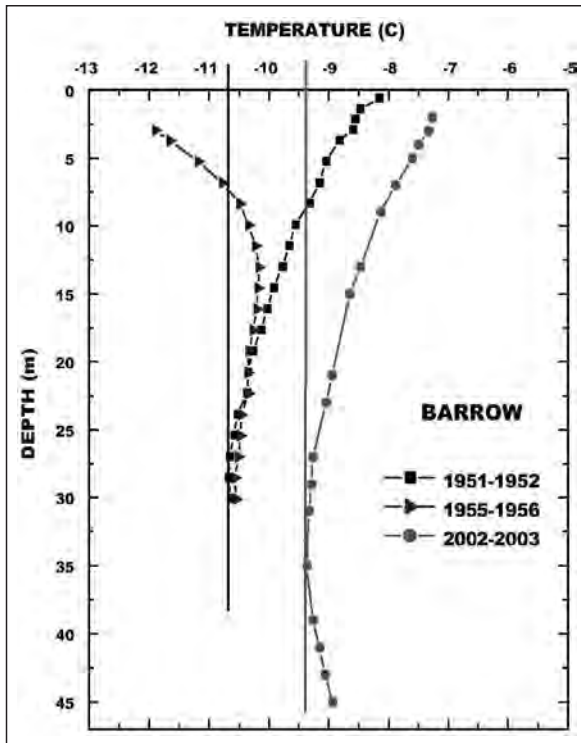


Figure 18. A time series of permafrost temperatures from 1951 to 2003 in a deep borehole at Barrow (based on data from Brewer and Romanovsky; see Nelson and others, 2008).

the Colville River, ranged from 3 to 4°C (5–7°F) for the Arctic Coastal Plain at Prudhoe Bay, and somewhat less at Barrow (fig. 18) and Barter Island (Osterkamp and Jorgenson, 2005) and to the south (Osterkamp, 2003). The warming of air temperatures was seasonal, greatest during winter (October through May) and least during summer (June through September). Snow covers were thicker than normal during the late 1980s and the 1990s, which contributed to the permafrost warming. At the turn of the century, permafrost temperatures showed that warming had slowed in the Prudhoe Bay area and to the south (Osterkamp, 2005, 2007).

Permafrost temperatures are not only sensitive to climate, but also vary with terrain conditions. One-time measurement of ground temperatures underneath a lake at Barrow (Brewer, 1958) show that depth of water can greatly influence ground temperatures and create an unfrozen zone beneath the lake bottom (fig. 19). Similarly, ground temperatures were warmer beneath a shallow lagoon, although temperatures remained below zero because the hypersaline conditions of nearshore water beneath the sea ice allows the water to cool below 0°C (32°F) (fig. 20). These warmer conditions under lagoons can affect permafrost temperatures for tens to hundreds of meters inland from the shore.

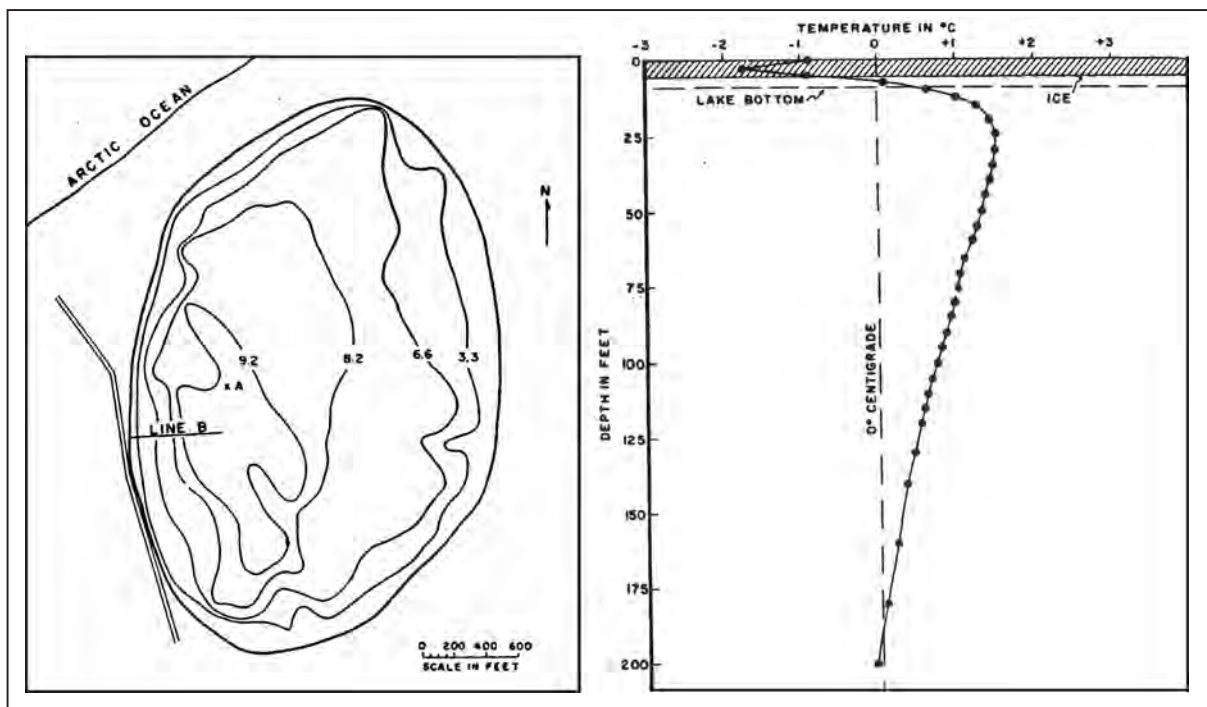


Figure 19. A temperature profile from a deep borehole beneath a lake near Barrow (Brewer, 1958). Note that there is an unfrozen zone (talik) in the sediments beneath the lake, but permafrost still exists at a depth of ~60 m (~200 ft).

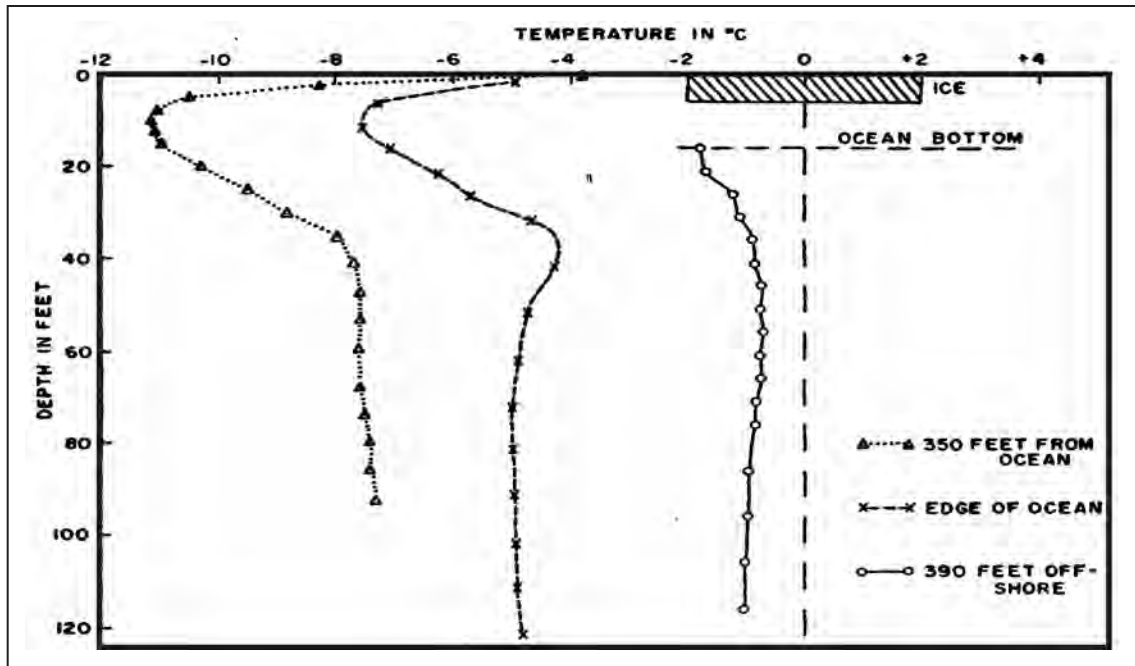


Figure 20. Temperature profiles from deep boreholes in relation to the shoreline of Elson Lagoon near Barrow (from Brewer, 1958). Note that deep temperatures are just below freezing under the lagoon and $\sim 6^{\circ}\text{C}$ ($\sim 11^{\circ}\text{F}$) colder inland from the shore.

ACTIVE-LAYER DYNAMICS

Active-layer thicknesses depend largely on the cumulative thermal history of the ground surface during the summer thaw period but can be significantly modulated by vegetation and site wetness (Romanovsky and Osterkamp, 1997). The depth of the active layer varies across the terrain and can be as little as 35 cm (14 in) in upland tussock tundra with organic-rich soils to as deep as 130 cm (51 in) in riverine tall willow shrub with sandy soils (Jorgenson and others, 2003c).

There is a large international effort by the Circumarctic Active Layer Monitoring (CALM) program to monitor

the response of the active layer to climate change (Brown and others, 2000; Hinkel and Nelson, 2003). The CALM network was established informally as a volunteer effort in 1991 and has grown to include 69 research sites in the circumarctic region. Investigators measure seasonal thaw depths across large plots using a standard protocol: at many sites soil and air temperature, and soil moisture content are also measured. At sites on the Beaufort Coastal Plain, mean thaw depths peaked during the record warm summer in 1998 but have not shown a consistent trend in depths since 1993 (fig. 21). Other recent analyses, using a slightly shorter data set for

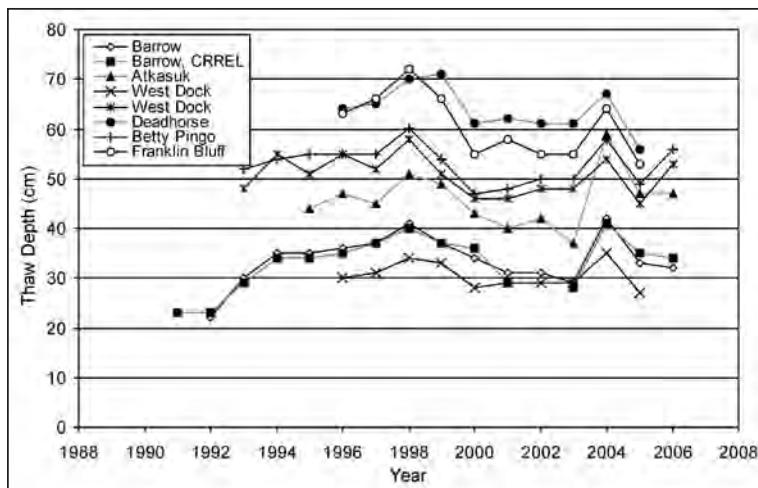


Figure 21. Maximum active-layer thicknesses at eight Circumpolar Active Layer Monitoring (CALM) sites on the Beaufort Coastal Plain (data from K. Hinkel).

the coastal plain and foothills regions (starting in 1995), show a pronounced decrease in active-layer thickness (Streletskiy and others, 2008).

Active-layer-thickness measurements at West Dock and Franklin Bluffs sites for a period of 16 years captured the effects of the record warm summers in 1989 and 1998 and, discounting the period around 1989, do not show significant trends (Osterkamp, 2005, fig. 22). These measurements, which are taken near the time of maximum thaw, show the effects of varying summer conditions rather than any definite trend. However, permafrost surface temperatures, as determined from borehole temperature measurements at the sites, generally warmed by 3 to 4°C (5–7°F) during this period, indicating that active-layer thicknesses in this region are not a good indicator of the effects of climate warming on permafrost temperatures. This probably is a result of the observed seasonality of the warming (i.e., warmer, winter conditions with little change in summer conditions). Thus, active-layer thicknesses do not reflect warming conditions when the warming occurs primarily in winter, which has been the case for the recent warming.

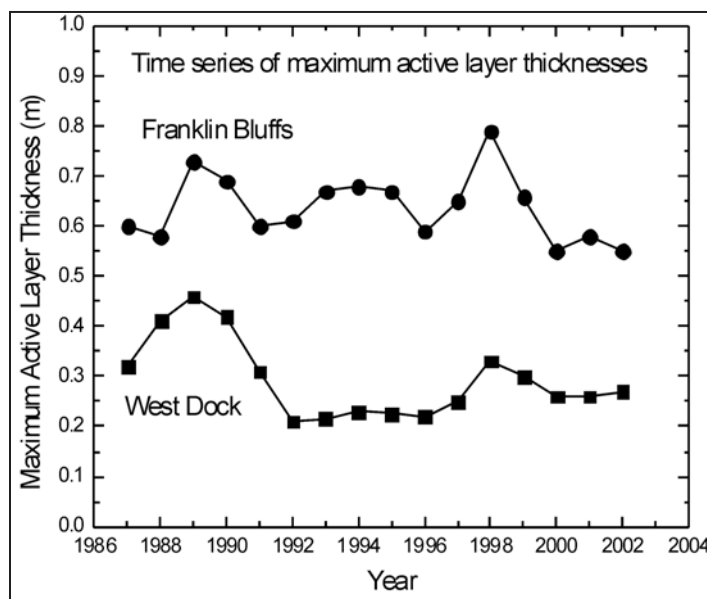


Figure 22. Maximum active-layer thicknesses at the West Dock and Franklin Bluffs near Prudhoe Bay from 1987 to 2002 (illustration by T. Osterkamp).

GROUND ICE

Ice in permafrost strongly influences the properties of frozen and thawing soil (Johnson, 1981). Ground-ice types varies widely in size, from microscopic inclusions to large masses up to 50 m (165 ft), and in distribution in the soil due to differences in soil texture, moisture, and thermal regime. Ice morphology is differentiated

by whether it is visible or not, is segregated in a soil matrix or in massive bodies, and by how it formed. In the coastal region of northern Alaska, ground ice exists in two main forms: (1) massive ground ice; and (2) porous and segregated ice, forming soil cryostructures. These ice types have variable percent ice volumes and distribution that greatly affect the relative sensitivity of permafrost to climate warming.

Massive ground ice occurs in three main forms: (1) ice wedges; (2) thermokarst-cave ice; and (3) ice cores of pingos. On the coastal plain, ice wedges are the most common type of massive ground ice, and they can be observed nearly everywhere (fig. 23). The presence of ice wedges can be easily noticed due to the polygonal surface patterns on the tundra. Ice wedges are formed by repeated contraction cracking of the soil (Leffingwell, 1915; Lachenbruch, 1962). During abrupt, cold temperature drops during the winter the frozen soil contracts and forms a crack (fig. 24). During the following spring, snowmelt flows into the crack and freezes. Because ice is weaker than the surrounding soil, a crack forms in nearly the same place the next winter and the process is repeated. The process, however, is

multi-dimensional so that the cracks form polygonal patterns on the ground, much like the desiccation cracks formed in drying, shrinking mud. When the soil between the wedges expands with warming during the summer, the expanding soil applies pressure near the wedges and deforms the soil upward to form ridges surrounding the low-center polygons. If the ice wedges thaw and the troughs deepen, high-center polygons can be formed.

The upper parts of ice wedges in the coastal region are located no deeper than 10–20 cm (4–8 in) beneath the permafrost table. As frequently seen along coastal exposures, the wedges penetrate deeper than the exposed bluffs. The average volume of ice wedges can be estimated to represent approximately 15–25 percent of the coastal exposures. However, these values vary between 1–2 percent and 40–45 percent in different sections. The highest ice wedge volume can be observed in bluffs ~5 m (~16 ft) high that formed in glaciomarine deposits near Cape Halkett (fig. 23). At such sites, the polygonal network

at the surface is very dense with spacing between ice wedges of 5–7 m (16–23 ft) and an ice-wedge width up to 3.5 m (11.5 ft). Relatively large ice wedges can be observed in the bottoms of old thaw-lake basins and on ‘primary land surfaces.’ The lowest ice-wedge volume is related to low accumulative surfaces such as coastal marshes, river deltas, and recently drained lake basins.



Figure 23. Big ice wedges in glaciomarine deposits at Point McLeod, Beaufort Sea coast (photos by M. Kanevskiy).

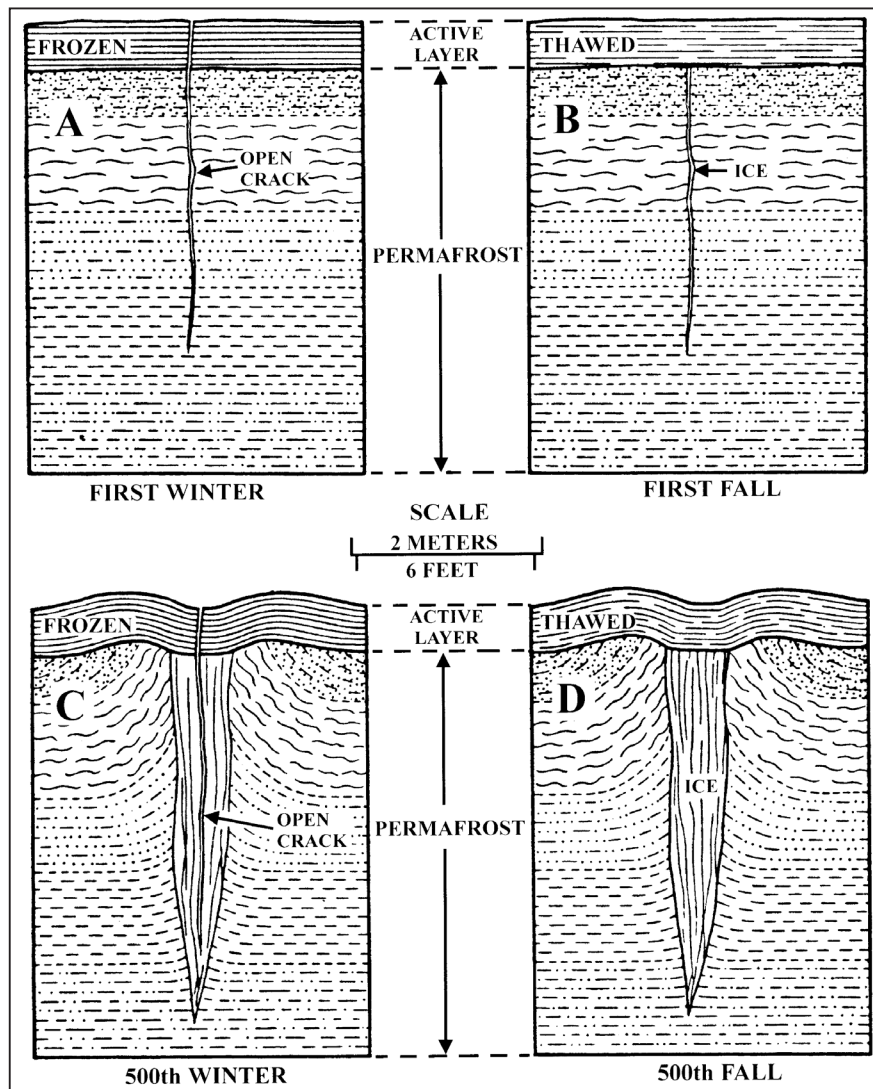


Figure 24. Diagram of ice-wedge formation (Davis, 2001, adapted from Lachenbruch, 1962).

These terrains have large ice-wedge polygons (up to 40 m [130 ft] across) and narrow ice wedges, usually less than 0.5 m (1.6 ft) wide. No wedges are found in the active eolian sand dunes.

Ice-wedge development has a large influence on modification of soil cryostructures. The growth of ice wedges induces upward displacement of the sediment layers along the ice wedge walls. This process considerably modifies the soil stratigraphy by creating vertical bands of coarse-grained sediments, and affects their redistribution within the active layer. Thickening of ice wedges, and seasonal contraction and expansion of soil between the ice wedges, leads to deformation of previously formed cryogenic structure and the development of vertically oriented cryostructures.

Thermokarst-cave ice (Shumskiy and Vturin, 1963; Shur and others, 2004), or pool ice (Mackay, 1997), is an unusual form of massive ice associated with degradation of ice wedges by the movement of water near the surface or underground. In some circumstances, water movement can stop and the refreezing of water in cavities results in formation of bodies in preexisting ice wedges (fig. 25). The thickness of these ice bodies can reach 0.7–0.8 m (2.3–2.6 ft).

Pingos (ice-cored, conical mounds) are abundant on the Beaufort Coastal Plain. More than 1,000 pingos have been identified in this area (Carter and Galloway, 1979; Ferrians, 1988). Pingos form in recently drained lake basins where unfrozen, moisture-rich lacustrine sediments that formed under a deep lake are exposed to freezing temperatures (Muller, 1959). The sediments must be permeable and thick enough that the thawed basin extends into permafrost. As permafrost aggrades downward into the thaw bulb, water migrates to the freezing front to form an ice core (Mackay, 1973). The core expands as pore water is continuously supplied

to the ice core and the surface is heaved upward. The closed-system pingos of the cold, continuous permafrost zone stop growing when the unfrozen pore water disappears. The largest pingo on the coastal plain, which has a height of 52 m (170 ft), is the Leffingwell Pingo near the Kadleroshilik River (fig. 26).

Surface sediments in the cold, continuous permafrost of the coastal plain are characterized by prevalence of the following cryostructures: crustal, pore, lenticular, layered, reticulate, ataxitic (chaotic, suspended), and organic-matrix ice (fig. 27). Porous, invisible cryostructure is typical of sands. Lenticular ice is formed mostly in silts in rapidly aggrading syngenetic permafrost. Silty clays and clayey silts, which are prevalent in the region, are characterized mainly by ataxitic (suspended) and reticulate cryostructures. The prevailing cryostructure of organic soils is organic-matrix ice, which can be ice rich (organic-matrix ataxitic) or relatively ice poor (organic-matrix porphyritic). Gravels have crustal cryostructure. The cryostructures are often complexly interbedded as illustrated by an example from slightly saline, glaciomarine deposits near Cape Halkett (fig. 28).

The volume and distribution of ground ice are closely related to soil texture and to the segregated ice structures associated with the textures (Jorgenson and others, 1997b, 2003a). This variation in turn can be partitioned by geomorphic unit to predict ice distribution across the coastal plain (fig. 29). Among soil textures, the mean volumetric moisture content was highest in massive organics (78 percent), intermediate in fines with organics (72 percent) and layered organics (68 percent), and lowest in massive sands (43 percent), layered fines (43 percent), and layered sands (40 percent). Among cryostructures, mean volumetric moisture content was highest for layered (77 percent), organic-matrix



Figure 25. Groundwater moving along the top of the permafrost or through wedge ice can create cavities in the wedge ice. Later freezing of the water in the cavities forms thermokarst cave ice (photos by M. Kanevskiy and T. Jorgenson).



Figure 26. The 52-m- (171-ft-) high Leffingwell Pingo near the Kadleroshilik River (photo by T. Jorgenson).

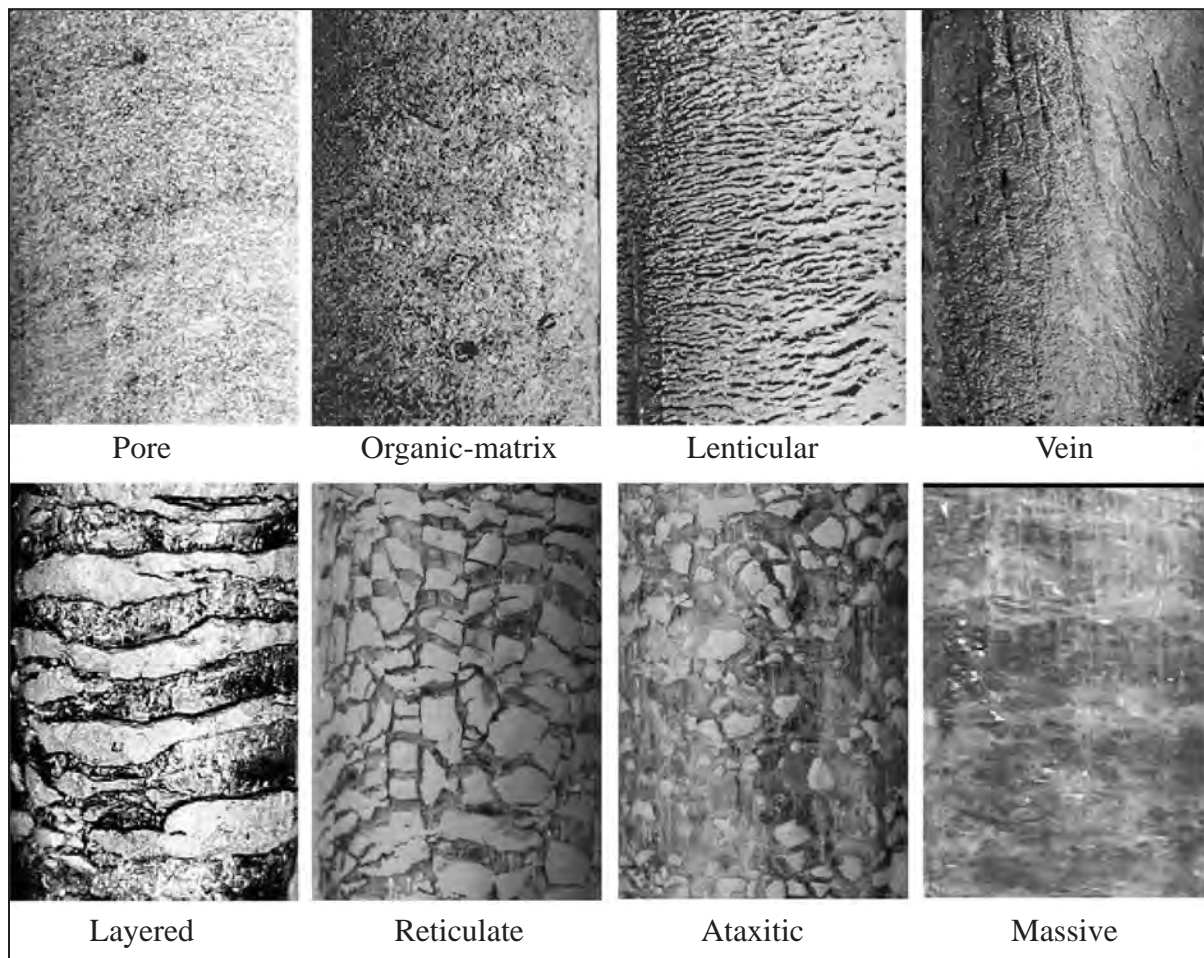


Figure 27. Main segregated ice structures typical for the coastal region of northern Alaska (photos by Y. Shur, T. Jorgenson, and M. Kanevskiy).

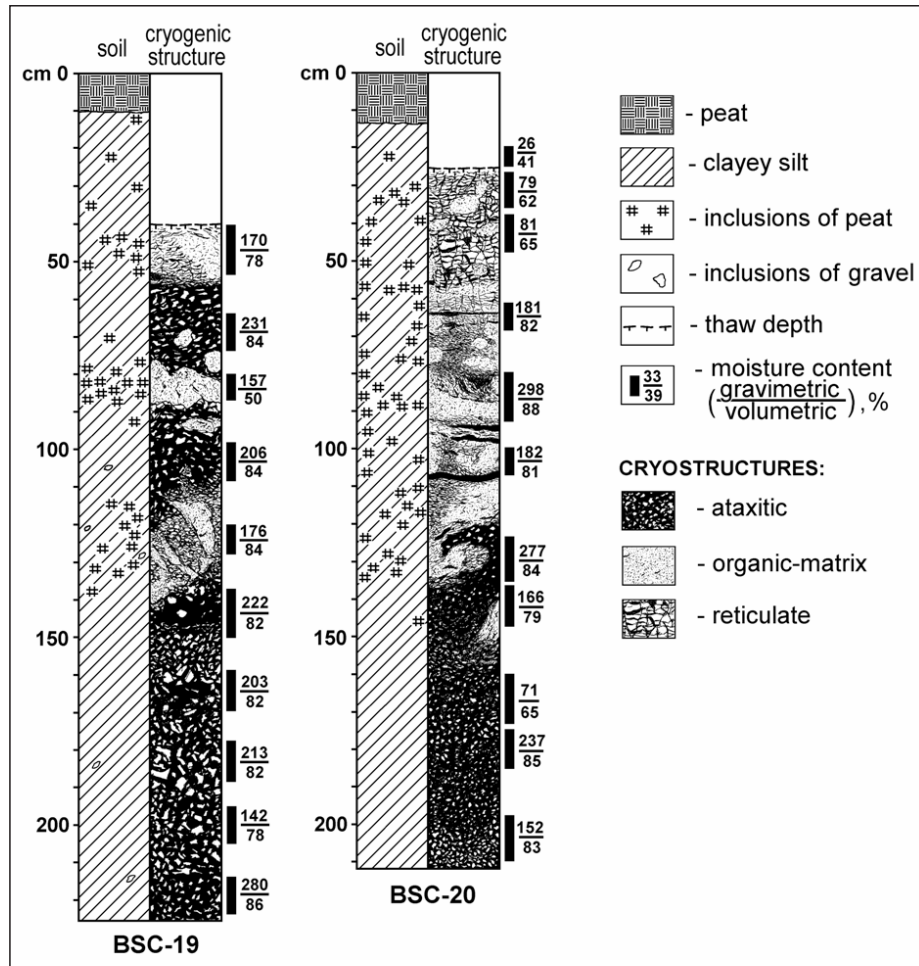


Figure 28. Cryogenic structures in glaciomarine sediments along Harrison Bay near Cape Halkett. The height of coastal bluffs is about 2.5 m (8 ft) (illustration by M. Kanevskiy).

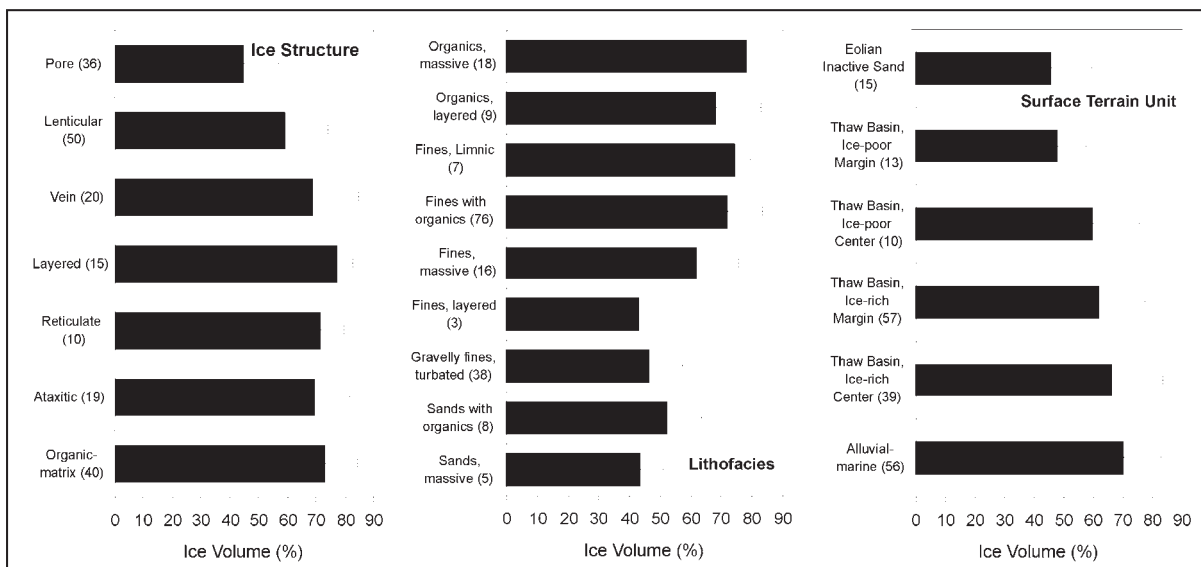


Figure 29. Volume of ground ice by ice structure, lithofacies, and terrain unit (Jorgenson and others, 2004).

(73 percent), reticulate (71 percent), ataxitic (70 percent), and veined (69 percent), and lowest for lenticular (59 percent) and pore (45 percent) cryostructures. Among terrain units, mean volumetric moisture content was highest in alluvial-marine deposits (71 percent) and ice-rich thaw basin centers (66 percent), intermediate in ice-rich thaw basin margins (62 percent) and ice-poor thaw basin centers (59 percent), and lowest in ice-poor thaw basin margins (48 percent) and eolian inactive sand (45 percent).

RESPONSE OF PERMAFROST TO CLIMATE CHANGE AND DISTURBANCE

Permafrost has responded to climatic change over millions of years, and most existing permafrost originated at the beginning of the Pleistocene 1.6 million years ago (Sumgin, 1927; Gold and Lachenbruch, 1973). The large increase in air temperature ($\sim 20^{\circ}\text{C}$ [$\sim 36^{\circ}\text{F}$]) at the Pleistocene–Holocene transition led to a considerable reduction in the permafrost regions. Evidence of permafrost south of the ice sheets is preserved in ice-wedge casts that have been found as far south as Iowa in North America and in middle Europe.

Permafrost is not connected directly to the atmosphere because its thermal regime is mediated by topography, surface water, groundwater movement, soil properties, vegetation, and snow. Surface water provides an important positive feedback that enhances degradation when water is impounded in sinking depressions. Groundwater in the active layer or in permafrost delivers heat and is typically surrounded by thawed zones. Soil texture affects soil moisture and thermal properties, such that gravelly soils tend to be well drained with deep active layers and organic soils tend to be poorly drained with shallow active layers. Vegetation has an important effect through the interception of solar radiation, growth of mosses and accumulation of organic matter, and interception of snow by shrubs. Snow protects soil from cooling in winter. Permafrost is greatly affected by these ecological components, therefore permafrost properties evolve along with the successional patterns of ecosystem development (Jorgenson and others, 1998). In turn, the patterns of ice aggradation and degradation influence the patterns of vegetation and soil development. This co-evolution of permafrost and ecological characteristics at the ground surface is most evident after disturbance, such as river channel migration, lake drainage, and fire (Shur and Jorgenson, 2007). This dependence of permafrost stability on both air temperatures and ecological factors greatly complicates the prediction of the consequences of climate change.

Thawing of ice-rich soils causes the surface to subside, creating depressions in the ground surface, termed thermokarst. The types of thermokarst and the ecological implications are extremely variable,

depending on climate, topography, soil texture, hydrology, and amounts and types of ground ice (Jorgenson and Osterkamp, 2005) (fig. 30). Thawing can proceed downward from expansion of the active layer, laterally from heat flow from surface and groundwater, internally from groundwater intrusion, and upward from thaw bulbs near surface water. Commonly observed patterns of permafrost degradation on the coastal plain include: (1) thermokarst lakes from lateral thermo-mechanical erosion; (2) thermokarst basins after lake drainage; (3) collapse blocks caused by the creation of thermo-erosional niches from water undercutting of ice-rich shores; (4) small, round, isolated thermokarst pits from surface thawing; (5) mixed thermokarst pits and polygons from initial ice-wedge degradation; (6) polygonal thermokarst troughs from advanced ice-wedge degradation; (7) thaw slumps and slides related to slope failure; (8) beaded streams; and (9) thermokarst gullies and water tracks from surface-water flow. Permafrost degradation resulting in these landforms nearly always involves positive feedbacks caused by dramatic thermal changes associated with surface or suprapermafrost groundwater movement. Thus, thermokarst can develop in both the discontinuous and continuous permafrost zones. Recent evidence demonstrates that ice wedges can melt even under cold-climate conditions, because the ice is located just below the active layer (figs. 31 and 32).

Thawing at the base of permafrost also can be a significant response. In particular, the thickness of Pleistocene-age permafrost was determined by the balance of the geothermal heat flux upward through the permafrost and heat losses from the surface during the earlier colder climate. With a constant heat input in the bottom and less heat lost out the top, permafrost can adjust to changes in climate, even cold climates, by thawing from the bottom.

Substantial effort has been made to model the effects of climate change on permafrost distribution. Site-specific models (Romanovsky and Osterkamp, 1997) demonstrate that changes in snow depth can be as important as warming temperatures. Landscape-level models that incorporate topography, vegetation, and soils have been developed that reasonably approximate permafrost distribution in the discontinuous zone, but have focused only on vertical heat transfer through soils and have ignored the lateral degradation of permafrost critical to many of the common types of thermokarst (Wright and others, 2003). Recent modeling efforts, however, have addressed the lateral degradation of permafrost near thaw lakes by coupling heat transfer with thaw subsidence (West and Plug, 2008). Index and climatically coupled numerical models have attempted to predict the changes in permafrost distribution in the northern hemisphere, based on regional climatic patterns. Of five models used to simulate permafrost changes, the



Figure 30. Photos of a variety of thermokarst landforms, including: (A) thermokarst lake, (B) collapse blocks undercut by thermoerosional niches, (C) thermokarst pit, (D) mixed pits and polygons, (E) polygonal trough network that creates high-centered polygons, (F) retrogressive thaw slump, (G) beaded stream, and (H) thermokarst gullies (photos by T. Jorgenson).

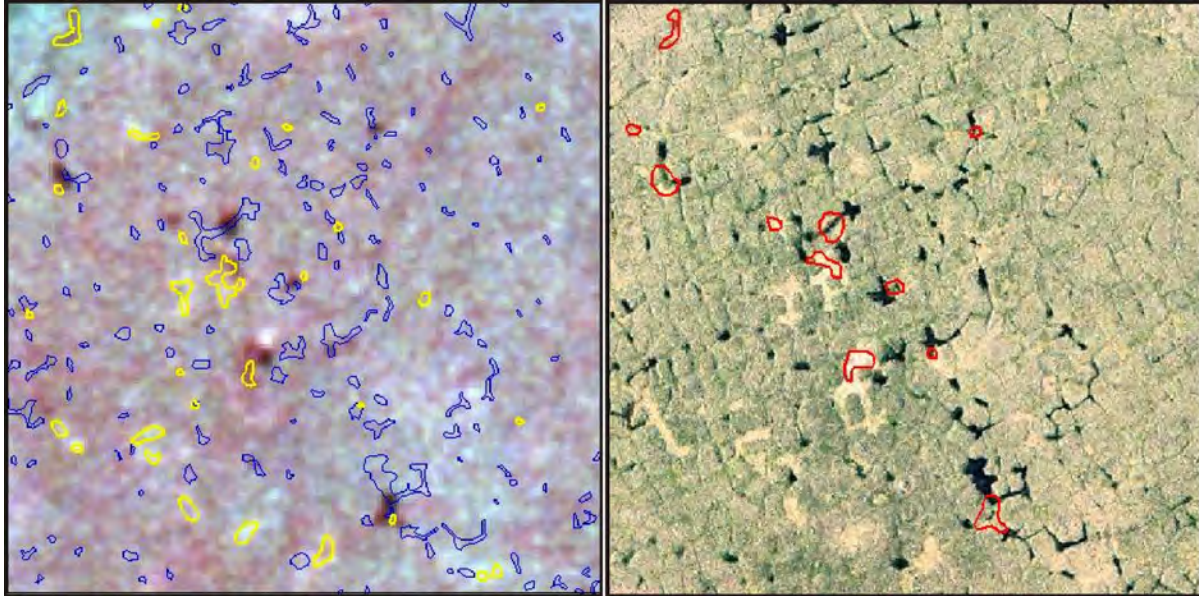


Figure 31. Airphotos from 1982 (left) and 2001 (right) showing extensive permafrost degradation over the period. Yellow lines represent thermokarst pits evident on a 1945 airphoto, red lines are pits evident in 1982, and blue lines are pits evident in 2001.

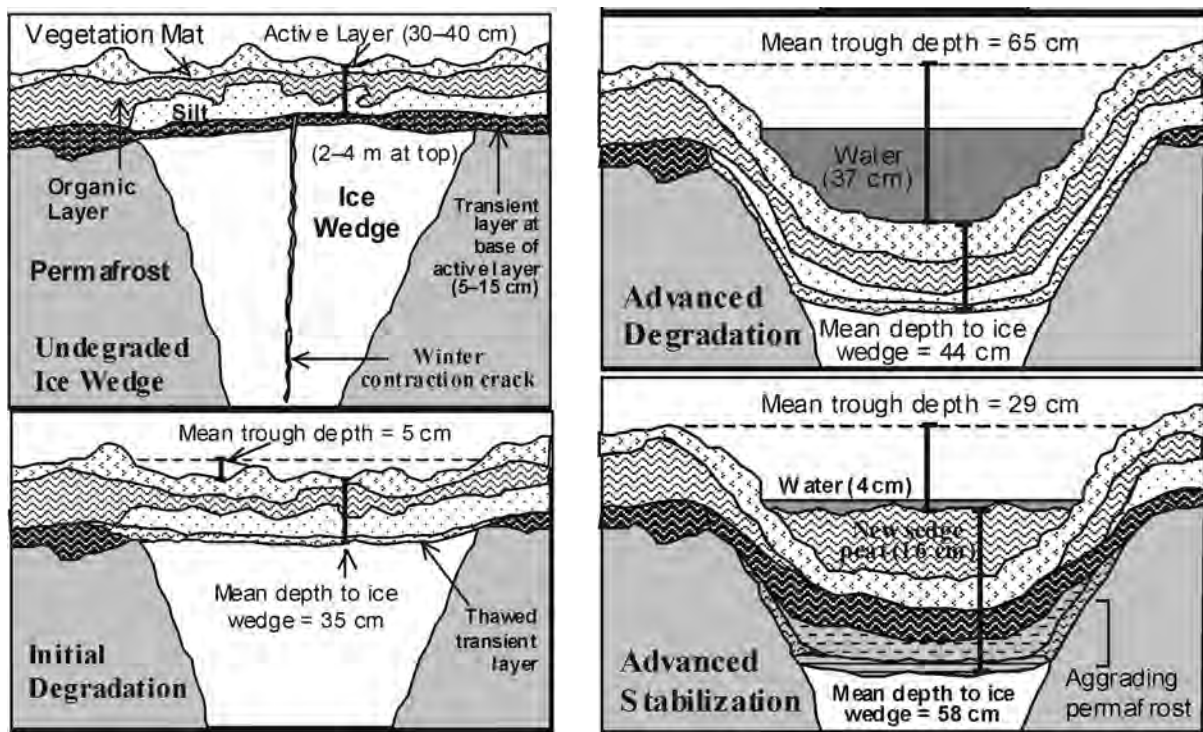


Figure 32. Diagram of the degradation and stabilization of ice wedges (from Jorgenson and others, 2006).

GFDL-R30_c model with intermediate results predicts the total extent of near-surface permafrost will decrease 23 percent by 2080 (ACIA, 2005).

Disturbance of vegetation and soil by human activity and wildfire are important factors contributing to localized permafrost degradation. Stripping vegetation by fire or human activities leads to an increase in the active layer and degradation of permafrost, which in many cases can be irreversible. Oil development, mining, and settlements have expanded rapidly since the beginning of the 20th century, causing localized degradation of permafrost (Brown and Grave, 1979). Fire, even in tundra regions, can have large effects

by eliminating the vegetation canopy and moss layer, removing a portion of the surface peat, and reducing the albedo (Racine, 1981; Racine and others, 2004). An immense wildfire spread near the Itkillik River in the foothills region in late summer of 2007 in response to very dry weather.

PATTERNED GROUND

One of the most striking features of the tundra of the coastal plain is the seemingly endless microtopographic variation of the ground surface (fig. 33). Although some microtopographic features, such as small dunes, ripples

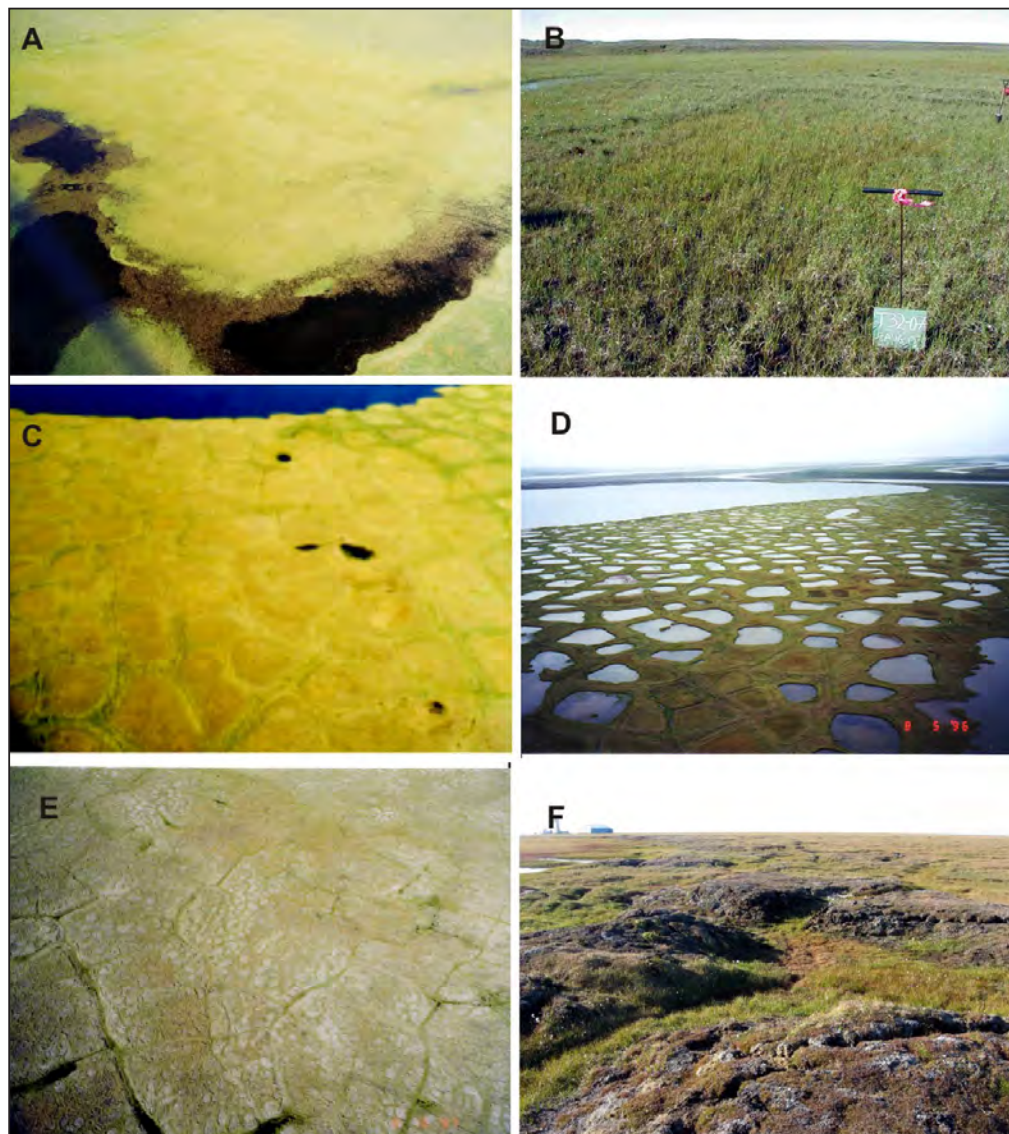


Figure 33. Ice aggradation and degradation in permafrost create a variety of surface patterns, including (A) nonpatterned ground, (B) disjunct polygon rims, (C) low-relief low-centered polygons, (D) high-relief low-centered polygons, (E) low-relief high-centered polygons with frost boils, and (F) high-relief high-centered polygons (photos by T. Jorgenson).

on riverbars, and streambanks result from erosional and depositional processes, the majority of features are caused by the aggradation and degradation of ground ice.

The aggradation of ground ice creates features such as hummocks, frost scars, ice-cored mounds, disjunct polygon rims, and low-centered polygons. In contrast, the degradation of ice, particularly wedge ice, creates features such as high-centered polygons, thermokarst gullies, collapse blocks, and beaded streams (fig. 30). Polygonal forms are by far the most common surface patterns, although frost scars also are widespread.

Frost boils (or frost scars) have been the subject of recent intensive studies because of their importance

to surface disturbance, nutrient cycling, carbon sequestration, and plant recruitment (Walker and others, 2004; Sutton and others, 2007; Kokelj and others, 2007). Peterson and Krantz (2003) provided a theoretical basis for differential frost heave as a triggering mechanism of patterned-ground formation. Recent analyses by Shur and others (2008), however, indicate that frost-boil formation also is dependent on frost cracking, differential vegetation colonization and peat accumulation, and ground-ice development (fig. 34). This scheme also shows the process of transformation of frost boils into earth hummocks.

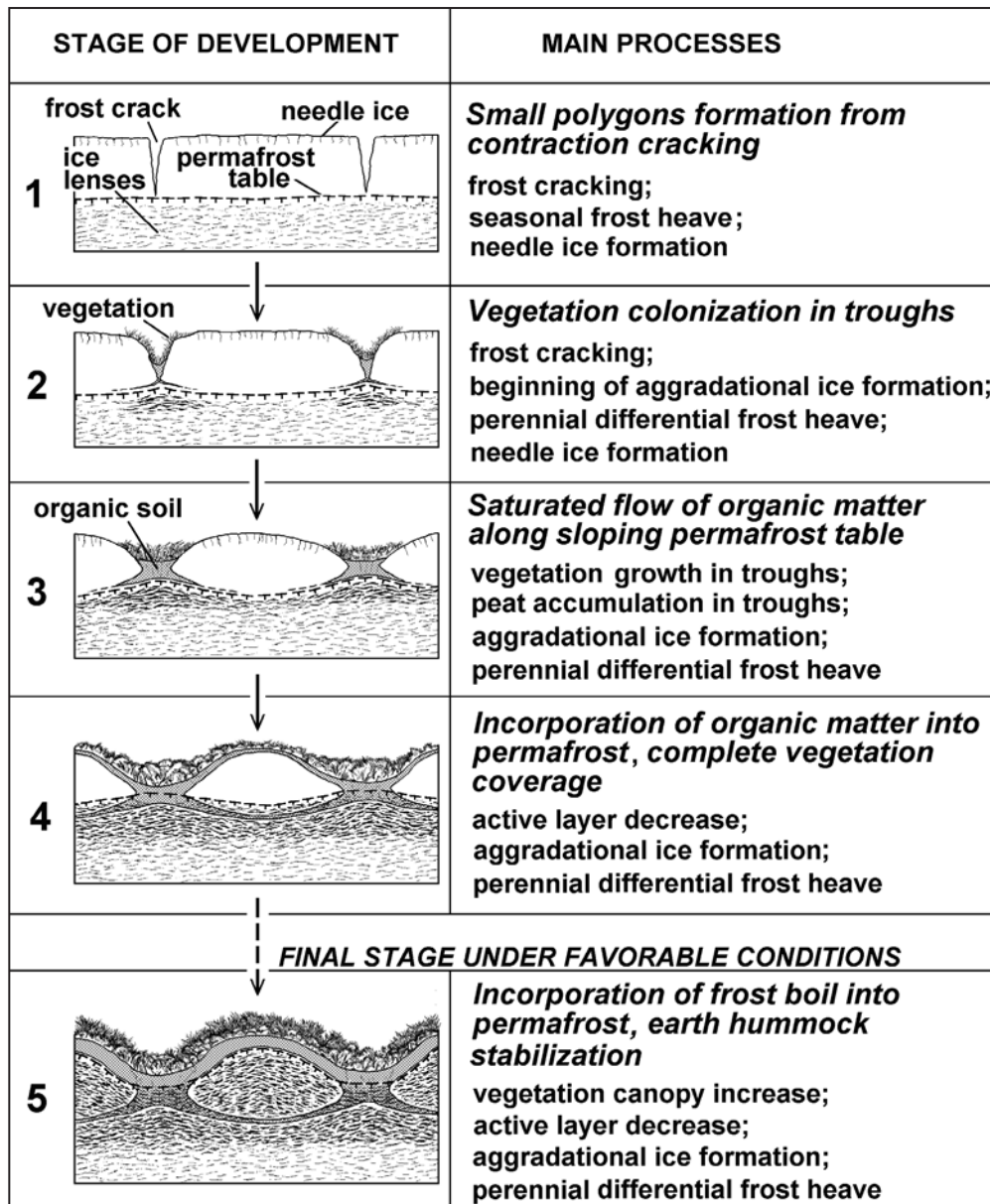


Figure 34. Successional stages in the formation of frost scars and earth hummocks (from Shur and others, 2008).

SOILS

Soils of northern Alaska are strongly influenced by permafrost with its low temperatures, impedance of drainage, freeze-thaw activity leading to cryoturbation, and ground ice aggradation. Early soil studies focused on soil description, classification, and terrain relationships (Tedrow and others, 1958; Drew and Tedrow, 1962; Holowaychuk and others, 1966; Brown, 1967, 1969; Tedrow, 1973). During the late 1970s and early 1980s, many studies were conducted under the International Tundra Biome studies (Everett and Parkinson, 1977; Everett, 1975, 1980; Everett and others, 1981; Everett and Brown, 1982) and under government and industry effort to assess environmental conditions in areas affected by oil development (Everett, 1980; Kreig and Reger, 1982; Walker and Everett, 1991; Walker and others, 1987). Several notable studies in the 1990s assessed soil–plant chemistry relations of divergent tundra ecosystems (Marion and others, 1989; Walker and others, 1998, 2003). More recent studies have focused on soil carbon and the potential consequences of climate change and coastal erosion (Bockheim and others, 1999; Ping and others, 1997, 2002; Michaelson and others, 1998; Hinkel and others, 2003a; Jorgenson and others, 2003a, 2005; Eisner and others, 2005).

Soil classification systems have evolved substantially over the years and in 1998 the U.S. soil taxonomy system added a new Gelisols order in recognition of the unique formative conditions created by permafrost (Kimble, 2004; Ahrens and others, 2004). The Gelisol order includes soils that have permafrost within 1 m (3.3 ft) of the surface or have permafrost within 2 m (6.6 ft) if cryoturbation features are present. The order was substantially revised in 2003 (Natural Resource Conservation Service [NRCS], 2003). Using the 1998 taxonomy, Jorgenson and others (2003c) documented a wide diversity of soil types, due in part to the sensitivity of the classification to small differences in organic depth, thaw depth, soil texture, moisture, and layering of horizons. The most common types in the eastern NPRA included Typic Aquorthel (11.5 percent of observations), whose wet, loamy soil lacks cryoturbation features, and Typic Historthel (8.6 percent), which is similar but has a 20–40 cm (8–16-in-) thick surface organic horizon. Typic Cryopsamment (8.0 percent) is a well-drained, sandy soil with an active layer greater than 1 m (>3.3 ft). Typic Aquiturbel (7.5 percent) is a wet, loamy soil, with evident cryoturbations. Typic Histoturbel (6.9 percent) is a wet, organic-rich soil with evident cryoturbation.

Soils are strongly correlated with microtopography (Ping and others, 2008). High-centered polygons are dominated by Ruptic Histoturbels (soil is broken by cryoturbation) and Typic Histoturbels are the main soil types, with Histic Aquiturbels and Glacic Histoturbels as minor components (fig. 35). Low-centered polygons

are dominated by Typic Histoturbels and Typic Historthels, with Glacic Historthels (underlain by massive ice below the active layer) as minor components. Nonpatterned areas in thaw lake basins are dominated by Typic Historthels and Glacic Aquorthels, with Ruptic Histoturbels and Glacistels as minor components. In deltas, Typic Aquorthels and Typic Historthels are the dominant soil types with Glacic and Sulfuric Historthels (saline soil with black mottling from sulfur reduction) as minor components.

The arctic tundra soils are known to accumulate and sequester organic carbon (Michaelson and others, 1996; Bockheim and others, 2003; Ping and others, 2008). In most soils of the coastal plain, cryoturbation is prevalent, except on young surfaces such as deltas, young lake basins, and floodplains. In deltas, organic carbon accumulates through burial by river sedimentation. Organic horizons only form after the establishment of sedge marsh vegetation. In drained-lake basins, organic carbon accumulates when marsh vegetation develops, followed by mixing and burial from bank erosion/collapsing and flooding. Once the lakes are drained and the land surface is raised due to ice-wedge formation, increased cryoturbation is evident, which churns the surface-organic matter down into the lower active layer and upper permafrost. Carbon accumulation was highest in the centers of polygons formed on ridges between the drained lakes due to increased surface age and cryoturbation. In exposed bluffs and lagoons, carbon accumulated and was sequestered through two main mechanisms. First, cryoturbation associated with patterned-ground formation churns surface-organic matter in the top 1 m (3.3 ft) (Bockheim and others, 1998; Ping and others, 1998, 2008). Second, growth of ice wedges deforms the surface organic matter downward as far as 3 m (10 ft) deep. Recent work indicates that organic carbon below 1 m (3.3 ft) is substantial and insufficiently accounted for in assessments of global carbon stocks (Jorgenson and others, 2003a, Bockheim and Hinkel, 2007; Ping and others, 2008).

VEGETATION

On the coastal plain and along the Beaufort Sea coast, vegetation patterns and productivity are affected by lacustrine processes and basin drainage, ice aggradation in basins to form older lowland ecosystems, fluvial processes along rivers, salinization and marine processes in coastal areas, and development of ecosystems on old, upland terrain surfaces. Vegetation, soil, and geomorphic components on the coastal plain have been studied extensively since the 1950s. Vegetation descriptions and plant inventories include those of Hanson (1953), Britton (1957), Spetzman (1959), Johnson and others, (1966), Wiggins (1962), Neiland and Hok (1975),

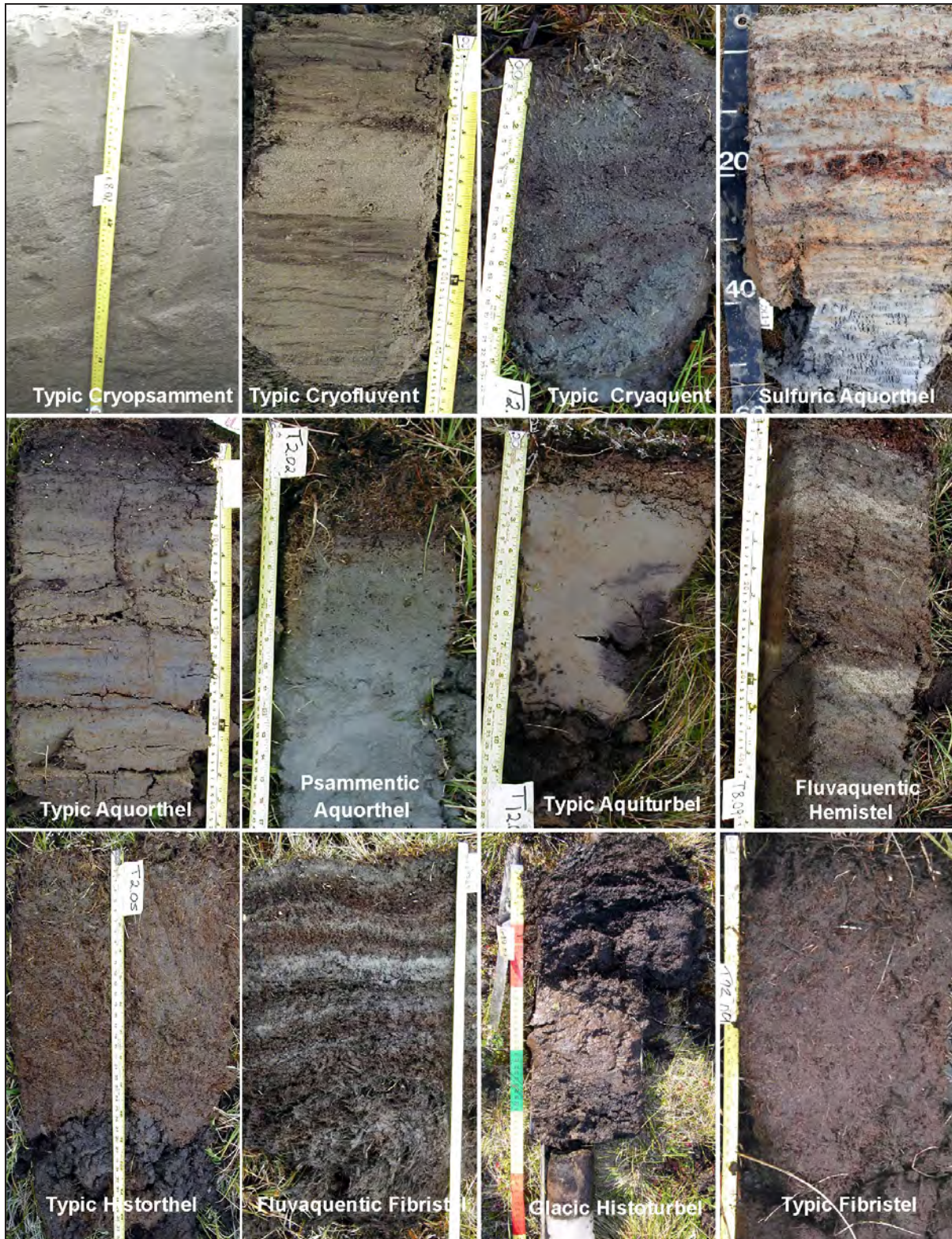


Figure 35. Photos of common soil types of the Beaufort Coastal Plain (photos by T. Jorgenson).

Brown and Berg (1980), Murray (1978), Webber (1978), Taylor (1981), Dunton and others (1982), Meyers (1985), and Walker (1985). Vegetation has been shown to be closely linked to soil and terrain patterns (Bliss and Cantlon, 1957; Cantlon, 1961; Tieszen, 1978; Peterson and Billings, 1978; Peterson and Billings, 1980; Walker and Webber, 1979; Walker, 1985; Walker and Everett, 1991; Walker and Walker, 1991; Walker and others, 2003; Jorgenson and others, 1996, 2003c). Mapping and remote sensing of plant communities and vegetation changes have been done by Webber and Walker (1975), Komarkova (1980), Walker and others (1980), Acevedo and others (1982), Walker and Acevedo (1987), Jorgenson and others (1994), Muller and others (1999), Ducks Unlimited (1998), Walker and others (2002, 2005), Jorgenson and Heiner (2003), Stow and others (2004), and Reynolds and others (2006). The most common local-scale ecosystems (ecotypes) and their associated plant composition recently mapped by Jorgenson and Heiner (2003) are described below (fig. 36).

Lowland lakes develop through a variety of processes, including: impoundment of water in low-lying basins; thermokarst of ice-rich sediments in old drained basins; and reconfiguration of small, shallow waterbodies by ice aggradation and organic-matter

accumulation in the margins of old basins (Jorgenson and others, 2006). Breaching and drainage of large, deep lakes creates lacustrine moist barrens, depending on how much of the basin is drained (fig. 33). Lacustrine wet sedge and moist sedge–shrub meadows develop on the newly exposed areas and usually are dominated by *Carex aquatilis*, *Eriophorum angustifolium*, *Salix ovalifolia*, and *Dryas integrifolia*, depending on drainage conditions. Lowland wet sedge meadows evolve from lacustrine wet sedge meadows in the basins after ice aggradation causes development of polygonal rims, raises the ground surface, and isolates the terrain from the effects of water in lakes. This wet, late-successional ecosystem is dominated by *Carex aquatilis* and *Eriophorum angustifolium*; other species include *C. saxatilis*, *C. chordorrhiza*, *E. russeolum*, *Salix planifolia pulchra*, and the mosses *Limprichtia revolvens*, *Aulacomnium palustre*, and *Scorpidium scorpioides*.

Upland ecosystems typically are associated with older, higher geomorphic units, such as old alluvial terraces, alluvial–marine deposits, and eolian inactive sand deposits that surround basins that stabilized during the mid Holocene. The surfaces have been modified only slightly by slope processes, organic accumulation, ice aggradation, accumulation of thin eolian silt, and minor thermokarst. Upland dry dwarf shrub,

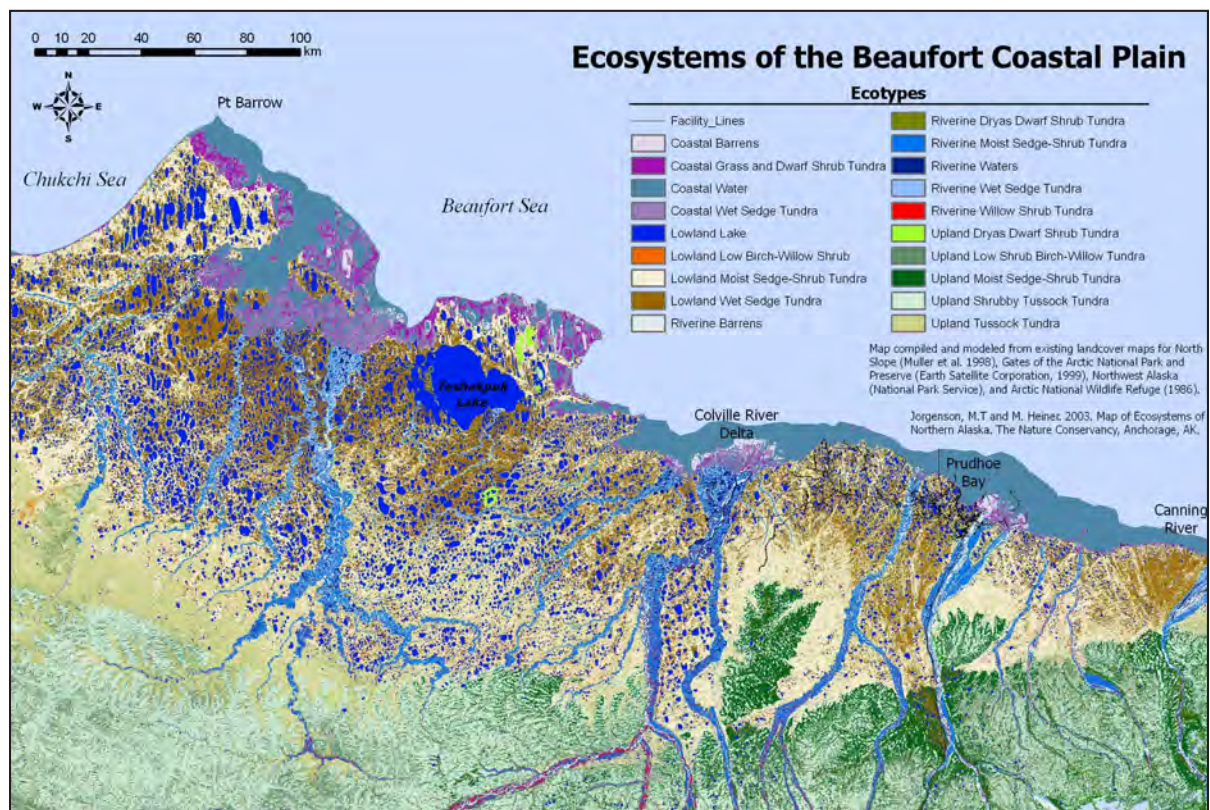


Figure 36. Map of ecotypes in the central–western Alaska Beaufort Coastal Plain (from Jorgenson and Heiner, 2003).

which occurs on windswept, well-drained upper slopes and ridges, has vegetation dominated by the dwarf evergreen shrub *Dryas integrifolia*, *Salix reticulata*, *Salix glauca*, *Arctostaphylos alpina*, *Arctagrostis latifolia*, and lichens (fig. 36). Upland moist low willow shrub, which occurs on well-drained, protected slopes has vegetation dominated by the low shrub *Salix glauca* (occasionally *Betula nana*), along with *Dryas integrifolia*, *Salix lanata richardsonii*, *Arctostaphylos rubra*, and mosses. Upland moist cassiope dwarf shrub, which occurs on moist broad ridges of old sand dunes, pingos, and the banks of drained-lake basins, has vegetation dominated by the dwarf shrub *Cassiope tetragona* and includes *Dryas integrifolia*, *Salix phlebophylla*, *Vaccinium vitis-idaea*, *Carex bigelowii*, *Arctagrostis latifolia*, *Hierochloa alpina*, *Pyrola grandiflora*, and *Saussurea angustifolia*. Upland moist tussock meadow, which occurs on gentle slopes and ridges on old terrain surfaces and ice-rich centers of drained-lake basins, has vegetation dominated by the tussock-forming sedge *Eriophorum vaginatum*. On acidic sites other plants include *Ledum decumbens*, *Betula nana*, *Salix planifolia pulchra*, *Cassiope tetragona* and *Vaccinium vitis-idaea*, and circumneutral sites usually include *Dryas integrifolia*, *Salix reticulata*, *Carex bigelowii*, and lichens and mosses. Upland dry barrens, which occur on eolian active sand and landslide deposits, have early colonizing species such as *Salix alaxensis*, *Festuca rubra*, and *Chrysanthemum bipinnatum*. The abundant ice wedges in old terrain surfaces are highly susceptible to thermokarst, forming areas of thermokarst pits and high-centered polygons, but on much of the coastal plain ice volumes are not sufficient to initiate thermokarst lakes.

Riverine areas are dominated by fluvial processes, although eolian and ice-aggradation processes also contribute to ecological development. Riverine moist barrens occur along the margins of active channels and along delta fringes, are subject to frequent flooding and sedimentation, and have scattered colonizers, such as *Deschampsia caespitosa*, *Chrysanthemum bipinnatum*, and *Salix alaxensis* (fig. 37). Riverine moist tall willow shrub occurs as narrow strips slightly higher on the floodplain, is subject to less flooding and sedimentation, has well-drained soils, and is dominated by *Salix alaxensis*, *Chrysanthemum bipinnatum*, *Bromus pumpellianus*, *Equisetum arvense*, and legumes. Riverine moist low willow shrub slowly replaces the tall willows as soils become seasonally saturated and *Salix lanata richardsonii*, *S. reticulata*, and *Equisetum variegatum* become dominant. On well-drained sandy or gravelly floodplains, riverine dry dryas dwarf shrub can develop and is dominated by *Dryas integrifolia*. Riverine wet sedge meadows, which occur on still higher, inactive floodplains, are characterized by saturated soils with interbedded mineral and organic sediments resulting

from occasional sedimentation and are dominated by *Carex aquatilis*, *Eriophorum angustifolium*, and *S. lanata richardsonii*. Lowland wet sedge meadows occur on abandoned floodplains that represent the oldest portions of the landscape. This ecosystem type has saturated soils underlain by extremely ice-rich permafrost that has contributed to elevating the floodplain surface and is dominated by plants similar to those on Riverine wet sedge meadows, but includes more *Dryas integrifolia* and other dwarf shrubs. At this stage, ice contents are sufficiently high that permafrost becomes susceptible to thermokarst and subsequent development of deep riverine lakes. Finally, eolian sand is frequently deposited in large dunes downwind of large, barren sandbars, contributing to the development of upland dry barrens, upland dry tall willow shrub, and upland dry dryas dwarf shrub (fig. 38).

Coastal ecosystems are salt-affected ecosystems that respond to differences in salt concentration, soil moisture and aeration, and sedimentation (Meyers, 1985; Jorgenson and others, 1997c). Coastal barrens are barren or partially vegetated (<30 percent cover) areas on active tidal-flat and delta-channel deposits where frequent sedimentation restricts vegetation establishment (fig. 36). Slightly brackish barrens with well-drained soils are colonized by *Deschampsia caespitosa*, *Equisetum arvense*, *Salix alaxensis*, and *Stellaria humifusa*, and more saline sites are dominated by *Elymus arenarius mollis*, *Stellaria humifusa*, and *Salix ovalifolia*. Coastal saline wet meadows are found on active and inactive tidal flats and have vegetation dominated by *Puccinellia phryganodes*, *Carex subspathacea*, *Carex ursina*, and *Stellaria humifusa*. Coastal brackish wet meadows predominantly occur on inactive tidal flats and have vegetation dominated by *Carex subspathacea*, *Dupontia fisheri*, *Salix ovalifolia*, with *Puccinellia phryganodes*, *Carex ursina*, and *Calamagrostis deschampsoides* as occasional associates. Coastal salt-killed wet meadows are barren or partially vegetated (<30 percent cover) areas where saltwater intrusions from storm surges have killed the original vegetation and salt-tolerant plants are actively colonizing. Common colonizing plants include *Puccinellia phryganodes*, *Stellaria humifusa*, *Cochlearia officinalis*, and *Salix ovalifolia*. Coastal moist willow dwarf shrub is found on moderately well drained, active and inactive tidal flats and has vegetation dominated by the dwarf willow *Salix ovalifolia*, along with *Calamagrostis deschampsoides*, *Elymus arenarius*, and *Carex subspathacea*. Coastal dry elymus meadows are found on well drained active tidal flats, delta active channel deposits, and sand dunes and are characterized by the presence of *Elymus arenarius mollis*, *Salix ovalifolia*, *Sedum rosea*, *Stellaria humifusa*, and *Deschampsia caespitosa*.



Figure 37. Photographs of lowland, lacustrine, and coastal ecosystems of the Beaufort Coastal Plain (photos by T. Jorgenson and J. Roth).

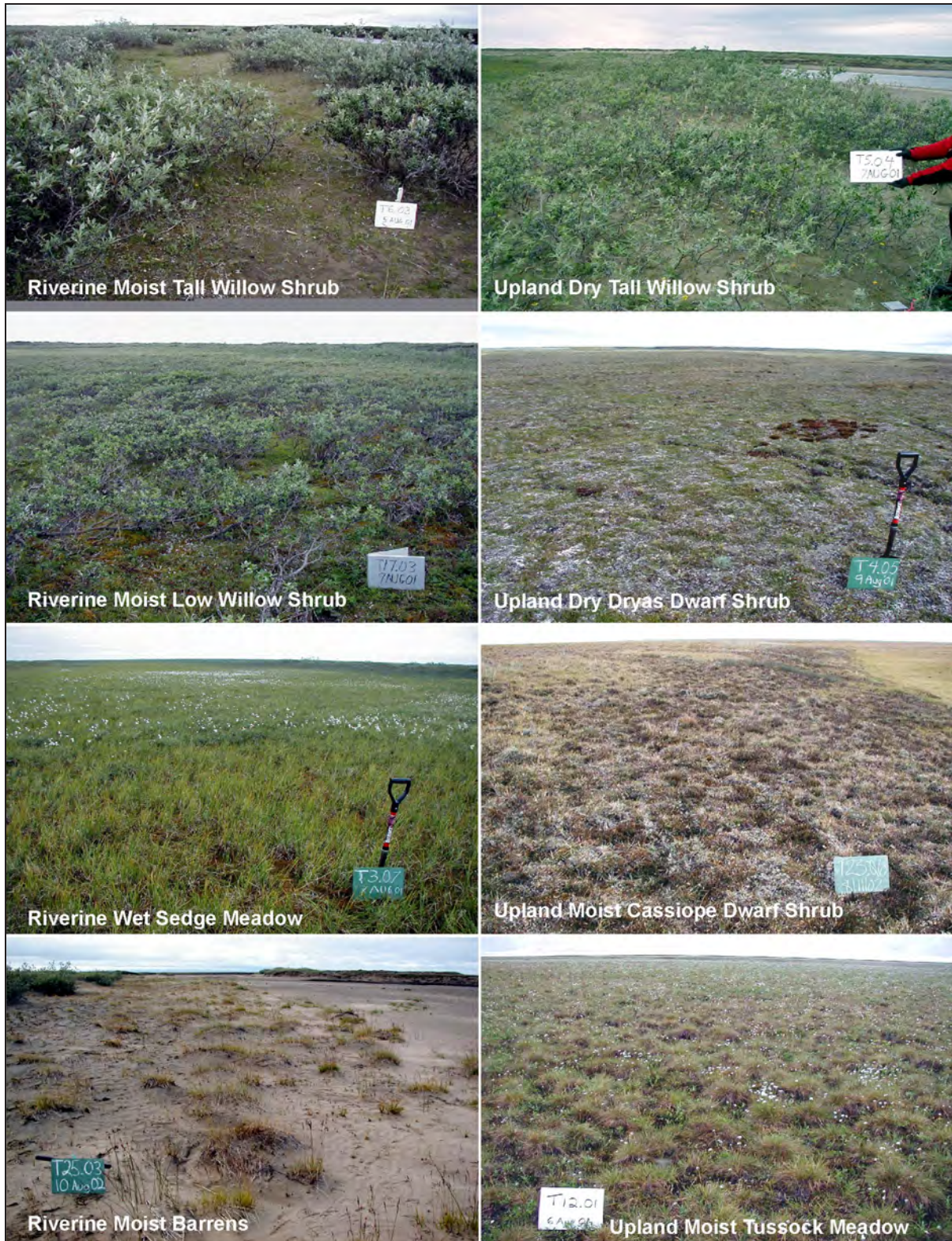


Figure 38. Photographs of riverine and upland ecosystems of the Beaufort Coastal Plain (photos by T. Jorgenson and J. Roth).

OCEANOGRAPHY AND SEA ICE

The mean annual sea level at Prudhoe Bay, the only water-level recording station along the Alaska Beaufort Sea coast has risen at 3.1 mm (0.12 in) per year over the last decade (NOAA data). This is slightly higher than the long-term, global mean sea level rise of 2.5 mm (.10 in) per year during the last 20 years (ACIA, 2005). Mean monthly water levels during the late summer, however, generally are 0.4 m (1.3 ft) higher than in winter due to frequent build-up of wind-driven water during the open-ice period (fig. 39). The daily tidal range is only 0.2 m (0.7 ft).

From a longer-term perspective, sea levels have changed radically between glacial and interglacial events, and thus have greatly affected coastal evolution. During the last glacial maximum (20 ka BP), sea level dropped by ~120 m (~390 ft), exposing the entire continental shelf (ACIA, 2005). During this time, a glacial ice shelf likely covered the Chukchi Borderland, effectively halting marine processes (Polyak and others, 2001). By ~15 ka BP the sea began to rise rapidly until 6 ka

BP and water inundated most of the continental shelf. During this time, the Arctic Ocean was reconnected to the Pacific Ocean and the locations of river deltas shifted rapidly inland. By 6 ka BP, sea levels stabilized within 2–3 m (7–10 ft) of their current level with only minor fluctuations since then (Mason and Jordan, 2001). The current Colville Delta was initiated around 4 ka BP (Jorgenson and others, 1998). The slowly rising sea level during this interval also differentially eroded the coast, leaving remnants of the original tundra surface as islands (Barnes and others, 1977; Naidu and others, 1984; Reimnitz and others, 1988).

Storm surges caused by high wind events can accelerate erosion, inundate low-lying tundra areas, and damage village facilities. Heights of storm surges are a function of wind stress and direction, water depth, and coastal morphology and thus can be highly variable along the coast (Henry and Heaps, 1976). The most notable storm surges were those of 1954, 1963, 1970, 1986, and 2000. The 1954 storm had a surge of ~3 m (~10 ft) at Barrow (Hume and Schalk, 1967). The 1963 storm at Barrow (fig. 40), which was the largest event

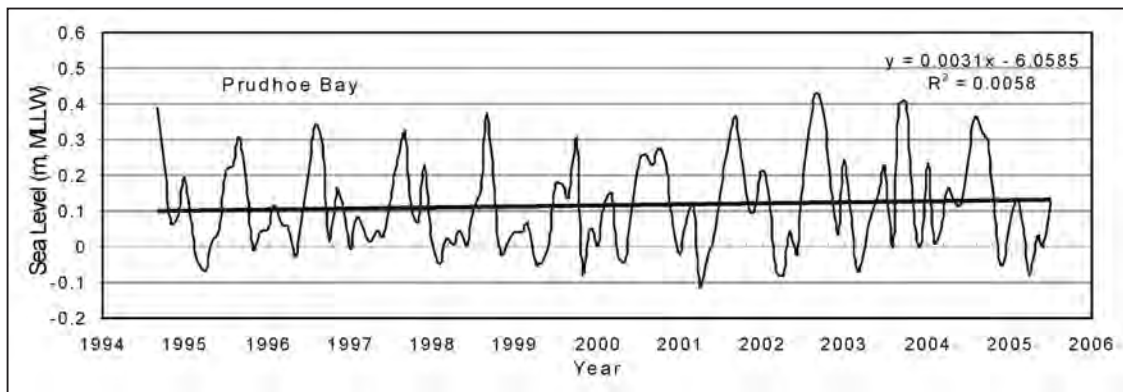


Figure 39. Mean monthly sea level at Prudhoe Bay, 1994–2006, showing an average increase of 3.1 mm/yr (NOAA data).



Figure 40. Flooding at Barrow caused by large storm surges in October 1963 (photo by G. Penning) and October 2002.

ever observed by long-term residents, had nearshore wave heights of 4–5 m (10–16 ft) and a surge height of 3.5 m (11.5 ft), and caused extensive damage to houses and roads (Reimnitz and Maurer, 1979; Lynch and others, 2003). The 1970 storm along the eastern Beaufort Sea coast had deep-water wave heights up to 9 m (30 ft), caused extensive flooding of low areas and left a driftline at a maximum height of 3.5 m (11.5 ft) in the Colville River delta, which was 0.5 m (1.6 ft) higher than that left by the 1963 storm (Reimnitz and Maurer 1979). The 1986 storm had a surge height of ~2 m (6.5 ft) and caused substantial erosion of the gravel beach at Barrow and flooded the runway at Kaktovik (Ahmaogak, 2004). The 2000 storm, which had deep-water wave heights of ~6 m (20 ft) and a surge height of ~3.5 m (~12 ft), destroyed low roads and homes at Barrow (Lynch and others, 2003), overtopped the runway, and damaged a protected landfill at Kaktovik, according to local observations. Another larger storm occurred soon after in 2002 (fig. 40).

Increased fetch resulting from sea-ice retreat can significantly increase wave heights. For example, for a storm that has average wind speeds of 15 m/s (49 ft/s) over a 24-hr period, an increase of the fetch from 160 km to 510 km (100 to 320 mi) potentially could increase wave height 25 percent, from 4.3 m (14.1 ft) to 5.5 m (18 ft). With the exception of the 2000 storm, the storms most notable for large surges (1954, 1963, 1986, and 2000) were fall storms when the ice retreat neared its maximum extent.

Sea ice dominates the nearshore environment for a 9-month period; it starts retreating from the coast in mid to late July, reaches a maximum during late September, and usually freezes back to shore by late

October (fig. 41). During the winter, the ice forms a gradient of energy, movement, salinity, and thickness that is classified into three zones: pack ice, floating-fast ice, and bottom-fast ice. Of particular concern for coastal ecosystems and local villages is the consistent retreat of sea ice during the summer since the 1950s. From 1979 to 2005, the minimum extent of summer sea ice has decreased by 30 percent (Fetterer and Knowles, 2004). The record retreat of sea ice in 2007 (fig. 41), has greatly heightened concern about an ice-free Arctic Ocean during the summer in the future (Stoeve and others, 2007). Previous record minimal extents for the entire Arctic Ocean were recorded in 2002 (Serreze and others, 2003) and again in 2005 (National Snow and Ice Data Center [NSIDC], 2005), although for the Beaufort Sea coast maximal retreats occurred in 2002 and 2004. In 2002, open water extended out 510 km (320 mi) at Barrow and 320 km (200 mi) at Barter Island, compared to the long-term averages of 160 km (100 mi) and 190 km (120 mi), respectively. Sea ice also is an important agent for scouring and redistributing sediments and carbon in the nearshore zone (Reimnitz and Barnes, 1974).

COASTAL DYNAMICS

COASTLINE TYPES

The near-shore Beaufort Sea is ice covered most of the year with generally open water from mid-July to mid-October. By early September, sea ice retreats northward to 300–500 km (185–310 mi) offshore near Barrow and 100–300 km (60–185 mi) offshore at Barter Island. During the open-water season, tides are on the order of 15 cm (5.9 in). Wind-driven waves during large storm events, however, can raise water levels as much as

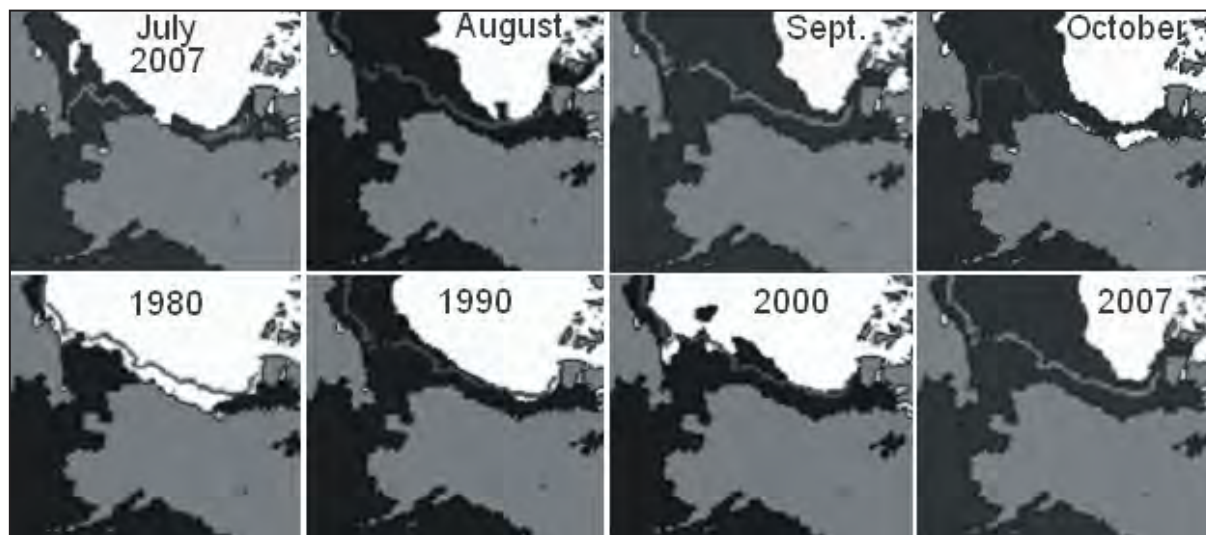


Figure 41. Extent of sea ice during summer months of 2007 (top row) compared to fall minimum extents in 1980, 1990, 2000, and 2007 (data courtesy of National Snow and Ice Data Center).

2 m (6.6 ft), inundate low tundra for several kilometers inland, and increase erosion (Reimnitz and Maurer, 1979; Kowalik, 1984). These environmental parameters strongly influence erosion by creating sea ice and limiting the open-water period, and by the occurrence of strong winds when the extent of open water is greatest. In addition to the effects of environmental forcing factors, the type and configuration of the shoreline has a major influence on coastal erosion (Barnes and others, 1988).

Recent mapping of the mainland coast of the Alaskan Beaufort Sea subdivided the coast into 48 landscape-level segments totaling 1,957 km (1,216 mi), with an additional 1,334 km (829 mi) of spits and islands (Jorgenson and Brown, 2005) (fig. 42). At this regional scale, mainland coasts were grouped into five broad classes: exposed bluffs (313 km [194 mi]), lagoons with barrier islands (546 km [339 mi]), bays and inlets (235 km [146 mi]), tapped basins (171 km [106 mi]), and deltas (691 km [429 mi]).

Exposed bluffs are present primarily in the western and eastern study area (fig. 43). Bank heights typically are 2–4 m (6.6–13.1 ft) and lithology varies from very

ice-rich, predominantly reworked marine silt along the western coast (Segment 1—Elson Lagoon to 15—Cape Halkett East Coast), to ice-poor sands in eolian deposits along the central coast (19—Fish Creek coast), to moderately ice-rich pebbly silty sand (Beechey sands according to Rawlinson, 1993) along the central to eastern coast (22—Oliktok coast to 47—Demarcation Bay). Ice wedges are estimated to occupy ~20 percent by volume of the upper permafrost in the higher, early Holocene to late Pleistocene deposits. Exposed bluffs have the highest mean annual erosion rates across all segments (2.4 m/yr [7.9 ft/yr]), the highest rates for any segment (8.3 m/yr [27.2 ft/yr] at 11—Drew Point Coast), and highest rate for any individual point (16.7 m/yr [54.8 ft/yr] at segment 14—Cape Halkett North Coast) on this coastal type. Low peaty shorelines with underlying lacustrine sediments occur where lakes have been drained by erosion of the bluff.

Deep bays and inlets (segment 2—Dease Inlet Coast West, fig. 42) are most common in the western coast, which is composed of ice-rich marine silt. These features typically formed from coalescence of large lakes that

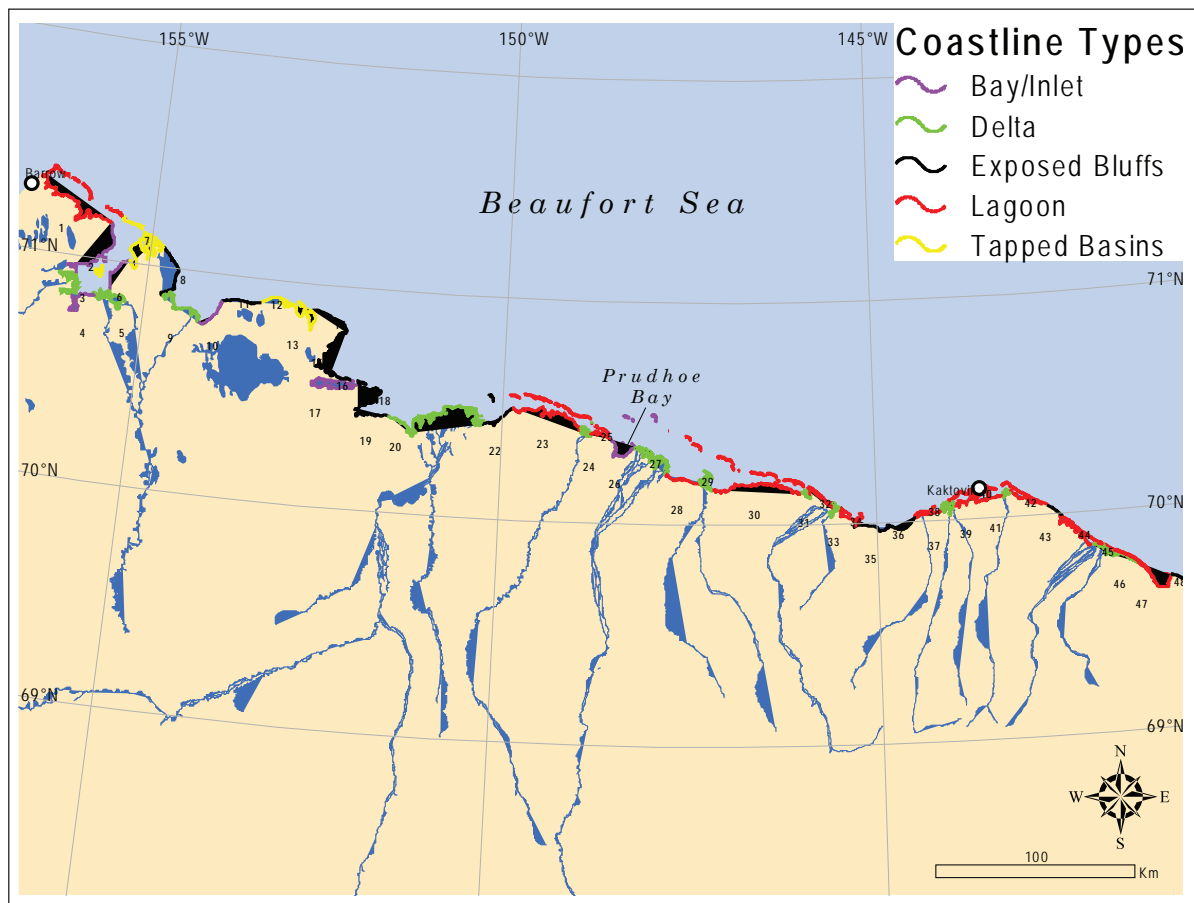


Figure 42. Map of coastline types (Jorgenson and Brown, 2005).



Figure 43. Photos of differing shoreline profiles (clockwise from upper left): Sloping high bank faced by a gravel beach at Beaufort Lagoon; moderately high bank with peat chunks blanketing beach along Elson Lagoon; tidal flats on the Colville River Delta; and an exposed high bank with collapsing blocks near Cape Halkett (photos by T. Jorgenson).

have been breached and flooded by seawater or from flooding of old floodplains during mid-late Holocene sea level rise. Bank heights generally are 2–3 m (7–10 ft) and ice-wedge volumes are assumed to be similar to those described for exposed bluffs. The mean annual erosion rate (2.0 m/yr [6.6 ft/yr]) for this coastal type is slightly less than that for exposed bluffs, presumably because of the longer fetch distance across the large bays.

Tapped basins are situated in extremely ice-rich marine silts found in the western portion of the area (segments 7—Tangent Point Coast to 13—Pogik Bay Coast, fig. 42). Thaw lakes in this area are unusually large, due to the low relief (Sellmann and others, 1975), and are occasionally breached by the sea as erosion proceeds landward. Observations are only available for small segments along the outer coast, thus little is known about erosion rates along the majority of the shoreline comprising inland tapped lakes. Ice-wedge volume averages 10 percent, although ice volumes probably are highly variable from <1 percent in recently tapped basins

to 20 percent in the older, higher surfaces (Jorgenson and Brown, 2005). Because of limited observations, estimates of erosion rates (1.7 m [5.6 ft] per year) are relatively unreliable for this shoreline type.

Lagoons with barrier islands are prevalent along the coast, and the mainland bluffs in the lagoons are similar to those described for exposed bluffs. The lagoons are bordered seaward by barrier islands and spits that protect lagoons and bluffs from high, storm-generated waves. Most barrier islands are sandy and some are gravelly. Lagoons generally have water depths of 2–4 m (7–13 ft), which reduce wave heights (fig. 44). Mean annual erosion rates (0.7 m/yr [2.3 ft/yr]) for this coastal type are the lowest for any type, except deltas.

Large and small deltas are found across the entire coast, with the Colville River Delta being the largest and best studied (Naidu and Mowatt, 1975; Walker, 1976; Jorgenson and others, 1997c). Localized sediment accumulation can be rapid (10 cm [3.9 in] or more) after large breakup or precipitation events (Walker,

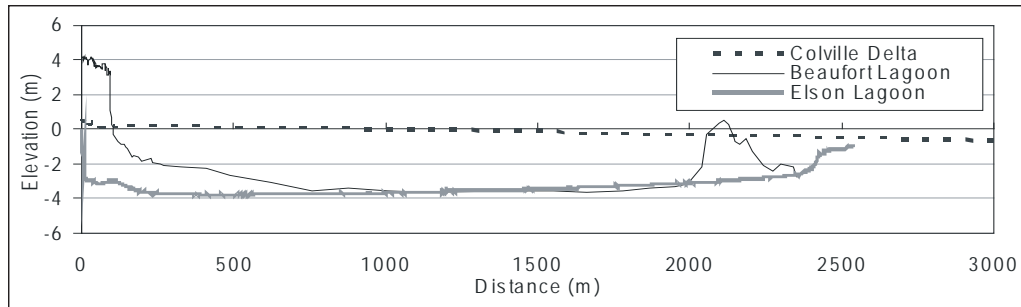


Figure 44. Representative nearshore bathymetry of the Colville Delta, Beaufort Lagoon, and Elson Lagoon along the Beaufort Sea coast.

1976). During spring breakup much of the sediment is deposited on land-fast ice and carried offshore by dispersing ice floes. Shoreline slopes are very gentle in deltaic environments with the ground elevation near mean sea level at the water's edge and gently rising to 0.5 to 1 m (1.6–3.3 ft) over a distance of several kilometers (fig. 44). Because deltas are formed by a network of distributaries, the total length of shoreline can be large. Ice contents and carbon contents are low due to the rapid accumulation of sediments. Although sedimentation and erosion are difficult to estimate for complex delta environments, Naidu and others (1999) estimated sedimentation rates of 1 kg/m^2 (0.2 lb/ft^2) for nearshore areas off the Colville River Delta.

COASTAL EROSION

Coastal erosion is the result of two main processes, mechanical erosion and thermal denudation (together often termed 'thermal erosion'), that can have either positive or negative feedbacks. During mechanical erosion, the dominant process, water removes unfrozen soil accumulated at the cliff, exposes the frozen soil, and occasionally creates erosion. Thermal denudation occurs through melting of ground ice and ice-rich soil, and subsequent gravitational removal of thawed material to the base of the cliff (Are, 1988; Shur and others, 2002).

Along the coast, mechanical erosion by waves is the governing process because cliffs are mostly 1–3 m (3–10 ft) high. At such cliffs, thermal denudation results in the accumulation of thawed material on the lower part of the cliff, while the upper part is protected by layers of peat and vegetation that remain attached to the surface. This accumulation of soil and peat on the cliff greatly reduces the rate of thermal denudation. During big storms, however, this protection is quickly removed, exposing permafrost to thawing; waves can cut deep niches at the base of a cliff, and big blocks of the shore can fall to the beach (fig. 30). Under

these conditions, one storm can cause several meters of shoreline erosion. Once the permafrost is exposed during a storm, the frozen ground is fairly resistant to mechanical erosion, limiting the effect of big storms. Given these various modes of erosion, a stretch of the shore can remain stable for a long time and then retreat rapidly in a year or two.

Using a coastal segmentation and classification approach to account for spatial variations, mineral sediment and organic carbon input from coastal erosion was estimated by Jorgenson and Brown (2005) to be $2,743 \text{ Mg/km/yr}$ [$4,867 \text{ tons/mi/yr}$] across the 1,957-km- (1,216-mi-) long mainland coast, which is less than half of the value ($6,600 \text{ Mg/km/yr}$ [$11,682 \text{ tons/mi/yr}$]) reported by Reimnitz and others (1988) for a 344 km (214 mi) section of rapidly eroding coast from Drew Point to Prudhoe Bay. Over the entire Alaska Beaufort Sea coast, mineral sediment input was estimated to be $3.3 \times 10^6 \text{ Mg/yr}$ [$3.6 \times 10^6 \text{ tons/yr}$]. Based on these limited data on soil organic carbon (Ping and others, 1997, 2002; Hinkel and others, 2003a; Bockheim and others, 2003), Jorgenson and Brown (2005) estimated soil organic carbon input to the Alaska Beaufort Sea averages 149 Mg/km/yr [264 tons/mi/yr] and totals $1.8 \times 10^5 \text{ Mg/yr}$ [$2.0 \times 10^5 \text{ tons/yr}$] over the entire coast. Erosion rates were found to be affected by both coastline type and soil texture (fig. 45) (Jorgenson and Brown, 2005).

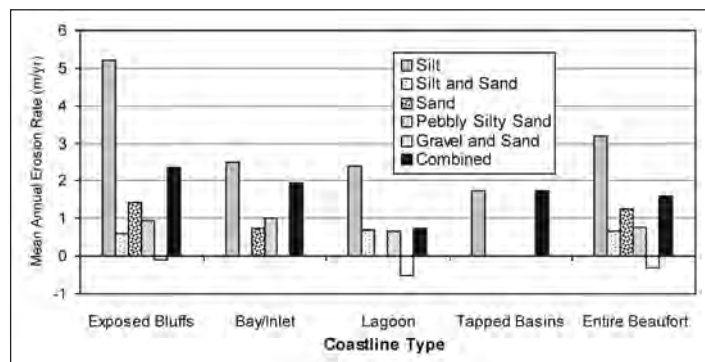


Figure 45. Erosion rates in relation to coastline type and shoreline soil texture (Jorgenson and Brown, 2005).

This page was intentionally left blank.

PART 2: OIL DEVELOPMENT

by Torre Jorgenson¹ and Caryn Rea²

HISTORY OF OIL DEVELOPMENT

There has been a long history of interest in the occurrence of oil on the Beaufort Coastal Plain beginning with the local Inupiat people and, later, western explorers. Surface oil was first reported by the English explorer T. Simpson in 1839 and later by U.S. Navy Lieutenant W.L. Howard in 1886. In 1901, W. J. Peters and F. C. Schraeder, both veteran Alaska geologists, mapped much of the western coastal area. Between 1906 and 1914 Leffingwell undertook several trips across the area and reported optimistically on the distribution and the potential of seepages. This documentation by Leffingwell (1919) provided the basis for the designation in 1923 of the Naval Petroleum Reserve 4 (later renamed National Petroleum Reserve–Alaska, or NPRA). Interest in the area's oil potential, however, really began in 1944 in response to oil shortages during the war. Subsequent exploration and drilling from 1944 through 1953 resulted in 80 core tests and test wells (Schindler, 2001). Although three oilfields (Simpson, Umiat, and Fish Creek) and seven natural gas fields (Barrow, Gubik, Wolf Creek, Meade, Oumalik, Umiat, and Square Lake) were found, they were not economic

to develop at the time. It was during this period that the U.S. Navy's Arctic Research Lab was established in 1947 and the Barrow gas field began production in 1950. More intensive geological surveys and industry-supported drilling took place between 1953 and 1968. Soon after gaining statehood in 1958, the State of Alaska selected land along the northern coast as state property and had its first lease sale in 1964. The Navy and later the U.S. Geological Survey had a major drilling program in the NPRA starting in 1975 and continuing until 1982.

After nearly a dozen unsuccessful wells, or 'dry holes', a major discovery was made at Prudhoe Bay State No. 1 by Atlantic Richfield Company (ARCO, now ConocoPhillips) and its co-owner Humble Oil (now ExxonMobil) and announced in March 1968. Sohio (now BP) drilled the confirmation well three months later close to the Put River. The Prudhoe Bay field (fig. 46) was initially estimated to contain 9.6 billion bbls of recoverable crude oil and more than 736 billion m³ (26 trillion ft³) of natural gas. The primary reservoir for the Prudhoe Bay oilfield is the nonmarine Ivishak Formation of the Sadlerochit Group, which at this location is nearly

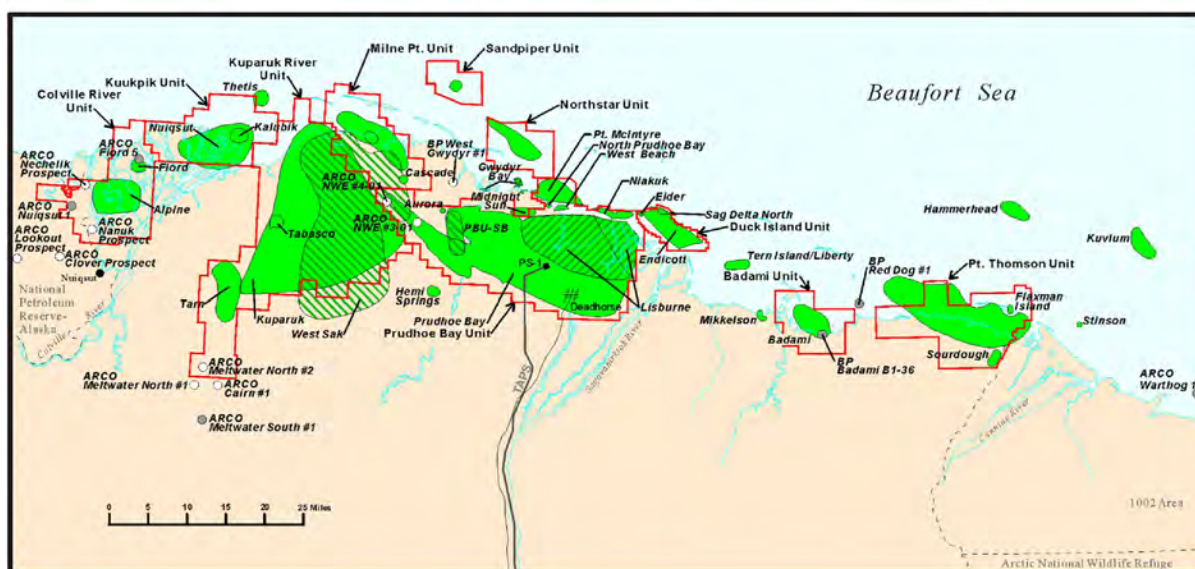


Figure 46. Distribution of oil reserves and oilfields in the central Beaufort Coastal Plain (map courtesy of Alaska Department of Natural Resources).

¹ABR Inc., Environmental Research & Services, P.O. Box 80410, Fairbanks, Alaska 99708-0410; currently employed by Alaska Ecoscience, 2332 Cordes Way, Fairbanks, Alaska, 99709; ecoscience@alaska.net

²Conoco Phillips Alaska, Inc., P.O. Box 100360, Anchorage, Alaska 99510-0360

2,750 m (9,000 ft) underground and up to 150 m (500 ft) thick. The Prudhoe Bay field was not produced until June 20, 1977, after completion of the Trans-Alaska Pipeline System (TAPS), which transported more than 1.5 million bbls of oil and gas liquids per day for more than a decade before initial decline began in 1988. The field still contributes about 5 percent of total U.S. production. Of the 29.4 billion bbls of in-place oil resource, recoverable oil has been revised upward to approximately 15.3 billion bbls through the use of gas re-injection, enhanced recovery techniques, and technology advances. To date, the Prudhoe Bay field has produced more than 10 billion bbls of crude oil, with 2004 production at ~475,000 bbls per day. Development of Prudhoe Bay and the transportation system necessary to move its crude oil to market cost more than \$25 billion. Almost 1,400 wells have been drilled.

Construction of the TAPS to transport the oil began in 1973, after Congress resolved Native claims to land along the right of way in 1971 and granted approval for the project. On June 20, 1977, the first oil was pumped through the pipeline.

Subsequent to this mega-development, oil exploration and development continued to expand eastward and westward (fig. 46). To the west of Prudhoe Bay, the Kuparuk field was discovered in 1969 and began producing in December 1981. Production from smaller developments followed, including Milne Point (1985), Lisburne (1986), Endicott (1987), Point McIntyre (1993), Niakuk (1994), Badami (1998), and the Kuparuk satellite fields (1998–2003). The Kuparuk field is the second-largest producing oil field in North America. More than 2.6 billion bbls of the estimated 6 billion bbls of original oil in place are expected to be recovered. The Kuparuk field currently produces about 140,000 bbls per day from ~950 wells. The producing reservoir is at depths of 1,675 to 1,980 m (5,500–6,500 ft) and the thickness of the oil-bearing rock is ~30.5 m (~100 ft).

Farther west of Kuparuk, the Alpine discovery was made in 1994, declared commercial in 1996, and oil production began in November 2000. Developed at a cost of more than \$1 billion by ConocoPhillips and its partner Anadarko Petroleum Co., Alpine is the largest onshore oilfield discovered in the United States in the last decade. Alpine produces ~125,000 bbls per day. Alpine, which is located 13 km (8 mi) northeast of the Inupiat village of Nuiqsut, is located on both state-owned and Native-owned lands. The original 16,188-ha (40,000-ac) oil field was developed from two drill sites on just 39.2 ha (97 ac), or 0.2 percent of the field area. Recent satellite developments to Alpine have come on line in the northern Colville River Delta (Fiord discovery or

CD-3 pad) and southern Colville River Delta (Nanuq discovery or CD-4 pad). ConocoPhillips Alaska, Inc. has proposed plans to expand Alpine by developing three satellite pads in the northeastern NPR-A.

Today, five of the United States' ten largest producing oilfields—Prudhoe Bay, Kuparuk, Point McIntyre, Alpine and Northstar (developed in 2001)—are located on the coastal plain or nearshore water of northern Alaska. A total of 33 discoveries had been put into production by 2002 (Bureau of Land Management [BLM], 2004).

Other large oil and gas resources (more than 991.2 billion m³ [more than 35 trillion ft³]) are known to exist and can be developed. The federal government estimates that perhaps three times this amount remains to be discovered in onshore and offshore areas. The State of Alaska and other interested parties are pursuing the development of a natural gas pipeline to reach potential markets. The pipeline project is estimated to cost more than \$30 billion (2007 dollars) and will require the producers to make long-term financial commitments to transport the gas. In addition, more than 20 billion bbls of viscous and heavy oil have been found. Viscous oil accounts for more than 5 percent of all the oil produced in Alaska and is expected to double over the next several years. Viscous oil is difficult and expensive to produce because it is cold and thick and will not flow to the surface as easily as oil from the main reservoirs.

During the 80-year period of oil and gas industrialization on the coastal plain, the most intense activity occurred during the 1970s and 1980s, when the massive Prudhoe Bay and Kuparuk oilfields as well as the TAPS were developed (BLM, 2004). During this period a large proportion of the roads, drilling pads, reserve pits, gravel mines, collector pipelines, and production facilities were built (figs. 47 to 49). From 1968 to 2001, total disturbed area grew from 277 to 7,158 ha (685 to 17,686 ac) (NRC, 2003; BLM, 2004).

Oil and gas development brought enormous revenues to state and local governments and a \$33-billion savings account (Permanent Fund) for Alaskans. This money has changed society by funding school construction, education, roads and airports, health clinics, and public safety officers throughout the state, and part of this fund is allocated to each resident annually. The vast majority of funds for Alaska state government spending come from the oil and gas industry; taxes and royalties account for more than 85 percent of the state's general fund. More than \$100 billion in state revenue have been provided by industry (adjusted to today's dollars) since production began in the late 1970s.

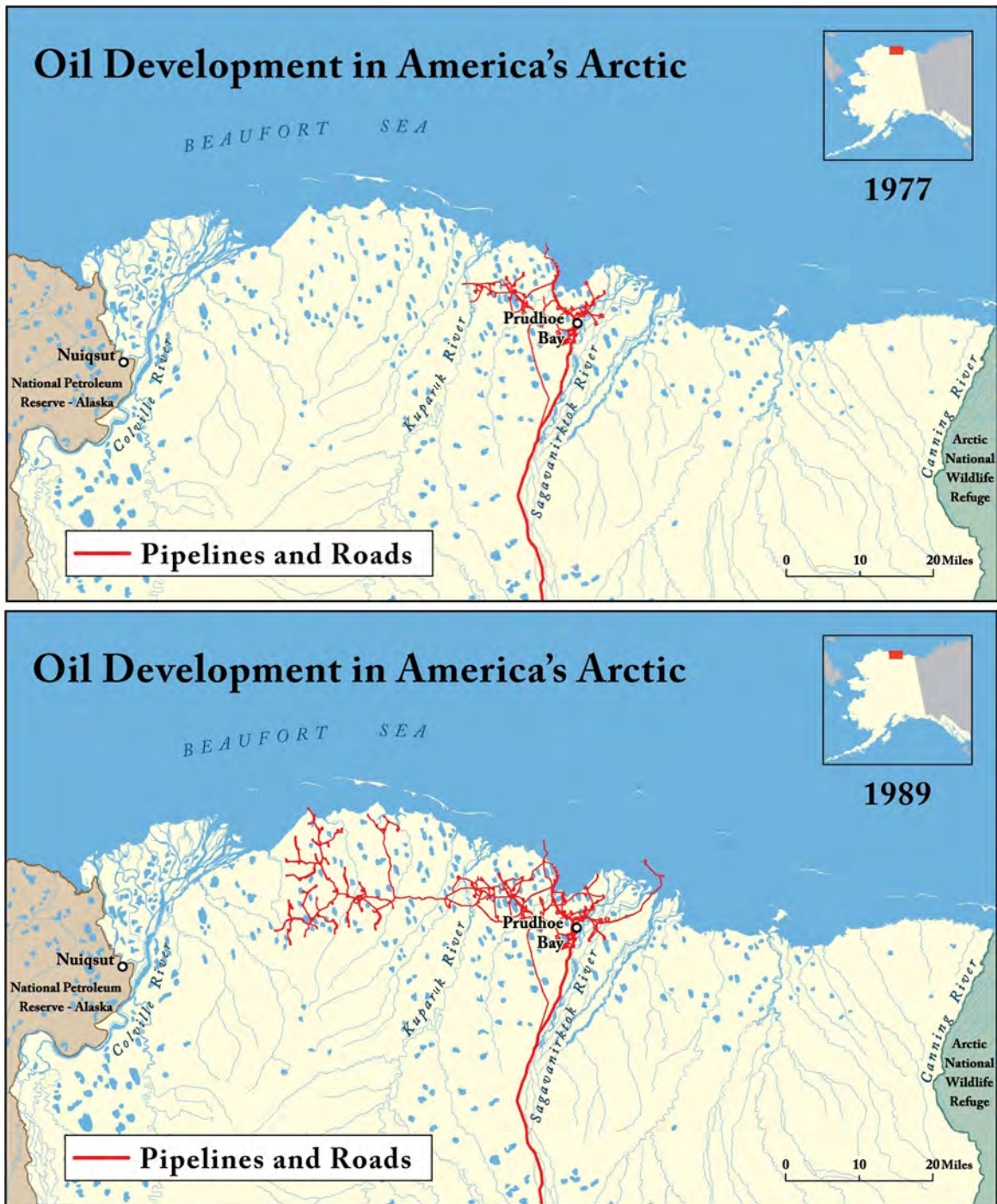


Figure 47. Historical development of oil facilities from 1977 to 1989 on the central Beaufort Coastal Plain. Development in Prudhoe Bay began in 1968. (Maps courtesy of Center for the Environment, Conservation GIS Center.)

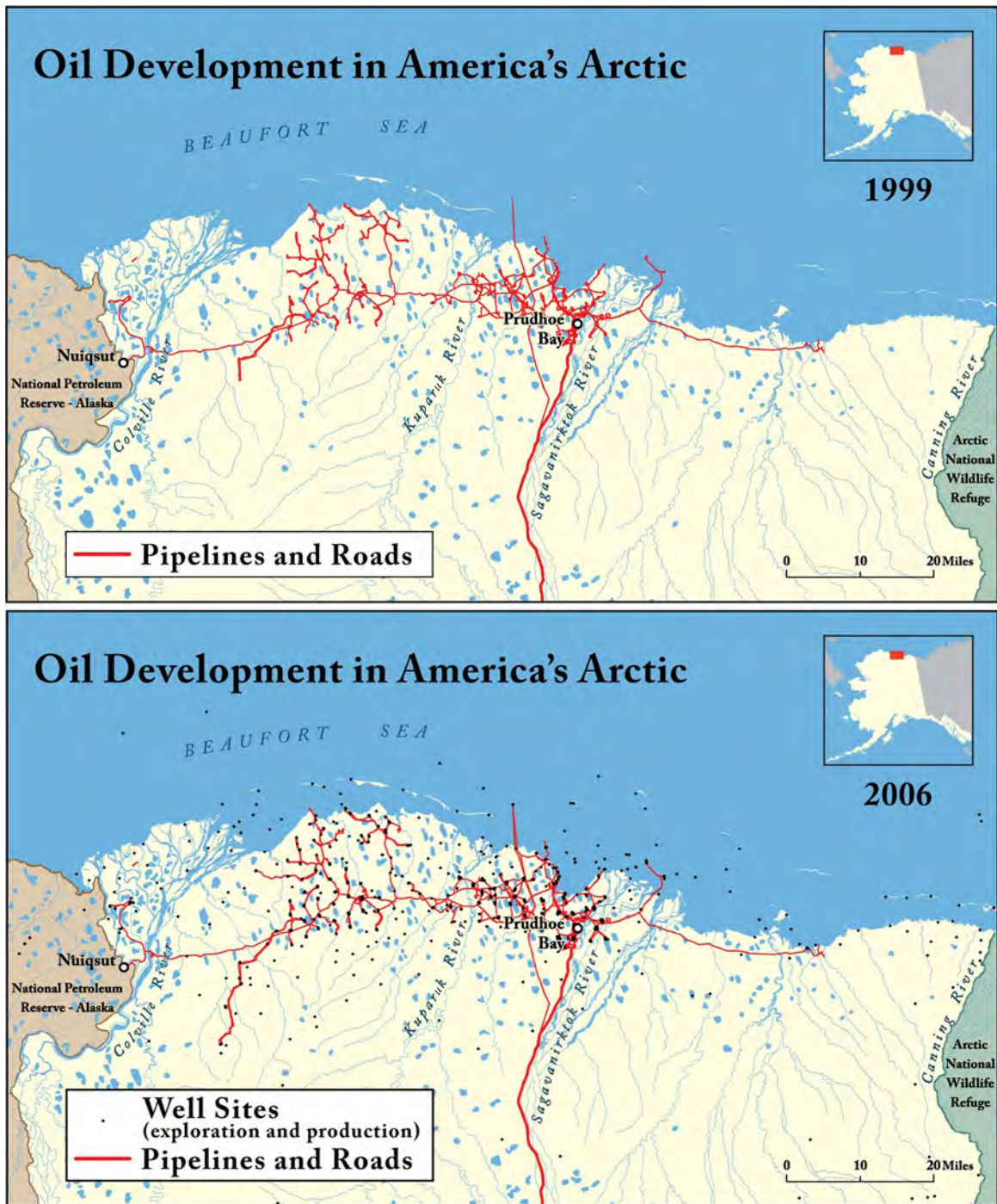


Figure 48. Extent of oil-related facilities from 1999 to 2006 (maps courtesy of Center for the Environment, Conservation GIS Center).

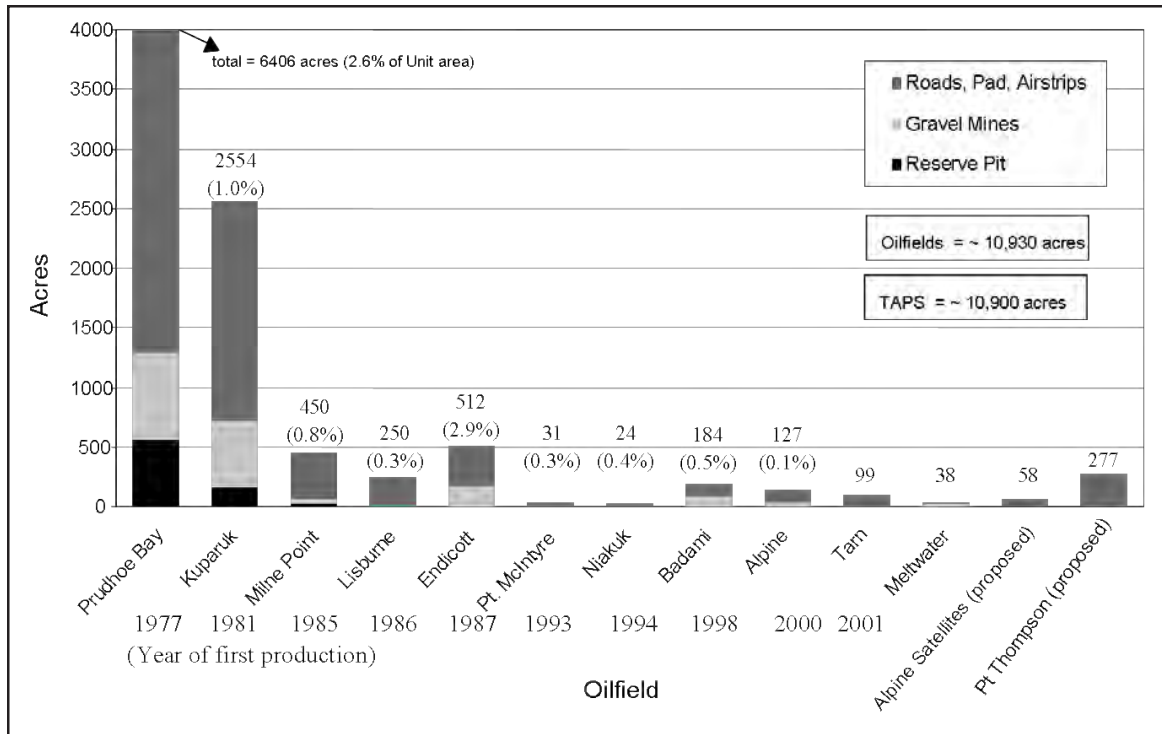


Figure 49. Changes in acreage of oilfield facilities from 1977 to 2001 (data from BLM, 2004).

SEQUENCE OF OILFIELD DEVELOPMENT

Oil development is accomplished through a sequence of seven major phases that take years, even decades, to complete, including initial reconnaissance and planning, seismic geophysical exploration, lease activities, exploratory drilling, appraisal, development and production, and decommissioning and restoration (Gilder and Cronin, 2000; NRC, 2003; BLM, 2004). The initial planning entails the review of existing geologic information, land status, maps, and remote sensing products.

Geophysical data are acquired through seismic surveys that are typically done in the winter onshore and during the summer offshore. Onshore surveys involve the overland transportation of survey crews using low-ground-pressure tire vehicles (for example, Rolligons), generation of micro-scale seismic inputs with vibrating feet attached to vehicles, and temporary installation of small geophones to record reflected seismic signals. Newer techniques use three-dimensional (3-D) seismic technology collected from dense sampling grids. The surveys require surface and air support and temporary base-camp facilities.

Leasing activity includes the auction process to obtain rights to explore and develop the minerals, and environmental reviews that can include field

assessments. Environmental assessments of physical, biological, and cultural resources may require the use of helicopters, Rolligons, and other wheeled vehicles.

Exploratory drilling is conducted in high-potential prospects to ascertain the geologic conditions, confirm the presence of hydrocarbons, and quantify the reserves. Most exploratory drilling is done during winter from temporary ice pads accessed by ice roads. The pads need to be sufficiently large to support the drilling rig, base camp, storage, water management, and waste disposal. Currently, drilling muds and cuttings are re-injected into subsurface formations on site or hauled off to a regional facility for injection.

The appraisal phase determines whether the reservoir is economically feasible and involves additional drilling supported from a larger base camp.

Development of support facilities and production of oil involves the construction of roads, airstrips, and drilling pads using gravel obtained from gravel mines, and installation of elevated or buried pipelines. Major support facilities include processing plants, water-supply plants, waste-handling facilities, power plants, base camps, and oil response facilities.

When all the economically producible oil reserves have been extracted, the facilities and hardware must be removed, and wastes and disturbed land must be cleaned up and reclaimed to the satisfaction of regulatory agencies.

ENVIRONMENTAL IMPACTS AND MITIGATION

A wide range of environmental impacts are incurred during the various phases of oil exploration and development (Gilders and Cronin, 2001; NRC, 2003). Air may be affected by emissions of carbon dioxide, carbon monoxide, methane, volatile organic hydrocarbons, halons, sulfur dioxide, nitrogen oxides, hydrogen sulfide, and dust particulates associated with flaring, combustion, road traffic, and chronic minor gas losses. Water may be affected by spills of oil and produced water, disposal of drilling waste, and discharge of treated grey water. Soil and vegetation can be disturbed by placement of gravel fill, gravel mines, off-road traffic, seismic activity, impoundments, dust from roads, and oil spills. Wildlife can be disturbed by direct habitat loss, disturbance or displacement by noise and human activity, blockage of movement by structures, and interception of birds by powerlines.

Knowledge of these impacts, however, has led to a concerted effort by industry and government to develop innovative technology and regulations to reduce the effects of development. Newer approaches have been directed at applying environmental stewardship, adhering to state and federal regulations, and minimizing corporate liability. The following discussion focuses on the main issues related to exploration, development, and decommissioning that have been the focus of regulatory concern and industry innovation. These issues include: tundra damage from seismic exploration, use of ice roads, drilling pads at exploratory well sites, environmental baseline studies, facility planning, gravel fill placement, water use, drilling waste, oil spills, garbage handling, wildlife displacement, and land rehabilitation.

Seismic exploration in the Arctic National Wildlife Refuge during the 1970s and early 1980s, which involved metal cleat-tracked seismic vehicles and tractor-pulled camp trains, caused substantial damage and has been the subject of long-term monitoring (Felix and Reynolds, 1989; Emers and Jorgenson, 1997). In response to concerns over tundra damage, the seismic industry has developed rubber-tracked vehicles, and routes camp-support facilities to wet tundra areas less susceptible to damage, which has resulted in much less damage (Jorgenson and others, 2003b). One problem that has delayed startup of seismic exploration until mid-winter, the Alaska State requirement of 30 cm (12 in) of soil freezing (frost), appears to have been resolved with the consensus that the initial standard was more conservative than necessary. However, because of the high density of 3-D seismic grids, environmental concerns remain high (NRC, 2003). The main variables for further reducing damage are requiring at least 25 cm (10 in) of snow, use of rubber-tracked vehicles (without cleats), limiting the

number of passes of vehicles over the same trail to two or fewer, pre-seismic route assessments to avoid sensitive habitats, and developing new camp-support equipment that uses rubber wheels or tracks instead of metal skis.

Ice roads have been used since the 1970s as an effective means of avoiding the impacts of building permanent roads (Keyes, 1977). Exploration drilling is limited to a brief window each winter when ice roads can be built in remote locations. Instead of constructing a gravel pad for exploration drilling, companies build temporary pads of ice that disappear after the well has been drilled, leaving virtually no trace (fig. 50). Temporary ice roads have long been used to support winter exploration drilling on the North Slope and some of the newer oil fields—including Alpine, Northstar and Badami—have no permanent road to the fields. The technology is well developed and there is a consensus that environmental impacts of ice roads are acceptable, given that the alternative would be permanent gravel roads. However, there still are visible impacts that persist for years to decades, and studies have been conducted to evaluate methods of further reducing impacts (Yokel and others, 2003). Most of the impacts appear to result during construction. Techniques to reduce impacts include pre-packing of snow, spreading additional snow, use of low-ground-pressure vehicles, avoiding excessive snow manipulation with bull-dozers and graders, and route selection to avoid sensitive vegetation. Proper route selection to emphasize areas of wet tundra with herbaceous vegetation has allowed ice roads to be built with only low-level, short-term impacts.

Exploratory well sites have evolved from thick gravel pads, to thin pads, to ice pads for one-season use, to insulated ice-pads for two-season use, and most recently to experimental elevated platforms (fig. 50). Earlier construction techniques and poor waste management led to a legacy of habitat damage, contamination, leaching of drilling waste that had been disposed of in surface impoundments, and corporate liability in the face of changing environmental standards. The current approach is to use an ice pad, incinerate burnable waste, and dispose of drill cuttings and liquid waste down permitted injection wells.

Environmental baseline investigations are proving to be important in minimizing damage and facilitating public acceptance of oil development (Jorgenson and others, 1997c). Of the many issues relevant to development, several bear special mention. First, all new projects have acquired high-resolution, georectified imagery (aerial or satellite) to provide a common base map for environmental and engineering studies. Second, hydrology has consistently been a high concern both from engineering and environmental perspectives. Stage-discharge, surface-water flow patterns, and cross-drainage issues have required extensive field



Figure 50. Production and exploratory well pads have decreased substantially in size over time. Production pads are shown on the top row, including well sites in the 1970s when drilling waste was disposed of in surface pits; late 1980s where drilling waste was buried in permafrost; and 2000s when drilling waste was re-injected (photos by T. Jorgenson). Exploratory well sites are shown along bottom row, including a site in the 1970s, 1980s, and 1990s. Note the decrease or elimination of gravel fill.

studies and two-dimensional hydrologic models have been used more frequently (BLM, 2004). Third, high-quality integrated-terrain-unit mapping (geomorphology, surface form, and vegetation) has become more common as the basis for habitat-use analysis, facility planning, oil-spill contingency planning, hydrologic modeling, seismic exploration mitigation planning, and facility planning (Jorgenson and others, 1997c, 2003c). Fourth, intensive studies of the abundance, distribution, and habitat use by fish and wildlife are more frequently being demanded by regulatory agencies and subsistence users in local communities (Moulton and George, 2000; BLM, 2004). Finally, knowledge of the nature and distribution of ground ice is important for facility planning and land rehabilitation to minimize thermokarst.

Facility planning to minimize impacts has focused on reducing the size of the development footprint, operation of roadless remote facilities, elevating pipelines to allow caribou passage, and avoidance of cross-drainage problems. Remote, small oilfields, and even individual drill pads, recently have been developed without permanent roads, relying instead on temporary ice roads in the winter and aircraft for year-round support.

Pipelines are now built with 1.5–2 m (5–7 ft) ground clearance for animal passage, and with periodic raised vertical U-shape loops to control oil loss in case of a spill and to allow pipeline expansion and contraction from temperature changes. Gravel ramps with buried pipelines were used in the 1990s, but recently have been associated with two oil spills. Finally, proper construction of bridges and installation of culverts to minimize impedance and impoundment of water remains problematic. Regulatory agencies have been favoring small bridges instead of large culverts because of problems associated with scouring, erosion, and ice-blockage of culverts. Because small culverts tend to settle with the ends bending upwards, designs have called for larger culverts and for better foundations designed to avoid thaw settlement. There also has been an emphasis on route selection to avoid the need for culverts, such as routing around drained-lake basins.

Gravel is needed for construction of roads, causeways, offshore islands, drilling pads, and airstrips, and must be extracted from riverbeds or gravel pits. The loss of habitat from the combined filled areas and excavated mine sites is by far the greatest impact of

oil development. By 2001, gravel fill covered 3,733 ha (9,224 ac) of tundra and nearshore areas in northern Alaska, and gravel mines affected 2,575 ha (6,363 ac) (NRC, 2003). Consequently, there has been a strong emphasis from regulatory agencies and environmental groups to reduce the size of the development footprint. Significant reductions have been accomplished through consolidation of facilities, use of ice roads to eliminate unnecessary gravel roads, directional drilling to reduce the number of pads, and down-hole injection of drilling waste to eliminate the need for surface disposal in reserve pits. Drilling advances and improved waste-management techniques enable the producers to significantly reduce the land area needed for oil field development (fig. 50). Wells that once were spaced about 36 m (120 ft) apart are now drilled as close as 3 m (10 ft). There have been dramatic reductions in the size of gravel pads used for drill sites from 80 ha (200 ac) (including reserve pits) to 4 ha (10 ac) (BLM, 2004). The percent of area covered by gravel, expressed as a percentage of the oilfield-unit boundaries has decreased from 2.6 percent for the older Prudhoe Bay to 0.2 percent for the new Alpine Development (Truett and Johnson, 2000). Gravel roads also tend to have indirect effects caused by dust, drainage impoundment, and thermokarst that can substantially increase the area impacted (Walker and others, 1987).

Today's drilling techniques have enabled industry to pinpoint the best subsurface locations, drill fewer wells, create less surface disturbance, and enhance oil recovery with fewer, more strategically placed production facilities. Extended reach directional drilling allows companies to reach deposits as far as 6.4 km (4 mi) away. Horizontal wells allow producers to run long sections of horizontal casing through an oil-bearing layer as thin as 1.8 m (6 ft), draining the deposit through openings in the casing. Horizontal wells can also use multiple horizontal sections to expose more than 6,100 m (20,000 ft) of reservoir rock in one well. In comparison, a vertical well might expose 60–90 m (200–300 ft) of reservoir rock. At least 90 percent of the wells now drilled in the Prudhoe Bay, Kuparuk, and Alpine oilfields are horizontal. This technology helps keep production up by tapping into deposits once thought to be uneconomic by accessing more of the reservoir to achieve higher production rates.

Drilling waste, including hydrocarbon- and salt-contaminated muds and cuttings, typically was discharged onto the tundra surface during the 1970s and early 1980s. At Prudhoe Bay the open, gravel-bermed, reserve pits developed in the 1970s typically contained 17–51 million L (4.5–13.5 million gal) of waste (ADEC, 1985). This created a huge liability to the oil industry as federal and state regulation of drilling-waste disposal and surface-water quality evolved. Industry has incurred enormous expense removing and disposing of this material, for a brief period in deep buried pits, and

more recently down injection wells after grinding up the material. Deep-well injection is now the only permitted means of disposal because of both environmental and liability concerns. The disposal of fluids still must be compatible with water in the deep formations and must not affect potential sources of drinking water.

Water use for ice roads, drilling, hydrostatic testing of pipelines, and camp facilities is of high concern to regulatory agencies, particularly to fisheries managers. In 2000, for example, 5.3 billion L (1.4 billion gal) of water were used by oilfields in northern Alaska, drawn from both lakes and wells (NRC, 2003). Water demand for construction and maintenance of ice roads and pads is ~1 million gals of water per mile (BLM, 2004). In Alaska, detailed lake inventories of water volume and fish populations are required by regulatory agencies for water withdrawal, and withdrawal is limited to 15 percent of water volume below maximum ice depth to protect fish.

Oil spills remain a common occurrence in northern Alaska, although the spills tend to be relatively small and cleanup technology has made substantial advances. Each year from 1977 to 1999 there was an average of 234 spills of crude oil and petroleum products with an average annual cumulative spill volume of 537 bbls (NRC, 2003). Seawater spills averaged 66 spills per year (incomplete data) with an annual average volume of 2,918 bbl. Most of the recent larger oil spills (up to 1 ha [2.5 ac]) have resulted from pipeline corrosion. A well-designed and implemented sequence of cleanup activities includes: control, containment, site assessment, oil removal and treatment, storage, disposal, risk assessment and remedial planning, and eventually ecological restoration and monitoring (Jorgenson and Cater, 1996). Cleanup techniques for tundra areas are well established (Nuka Research and Planning Group [NRPG], 2004).

Populations of predators, such as arctic foxes, glaucous gulls, grizzly bears, and ravens, have all increased around oil development, which has led to increasing concern about the effects of their predation on nesting birds in the oilfields (Truett and others, 1997). Their increases have been attributed to unenclosed garbage, landfills, and feeding by oilfield workers. Animal-proof dumpsters are now preferred, feeding of wildlife has been banned, and new developments handle solid waste without landfills.

Effects of development on caribou populations, one of the main animals used for subsistence in northern Alaska, has remained one of the most controversial issues of oil development. The original high density of development, heavy traffic, low pipeline heights, and routing of pipelines adjacent to roads have contributed to the displacement of caribou from portions of the older oilfields and lower reproductive success (Curotolo and Murphy, 1986; Cameron and others, 1995). Raising

pipelines to a minimum of 1.5 m (5 ft), separating pipes from roads, and controversial seasonal road restrictions have helped reduce deleterious effects.

Rehabilitation techniques for treating abandoned land have been developed through long-term research in the oilfields (Mitchell and others, 1974; Jorgenson and Joyce, 1994; Jorgenson and others, 1995; Jorgenson, 1997; Forbes and McKendrick, 2004). Federal regulatory agencies have emphasized the removal of gravel fill as the most effective approach to reestablishing the hydrologic and soil conditions for wetland restoration (Kidd and others, 2004). This strategy has been coupled with the requirement to reuse gravel from abandoned roads and pads. For areas where gravel removal is not practical, indigenous nitrogen-fixing legumes have provided the best plant growth on dry, thick gravel fill.

Newer oil developments have been applying a set of best-management practices for minimizing environmental impacts during the various stages of arctic oil development (Truett and Johnson, 2000):

OIL EXPLORATION:

- Conduct baseline archeological, wildlife, habitat, and hydrology studies for facility planning.
- Obtain high-resolution, georectified imagery for field studies and mapping.
- Create integrated-terrain-unit maps of exploration area for impact analysis.
- Conduct all exploration activities during winter when wildlife is mostly absent and tundra impacts are reduced.
- Perform exploratory drilling during a single winter, rather than over multiple years.
- Use insulated ice pads for multi-winter drilling.
- Reduce size of ice pads for drilling to reduce water use.
- Construct ice roads to exploration sites.
- Use specifically designed vehicles for winter tundra travel to reduce surface damage.
- Re-inject drilling mud into confining geological zones.
- Prohibit feeding of wildlife and hunting to reduce effects on predator populations and reduce chances for harmful human-wildlife encounters.

FACILITY PLANNING:

- Minimize facility size and wellhead spacing to reduce coverage of tundra.
- Design pipeline vertical support members to allow for unanticipated expansion.
- Design facility for zero discharge of solid and liquid wastes; re-inject drilling waste.
- Use existing roads and pads.
- Recycle gravel from unused or abandoned facilities.
- Use existing production and power generation wherever feasible.
- Consider future development potential when siting road and pipeline routes.
- Identify surface-water movement patterns to avoid cross-drainage problem areas and design proper cross-drainage structures that do not ice up during winter and spring.
- Elevate pipelines to 1.5 m (5 ft) or more to allow passage of caribou and snowmobiles.
- Compile and analyze historical wildlife use of area to avoid high-use areas.
- Coordinate with regulatory agencies and local communities.
- Identify potential oil-spill patterns and sites for pre-staging containment and cleanup equipment.

CONSTRUCTION AND OPERATION:

- Construct pipelines during winter from ice roads.
- Restrict on-tundra activities to permitted areas.
- Designate fuel storage and transfer locations away from waterbodies and wetlands.
- Use small portable containment devices during all fuel transfer operations.
- Enforce speed limits in project areas to reduce accidents that may damage the tundra.
- Prohibit work in fish-bearing streams.
- Conduct all major activities, like pipeline and bridge construction, and gravel mining, during winter.
- Maintain continual on-site environmental presence during construction to ensure compliance with permit requirements.
- Clear culverts before breakup.
- Prohibit hunting by personnel and restrict public access.
- Provide environmental training to personnel to help avoid potential impacts.

This page was intentionally left blank.

PART 3: TOUR OF PRUDHOE BAY AND KUPARUK OILFIELDS

by Torre Jorgenson¹

OVERVIEW

The Prudhoe Bay (fig. 51) and Kuparuk oilfields are the two largest oilfields in the United States and Prudhoe Bay is the 18th largest oilfield discovered in the world (Bird and Houseknecht, 2006). Four other adjacent

oilfields, Point McIntyre, Endicott, Alpine, and North Star also are among the top ten U.S. oilfields. Together they have contributed about 20 percent of U.S. domestic production annually since oil production began in 1977.

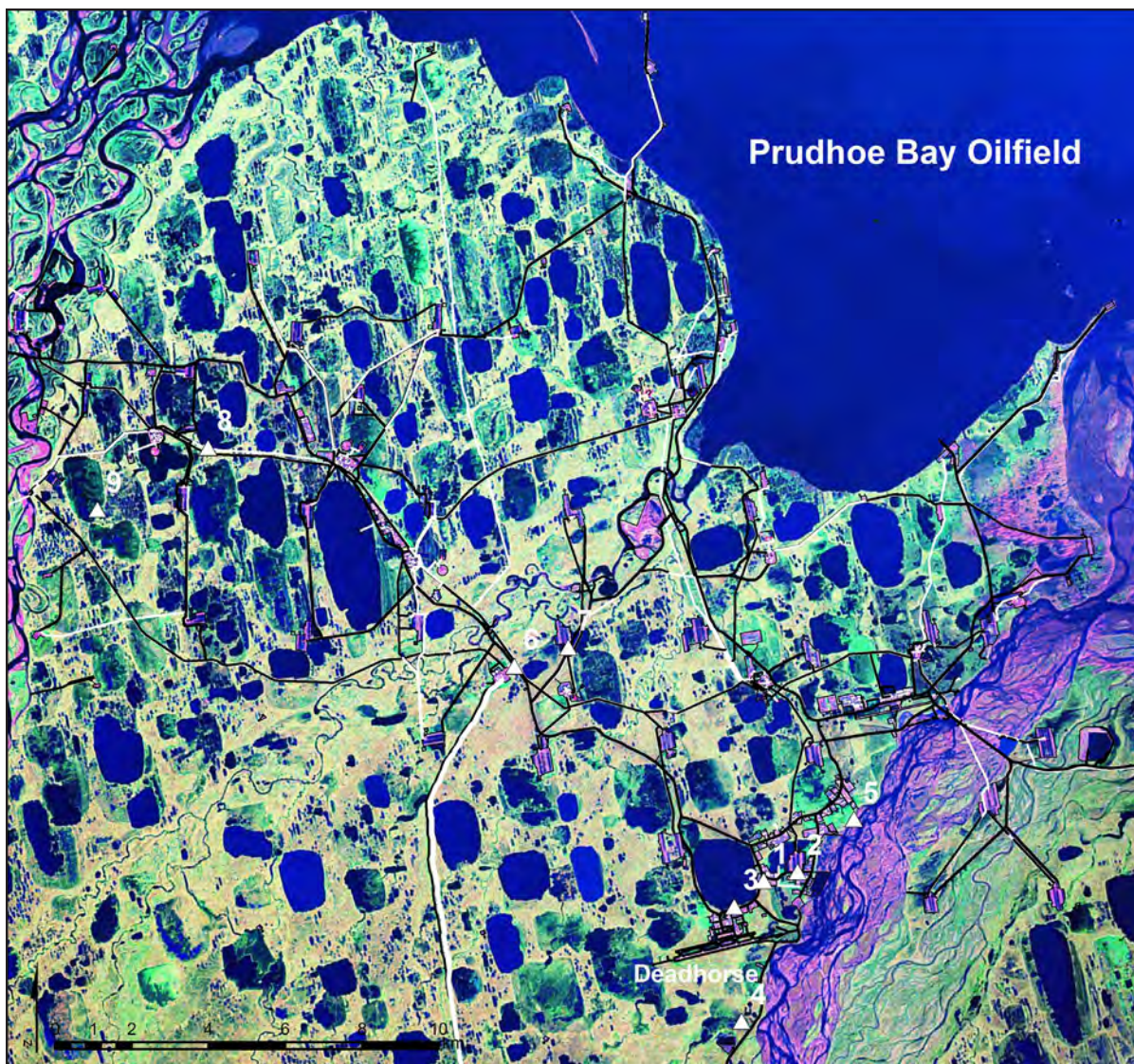


Figure 51. Landsat image of the Prudhoe Bay oilfield. Numbers indicate tour stops at: (1) Deadhorse oilfield support facilities, (2) Drill Site 12, (3) dust impacts near Coleen Lake, (4) pipeline trenching trials, (5) Sagavanirktok riverbank exposure, (6) Pump Station 1, (7) Drill Site 7 impoundment, (8) GC2 oil-spill restoration, and (9) Betty Pingo research site.

¹ABR Inc., Environmental Research & Services, P.O. Box 80410, Fairbanks, Alaska 99708-0410; currently employed by Alaska Ecoscience, 2332 Cordes Way, Fairbanks, Alaska, 99709; ecoscience@alaska.net

These fields, along with more recent developments, have produced ~15 billion bbls of oil over the past 30 years.

Extracting, processing, and transporting crude oil at Prudhoe Bay requires an extensive network of roads, industrial facilities and pipelines that together constitute one of the world's biggest industrial complexes. By 2001, overall development in the oilfields directly affected 7,023 ha (17,354 acres), including 115 drilling pads, 644 km (400 mi) of road, 724 km (450 mi) of pipeline, five docks, and 25 production, processing, seawater treatment and power plants (National Research Council [NRC], 2003).

Oil extraction starts at the wellheads (some may have 30 or more) of a drill site, and the oil is gathered in the manifold building at the drill site (fig. 52). The manifold building controls the pumping rate and pressure, and has the ability to release uncontrollable surges in pressure by redirecting gases to a flare pit. From the manifold building, the produced oil, natural gas, and brine travel in pipelines to separation facilities (called gathering centers in Prudhoe Bay and central production facilities in Kuparuk), where the crude oil is separated from the natural gas and water (fig. 53). The produced water is

returned to the drill sites for re-injection to maintain pressure in the formation, and the natural gas is piped to a central gas facility (CGF). At the CGF, the heavier natural gas liquids are separated and piped to Pump Station 1. Lean gas is separated for re-injection at individual drill sites to help maintain formation pressure or is piped to the central compressor plant, which re-injects it for long-term storage. Seawater is processed at a seawater treatment center to remove sediments and kill bacteria that might degrade crude oil, and then injected into the formation as necessary to maintain subsurface pressure. Crude oil from all the separation facilities at the various oilfields is piped to Pump Station 1 for pumping down the Trans Alaska Pipeline System (TAPS) to the marine terminal in Valdez for shipment to market.

Crude oil has been pumped through the TAPS for more than 30 years, starting in 1977 (fig. 54). Throughput peaked in 1988 at an average of 2,033,082 bbls per day and a total of 744,107,855 bbls for the year (Alyeska Pipeline Service Company [APSC], 2008). By 2006, throughput had dropped to a daily average of 759,081 bbls and an annual total of 277,064,405 bbl. Cumulative output from 1977 through 2006 was 15.3 billion bbl.

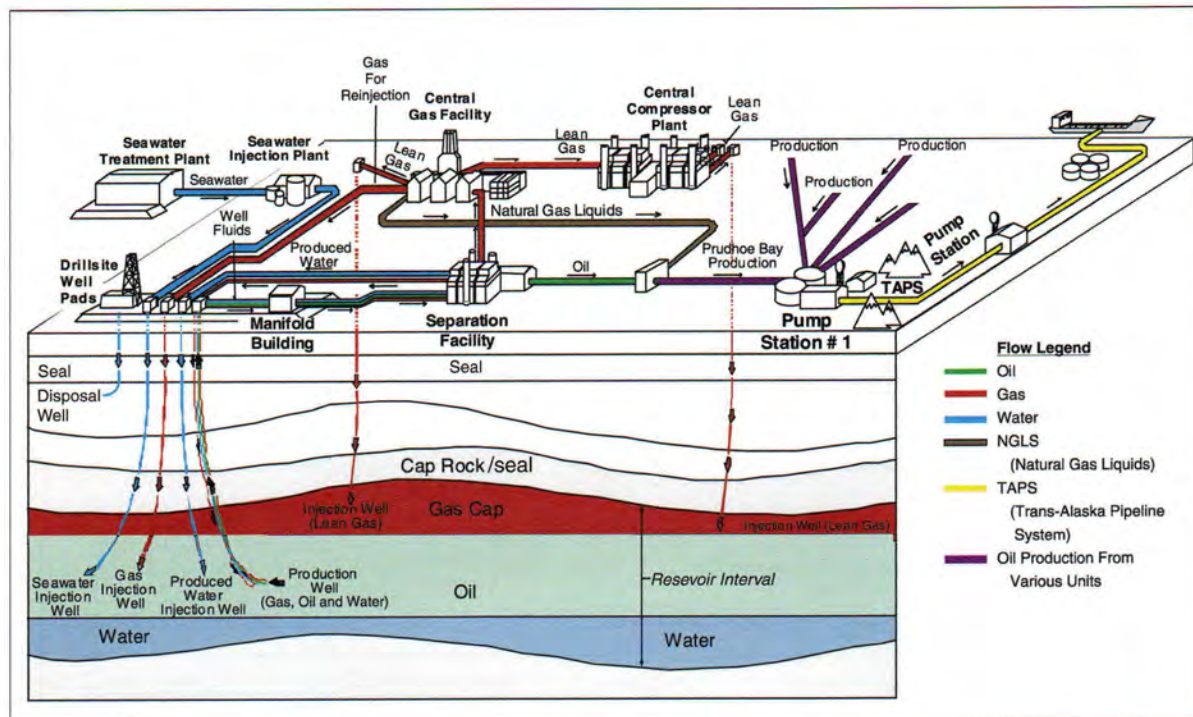


Figure 52. Diagram of oilfield facilities in Prudhoe Bay, illustrating the flow of crude oil from a drill site to Pump Station 1 (NRC, 2003).

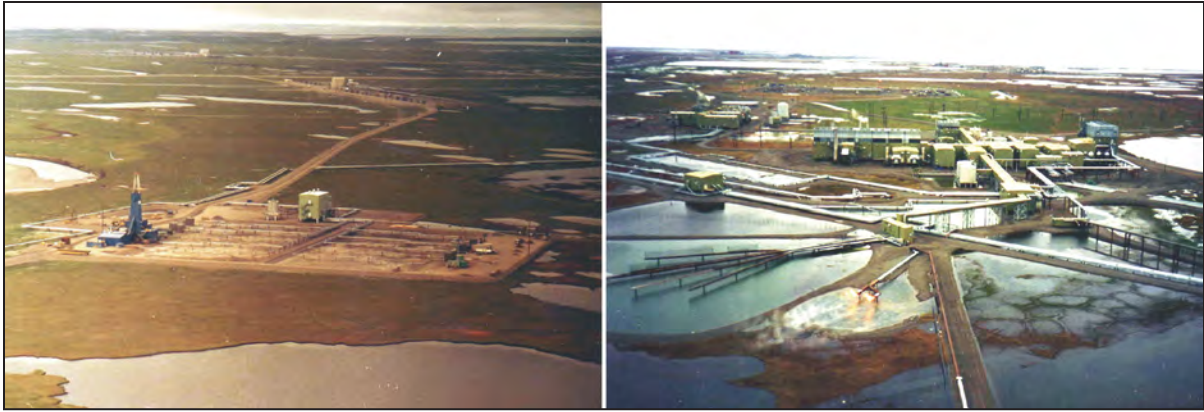


Figure 53. Aerial views of a drill site with a drill rig and a central processing facility with large flare pits for venting uncontrollable pressure surges (photos by T. Jorgenson).

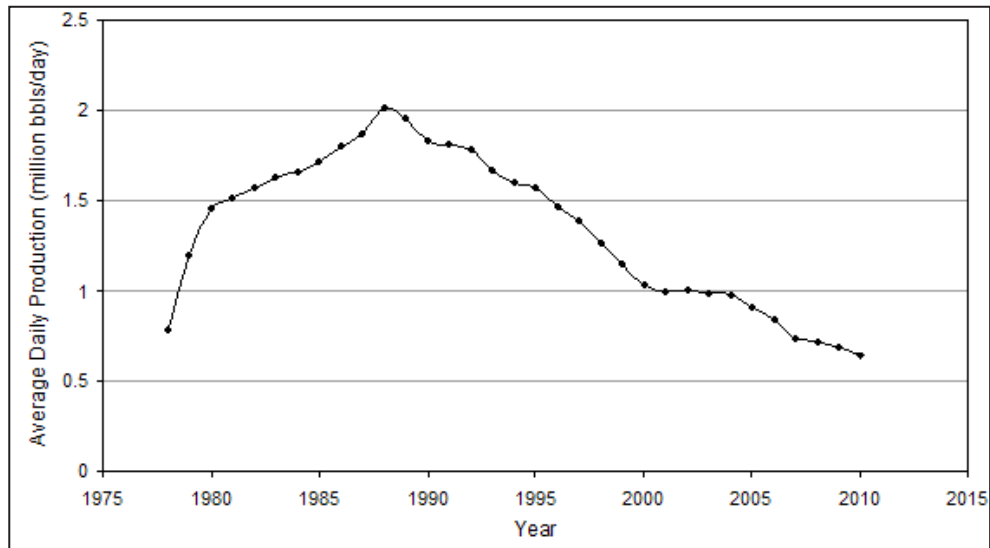


Figure 54. Annual throughput of crude oil in the Trans-Alaska Pipeline System since 1977.

STOP 1: DEADHORSE FACILITIES

Deadhorse, named after an early pioneer construction company, is the regional center for support services for oilfield development (fig. 55). Deadhorse is the end of the Dalton Highway, at Mile 414, about 800 km (500 mi) north of Fairbanks. From here, road access to the Arctic Ocean and the oilfields is restricted by the oil companies, although access is granted to guided tours. Deadhorse includes an airport, transportation companies, pipeline construction and drilling companies, worker housing, small stores, a service station with gas and tire service, and a couple of hotels. Scheduled airline flights connect to Fairbanks, Anchorage, and North Slope villages. Between 3,500 and 8,000 people work in the oilfields, depending on how busy the oil operations are, and some live year-round in Deadhorse.

Deadhorse has some of the most heavily impacted terrain from oil development because there was little environmental oversight during early years of construction. There are thick accumulations of road dust on the adjacent tundra from heavy traffic, substantial tundra damage from off-road travel, and numerous gravel pads contaminated by poor fuel and material handling procedures. One facility at Deadhorse specializes in thermal remediation (burning) of hydrocarbon-contaminated soils. The thermal remediation unit was originally brought up in 1991 to treat gravel and tundra contaminated by crude oil at the S.E. Eileen exploratory well site (Jorgenson and others, 1991). The Alaska Department of Environmental Conservation keeps a database of contaminated sites in Deadhorse, such as the Deadhorse Hotel pad, Deadhorse airport, Childs Pad, and the VECO Fracmaster Pad.



Figure 55. Airphoto of oilfield support services at Deadhorse, showing dense development of facilities.

STOP 2: OIL OPERATIONS AT DRILL SITE 12

The drill site is the principal facility for extracting produced oil, natural gas, and water from deep oil-bearing formations; the products are then piped to a central processing facility for separation (fig. 56). The facility also re-injects natural gas and seawater to maintain fluid pressure in the formation and to store the natural gas for later production. A drill site is composed of a 1.5-m- (4.9-ft-) thick gravel pad to provide a thermally stable foundation for the infrastructure, open reserve pits surrounded by gravel berms to contain drilling waste (older sites), wellheads surrounded by metal sheds, small-diameter pipelines that move fluids to the manifold building, and a flare pit for burning natural gas during times of uncontrollable pressure surges.

Drill Site 12, built in the mid-1970s is representative of the old approach to drill-site construction. Early drill sites are relatively large and there was no attempt to site facilities away from lakes, basins, or areas of water flow. The outline of Drill Site 12 occupies 21.6 ha (53.4 ac) and the wellheads are relatively widely spaced. By the late 1990s, the sizes of the gravel pads were substantially reduced, wellheads were closely spaced, and open reserve pits were eliminated in favor of re-injection of wastes.

The reserve pits are designed to contain the muds and cuttings from the drilling process. When a well is started (spudded), a drilling mud is created by mixing a bentonite clay with water to produce a viscous, thixotropic solution. The mud is needed to lubricate the well bore, overbalance the formation pressure to prevent blowouts, and remove cuttings from the well bore. As the formation is drilled, rock material is ground up, some into large particles and some pulverized and suspended in the mud system. The process raises the viscosity to a point where the mud is not easily pumped. As the rock-laden mud circulates to the surface, it is passed over 80-mesh shaker screens to remove coarse material.

Concern about contamination of adjacent wetlands by hydrocarbons, heavy metals, and salts leaching from the early reserve pits (Woodward and others, 1988) led to an agreement in 1996 between the Environmental Protection Agency, the Alaska Department of Environmental Conservation, and the oil industry to develop closure plans by 2002. North Slope operators soon began cleaning out their in-field reserve pits. In an early approach to disposal and long-term sequestration, drilling waste from multiple drill sites was buried and capped in a deep pit near Drill Site 16 for permanent isolation in permafrost. Starting in 1995, the mud and cuttings were taken to a large-scale grind and injection plant near Drill Site 4-19 in the Eastern Operating Area. In the process, large particles are removed from the drill cuttings through the use of shakers, demanders, de-silters, and centrifuges. The remaining fine material is run through a ball mill to grind it until it is fine enough to not plug the openings for the subsurface

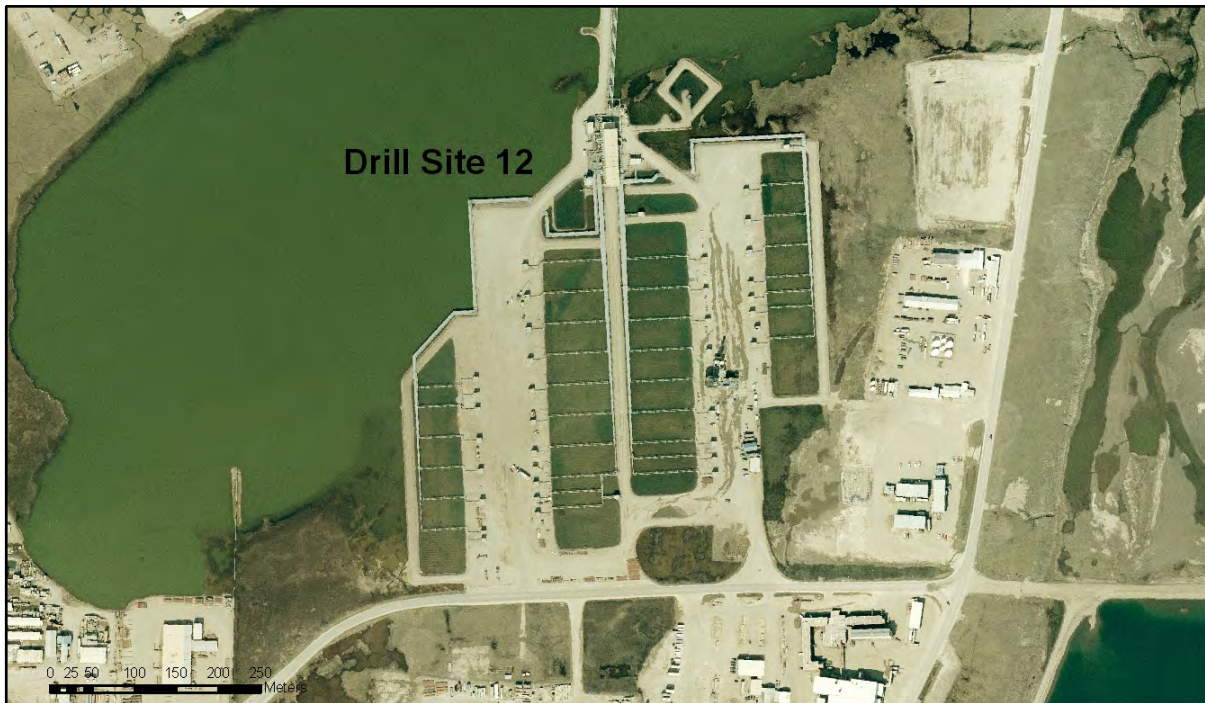


Figure 56. Airphoto of Drill Site 12 showing a typical layout of a drill site that was developed according to the design and engineering techniques used during the 1970s.

formation and is pumped 600–3,000 m (1,970–9,840 ft) deep into the ground. The grind-and-inject technology has enabled oilfield operators to achieve ‘zero discharge’ of drilling wastes and eliminate the need for reserve pits at new drill sites. By 2000, some 917,520 m³ (1.2 million yd³) of solid material—mostly cuttings—had been pumped down hole in the oilfields. About 513 of 605 reserve pits statewide had been cleaned out by 2007, while another 17—mostly on the North Slope—are expected to be closed within the next year, according to DEC. Another 57, mostly North Slope sites, are slated for future corrective action, and all inactive reserve pits owned by BP, ConocoPhillips Alaska Inc., and ExxonMobil Production Co. are currently expected to be closed by 2014. Of several viable options available, grind-and-inject disposal has proven to be a cost-effective approach, costing about \$91/m³ (\$100/yd³), and offers the prospect of being a permanent solution.

STOP 3: DUST IMPACTS

Heavy traffic along the main arteries of the oil fields creates dust clouds that drift off the gravel roads and deposit silt on the adjacent tundra (figs. 57 and 58). Near especially heavily traveled roadways, accumulations can be as thick as 25 cm (10 in) (McKendrick, 2000) and eliminate all vegetation up to 5 m (16 ft) and sensitive mosses up to 20 m (65 ft) away from the road (Everett, 1980; Spatt and Miller, 1981; Walker and Everett, 1987; Auerbach and others, 1997). The dust smothers vegetation, increases pH and thus affects nutrient availability, shifts species composition toward more disturbance and alkaline tolerant species, increases active-layer thickness, accelerates spring snow-melt, and causes thawing of ice-wedges in the permafrost. The use of a pebble-rich asphalt, called chip-seal, along portions of the heavily used spine roads has eliminated further dust-fall in treated areas.

STOP 4: BURIED PIPELINE TRENCHING TRIALS

Trenching trials were conducted by BP near Material Site 3, ~2 km (1.2 mi) south of Deadhorse along the Dalton Highway, during February 2002 to test the feasibility and economics of a variety of trenching equipment and soil-handling processes for burying a gas pipeline (fig. 59). The current method of excavating a pipeline ditch in permafrost soils is to drill and blast the ditch to fracture the permafrost and then excavate the blasted material with backhoes. An alternative method, which has been used successfully in non-permafrost areas, is to excavate the trench with wheel or chain trenching machines. Potential advantages of the trenching machine include: smaller cross-section and volume of material displaced, more stable trench, closer proximity for a side boom to lay the



Figure 57. A 2004 airphoto reveals ice-wedge degradation caused by heavy dust loads along heavily traveled roads in areas of dense development. Thermokarst can extend 50 m (165 ft) from the road.



Figure 58. Views in 2004 of degrading ice wedges caused by dust from a road in Deadhorse (photos by T. Jorgenson).

pipeline in the trench, grinding of soil and bedrock to make more suitable backfill material, smaller footprint, better chance for rehabilitation, and less equipment on the right-of-way.

The trenching trials evaluated the trench production rates of five varying techniques, relative to a standard full-trench technique used as the baseline condition. The test trials evaluated the ability of equipment to: (1) trench at variable depths in situations with variable terrain; (2) complete a full-width trench after a shallow and deep pass; (3) excavate a single-slot trench in advance of the full-width pass; (4) excavate two narrow trenches (one on each side of the final trench) in advance of the full-width pass; and (5) trench two narrow side-by-side trenches at half depth in advance of the full width pass (fig. 60). Testing was done with 1660 and 1260 HD trenchers (fig. 61).

Revegetation of the trench berms was initiated in 2003, by hand spreading of fertilizer and the native-grass cultivar *Puccinellia borealis* (ABR, 2007). Monitoring of the site since 2003 has revealed substantial thaw settlement along many of the trenches, which were backfilled with ice-rich permafrost soil (fig. 62). Due to continued thaw settlement of the trenches below tundra grade and impoundment of water that is preventing plant growth, additional remedial measures are being planned to backfill the trenches and perform additional revegetation work.



Figure 59. A 2007 airphoto of berms left over from trenching trials that evaluated five methods for burying a cold gas pipeline.

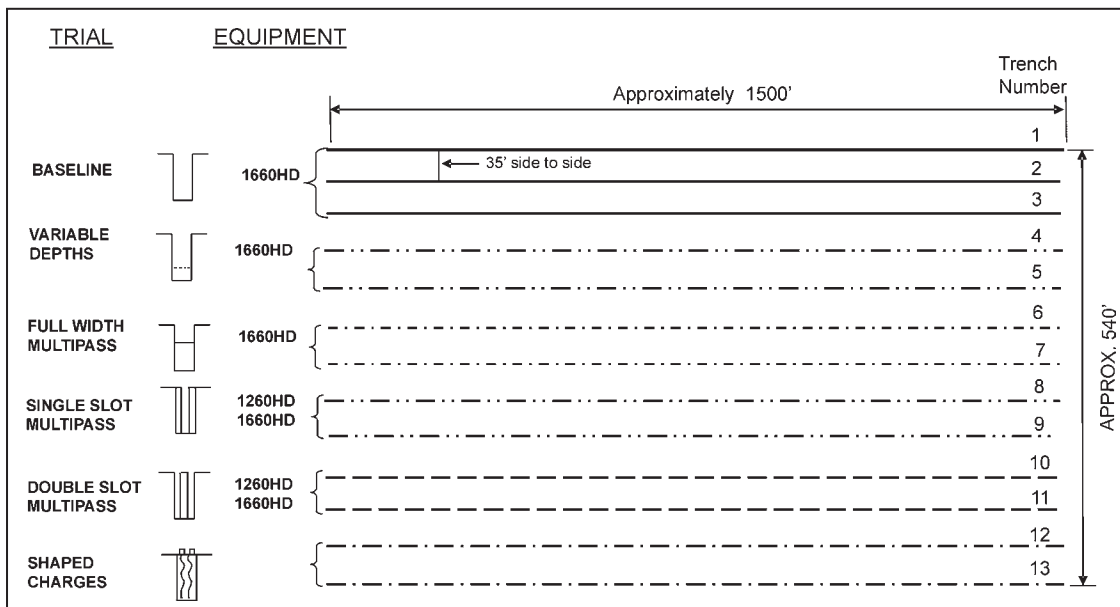


Figure 60. Layout of the trenching trials at Material Site 3 for evaluating the feasibility and costs of various techniques for creating a trench for a buried gas pipeline (courtesy of BP).



Figure 61. View of a chain-trenching machine showing the initial shallow pass and the stockpiling of soil material for later backfilling of the trench (photo by D. Blanchet).

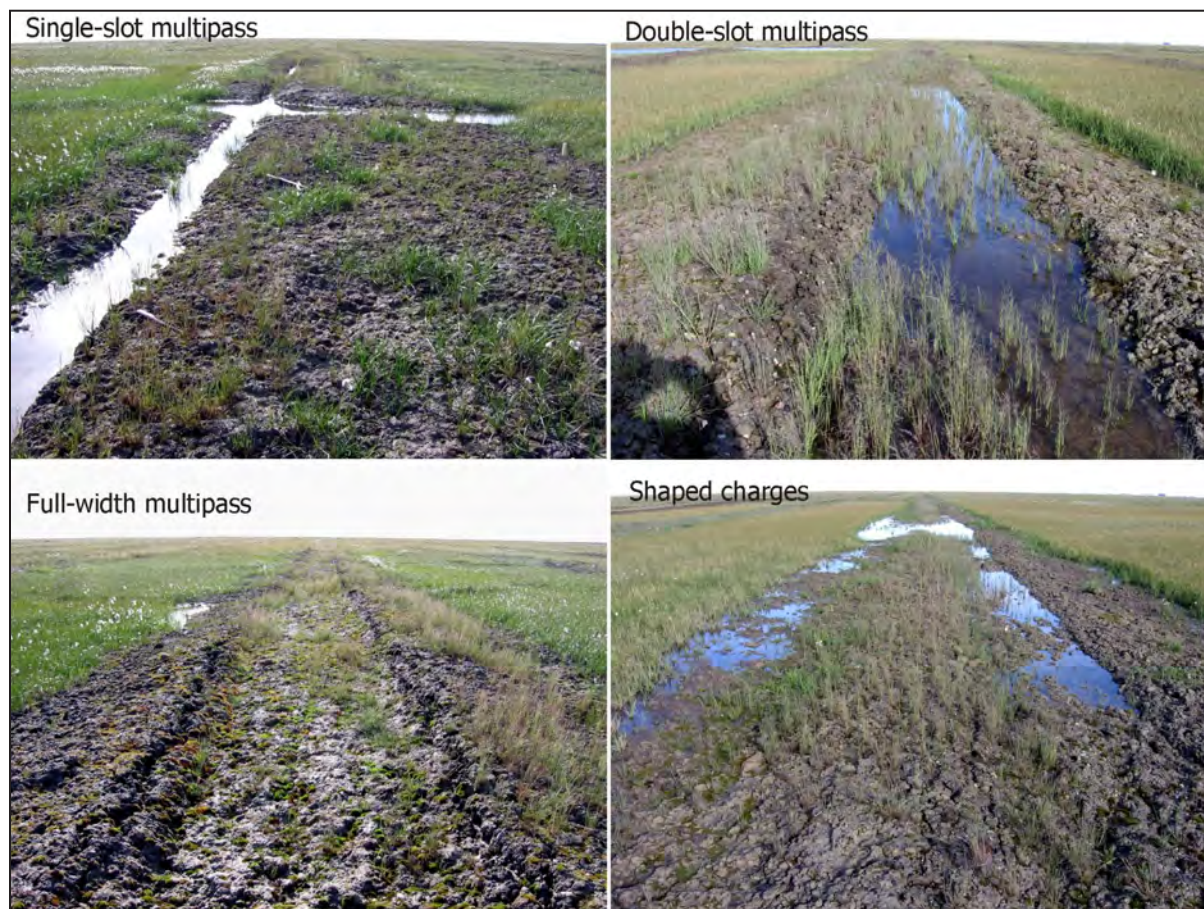


Figure 62. Views in 2006 of trenches created in 2002 by four trenching techniques and subsequently backfilled with ice-rich spoil material (photos by ABR).

STOP 5: RIVERBANK EXPOSURE ALONG SAGAVANIRKTOK RIVER

Deadhorse is situated next to the Sagavanirktok ('Sag') River (fig. 63), a large braided river system whose headwaters originate in the Brooks Range, and which drains about 4,817 km² (1,860 mi²). In the lower stretch of the river the floodplain is 12.5 km (7.8 mi) wide, although a 4.2-km- (2.6-mi-) wide section of coastal plain deposits separates the two main channels. Discharge of the Sag River has been continuously monitored at Pump Station 3 since 1982. The floodplain has broad expanses of barren, gravelly channel deposits created by active bed-load movement and highly varying rates of discharge, from peak flows during spring snowmelt to low flows during mid-summer. Most of the remaining floodplain is occupied by inactive channel deposits with gravelly soils, and supports expansive terraces with dryas dwarf shrub vegetation. Thick accumulations of fine-grained overbank deposits are uncommon.

The inactive-floodplain overbank deposits have thick accumulations of fine-grained sediments with abundant ground ice (fig. 64). The ice wedges, and the segregated ice in soils between the wedges, deform and raise the



Figure 63. A 2007 airphoto of riverbanks along the Sagavanirktok River near Deadhorse.



Figure 64. Views of a soil exposure along the bank of the Sagavanirktok River illustrating a 1.5 -m- (4.9-ft-) wide ice wedge and cryoturbation of soil horizons, along with reticulate to ataxitic ice morphologies (photos by T. Jorgenson).

surface during floodplain development (Shur and Jorgenson, 1998). Ice wedges of inactive floodplains typically are modest in size (1–2 m [3.3–6.6 ft]) and cause the deformation of soils into low-centered polygons with low rims. The fine-grained soils support the formation of well-developed reticulate and ataxitic (suspended) ice structures that typically occupy 70–80 percent of the soil volume. Soils are greatly deformed by the syngenetic ice development, active layer processes, and repeated freezing and thawing of the transient layer at the top of the permafrost.

STOP 6: PUMP STATION 1

It is from Pump Station 1 (PS-1) that Alyeska's Trans-Alaska Pipeline System (TAPS) begins its long and rugged run to the port of Valdez, where the oil is transported by oil tankers to the lower 48 states (fig. 65). At startup in 1977, there were eight pump stations operating the TAPS system, although the original design called for 12 (APSC, 2008). Two pump stations (2 and 7) were added in 1979–1980. At maximum throughput there were 11 pump stations. By 2004, the number of pump stations had been reduced to six (Pump Stations 1, 3, 4, 7, and 9), while PS-5 is a relief station. Each pump station has 10–25 Alyeska employees that work 12-hour daily shifts on a 1-week-on/1-week-off, or 2-weeks-on/2-weeks-off schedule.

At PS-1 the produced crude oil is metered from the sales pipelines carrying separated oil ready for refining from the various oilfields and is gathered in large storage tanks (fig. 66). The oil then flows to the booster pump room and the main turbine room to create the pressure for pushing the oil through the pipeline. The oil flows from the main turbine room through the pig-launching building, where pipeline inspection gauges ('pigs') are regularly sent through the line. Different types of pigs are used for various functions. Some remove buildup of paraffin on the insides of the pipe. Other pigs are equipped with complex electronics that relay radar scans and fluid measurements as they travel down the line; the data they report can be used to assess pipeline integrity. A control room directs the operations and coordinates throughput with other pump stations. Other support facilities at the pump station include offices and living quarters, shops, fuel-handling buildings, and communications. PS-1 was built in the middle of a lake basin, which was purposely drained to provide terrain with relatively low soil ice contents (fig. 65). PS-1 has five refrigerated foundations to ensure the stability of the foundations on permafrost.

Like most stations, PS-1 has two mainline full-head pumps capable of pumping ~1 million bbls per day (APSC, 2008). The full-head pumps are two-stage pumps with impellers in series with one inlet and outlet, each capable of pumping 75,700 L/min (20,000 gal/min). In addition, PS-1 has additional booster pumps to move oil from the storage tanks to the main line and to boost oil pressure. At PS-1 the crude oil is injected into the pipeline at 45.6°C

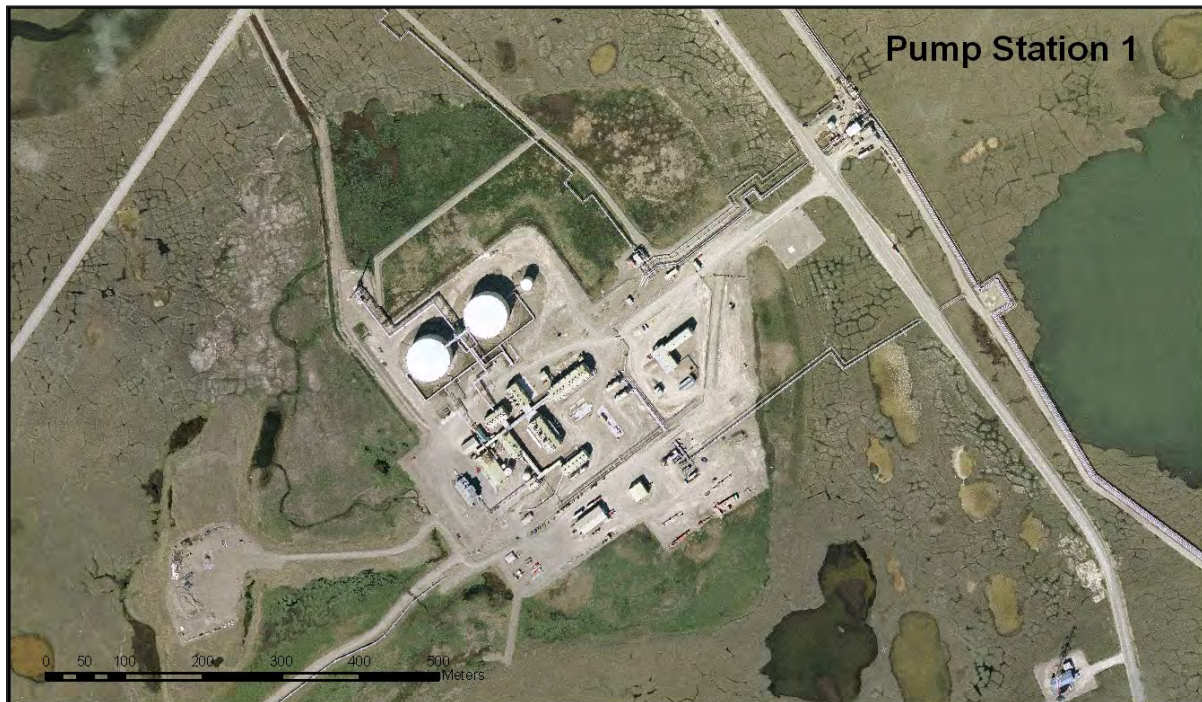


Figure 65. A 2007 airphoto of Pump Station 1, the start of the Trans-Alaska Pipeline.

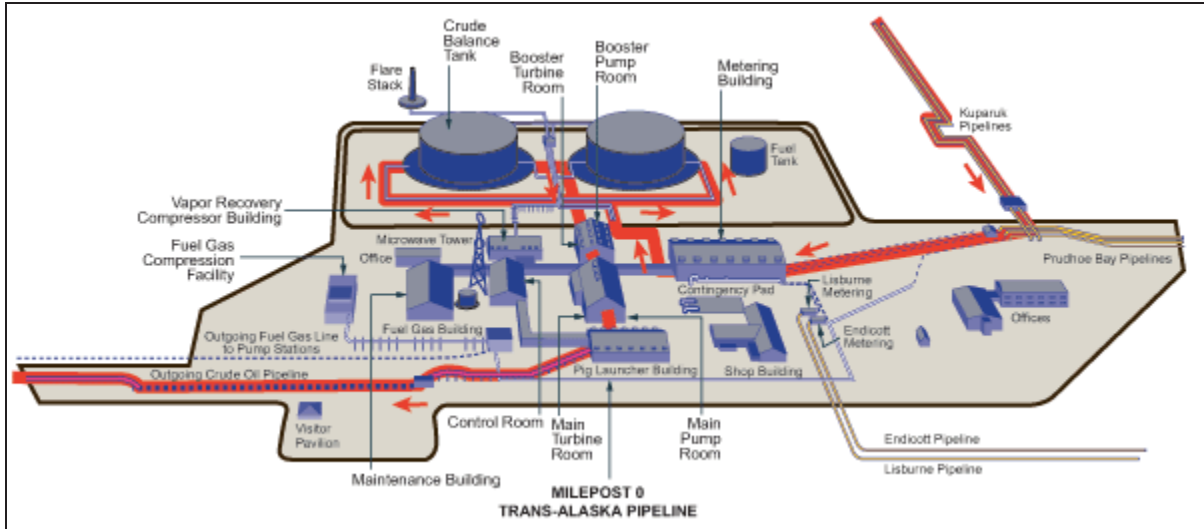


Figure 66. Layout of the facilities at Pump Station 1 (BLM, 2003).

(114°F) and by the time it reaches the terminal at Valdez the temperature drops to ~18°C (~65°F). Over the 9-day travel period, the oil moves at an average of 6 km/hr (3.7 mi/hr). At capacity, the pipeline holds 9 million bbl. Additional holding capacity is available at the pump stations to adjust oil throughput along the many segments and varies from 420,000 bbls at the gathering point at PS-1, 150,000 bbls at PS-5 on the south side of the Brooks Range, to 55,000 bbls at the other pump stations. The pipeline is designed to operate at a maximum of 8,136 kPa (1,180 psi). At Pump Station 1, drag-reducing agents are added to enhance flow and throughput with fewer pumps. They were first used in 1979 (fig. 67).

The TAPS is an engineering marvel that crosses 1,287 km (800 mi) of rugged terrain, including two high mountain ranges, 800 rivers and streams, and three major active faults with high earthquake hazard. It consists of the pipeline, pump stations, a marine terminal, and associated facilities and systems. About 676 km (420 mi) of the 122-cm- (48-in-) diameter pipeline are built above ground on vertical support members (VSMs), 605 km (376 mi) of pipe are buried below ground using conventional methods, and 6.4 km (4 mi) are below ground in areas requiring special refrigeration. At the river and stream crossings, the pipe either bridges the waterways or is buried below them. At 13 locations, special bridges were built, including two suspension bridges.

To protect the integrity of the hot-oil pipeline in permafrost terrain, which occurs along ~75 percent of the route, much of the pipeline is built on VSMs (fig. 68). A total of 78,000 VSMs were used, including 16 different types to accommodate the variety of soil and permafrost conditions. They typically are 46 cm (18 in) in diameter and are embedded to depths of 4.6–21.3 m (15–70 ft). The standard VSMs are ~18 m (~60 ft) apart, while anchor-support VSMs are 245–550 m (800–1,800 ft) apart. In areas of warmer permafrost, particularly in central Alaska, 61,000 of the vertical support members are fitted with heat pipes (two per VSM) or thermal siphons that help protect the thermal stability of the permafrost by enhancing the loss of heat from the ground during winter.



Figure 67. A gooey, drag-reducing agent is injected into the pipeline to reduce friction, increase throughput, and reduce the number of turbines needed to push the oil (BLM, 2003).

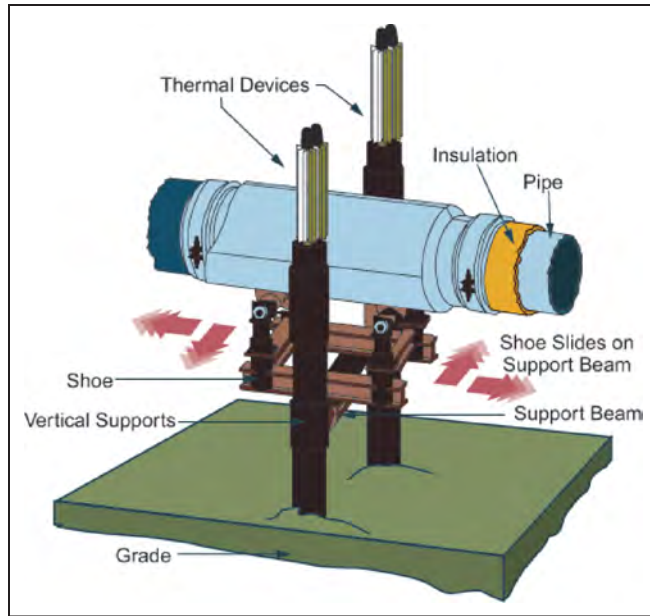


Figure 68. A diagram of the Trans-Alaska Pipeline System showing the special designs needed for cold climates, permafrost terrain, and seismically active conditions (illustration courtesy of Alyeska Pipeline Service Company). The thick insulation helps maintain the temperature and viscosity of the hot oil in the pipeline. The sliding shoes allow the pipeline to move as it contracts or expands during changing temperatures or in response to shifting ground during earthquakes. The vertical support members fitted with heat pipes, or thermal siphons, help protect the thermal stability of the permafrost by enhancing the loss of heat from the ground during winter.

Above-ground portions of the pipeline are built in a zigzag pattern to allow for thermal expansion (fig. 69). Each 12.2-m (40-ft) length of pipe expands and contracts 0.8 mm (0.03 in) with each 5.6°C (10°F) change in temperature. Consequently, there was ~23 cm (~9 in) of longitudinal expansion along a typical 220-m (720-ft) straight above-ground segment from the minimum length at the time of tie-in temperature during winter construction to the maximum length when hot oil started flowing and operating temperatures were achieved.

Control valves are strategically placed along the pipeline to permit isolation of sections of the pipeline and minimize the volume of potential spills. Of the 177 valves along the pipeline, 81 are check valves, 71 gate valves, 24 block valves, and one is a ball valve (fig. 70).

Actual pipeline construction began in April 1974 and was completed in June 1977 at a cost of approximately \$8 billion. At the time, it was the largest privately-funded construction project in history. Approximately 2,000 contractors and subcontractors, as well as ~70,000 workers, were employed to work on the project. TAPS is operated by Alyeska Pipeline Service Company on behalf of six owner companies. Federal and state governments cooperatively oversee the TAPS through the Joint Pipeline Office.



Figure 69. Views of the beginning of the Trans-Alaska Pipeline System at Milepost 0 and of the zigzag construction of the pipeline design to allow thermal expansion and contraction (BLM, 2003).

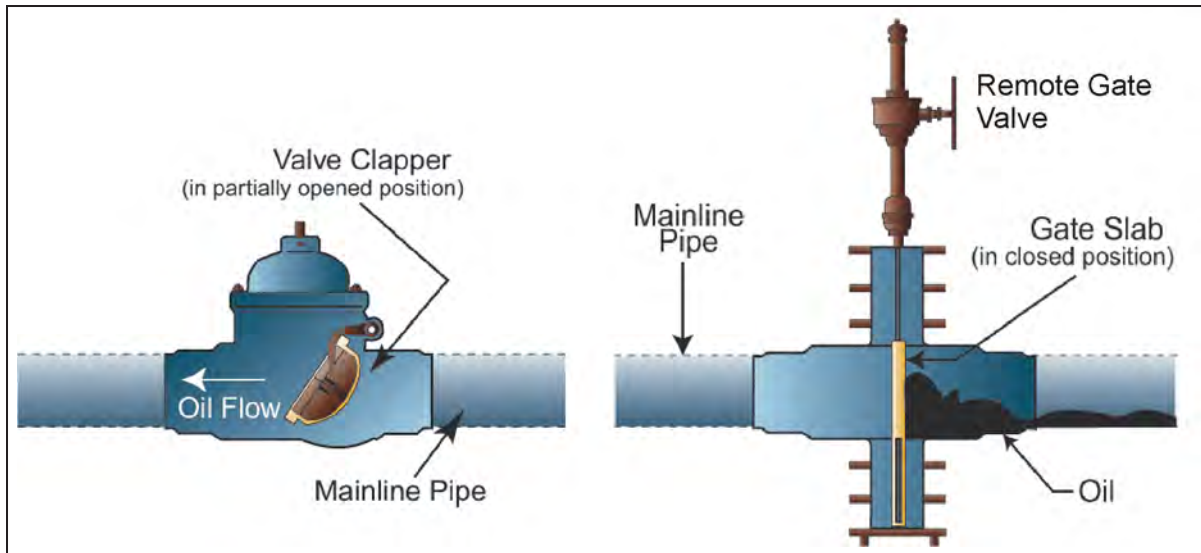


Figure 70. Diagrams of a check valve (with valve clapper) and gate valve used by the TAPS to control oil movement (BLM, 2003).

STOP 7: IMPOUNDMENT AT DRILL SITE 7

The impoundment of water by roads and pads is an extensive indirect impact of oil development in the Prudhoe Bay oilfield (Klinger and others, 1983; Walker and others, 1987; Auerbach and others, 1997; McKendrick, 2000; NRC, 2003). During early oilfield development little concern was paid to facility design and placement, leading to many road and pads being built within lakes, drained-lake basins, and across drainage-ways (fig. 71). In the Prudhoe Bay oilfield, impoundments covered 22 percent of the highly developed portion of the oilfield and 3 percent of the broader oilfield (Walker and others, 1987). Drill Site 7 provides a dramatic example of gravel fill placement in the middle of a lake and the constraint of water movement by two roadways.



Figure 71. A 2007 airphoto of an impoundment caused by parallel gravel roads near Drill Site 7. During the 1970s, little effort was undertaken to site facilities to avoid impedance of cross-drainage flow.

The flooding of wet and moist tundra, which typically occurs in low-lying lake basins, has many ecological effects (NRC, 2003). The additional water drowns and kills vegetation, can lower the albedo, increase heat flow to surface soils, and cause thermokarst. The high seasonal fluctuations in water levels in drained-lake basins, which provide high-value bird habitat, are deleterious to nesting birds (Truett and others, 1997).

STOP 8: OIL SPILL CLEANUP AND RESTORATION NEAR GC2

The largest spill in the history of the Prudhoe Bay oilfield originated from the transit line that delivers oil from Gathering Center 2 to the trans-Alaska pipeline. The spill was discovered on March 2, 2006, by a British Petroleum employee (Bailey, 2006). An estimated 760 m³ (200,000 gal) leaked from the pipe and flowed across the tundra underneath the snow. The leak originated from a one-quarter-inch hole in the bottom of a section of line buried under what is termed a caribou crossing, a gravel-covered culvert designed to allow animals to cross over a pipeline as opposed to going under an elevated pipeline. Because winter snow covered the leaking oil, the spill remained undetected by pressure sensors for several days until a well-pad operator smelled the oil fumes. The hole was determined to have been caused by corrosion associated with sulfate-reducing bacteria inside the pipeline. The spill affected 0.8 ha (1.9 ac) of moist sedge-shrub tundra between the southern shoreline of Q Pad Lake and the pipeline access road south of the lake, as well as a portion of Q Pad Lake itself (fig. 72). The boundary of the spill was established by digging pits in the snow to search for visible oil.

Cleanup and oil recovery began immediately and progressed in two phases. During Phase 1, much of the free product that had pooled in polygon troughs and local depressions was removed with pumps and suction hoses. Next, clean snow was collected from Q Pad Lake and packed onto the site to absorb free oil from the tundra surface. In Phase 2, the remaining oil was removed by mechanically sweeping and ‘trimming’ the tundra surface (fig. 73). Both of these operations were intended to remove surface oil and oil-saturated organic soil, while leaving the bulk of the plant root material intact wherever possible. However, the irregular surface of the tundra and the presence of subsurface oil contamination, especially above and within ice wedges along polygonal troughs, required much of the site to be trimmed to a depth below the plant rooting zone. The excavation was guided by sampling soil periodically at selected locations to determine the presence or absence of hydrocarbon contamination. These results were used to delineate areas that met cleanup criteria specified by the Alaska Department of Environmental Conservation. Cleanup operations were completed on April 19, 2006.



Figure 72. A 2007 airphoto of the GC2 oil spill site (dark soil in center) after cleanup and ecological restoration.

Restoration treatments began on April 19, 2006 (Cater, 2007). The excavated area was backfilled with clean tundra soil until the new surface was brought up to slightly higher than original tundra grade. The soil was obtained from the Put River mine site where the organic mat had already been excavated and stockpiled in preparation for gravel mining. Intact blocks of frozen tundra soil with dormant vegetation also had been stockpiled, and these were placed on top of the backfill material to provide native plant materials for vegetation recovery. The final ground surface elevation was 15–30 cm (5.9–11.8 in) higher than the original tundra surface to compensate for the settlement that was expected to occur in the backfill material. Large blocks of frozen soil were wrapped with erosion control blankets and placed on the lake shoreline to reduce the risk of erosion. Shore-seal booms were



Figure 73. Views of techniques used to clean up a crude oil spill near GC2 in Prudhoe Bay and to restore tundra vegetation damaged by the oil and the cleanup (photos by T. Jorgenson and T. Cater).

installed along the shoreline of the backfilled area to dampen wave action, minimize erosion, and contain any sheens from residual oil. The frozen blocks of dormant tundra were covered with ~0.5 m (~1.6 ft) of clean snow to prevent early sprouting and mortality of plants, reduce solar radiation on the barren surface and heat flow into the permafrost, and provide a source of water for plant growth in early spring. In early June, the area was fertilized, and soil blocks that had landed upside down during initial placement were overturned. In 2007, additional fresh tundra sod blocks from the Put 23 mine site were hand transplanted over ~100 m² (1,075 ft²) beneath the pipelines and near the spill origin by the Barrow Village Response Team (fig. 74).



Figure 74. Views in 2007 of regrowth of tundra sod chunks spread during the winter and hand transplanting of live tundra sod mats during the summer to help restore the tundra damaged by the oil spill and cleanup at the GC2 oil spill (photos by T. Cater, ABR, and BP, 2007).

STOP 9: BETTY PINGO

Betty Pingo is the largest steep-sided pingo in the Prudhoe Bay oilfield (fig. 75) and measures 14 m (46 ft) tall and 150 m (492 ft) in diameter (Walker and others, 1985). Walker and others (1985) mapped 766 mounds within the Beechey Point Quadrangle and differentiated 373 as steep-sided pingos and 393 as broad-based mounds (fig. 76). The steep-sided pingos have small basal diameters (<200 m [<650 ft]), steep side slopes, and primarily occur in drained-lake basins (fig. 77). In contrast, the broad-based mounds have much larger mean diameters (242 m [794 ft]) and commonly occur outside recognizable lake basins indicative of ancient origins. Coring of one broad-based mound, C-60 in the Kuparuk oilfield, revealed a massive ice core, indicating that they too are pingos (Walker and others, 1985). The largest pingo (52 m [170 ft] tall) on the coastal plain is the Leffingwell Pingo near the Kadleroshilik River and was originally surveyed by Leffingwell (1919). Although he speculated on an origin involving water under pressure (artesian), it was Porsild (1938) who identified the basic mechanism of hydrostatic pressure involved in the formation of pingos.

The Betty Pingo site became a prominent monitoring site under a major study of land–air–ice interactions funded by the National Science Foundation (Kane and Reeburgh, 1998). A 1-km by 1-km (0.6-mi by 0.6-mi) grid was established in 1993 for monitoring maximum seasonal thaw depths as part of the Circumarctic Active Layer Monitoring (CALM) program (Brown and others, 2000; Hinkel and Nelson, 2003). At the Betty Pingo grid, mean thaw depths peaked during the record warm summer in 1998, but have not shown a consistent trend in depths since data were first collected in 1993 (figs. 21 and 78).

A continuous record of meteorological, hydrological, and soil data has been collected at Betty Pingo since 1994, as well as at nearby sites at West Dock (1995) and Putuligayuk River (1999) to the east (Mendez and others, 1998; Kane and others, 2000). Radiation and soil temperature information is collected over a wet, marshy location by the main meteorological tower (Betty Wetland/Met, 70°16'46.3" N, 148°53'44.5" W) and also from a drier, higher location a few meters away (Betty Upland, 70°16'46.9" N, 148°53'46.5" W). A rain gauge collects precipitation data, while soil moisture is measured using time domain reflectometry. The data help characterize the 471 km² (182 mi²) watershed of the Putuligayuk River, which is totally confined to the low-gradient coastal plain dominated by wetlands, ponds, and wind-oriented lakes. The USGS gauged the 'Put' for 15 years, from 1970 to 1986 (data for 1980 and 1981 missing). Surface drainage from the smaller Betty Pingo catchment (8.15 ha [20.14 ac]) is quantified by means of a V-notch weir. The water equivalent of the snowpack is measured late each spring at these sites just before melt begins (Kane and others, 2000).



Figure 75. A 2004 airphoto of the Betty Pingo (top, center).

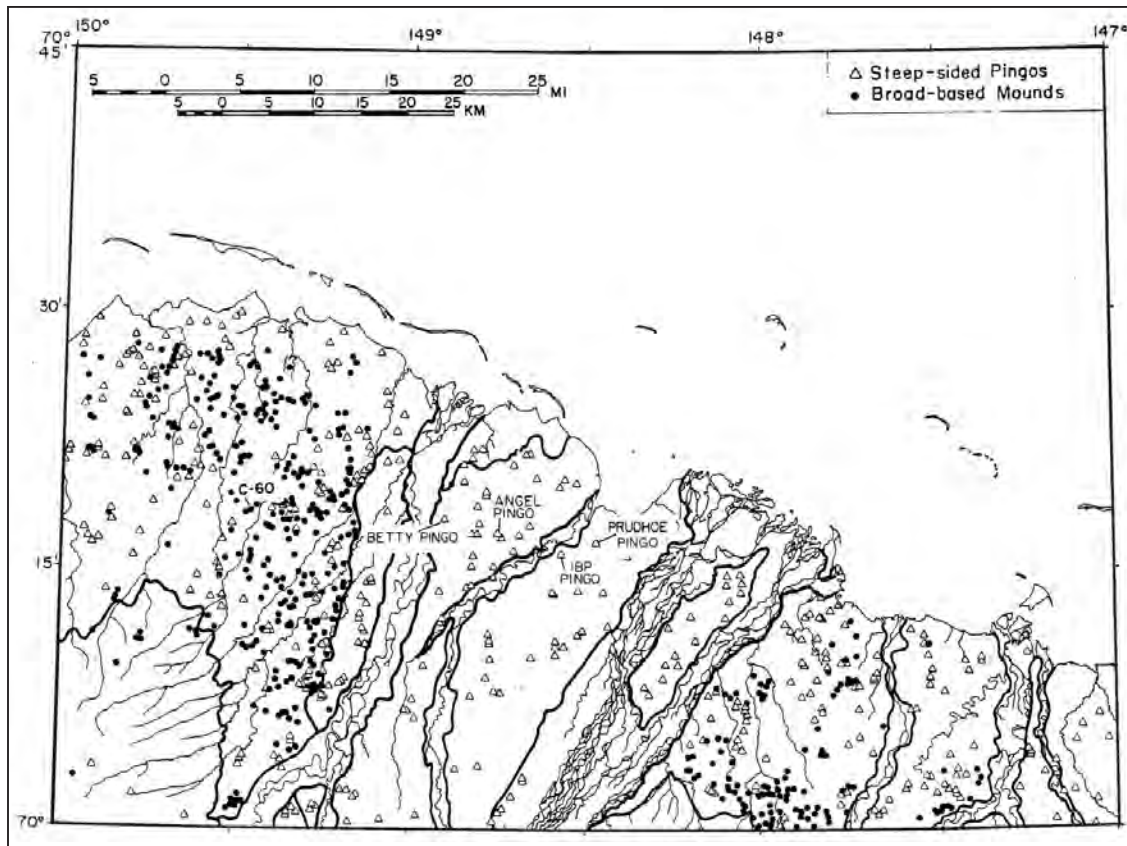


Figure 76. Distribution of 766 steep-sided pingos and broad-based mounds within the Beechey Point Quadrangle encompassing the Prudhoe Bay and Kuparuk oilfields (from Walker and others, 1985).



Figure 77. The Prudhoe Pingo (photo by D. Kane).

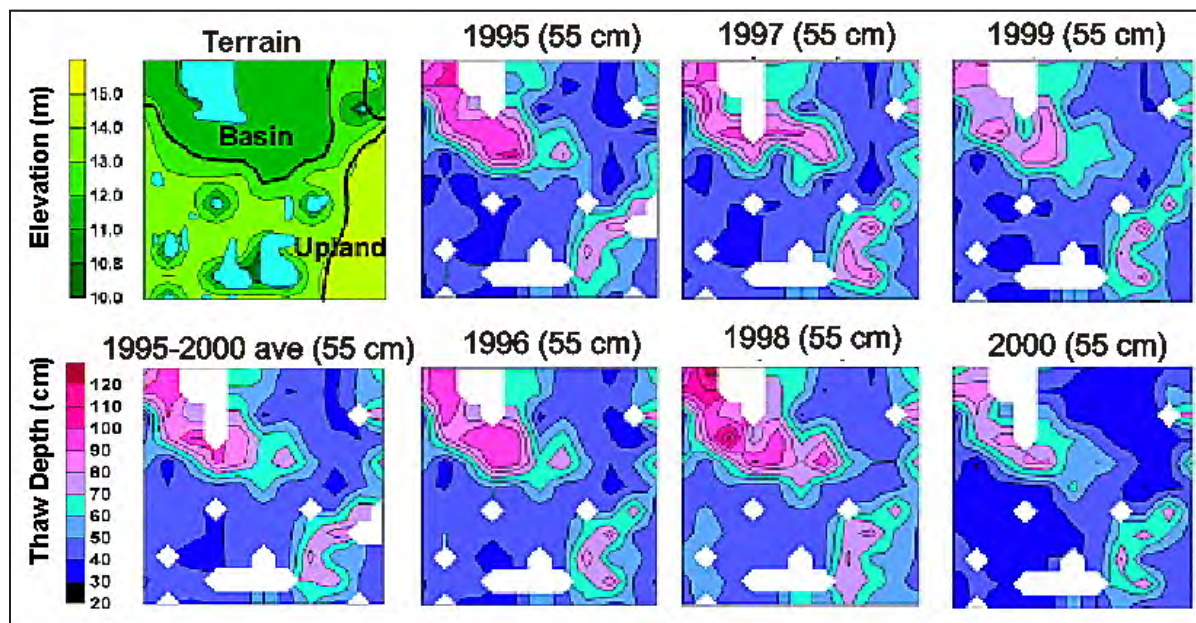


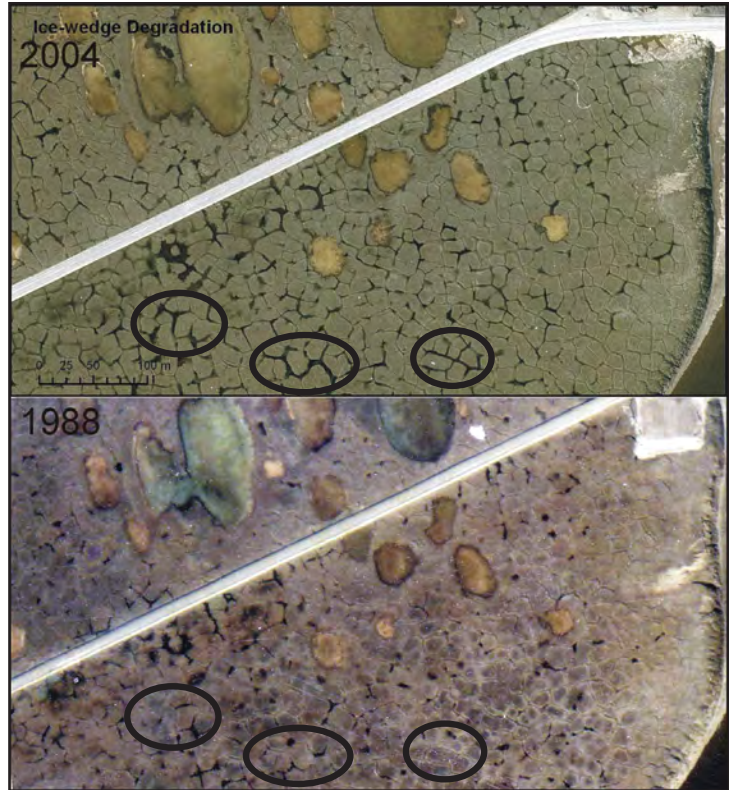
Figure 78. Maps of topography (upper left) and thaw depths extrapolated from the 100-m- (330-ft-) spaced measurements from the Circumarctic Active Layer Monitoring grid at Betty Pingo (adapted from Hinkel and Nelson, 2003).

STOP 10: ICE-WEDGE DEGRADATION

Ice wedges are particularly sensitive to disturbance and climate change because they form just below the active layer (Jorgenson and others, 2006). At this site adjacent to the west bank of the Kuparuk River, a comparison of 1988 and 2004 airphotos reveals extensive new degradation both near and far from the road (fig. 79).

Observations by Jorgenson and others (2006) in the National Petroleum Reserve—Alaska indicate that there has been a dramatic increase in the degradation of ice wedges, presumably due to climate warming during the last two decades. They inferred from climate and thaw-depth data that the degradation was initiated by the unusually warm and wet summer in 1989. This degradation is also prevalent in the Kuparuk and Prudhoe Bay oilfields.

Figure 79. A comparison of airphotos from 1988 and 2004 reveals extensive degradation of ice wedges on coastal plain deposits adjacent to the Kuparuk River.



STOP 11: TUNDRA FROST SCARS

Frost scars, also called frost boils, play an important role in tundra ecosystems by disturbing the surface, affecting the burial of organic matter deep into the soil profile, influencing the flux of trace gases to the atmosphere and the flux of water and nutrients to streams, and affecting wildlife habitat (Walker and others, 1980; Walker and others, 2004; Sutton and others, 2007; Bockheim and Hinkel, 2007). They are especially prevalent on upland terrain in the Kuparuk region (figs. 80 and 81). These features are described in Part 1.



Figure 80. Aerial view (left) of abundant frost scars on coastal plain deposits in the Kuparuk oilfield, and a ground view of active frost scars near Galbraith Lake (right) in the Brooks Range (photo by T. Jorgenson).



Figure 81. Frost scars evident on a 2004 airphoto.

STOP 12: KUPARUK OPERATIONS CENTER

The Kuparuk oilfield is the second largest producing oilfield in the United States (fig. 82). The Kuparuk River Unit (with satellite fields), before it incorporated several satellite fields into the newly renamed Greater Kuparuk Unit, was estimated to have had 2.9 billion bbls of reserves. It was deemed economic for development in 1977 after completion of the Trans-Alaska Pipeline. About 2,000 directional or horizontal wells have been drilled to fully develop the Kuparuk River field. Kuparuk includes three large central production facilities and a seawater treatment plant for use in production. The seawater is mixed with water produced during oil extraction, and this mixture is injected into appropriate zones in the subsurface. The Kuparuk Operation Center comprises a Central Production Facility 1, housing and dining facilities, management offices, a wastewater treatment plant, shipping facilities, and maintenance shops (fig. 83). Kuparuk-associated solid wastes are shipped to the regional landfill at Prudhoe Bay, and hazardous wastes initially were shipped 3,220 km (2,000 mi). Advances in recycling and a 95 percent reduction in construction and waste material at the Kuparuk River Unit won the U.S. Environmental Protection Agency's (EPA) Evergreen Award for Pollution Prevention in 1999.

At a central processing facility the oil produced from the drill sites is treated to separate the crude oil, natural gas, and brine extracted from the subsurface formations. This involves multiple stages where the mixture is separated at varying pressures and then run through a sequence of coolers, separators, scrubbers, heaters, and compressors (fig. 84). After separation the crude oil is sent down the sales line (a line carrying separated oil product ready for sale to a refinery) to Pump Station 1, the natural gas is sent to the Central Gas Facility for re-injection, diesel-range hydrocarbons and gas are portioned off for oilfield use, and water is returned to the drill sites.

STOP 13: REHABILITATION OF GRAVEL WASHOUTS AT CULVERTS

Adequate design of cross-drainage structures is difficult on the flat coastal plain environment (fig. 85). Culverts are used in most situations to provide hydrologic connections beneath the gravel, but culverts often stay frozen during the early summer and delay movement of water during snowmelt. Although substantial effort is made to thaw and clear culverts prior to breakup, culverts occasionally have difficulty passing the high spring discharge or they can create scour problems near the roadbed. In addition, thaw settlement beneath the culverts and heavy road traffic often cause the culverts to be depressed in the middle and uplifted at the ends (fig. 86). Inadequate culvert design at small stream crossings has led to occasional scouring and gravel deposition on the adjacent tundra. During the early 1990s, there was a large effort to remove the gravel, which was considered non-permitted gravel fill, from the tundra (Ott, 1993b). In more recently developed oilfields, considerable attention has been paid



Figure 82. Landsat image (circa 2000) of the Kuparuk oilfield. Numbers indicate tour stops at: (12) Kuparuk Operations Center, (13) gravel washout, (14) Mine Site D, (15) oil spill near Drill Site 2U, (16) young and old drained lake basins near CPF3, (17) Drill Site 3O, (18) Drill Site 3R, and (19) coastal margin near Oligtok Point.



Figure 83. Airphoto of the main operations center in the Kuparuk oilfield. The center includes Central Processing Facility 1, housing and logistical support facilities, Mine Site C, and the start of the major oil pipeline from Kuparuk to Pump Station 1.

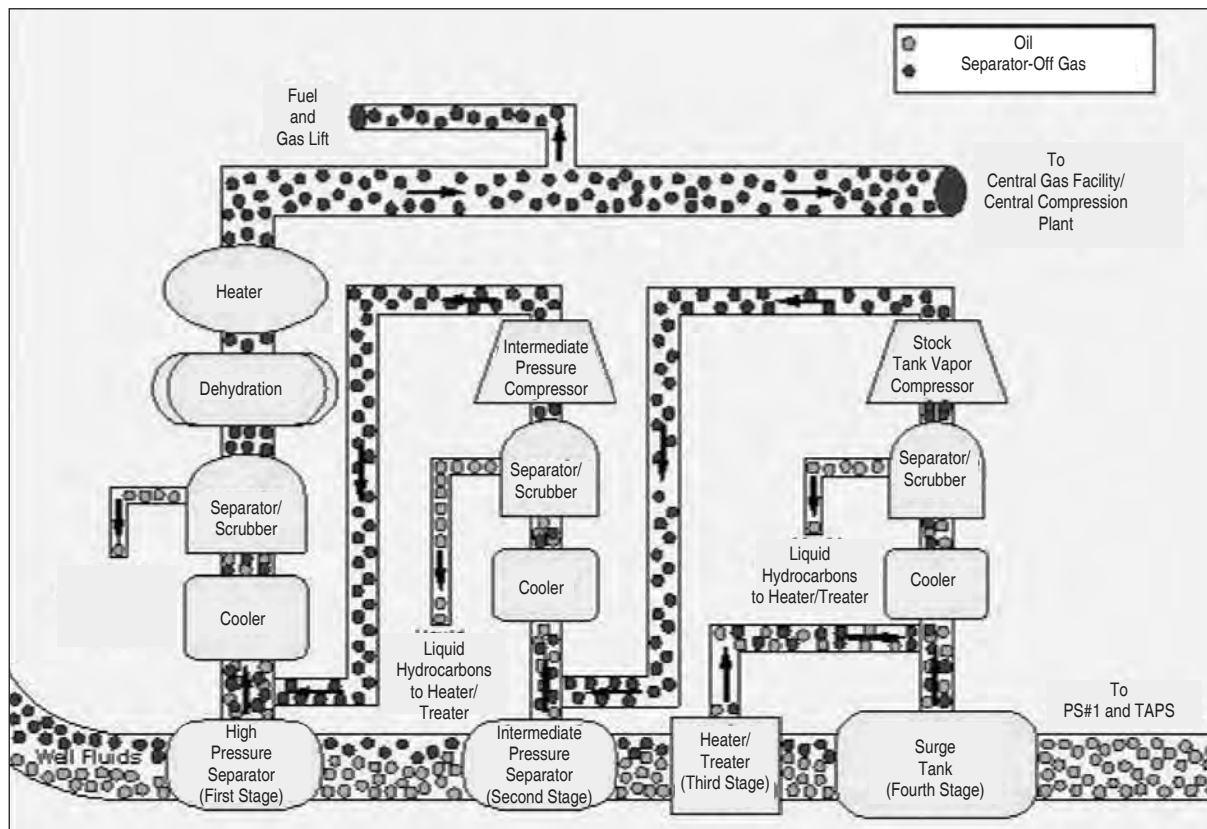


Figure 84. Diagram of the processing stream for produced oil at a central processing facility (courtesy of Alaska Division of Oil & Gas).



Figure 85. A 2004 airphoto of the location of a gravel washout downstream (above the road) of the main spine road near the Kuparuk operations center.



Figure 86. Views of problems associated with culverts and gravel deposition on tundra, including: (A) the deposition of gravel on tundra, and (B) uplifting of culvert ends that reduce passage of water when water levels are low. To remove gravel outwash from the tundra, (C) large backhoes, and (D) hand labor and a conveyor-belt system have been used (photos by T. Jorgenson and T. Cater).

to locating roads and pads on higher terrain to avoid cross-drainage problems (BLM, 2004). In the new Alpine oilfield, culverts were sited in the lowest microsites along ice-wedge troughs and were underlain with insulation and a gravel bed to prevent settling and blockage of the culverts. Follow-up hydrologic monitoring indicates the better-designed culverts to be functioning well.

In areas where the gravel is relatively thin, tundra vegetation is able to sprout up through the gravel, but in areas where the gravel is >10 cm (>4 in) thick the surface remains barren for long periods until the gravel is colonized by species adapted to disturbed sites (Jorgenson, 1988; McKendrick, 2000). To clean up the gravel at numerous stream crossings, specially equipped backhoes, vacuum trucks ('supersuckers'), and hand labor were used to remove the gravel (Ott, 1993a). Fertilizer has been applied at some sites to enhance recovery.

STOP 14: LAND REHABILITATION AT MINE SITE D

Mine Site D, which was excavated in the late 1970s to provide gravel for roads and pads in the Kuparuk oilfield, has two main components: the deep gravel pit and the extensive overburden stockpile derived from silty sand deposits unsuitable for road material. Beginning in the late 1980s, the area became the site for intensive research into the rehabilitation of abandoned mine sites (fig. 87). To enhance the availability of deepwater (>2 m [>6.6 ft] deep) habitat for overwintering fish in a region dominated by shallow lakes that freeze to the bottom in the winter, channels were cut to connect the adjacent stream to the pit; the pit was then flooded. Grayling were later transplanted into the resulting lake and it has become a popular spot for sport fishing (Hemming, 1988; Hemming, 1995).

In 1992, an experiment was initiated to evaluate the feasibility of creating wetlands on a dry overburden stockpile (fig. 88) by constructing a large berm to collect snow and smaller berms to impound the meltwater (Jorgenson and others, 1992a). The developing waterbody was infused with invertebrates and microorganisms by pumping water from a tundra pond into the basin. Sprigs of *Arctophila fulva*, an important aquatic grass for algal growth, invertebrates, and waterbirds (Bergman and others, 1977), were transplanted into the perched pond after previous research had shown that it was readily amenable to transplanting (Moore and Wright, 1991; McKendrick, 1990).

The abandoned gravel pad along the access road to the pit, which was used as a staging area during mining, was used for evaluating several techniques for rehabilitating gravel pads (fig. 88). Experiments were set up to evaluate polygonal patterns of low berms that were created to capture snow and enhance meltwater input and soil



Figure 87. A 2004 airphoto of Mine Site D after completion of rehabilitation activities that included: (1) connection of the mine site to the adjacent creek to provide deep-water fish habitat, (2) creation of large berms to collect snow and impoundments to create perched ponds, (3) revegetation of the overburden stockpile, and (4) revegetation experiments on thick gravel fill.

moisture, the addition of organic-rich topsoil to enhance long-term soil properties, mulching to reduce evaporation, and application of various plant cultivation techniques (Jorgenson and Cater, 1992). The combination of berms, organic topsoil, mulching, and seeding with native-grass cultivars resulted in the highest plant cover values of any experimental treatment evaluated in the Kuparuk Oilfield (Jorgenson and others, 1995, 2003d). While the costs are modest, the availability of organic topsoil in the oilfields is limited. The seeding of locally collected legumes have been evaluated at mine sites D and F because of their symbiotic relationship with nitrogen-fixing bacteria that can provide a long-term source of nitrogen on extremely nutrient-poor gravel fill. Since its planting in 1989, vegetation in the polygonal basins has slowly diminished, while the legumes in the adjacent demonstration plot have spread vigorously.



Figure 88. Mine Site D in the Kuparuk oilfield has been the site of wide-ranging rehabilitation studies including the flooding of the mine site to create fish overwintering habitat, testing of techniques for rehabilitating thick gravel pads by creating low-centered polygons to capture snow and seeding with legumes, and converting dry overburden stockpiles to wetlands by impounding snowmelt into perched ponds and planting *Arctophila fulva* sprigs (photos by T. Jorgenson and T. Cater).

STOP 15: OIL SPILL CLEANUP AND RESTORATION NEAR DRILL SITE 2U

In late August 1989, an estimated 300–600 bbls of crude oil and produced water were accidentally released from a valve in a production flowline from Drill Site 2U in the Kuparuk oilfield (fig. 89), contaminating 0.6 ha (1.5 ac) of arctic coastal tundra (Jorgenson and others, 1991). The incident was the first significant oil spill to occur in the Kuparuk oilfield. Initial cleanup activities were conducted in 1989, and additional contaminated soil was scraped from the frozen tundra surface in April 1990. Bioremediation treatments were applied during 1990–1992 to reduce remaining hydrocarbon contamination, while promoting recovery of the damaged ecosystem. At the time of the 2U spill, information was lacking on the long-term consequences of oil spills in the Arctic, with respect to both oil contamination and ecological damage incurred during cleanup.

Cleanup techniques included containment with sandbags and absorbent materials, flushing the surface with warm and cold water to float and remove oil, physical removal of contaminated debris by raking and swabbing with absorbent material, and the use of plywood boardwalks to prevent trampling (fig. 90). The volume of crude oil



Figure 89. A 2004 airphoto of the location of the oil spill (marked with black outline and above pipeline intersection) that occurred in 1989 near Drill Site 2U.

remaining on the ground after initial cleanup was estimated at 18–50 bbls, equivalent to 0.6–1.7 L/m² (0.02–0.04 gal/ft²) if spread out evenly over the site. Because the stringent cleanup criterion of 500 mg/kg Total Petroleum Hydrocarbons (TPH) was not met during the fall cleanup, and bioremediation was considered unlikely to achieve that level in a timely manner, additional cleanup was done in April 1990 using a grader and loader to scrape 2–5 cm (0.8–2 in) of visually contaminated soil from the surface. The scraping yielded 137 m³ (179 yd³) of material, which contained approximately 70 percent snow and 30 percent organics. The material was thawed in a snow melter to separate the water from the particulate material for disposal. Final cleanup was completed in May 1990 when oily patches exposed to solar radiation had thawed. Hand raking of the oily patches yielded 15 m³ (19.6 yd³) of oily moss and soil.

Bioremediation treatments were applied during summers 1990–1992 to enhance biodegradation of remaining hydrocarbons. Treatments included: (1) removal of snow in April to enhance early thaw and lengthen the growing season; (2) dewatering the site with pumps to lower the water table to facilitate aerobic microbial activity; (3) watering during dry periods to maintain proper soil moisture; (4) fertilization to enhance microbial growth; (5) liming to control pH; and (6) mechanically perforating the soil with tines to improve soil aeration. In addition to these bioremediation efforts, thaw settlement was minimized by backfilling thermokarst troughs with organic soil.

Intensive, long-term monitoring of the site was conducted during the first seven years (1990–1996), with additional follow-up sampling in 2000 at the request of the Alaska Department of Environmental Conservation to provide data for negotiating close-out of the site and to document the fate of hydrocarbons after a longer period (Cater and Jorgenson, 2001). Monitoring revealed that the mean TPH concentration initially was 16,342 ppm (mg/kg, dry wt. basis) after fall cleanup, 3,446 ppm at the end of the first growing season in 1990, and 687 ppm in 1996 (fig. 91). In 2000 after TPH methods had been discontinued, analysis of diesel-range organics revealed a mean hydrocarbon concentration of 663 ppm. Total live vegetation cover increased from 11 percent after the first growing season in 1990 to 64 percent by 1996, as compared to 58 percent in undisturbed reference tundra, mostly due to the recovery of the sedges *Carex aquatilis* and *Eriophorum angustifolium*. By 1996, mean thaw depth in the affected area (46.3 cm [18.2 in]) was not significantly different from the unaffected adjacent tundra (41.6 cm [16.4 in]). Some thermokarst and increased surface water was evident shortly after the cleanup, but after organic soil was backfilled in troughs to stabilize the surface, the extent of thermokarst was not visually different from 1996 to 2000.

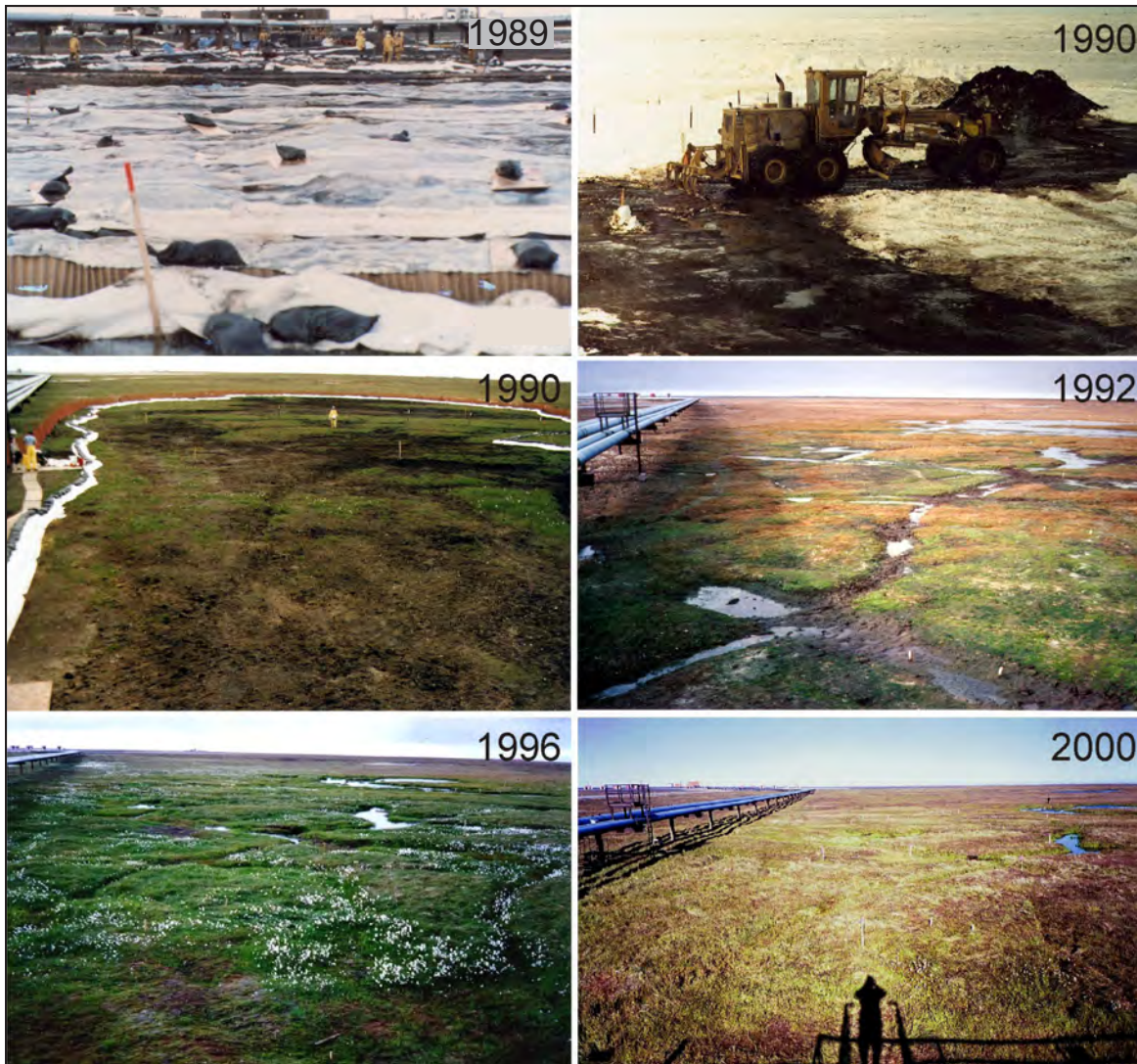


Figure 90. Views of the cleanup of oil spill site after initial flushing in fall 1989 and mechanical scraping in winter 1990. Vegetation was allowed to recover assisted only by fertilization and showed fairly rapid recovery from 1990 to 2000 (photos by T. Jorgenson and T. Cater).

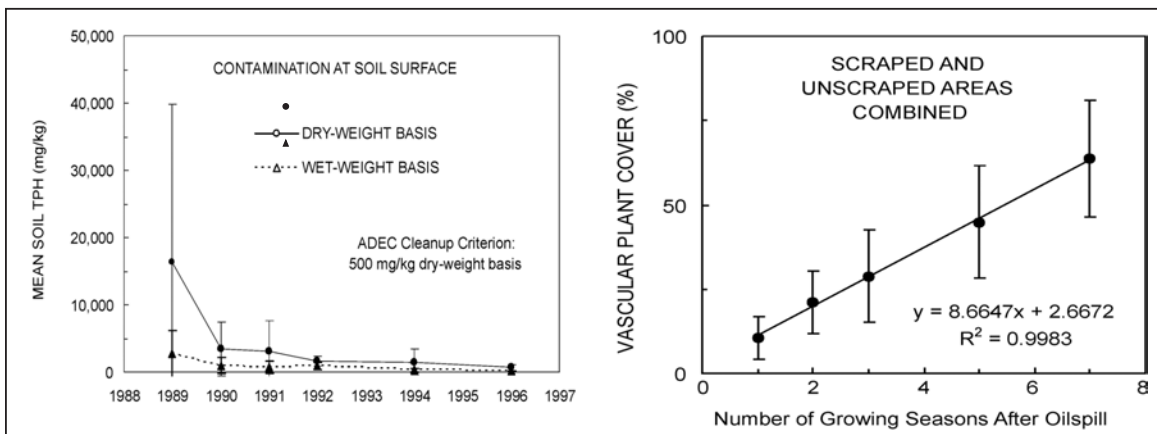


Figure 91. Changes in the concentrations of Total Petroleum Hydrocarbons (TPH) and percent of total live cover from 1989 to 1999 at a crude oil spill near Drill Site 2U (Cater and Jorgenson 2001).

STOP 16: DRAINED-LAKE BASIN AT CPF-3

Lakes (19 percent of area) and drained-lake basins (48 percent) dominate the landscape in the Kuparuk oilfield (Roth and others, 2007) and profoundly influence the hydrology, soils, vegetation, and wildlife use of the coastal plain environment. Recent work on the evolution of lakes and basins indicates that most of the lakes in this region are simply catchments of water in low-lying depressions and not thermokarst lakes (Jorgenson and others, 2006). Extensive coring and estimates of thaw settlement characteristics reveal that there is not enough ground ice in the coastal plain deposits to allow the formation of true thermokarst lakes (Pullman and others, 2007). In very old basins, such as on the left side of figure 92, numerous small ponds develop from the aggradation of ice and subdividing of larger waterbodies. Some have interpreted these small ponds to be small thaw ponds that eventually coalesce into larger waterbodies, but the presence of abundant limnic sediments in soils adjacent to the ponds and stable pond margins indicate that the ponds are infilling and shrinking instead of expanding.

Basins dramatically alter the hydrologic patterns of the landscape (Kane and others, 1992, Hinzman and others, 1998). Often the lakes and basins are hydrologically isolated and the drainage patterns are interrupted or indistinct. The annual water balance is dominated by the input of snowmelt during breakup. During the summer, however, water levels gradually draw down because of the very low amount of precipitation. Because of the seasonal patterns in the water balance and the poorly developed drainage network, river discharge from small streams that originate on the coastal plain becomes very low during the summer (McNamara and others, 1997).

Soils in drained-lake basins accumulate thick surface-organic horizons relatively rapidly because of the wet, anaerobic conditions (Hinkel and others, 2003a; Bockheim and others, 1999; Jorgenson and others, 2003c). While there has been considerable debate as to the long-term carbon balance of upland tundra (Oechel and others, 1993; McGuire and others, 2006), drained-lake basins with their relatively rapid peat accumulation are substantial sinks for carbon. Newly drained basins are devoid of ice wedges, although segregated ice can be substantial in thin bands below the active layer. At older stages of development, ice-wedges grow to 2–3 m (7–10 ft) in width and substantially deform the soils and surface topography.

Vegetation in the drained-lake basins shows dramatic shifts in species composition over time as nutrient availability and soils are altered by the changing surface drainage conditions associated with aggrading ground ice. The amount of drainage can be highly variable depending on the bathymetry of the lake and the depth of



Figure 92. A 2004 airphoto of a young, ice-poor, drained-lake basin (surrounding large pond on right) and an old, ice-rich lake basin (left side with many small ponds). The ice-poor basin lacks well-developed ice wedges and has numerous small ice-cored mounds (small white dots). The ice-rich basin has well-developed low- and high-centered polygons associated with well-developed ice wedges and numerous infilling small, shallow ponds.

the incised outflow channel, ranging from fully drained basins with exposed mudflats, to partially drained basins with only shallowly sloping margins exposed. In fully drained basins, the surface is rapidly colonized by *Senecio congestus*, *Deschampsia caespitosa*, *Puccinellia langeana*, and *Carex aquatilis* (Jorgenson and others, 2003c). In shallow water, the aquatic grass *Arctophila fulva* quickly exploits the nutrient-rich sediments. At the latest stages of lake-basin development, the surface becomes highly polygonized or has abundant narrow irregular string-like ridges. The better-drained areas have species typical of moist sedge-dwarf shrub tundra, while the oligotrophic wet meadows are dominated by *Carex aquatilis*, *Eriophorum angustifolium*, *Carex membranacea*, and *Salix lanata*.

Studies of bird use of arctic wetlands have revealed the importance of the complex wetlands in drained-lake basins (Bergman, 1977; Moitoret and others, 1996; Troy, 2000). The basins provide mosaics of shallow ponds, deep water, sedge and grass marshes, and raised tundra that provide a high interspersed of high-quality foraging, nesting, and breeding habitat.

STOP 17: BURIED RESERVE PIT AT DRILL-SITE 30

In response to concerns about the surface disposal of drilling waste in above-ground reserve pits, several drill sites in the Kuparuk oilfield disposed of drilling waste in deep sumps capped by thick overburden, with the concept that the waste would remain frozen and isolated in the permafrost. The below-ground-freeze-back technique for immobilizing drilling waste in permafrost was used at Drill Site 30. A deep sump was excavated in 1988 at the time of drilling and the overburden was stored on temporary ice pads on the north and south ends of the pits (fig. 93). In 1989, drilling muds and cuttings were disposed of directly to the pit, the waste was allowed to freeze back under the cold temperatures, and capped with a thick layer of the organic-rich overburden. In 1990, the cap was seeded with native grass cultivars and fertilized (Jorgenson and Cater, 1992).

Monitoring in 1991, 1992, and 1993 (Cater and Jorgenson, 1994) and 2000 (Bishop and others, 2001) revealed ~30 cm (~12 in) of subsidence of the north cap and ~40 cm (~16 in) of subsidence of the south cap, leaving the caps 20–30 cm (8–12 in) higher than the adjacent tundra. Mean thaw depths on the caps ranged from 57.1 cm (22.5 in) to 58.2 cm (22.9 in) in 2000. Total live vegetation cover increased from 16.3–28.9 percent in 1990 to 68.0–81.7 percent in 2000 on the two caps (Bishop and others, 2001). Over the intervening years, substantial ground settlement has occurred over thawing ice wedges in the areas of the temporary ice pads. In addition, small impoundments developed along a portion of the margins of the overburden cap.



Figure 93. A 2004 airphoto of Drill Site 30, which was developed in the mid-1980s. Drill-site development during that period included smaller gravel pads, compact placement of well sites (small boxes in center of pad), and burial and capping of drilling waste deep in permafrost (left side of pad).

STOP 18: LAND REHABILITATION AFTER GRAVEL REMOVAL

Placement of gravel fill for roads and pads is necessary during oil development to provide a stable surface for facilities and travel. After abandonment the dry, nutrient-poor gravel provides a very poor substrate for plant growth so productivity of reclaimed land remains low (Johnson, 1981). One strategy for improving the growing environment to one that is more conducive to restoring tundra plant communities similar to those lost under the fill is to remove the gravel (Jorgenson and Joyce, 1994; Jorgenson and others, 1995; McKendrick, 2000; Forbes and McKendrick, 2004; Kidd and others, 2004). To test revegetation techniques after gravel removal, an experiment was initiated in 1992 at a small section of road that had been removed in 1991 to compare the performance of five revegetation treatments (fig. 94). The treatments included natural recovery alone, natural colonization assisted with fertilizer, seeding with indigenous native plants, seeding with native grass cultivars, and transplanting of tundra plugs (Cater and Jorgenson, 1993). Other large experiments involving land rehabilitation after gravel removal have occurred at the S.E. Eileen exploratory well site (Jorgenson and others, 1992b), North State 2 exploratory well site (Jorgenson and others, 1993, Kidd and others, 2004), the Prudhoe Bay Operations Center (Kidd and others, 2006), and the Mobile Z Airstrip (ABR and BP, 2007).

Monitoring of surface stability, soil chemistry, and vegetation growth in 1995 and 1999 indicated substantial thaw settlement and good performance of many of the revegetation treatments (Bishop and others, 2000). Measurements of ground surface elevations and thaw depths revealed that the surface had subsided an average of 10 cm (3.9 in)



Figure 94. A 2004 airphoto of Drill Site 3R showing the thin, polygonized gravel fill (center of photo) remaining after removal of the short gravel road going directly to the drill site.

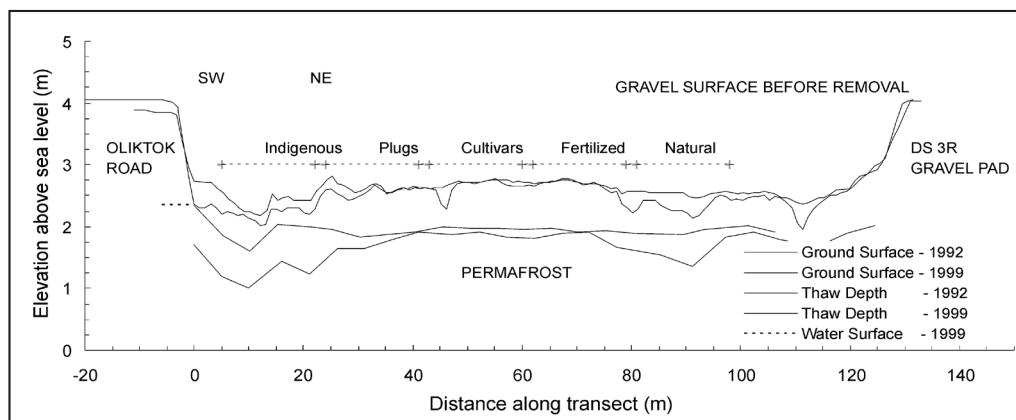


Figure 95. Cross-sectional profile of elevations of the ground surface and permafrost table across a former gravel road at Drill Site 3R (Bishop and others, 2000). Dashed line and cross-marks show boundaries of treatments. Original gravel surface before removal was even with Oliktok Road.

over 7 years and up to 25 cm (9.8 in) in areas underlain by ice wedges (fig. 95). After seven years, the native grass cultivars showed the greatest gains in total live cover (80 percent), followed by the plug transplants (55 percent). The dominant species in the cultivar mix were *Arctagrostis latifolia*, *Deschampsia beringensis*, and *Festuca rubra*, while the plugs were dominated by *Carex aquatilis*. Fertilized (33 percent) and seeding of indigenous species (32 percent) showed intermediate results, while the natural treatment lagged far behind (9 percent). The indigenous seed was mostly composed of *Carex aquatilis*, *Eriophorum angustifolium*, and *Puccinellia langeana*, but only the latter grew successfully from seed (fig. 96).

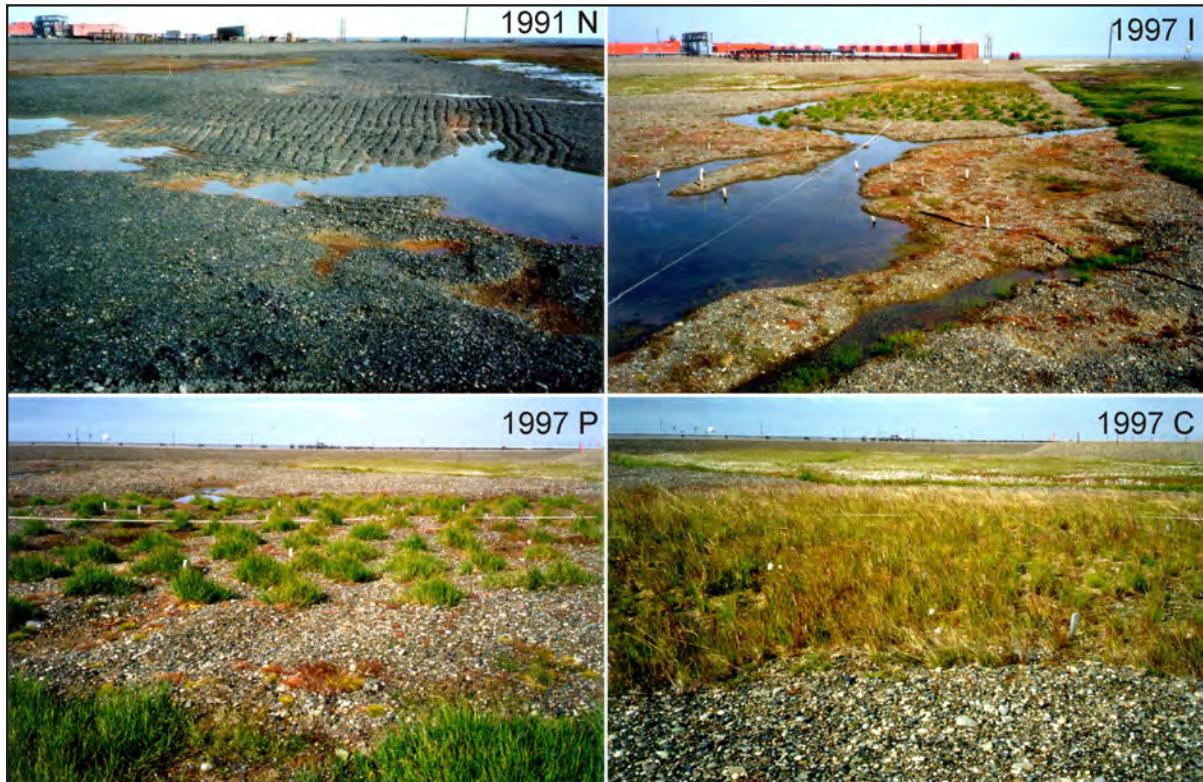


Figure 96. Views of the remaining gravel fill after most of the material had been removed from an abandoned entrance road to Drill Site 3R (Jorgenson and Cater, 1992; Bishop and others, 2000). The views include (N) the site the summer after gravel removal in 1991, and (I) the indigenous seed treatment, (P) the plug transplants, and (C) the native grass cultivars in 1997.

STOP 19: OLIKTOK POINT, ARCTIC OCEAN, AND SALT-KILLED TUNDRA

The main spine road in the Kuparuk oilfield ends at the Seawater Treatment Plant (STP) at Oliktok Point (fig. 97). The STP treats seawater to kill bacteria and pumps it to the central processing facilities for later injection into the subsurface formations to maintain pressure and drive oil to the oil wells. Oliktok Point also is the site for a Distant Early Warning (DEW) station.

The DEW line station at Oliktok Point was constructed by the U.S. Air Force between 1954 and 1955 and has been active ever since. It is now known as the Oliktok Long Range Radar Station (LRRS). It was part of an extensive network of radar sites constructed in the 1950s to detect warplanes from the former Soviet Union during the Cold War (fig. 98). The installation was originally constructed as an auxiliary station. It consisted of a 25-unit module train, radome radar, and support facilities. In the mid-1980s, a Minimally Attended Radar was installed, which reduced the number of workers required to operate the facility. Generally, two contract personnel are stationed at the Oliktok LRRS installation year-round. The installation presently consists of a 22-unit module train containing living quarters, a power generation plant, sewage and water systems, and an incinerator. The module train is attached to the radome tower. The radome tower houses the rotating radar, which is supported on a steel-framed platform straddling the modular train. A 1,225-m- (4,020-foot-) long lighted gravel runway is also part of the facility.

The Oliktok LRRS is the site of a highly unusual polar bear attack that occurred on December 1, 1993 (USFWS, 1993). According to reports submitted to the U.S. Fish and Wildlife Service, a 2.4-m- (8-ft-) tall adult polar bear



Figure 97. A 2004 airphoto of Oliktok Point on the northern end of the Kuparuk oilfield. Evident in the airphoto are sediment-laden nearshore water of Simpson Lagoon, gravel beaches, tidal ponds, halophytic wet meadows, and salt-killed tundra (white areas in center).

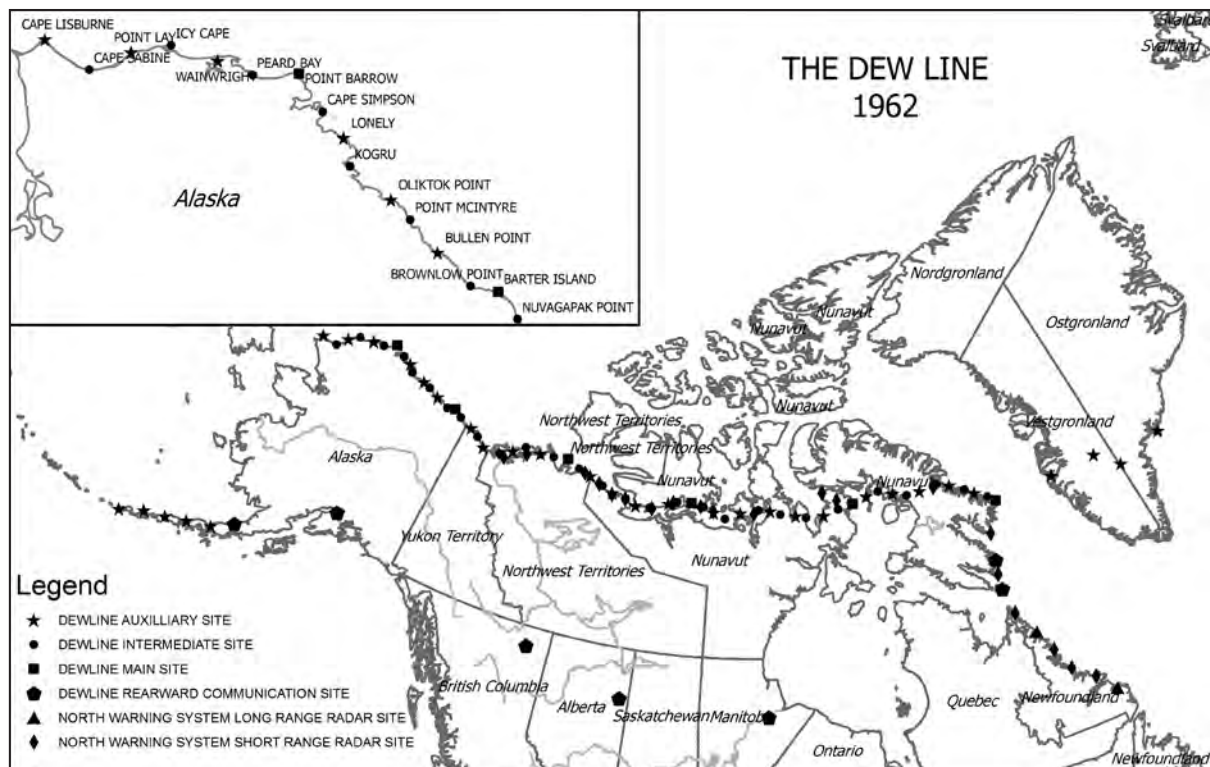


Figure 98. Map of the network of Distant Early Warning (DEW) stations built across the North American Arctic (courtesy of the North American Air Defense Online Radar Museum).

approached the facility living quarters and peered into a ground floor window. Workers saw the bear looking in and swatted the window with a magazine to frighten it away. It returned a short time later, and they swatted the window again. After a third return and window swat, the bear came crashing through the glass and attacked the men inside. It made its way into the facility library before it was shot and killed by a fellow worker. One severely injured man, a nonmilitary construction worker, was flown to the ARCO Kuparuk medical facility and later to an Anchorage hospital where he was treated in intensive care. According to a polar bear biologist with the USFWS, that bear and two or three others seen in the Oliktok Point area in previous weeks were probably attracted by the whale meat stored there by Inupiat whalers.

Oliktok Point has extensive areas of coastal habitats including gravel beaches, barren mudflats, halophytic wet meadows, and salt-killed tundra (fig. 99). The saline fringe supports halophytic meadows dominated by *Carex subspathaceae*, *Puccinellia phryganodes*, *Carex ursina*, *Cochleria officinalis*, and *Stellaria humifusa*. The active sediment deposition, saturated anaerobic soil conditions, and high salinity combine to create very picturesque soils with dramatic orange (iron oxidation) and black (sulfur reduction) mottling. Large storms in 1963 and 1970 flooded extensive areas along the coast and the brackish water killed the freshwater wet and moist tundra. Loss of live vegetation has led to degradation of ice wedges.

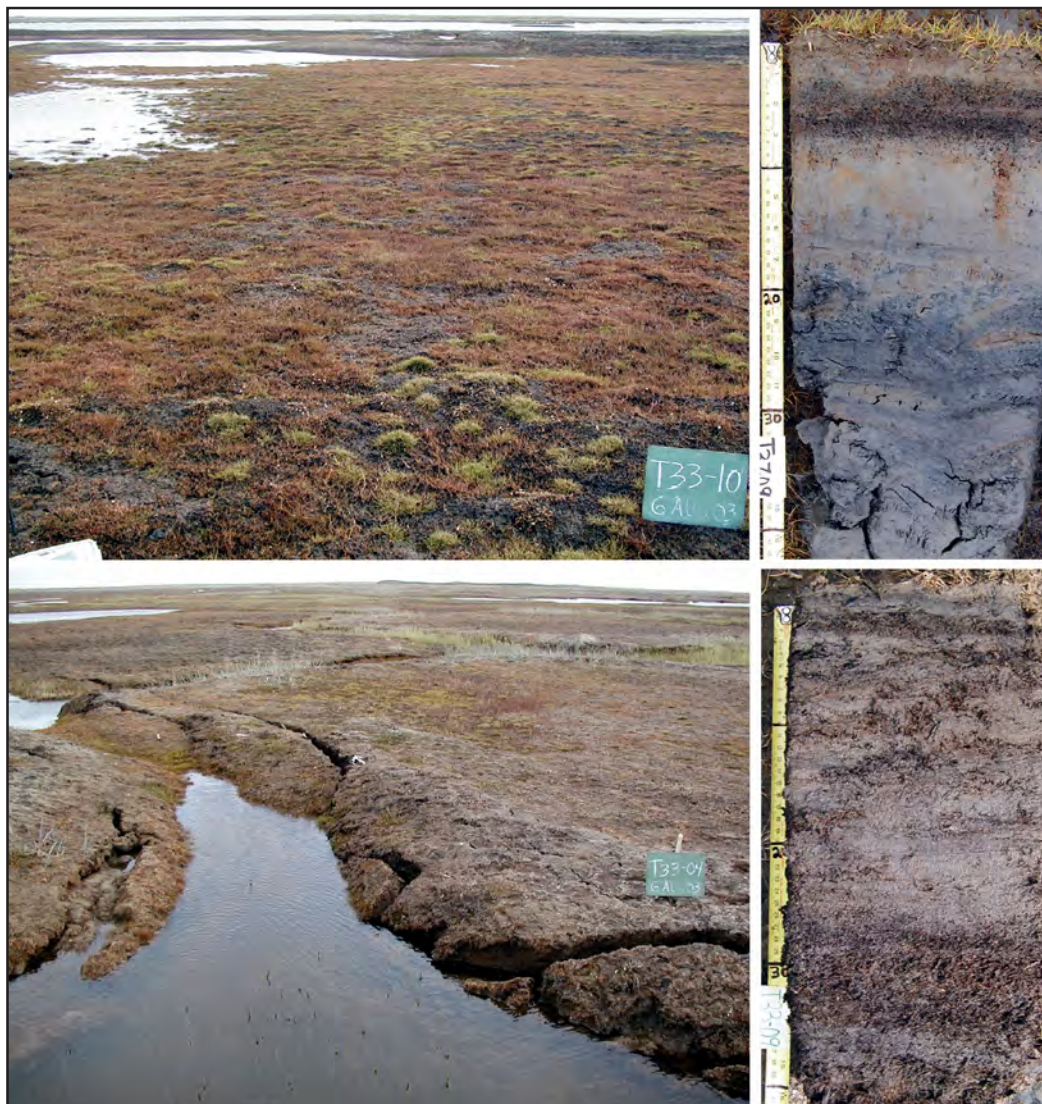


Figure 99. Coastal meadows occupy a thin band of salt-affected habitats along the Beaufort Sea coast. Saline wet meadows (above) and tundra killed by saltwater (below) during large storms in 1963 and 1970 are prevalent (photos by T. Jorgenson).

This page was intentionally left blank.

PART 4: TOUR OF THE COLVILLE RIVER DELTA

by H. Jesse Walker¹ and Torre Jorgenson²

OVERVIEW

This part of the field guide deals with specific landforms and processes to be examined along the field-trip route in the Nechelik Channel in the Colville River Delta (fig. 100). They are discussed below in the sequence numbered on the map. This section of the guidebook is mainly descriptive and historical and is designed to serve as a stimulus for discussion at various stops.

The Colville River is the largest river on Alaska's North Slope and is one of eight major rivers with significant freshwater input to the Arctic Ocean (Walker, 1983). The Colville enters the Beaufort Sea midway between Barrow and Kaktovik. It drains ~29 percent (53,600 km² [20,695 mi²]) of the North Slope of Alaska, with most of the watershed in the foothills (64 percent) and smaller areas in the Brooks Range (26 percent) and coastal plain (10 percent; Walker, 1976). The head of the delta is located near the mouth of the Itkillik River (Arnborg and others, 1966). Below the Itkillik River, the area encompassed by the floodplain of the delta and water within the fringe of the delta covers 666 km² (257 mi²). The Colville River, with its large discharge and heavy sediment load, produces a deltaic system shaped by the dynamic interaction of depositional and erosional processes, sea-level changes, glaciations and major drainage changes, permafrost development, wind activity during dry climatic periods, and lake development (Hopkins, 1982; Dinter, 1985; Rawlinson, 1993).

The remarkable environment of the delta has been the subject of numerous studies conducted over the last four decades. Much of the information on the geomorphology and hydrology of the delta was gathered by Walker and his associates over more than three decades (Walker and Arnborg, 1966; Walker, 1976, 1994) and later by Jorgenson and his colleagues in the 1990s in preparation for oil development (Jorgenson and others, 1993, 1996, 1997b, 2003c). Other important studies on the geomorphology of the delta and nearby coast include those of Carter and Galloway (1982, 1985), Reimnitz and others (1985), and Rawlinson (1993). Several major multi-disciplinary research efforts have been conducted, including a study of nearshore aquatic and marine environments by the University of Alaska (UAF, 1972), the investigation of the coast and shelf of the Beaufort Sea by numerous organizations during the 1970s (Reed

and Sater, 1974), and numerous studies conducted under the Outer Continental Shelf Environmental Assessment Program.

The delta is bounded on both sides by old alluvial terraces that are traceable from the coast to above the Itkillik River (fig. 101). Fossil wood collected at the base of exposures yielded ages of 48–50.6 RC ka BP, suggesting that the terraces and underlying deposits of gravelly sand were formed during the last interglacial period (Carter and Galloway, 1982). These deposits are part of the Gubik Formation (Black, 1964; Carter and others, 1977), a series of unconsolidated deposits that record a complex marine and alluvial history spanning ~3.5 million years (Carter and others, 1986). Modern sandy deltaic sediments in the delta generally range from 5 to 10 m (16 to 33 ft) below sea level and are underlain by 6–12 m (20–40 ft) of gravelly riverbed material (glaciofluvial outwash) and 20 m (65 ft) or more of interbedded silts, clays, and organics indicative of marine or deltaic sediments associated with the Gubik Formation (Miller and Phillips, 1996). The surficial geology of the central Arctic Coastal Plain has been mapped (1:63,360 scale) by Carter and Galloway (1985) and Rawlinson (1993).

The delta has two main distributaries, the Nechelik (western) Channel and the Colville East Channel. These two channels carry about 90 percent of the water through the delta during flooding and 99 percent during low water (Walker, 1983). Smaller channels branching from the East Channel include the Sakoonang, Tamayayak, and Elaktoveach channels. Most of the water is carried through the delta during spring breakup (fig. 102). Monitoring of peak discharge was begun in 1962 by Arnborg and others (1966), measured sporadically during the 1970s by Walker (1974) and the USGS (1978), and continuously from 1992 until present in association with oil development studies (Jorgenson and others, 1993, 1996; Shannon and Wilson, 1996, 1997; Michael Baker, Inc., 2000, 2007) (fig. 103). Determination of peak discharge is complicated by the persistence of thick ice in the main channel, ice floes, and occasional ice jams. The high sediment load during spring flooding can leave thick silt deposits on the bank and the silt can form distinctive layers in the peat accumulating on the floodplain (fig. 104).

¹Department of Geography and Anthropology, Louisiana State University, Baton Rouge, Louisiana 70803

²ABR Inc., Environmental Research & Services, P.O. Box 80410, Fairbanks, Alaska 99708-0410; currently employed by Alaska Ecoscience, 2332 Cordes Way, Fairbanks, Alaska, 99709; ecoscience@alaska.net



Figure 100. Landsat image (circa 2000) of Colville River Delta showing the location of the tour stops described in the guidebook.

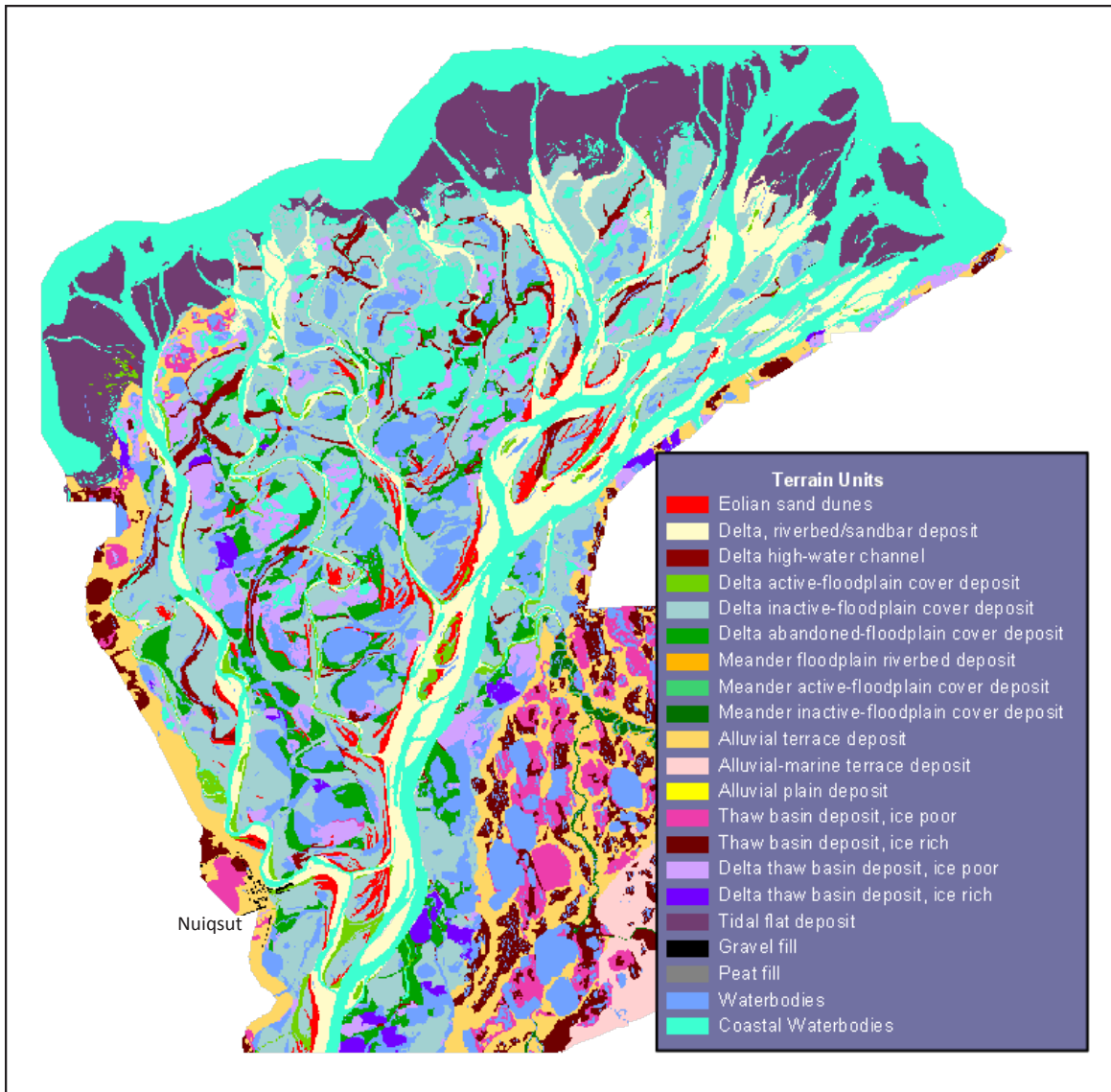


Figure 101. Map of geomorphic units on the Colville River Delta and adjacent terrain (Jorgenson and others, 1997).



Figure 102. Photograph of flooding during spring breakup on the Colville River Delta showing the persistence of ice in the deep part of the distributary channels (photo by P. Banyas).

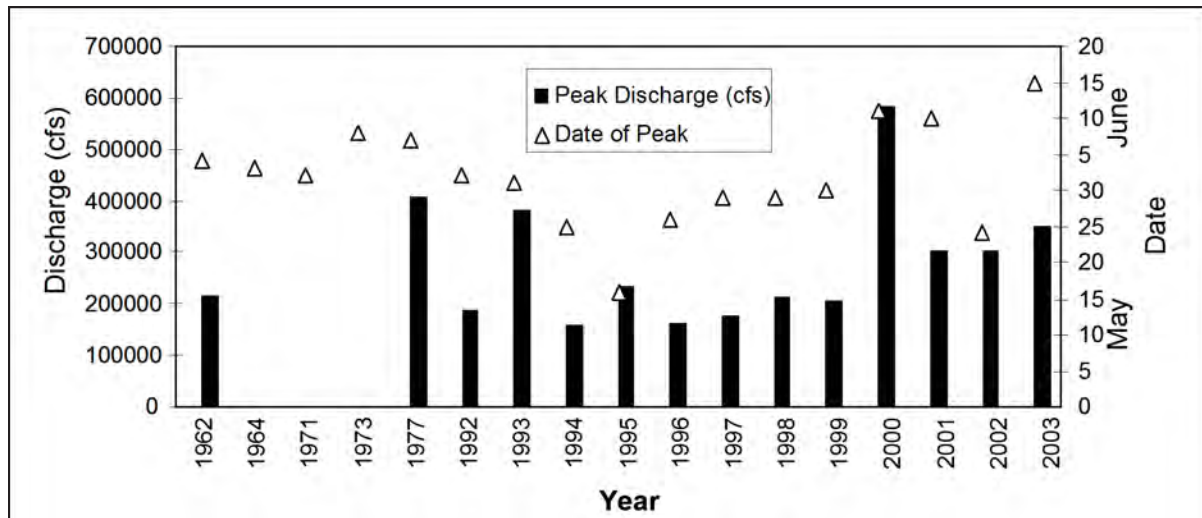


Figure 103. Volume (left y-axis) and date (right y-axis) of annual peak discharge at the head of the Colville River Delta, 1992–2007 (data from Arnborg and others, 1966; USGS, 1978; Jorgenson and others, 1996, Shannon and Wilson, 1996, 1997; Michael Baker Jr., 2007).



Figure 104. Sedimentation during spring breakup can deposit thick layers of mud (left, 1962) that can form distinctive layers in the soil profile (right, 2003) (photos by J. Walker and T. Jorgenson).

Similar to most large deltas around the world, the Colville River Delta is characterized by migrating distributary channels, waterbodies of various origins, natural levees, sand dunes, sand bars, and mud flats (Walker, 1976, 1983). Unlike deltas in temperate climates, however, it is greatly influenced by two other factors: low temperatures, which preserve most of the annual precipitation until spring breakup, and the presence of permafrost (Walker, 1976). Permafrost affects the seasonal character of river discharge and the timing and nature of erosion, contributes to the accumulation of ice and organic matter, and causes the development of distinctive surface features such as ice-wedges and ‘thaw’ lakes formed by thawing of ice-rich sediments (Walker, 1976; Jorgenson and others, 1996).

Landforms within the delta are highly complex as a result of fluvial (flowing water) deposition, eolian (wind) transport, development of thaw lakes, and marine processes. Floodplain deposits comprise various materials (silt, sand, gravel, peat, and ice) and can be subdivided into five classes of terrain units (riverbed, high-water channel, and active, inactive, and abandoned floodplain cover deposits), depending on the type of material and depositional process (fig. 105). Riverbed/sandbar deposits occupy a large portion of the delta, with the size of bars increasing and sediment grain size decreasing in a downstream direction. Gravel bars are rare, consisting of a few patches of gravel near the head of the delta (Walker, 1976). Over time, the floodplains increase in height as sediments and organic material

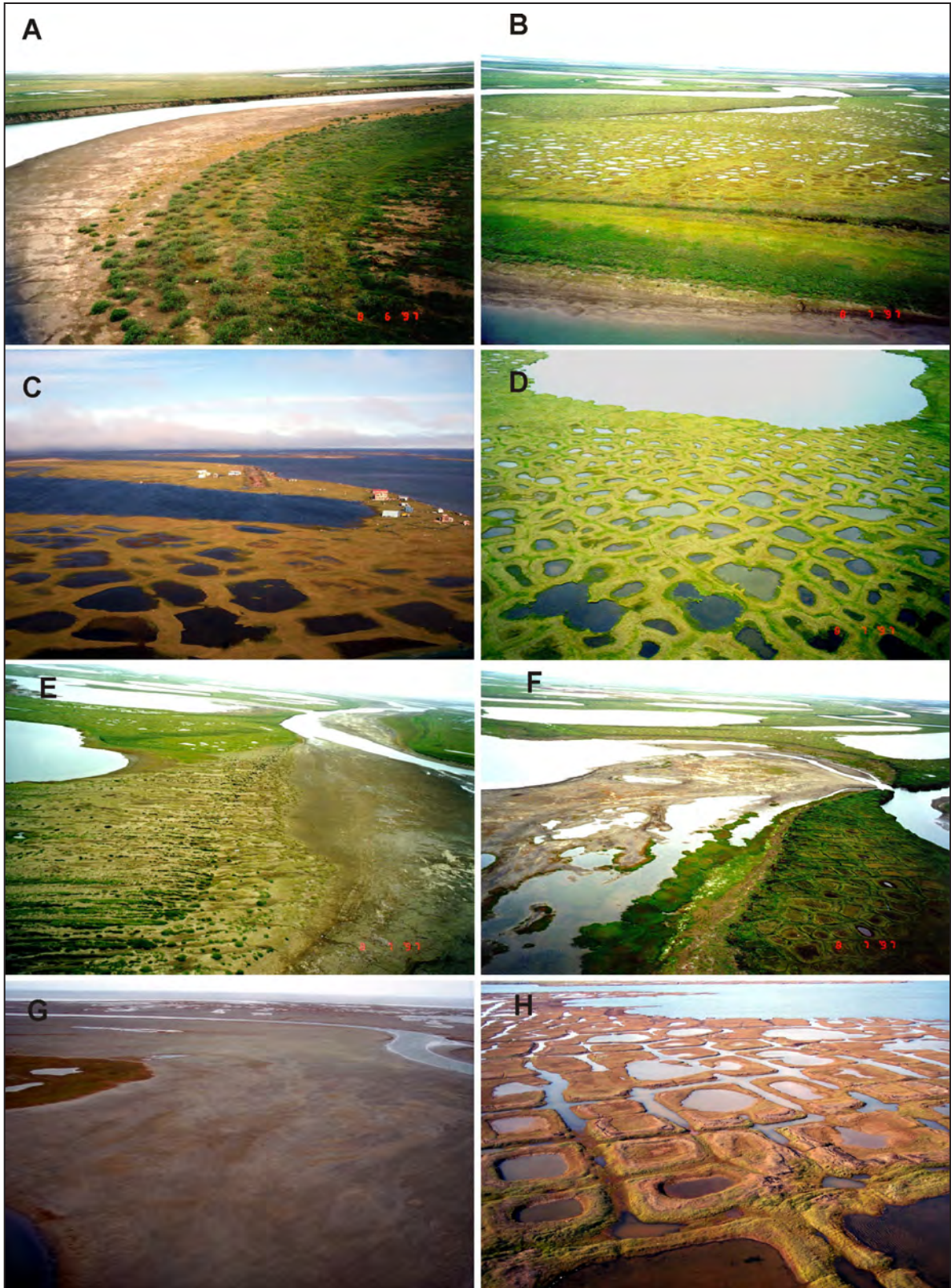


Figure 105. Depositional environments of the Colville River Delta, including (A) channel deposits along a point-bar, (B) floodplain steps of overbank deposits, (C) Helmerick's homestead on an inactive floodplain, (D) ice-rich abandoned floodplain with thaw lake, (E) sand dune, (F) tapped lake, (G) tidal flat, and (H) salt-killed tundra (photos by T. Jorgenson).

accumulate at the surface and ice forms in the underlying permafrost (Jorgenson and others, 1996). Riverbanks along the older, higher floodplain deposits generally range from 6 m (20 ft) above low water level near the head of the delta to 1 m (3.3 ft) at the outer edge of the delta, although some banks that have cut into sand dunes and old alluvial terraces are 7–9 m (23–30 ft) high (Ritchie and Walker, 1974).

The accumulation of peat in these fluvial sediments and other stable surface deposits is an important factor contributing to the development of the arctic landscape. The accumulation of peat has contributed substantially to floodplain deposits, raising the surface of the floodplain and altering flooding frequency. The thickest accumulation of peat found thus far on the delta is 2 m (6.8 ft), with an age of 4.1 cal ka BP (Jorgenson and others, 1996). The development of a peat layer at the surface also is important for insulating the underlying permafrost and enhancing further ice accumulation. Disruption of the surface peat layer can have serious consequences for the thermal stability of underlying ice-rich sediments.

Windblown sand and silt have accumulated at the surface of most deposits on the Colville River Delta and transportation corridor and have formed prominent sand dunes in the delta (Carter, 1981; Walker, 1976). Active sand dunes are common along the western banks of channels downwind from large river bars (Walker, 1983). Older, stabilized dunes are also common and are frequently capped by a thin layer of windblown silt.

Thaw lakes are found throughout the delta, particularly on older, ice-rich floodplain deposits. A particular form of thaw-lake development in deltas is the 'tapped' lake, which is formed by erosion of meandering channels into the sediments that contain the lake, causing it to drain (Walker, 1978). Tapped lakes then are subject to flooding and filling by sediments deposited during floods.

Marine processes are most active during the short ice-free period and contribute to the build-up of tidal flats along the outer edge of the delta (Ritchie and Walker, 1974). The nearly flat, barren mud and sand flats are flooded periodically by tidal waters and storm surges. Much of the material in the tidal flats is deposited during spring floods following breakup. Because river flooding and breakup occur before the sea ice breaks up, floodwater from the river deposits sediment as it floods over the sea ice. Rising sea levels (2–3 mm/yr [0.08–0.12 in/yr]; ACIA, 2005) probably have contributed to the accumulation of sediments on the tidal flats and increased the frequency and extent of flooding on the older, higher floodplain deposits that developed during an earlier era (Jorgenson and others, 1996).

Permafrost is of serious concern for engineering design. The volume of segregated ice in the top 2 to 3

m (7–10 ft) of older floodplain deposits on the Colville River Delta typically ranges from 70 to 85 percent (Jorgenson and others, 1996). Ice wedges are vertically oriented masses of ice that taper downward and develop by water repeatedly filling and freezing in cracks formed at the surface by thermal contraction. Ice wedges generally are less than 3 m (10 ft) wide and 5 m (16 ft) deep (Black, 1976), but occasionally may be up to 25 m (80 ft) deep (Carter, 1988). On older portions of the delta, ice wedges may occupy as much as 20 percent of the near-surface sediments (Jorgenson and others, 1997b). Another indicator of the very high ice content in the higher, older floodplain deposits on the Colville River Delta is the depth (3 to 4 m [10–13 ft]; Moulton, 1996) of thaw lakes in the delta (Jorgenson and others, 1996). These depths suggest that excess ice constitutes half or more of the volume of the top 6 to 8 m (14–26 ft) of sediments, which are highly unstable when thawed.

Ground ice morphology and volume are related to formative processes (fluvial, eolian, marine, and organic) and change as the landscape evolves (fig. 106) (Jorgenson and others, 1998, Shur and Jorgenson, 1998). Delta riverbed deposits have massive or crossbedded sandy sediments that accumulate rapidly due to frequent flooding (every 1–2 years), have no organic-matter buildup, and have low ice contents (40–50 percent). Active floodplains have layered or massive fines on top of sandier riverbed materials, still have rapid material (mostly sediments) accumulation rates (26.5 cm [0.87 ft]/100 yr) due to slightly less-frequent flooding (every 3–4 years), lack organic-matter buildup, and have intermediate ice volumes (60–70 percent) associated with the development of lenticular and pore ice. Inactive floodplains have interbedded mineral and organic layers indicative of infrequent flooding (5–25 years), much lower material (mostly ice and organics) accumulation rates (7.3 cm [0.24 ft]/100 yr), and have high ice contents (70–80 percent) associated with development of vein, reticulate, ataxitic, and wedge ice. Abandoned floodplains have massive or layered organic accumulations at the surface due to very infrequent flooding (25–150 years). They have very low material (mostly organics and ice) accumulation rates (2.4 cm [0.08 ft]/100 yr), and have very high ice contents (80–90 percent) associated with organic-matrix ice and wedge ice. The density of ice wedges varies dramatically through this sequence (fig. 107). By this stage, the surface has accumulated so much ice that it becomes unstable and prone to thaw-lake development. Tapping of thaw lakes by meandering channels can drain the lake and the lower surface is subject again to the processes described above.

Landscape change on the Colville River Delta primarily is driven by fluvial erosion and deposition along river channels and the development of thaw lakes

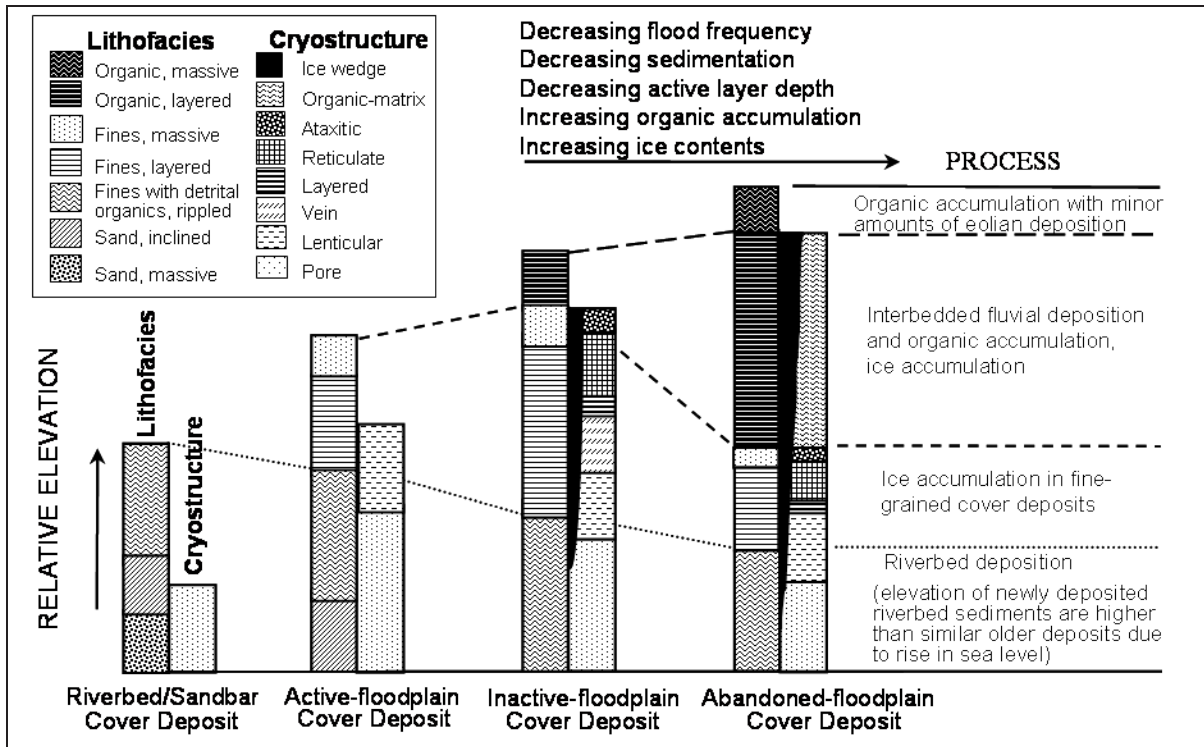


Figure 106. Diagram of the evolution of soil stratigraphy and ice morphology during floodplain development on the Colville River Delta (Jorgenson and others, 1998).

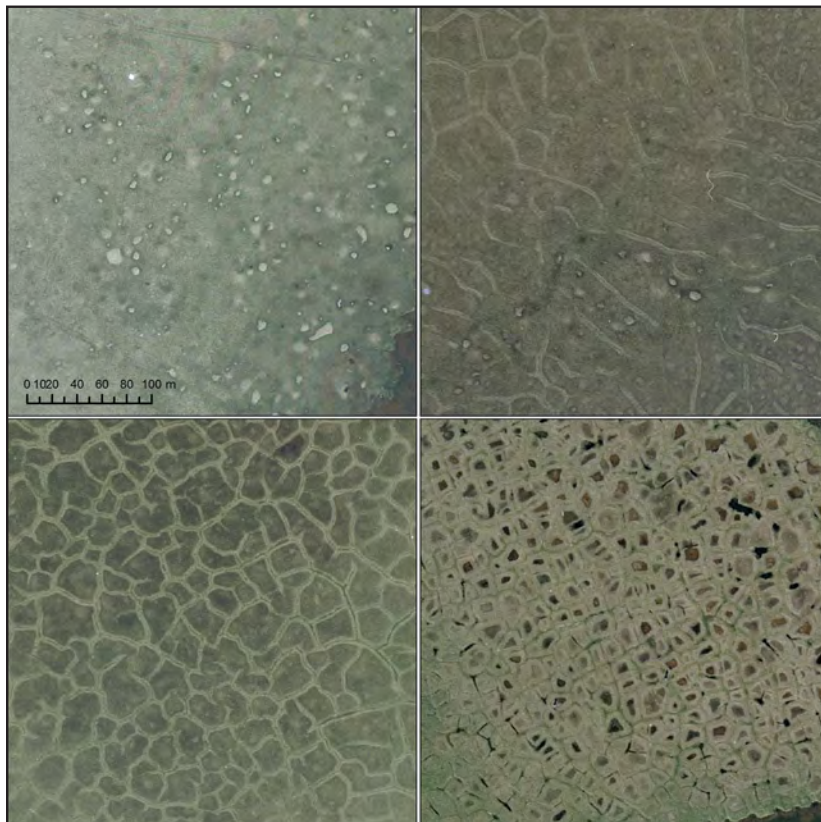


Figure 107. Photos showing aerial views of development of ice-wedge polygons associated with nonpatterned ground with occasional ice-cored mounds evident as small gray patches (upper left), disjunct (upper right), low-density (lower left), and high-density polygons (lower right), Colville River Delta (photos from Jorgenson and others, 1997b).

in ice-rich sediments (Walker, 1976, 1983; Jorgenson and others, 1993; Rawlinson, 1993). An analysis of landscape change by Jorgenson and others (1993) revealed that 7.6 percent of the area has been affected by erosion, deposition, or water-level changes over a 37-year period between 1955 and 1992 (fig. 108). Most of this change resulted from erosion (1.3 percent) and deposition (2.6 percent) of sediments within the main channels and adjacent barren riverbed deposits. Erosion of banks along older, higher floodplain deposits was somewhat lower (1.0 percent) than along active channels. Drainage of thaw lakes and deposition of sediments in drained-lake basins accounted for a moderate landscape change (1.8 percent), while water-level changes also affected some areas (0.9 percent). Within the main channels, most of the erosion and deposition resulted from lateral movement of channels across barren riverbed and from migration of mid-channel bars. In the East Channel, mid-channel bars migrate as much 10.7 m (35 ft) per year as material is eroded from the upstream end and deposited below the downstream end. Other portions of the riverbed along point bars and where channels split show similarly high rates of erosion and deposition.

Although the extent of erosion along the banks of older, higher portions of the floodplain is less than in barren riverbed deposits, it still can be considerable. In the East Channel, erosion generally is greatest at the unprotected ends of narrow islands, where erosion rates of 2.1–4.3 m (7–14 ft) have been measured (Jorgenson and others, 1993). Along the sides of islands and cutbanks in meandering channels, erosion rates can exceed 0.9 m (3 ft) per year; for instance, erosion at two sites along the Nechelik (Nigliq) Channel averaged 0.9–1.8 m (3–6 ft) per year over a 23–30-year period (Walker, 1983). However, averaging rates over a long period can mask the episodic nature of erosion, in that undercutting of 7.6–9.1 m (25–30 ft) may result from a single storm (Walker and Morgan, 1964). At the main pipeline crossings on the East Channel, erosion of the banks averaged 36.6 cm (1.2 ft) per year.

Factors influencing erosion along river channels include the timing of flood events and the accumulation of peat and ice in the older floodplain deposits. Although spring breakup is normally the largest flooding event each year, the amount of erosion at that time can be limited by the frozen active layer and ice frozen to the surface of the riverbed (Carter and others, 1987). Thermal erosion of banks occurs during floods and lower flow stages later in the season. Thermal erosion of ice-rich sediment at and below the water surface leads to the

collapse of large blocks, a predominant factor in bank erosion (Walker and Morgan, 1964; Walker and Arnborg, 1966; Ritchie and Walker, 1974). Peat-rich soils tend to have lower erosion rates (0.8 m [2.5 ft] per year) than highly mineralized soils (2.0 m [6.5 ft] per year), presumably because of the protection provided by the fibrous mats of peat (Walker, 1983) and the slower thawing of ice-rich organic matter.

Erosion of shorelines in large thaw lakes isolated from rivers is caused both by wind-driven waves and by melting of ice-rich sediments. Erosion rates of exposed shorelines in the large thaw lakes of the central delta generally are much higher (up to 1.8 m [6 ft] per year) than in smaller lakes with more protected shorelines (Jorgenson and others, 1993). The erosion of ice-rich sediments by thaw-lake processes illustrates an important paradox about the stability of floodplain deposits in the delta: the oldest, highest terrain units contain such high ice contents that they have become the most unstable and erodible areas. Indeed, the high proportion of surface area covered by thaw lakes in the central delta (oldest areas), and the general occurrence of abandoned floodplain deposits as small patches surrounding large thaw lakes, indicate that most of the older, ice-rich deposits already have been lost to erosion by thaw lakes.

Changes in the extent of tidal flats along the lower Nechelik Channel indicate that tidal flats expand into nearshore waters at a rate of up to 6.7 m (22 ft) per year at the mouths of channels emptying directly into the Beaufort Sea (Jorgenson and others, 1993). In most areas of the delta, however, the expansion rate is much lower (about 42.7 cm [1.4 ft] per year; Reimnitz and others, 1985).

The delta has long been recognized as one of the most productive deltas for fish and wildlife on the arctic coast of Alaska (Gilliam and Lent, 1982; Divoky, 1984). The area is important for tundra swans (*Cygnus columbianus*), brant (*Branta bernicla*), yellow-billed loons (*Gavia adamsii*), greater white-fronted geese (*Anser albifrons*) and a variety of other migratory birds (Rothe and others, 1983). Arctic (*Coregonus autumnalis*) and least cisco (*Coregonus sardinella*) overwinter in the delta and support the only commercial fishery on the North Slope (NOAA/OCSEAP, 1983; Moulton, 1996). Caribou (*Rangifer tarandus*) from both the Central Arctic Herd and the Teshekpuk Herd use the delta (Gilliam and Lent, 1982). The area's resources are important to the subsistence economy of the Nuiqsut villagers.

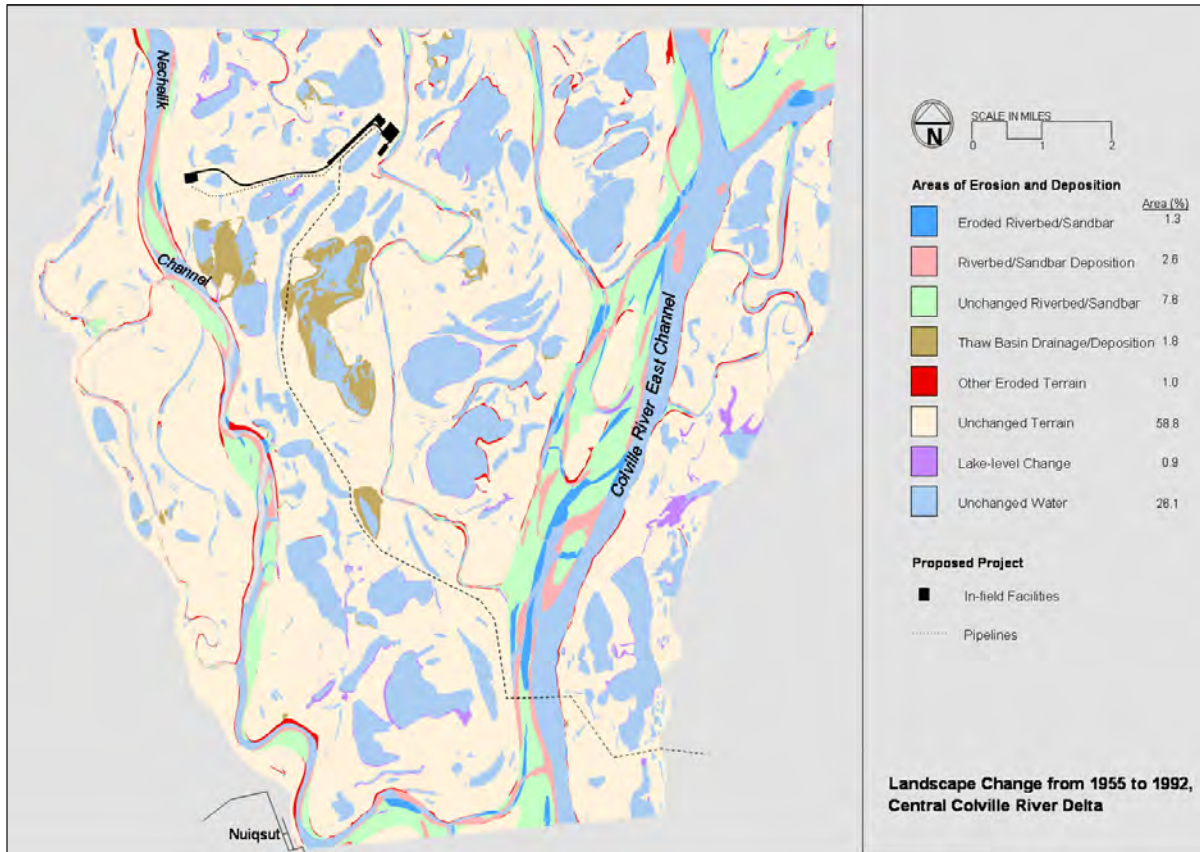


Figure 108. Map of changes in the landscape of the Colville River Delta from 1955 to 1992 due to channel erosion, deposition, and lake drainage (from Jorgenson and others, 1996).

STOP 1: NUIQSUT

The modern village of Nuiqsut, meaning “a beautiful place over the horizon,” was established in 1972 near the head of the Nechelik Channel, which is the westernmost distributary of the Colville River. It is at a location that provided relatively close and easy access to the main channel (fig. 109). The actual ancestral location of Nuiqsut was on an island near the mouth of the main channel, which was not ideal for the location of present-day Nuiqsut. At the time of the founding of Nuiqsut there were only a few locations with buildings in the delta: one was the Woods’ home at Niglik, a second was the Helmericks’ hunting camp near the mouth of the main channel, and a third was the Arctic Research Laboratory (ARL)’s Camp Putu that served as a base for research from 1962 to about 1978. It was from that base that most of the early research on the delta was conducted. Nuiqsut was founded by 27 families who moved by snowmachine from Point Barrow in April 1973 (fig. 110). They lived in tents (protected by snow blocks during winter) for about 1½ years before housing was developed by the Arctic Slope Regional Corp. (fig. 111). Today, Nuiqsut, classified as a second-class city, has a population of more than 500. It has a modern school system, health-care facilities, fire department, electrical service, a recreation center, heated water storage tanks, a post office and an air field. Hunting (primarily caribou, seals, and whales), trapping, and fishing (mainly white fish) are still practiced intensively. However, many other occupations, such as those associated with city services and the oil companies, are now common. The harsh climate (low temperatures and long-lasting snow and ice covers) and permafrost are imposing constraints that must be dealt with; examples of adjustments to the environment are numerous. One of the most conspicuous is the technique of protecting the integrity of permafrost by raising structures that might cause thawing some distance above the tundra surface. This is done in two ways—by placing structures on pilings (such as the village’s school buildings) or by establishing a foundation of sand and gravel (often with high-strength geofabric included) as under many of the houses and streets (figs. 112 and 113).

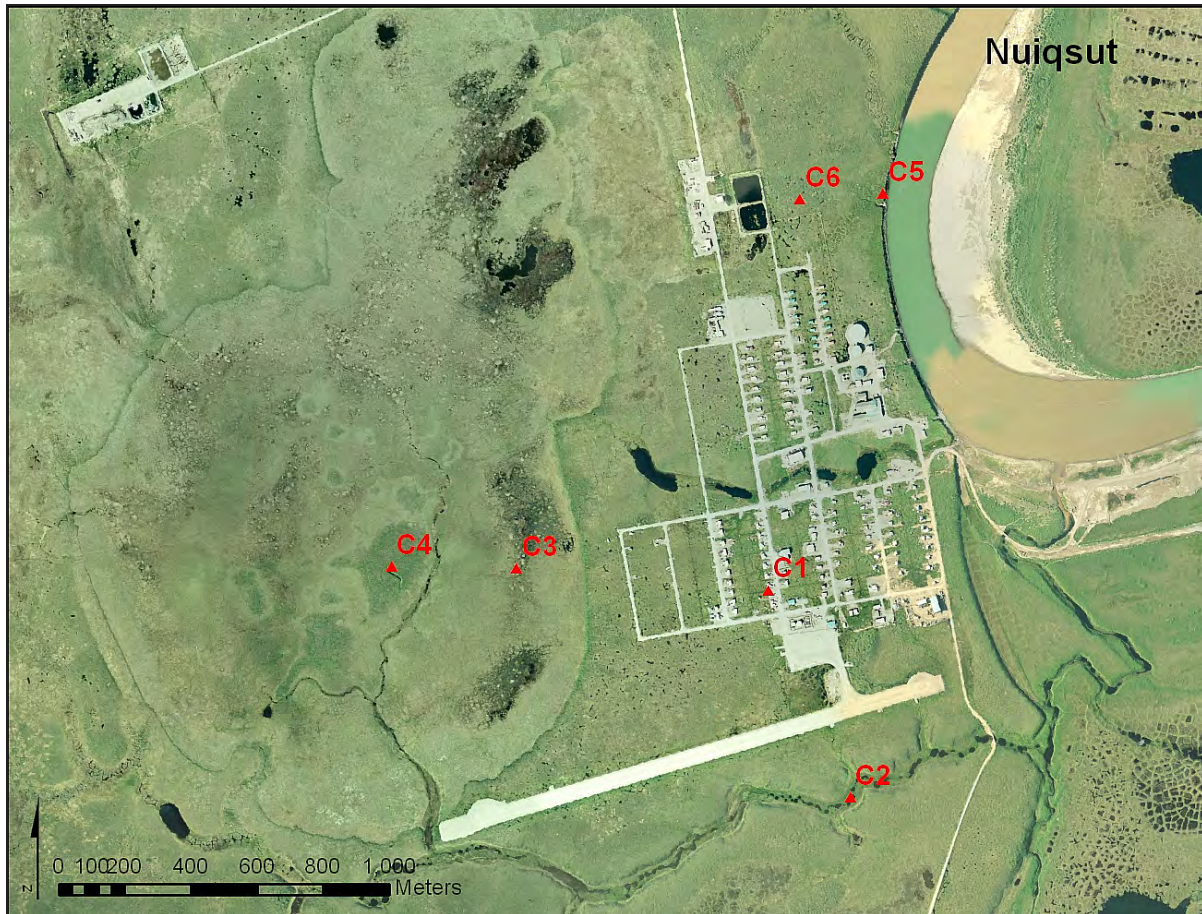


Figure 109. A 2004 airphoto of the Native village of Nuiqsut, situated on a high west bank of the Niglik channel of the Colville River. The numbers represent four stops.

In 1981, construction began on the 1,500-m- (4,920-ft-) long runway that now forms the southwest border of the village (fig. 114). Some 200,000 m³ (261,580 yd³) of sand and gravel were dredged from the thalweg portion of Nechelik Channel (fig. 115), piped to the runway site, and placed directly on the tundra surface (fig. 116). This method of sand and gravel acquisition is made possible because of the presence of the talik beneath the river bed. It proved so successful that dredging beneath the river continued during 1982 and was begun shortly thereafter along the Kokolik and Meade rivers. In the Colville, gravel obtained from as deep as 18 m (60 ft) beneath the river surface was crushed and used as topping for the runway. Some 500,000 m³ (653,950 yd³) of sand and gravel were stockpiled. During construction, environmental damage to the tundra surface near the runway was minimal because of the effective control of runoff from the hydraulic operation and the reduced need for vehicles impacting the tundra outside the runway right-of-way. Prior to runway construction a survey of the characteristics of the tundra base was made in order to see, over time, the effect of the fill on numerous ice-wedges that crossed the area and the permafrost that underlay it (fig. 116). In addition, some monitoring of the river channel was maintained for several years.

Of course, permafrost can be advantageous to human endeavors as well. When the move was made to the riverbank on the Nechelik Channel, there was no electricity and therefore no refrigerators or deep freezers. As in pre-contact times the Inupiat took advantage of the low temperatures of the permafrost by digging ice (permafrost) cellars in which they stored fish, caribou, and other meats. Today, virtually all ice cellars in Nuiqsut have been replaced by freezers, which can be found in every house.

With the development of the Alpine oilfield, natural gas became available. A gas line was buried in a trench across the floodplain from the pipeline crossing at the East Channel, buried underneath the Nechelik Channel, and is distributed throughout the village in buried pipes (fig. 117). In 2008, the gas was hooked up to individual houses, substantially reducing heating costs.

Figure 110. Inupiat camping at the site of the future Nuiqsut village (1973 photo by J. Walker).

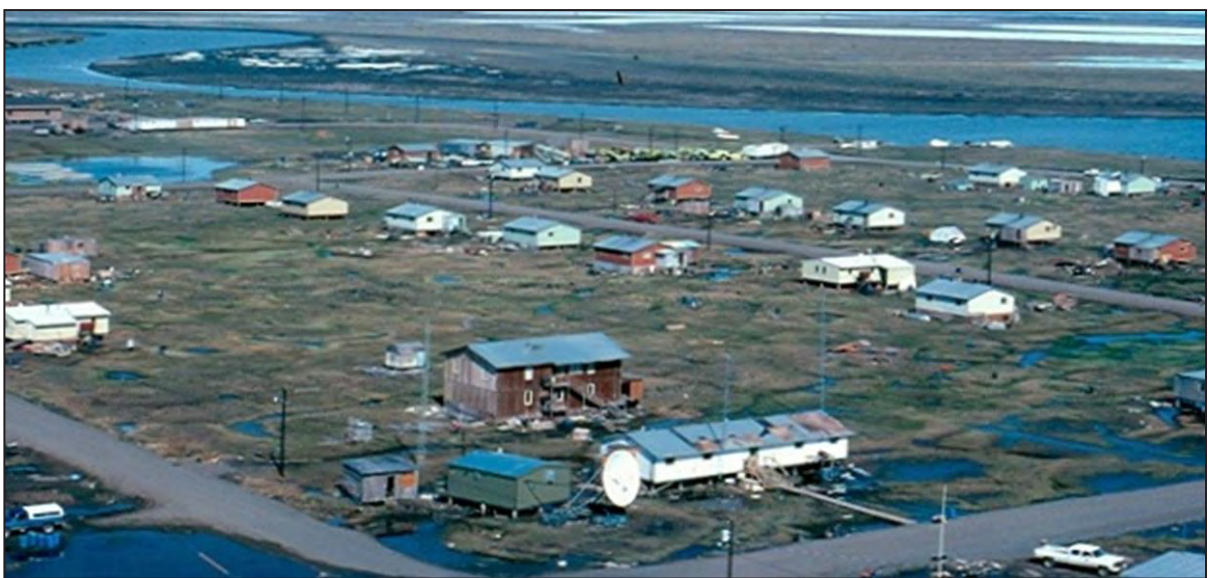


Figure 111. Nuiqsut village in 1982 (photo by J. Walker).

Figure 112. Nuiqsut schoolhouse on pilings (1984 photo by J. Walker).



Figure 113. House pad under construction (1983 photo by J. Walker).



Figure 114. Runway under construction (1981 photo by J. Walker). Note beaded stream.



Figure 115. The Nivakti dredging gravel from the bottom of the Nechelik Channel near Nuiqsut in 1982. Note the caribou rack on the dredge (photo by J. Walker).

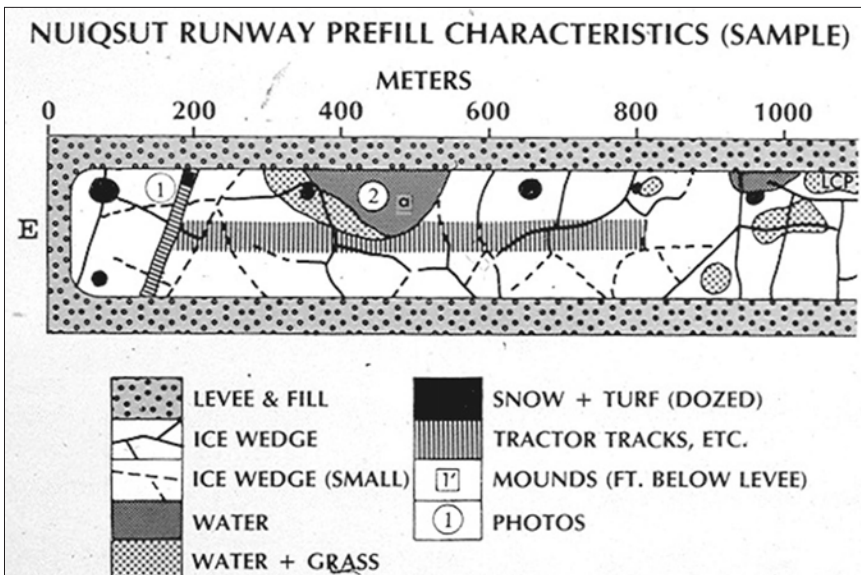


Figure 116. Survey of runway location prior to fill (Walker, 1994).



Figure 117. Photograph of buried gas pipeline in Nuiqsut installed in 2006. The pipeline delivers gas from the Alpine central processing facility to the powerplant, community buildings, and houses (photo by T. Jorgenson).

STOP 2: BEADED DRAINAGE

The small (4-km- [2.5-mi-] long) beaded stream carries water from the surrounding tundra to the floodplain of the Nechelik Channel (fig. 118). Beaded streams are common on the Beaufort Coastal Plain and the Brooks Foothills of northern Alaska, where ice wedges are abundant in the permafrost (Washburn, 1973). The beads (pools) typically are roughly circular, 1 to 5 m (3.3–16.4 ft) across, and up to 2 m (6.6 ft) deep. Pools commonly are connected at fairly regular intervals by shallow, steep-sided, channel segments. The beads are thought to be the result of the thawing of ice at the intersections of ice-wedge polygons (Péwé, 1966). During periods of low rainfall in mid-summer, channel flow is reduced but the pools continue to maintain water (Oswood and others, 1989). Organic concentrations in the water tend to be high and dominated by dissolved rather than particulate organic carbon (Oswood and others, 1989).

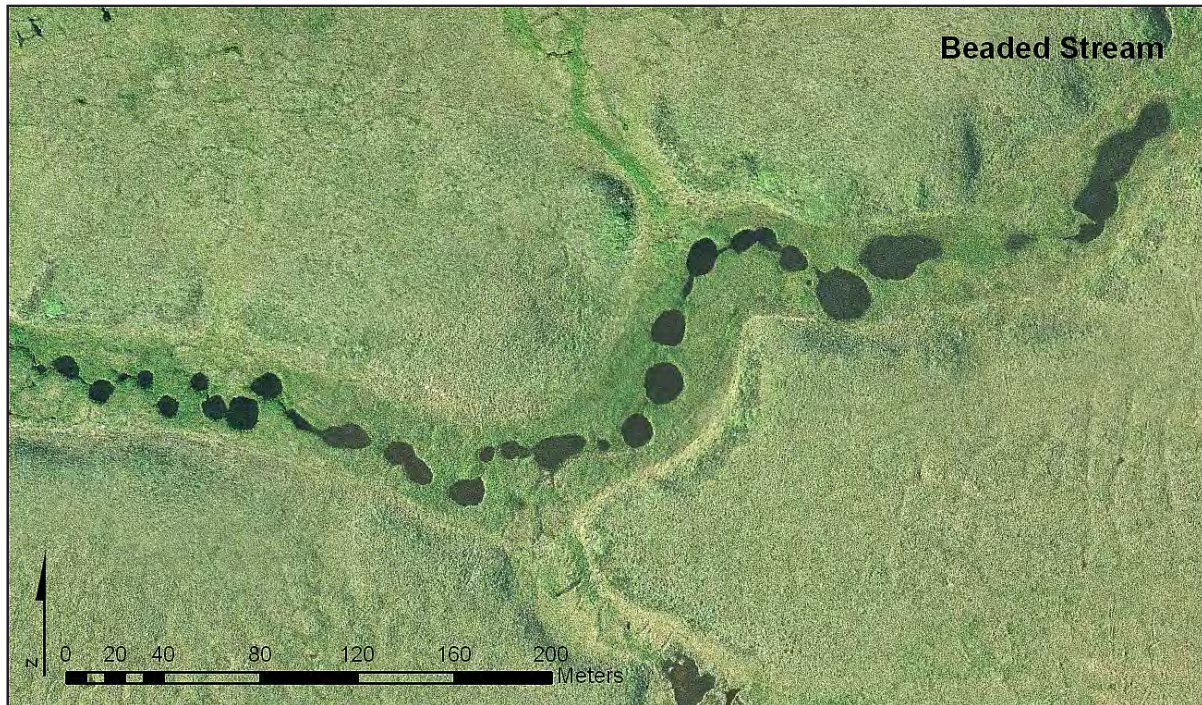


Figure 118. A 2004 airphoto of a beaded stream just south of Nuiqsut (Stop 2 on fig. 109). Beaded streams are formed in part from the thawing of massive ice at the intersections of the polygon network of ice wedges.

STOP 3: DRAINED LAKE AND ICE-CORED MOUNDS

Oriented lakes and the basins formed after lake drainage, which are common across the coastal plain of the North Slope, are present both to the west and east of the Colville Delta. A large (2.5 km² [~1 mi²]) oriented lake recently drained into a small channel that flows east just to the south of the present-day runway (fig. 119). Lakes have been tapped and drained by migrating channels on the Colville Delta at various times through the Holocene, creating a mosaic of drained lakes that are in various stages in the development of tundra vegetation and ice-wedge polygons. On the coastal plain deposits west of the Colville River, which have slightly pebbly loamy soils, the erosional sorting of materials within the lake creates silty centers and sandy margins. These silty centers tend to develop high concentrations of segregated and wedge ice and thus become uplifted in the middle (fig. 120).

In recently drained basins, the formation of small ice-cored mounds is common (fig. 119). Massive ice tends to develop in areas where the organic mat becomes sufficiently thick that the entire active layer is composed of peat. Presumably, during freeze-back in the fall, water easily migrates through the hydraulically conductive organic matter and accumulates at the freezing front at the top of the permafrost. Because the radius of water movement around the mounds is small, the mounds tend to grow only to 5 m (16.4 ft) in diameter and 0.5 m (1.6 ft) in height (fig. 121).

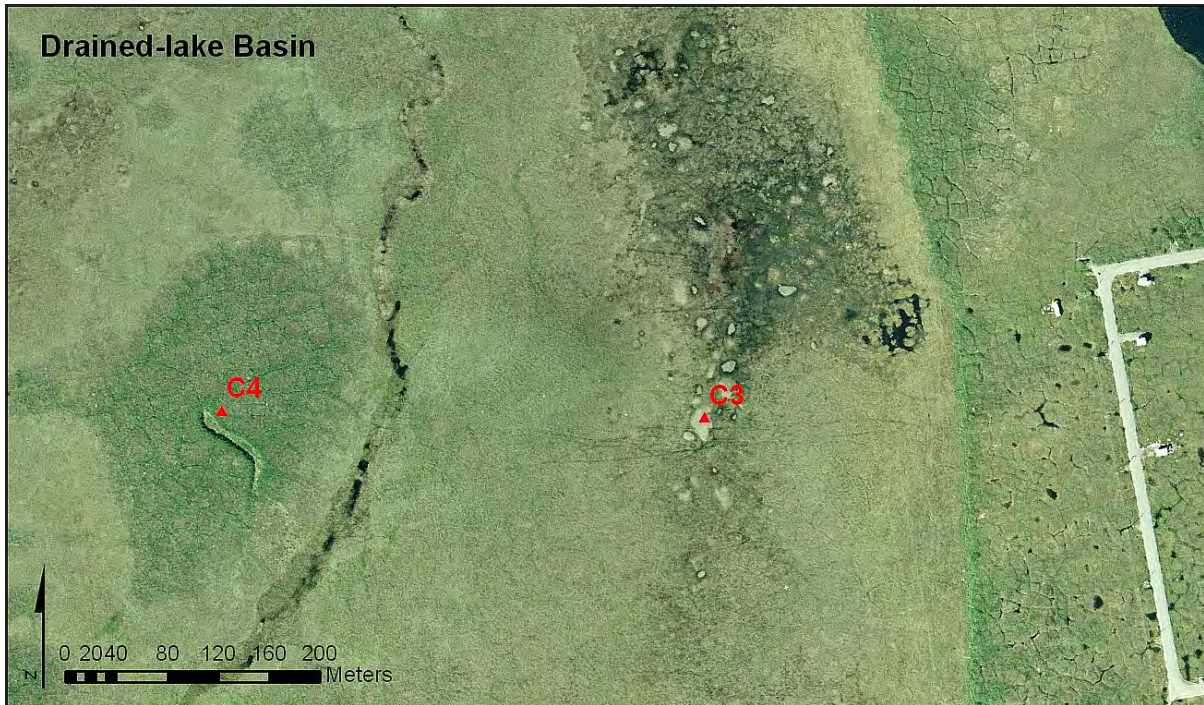


Figure 119. A 2004 airphoto of a young drained-lake basin on coastal-plain deposits adjacent to the Colville River Delta, near Nuiqsut (Stops 3 and 4). The nonpatterned surface lacks the polygonal patterns associated with well-developed ice wedges. The small white patches are 0.5-m- (1.6-ft-) high ice-cored mounds (C3). A pingo has formed in the middle of the basin (C4).

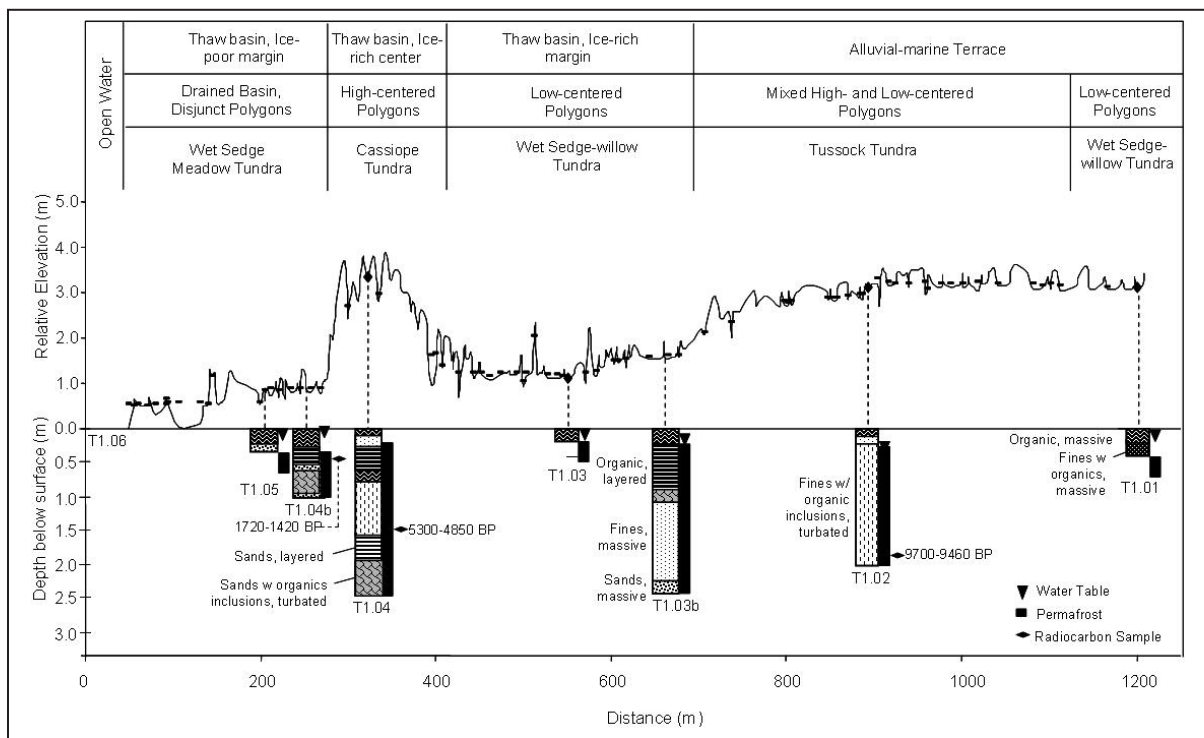


Figure 120. Topographic profile of a drained lake basin on the coastal plain west of the Colville Delta.



Figure 121. Ice-cored mounds typically form only in young drained-lake basins. They often have dead vegetation (*Carex aquatilis* and mosses) that indicate that they were formed recently. They typically have 0.5 m (1.6 ft) of poorly decomposed peat over clear, massive ice 0.3–0.5 m (1–1.6 ft) thick.

STOP 4: PINGO IN DRAINED LAKE

A small pingo occurs in the center of the recently drained lake basin west of Nuiqsut (fig. 119). The pingo is only ~3 m (~10 ft) high, has gently sloping sides, and is rather indistinct within the basin. The small stature of the pingo presumably is due to the nature of the talik, which forms a reservoir of unfrozen water that is the source for the growth of the ice core, and the sandy loamy material, which limits the rate of water migration through the sediments to the downward freezing front. One side of the pingo has been breached and that may have contributed to stalling of pingo formation (fig. 122). Because the surface of the pingo has been uplifted above the adjacent wet tundra, the better drained soils of the slopes support robust vegetation dominated by *Salix lanata*.



Figure 122. Photograph of a small pingo formed in the center of a recently drained lake basin. The pingo is vegetated with *Dryas* dwarf shrubs and low Richardson willow. Location of the pingo is shown in figure 119.

STOP 5: THE GUBIK FORMATION

Most of the landscape to the west of the Colville River Delta is dominated by the ‘Gubik Formation’, which is a generic term for all unconsolidated Quaternary sediments in the region (Black, 1964). In the high bluff near Nuiqsut (fig. 123), the deposit is a heterogeneous mixture of silts, sands, and gravels, with some boulders and fossil fragments of various types (including mammoth and mastodon). The banks rise 8–10 m (26–33 ft) above normal river level and, where adjacent to the active channel, are subject to erosion by the river. The erosion of the riverbanks at Nuiqsut has been monitored since 1962, beginning more than 10 years before the founding of the village. During most of the year, the riverbanks are protected by deep snowdrifts. However, with snowmelt, water begins to flow and the river stage rises. With breakup and the flooding that accompanies it, flowing water not only melts and erodes the protective snow cover but begins to undercut the bank, developing a thermo-erosional niche (fig. 124). The niche continues to widen and deepen as the stage, velocity, and temperature of the water

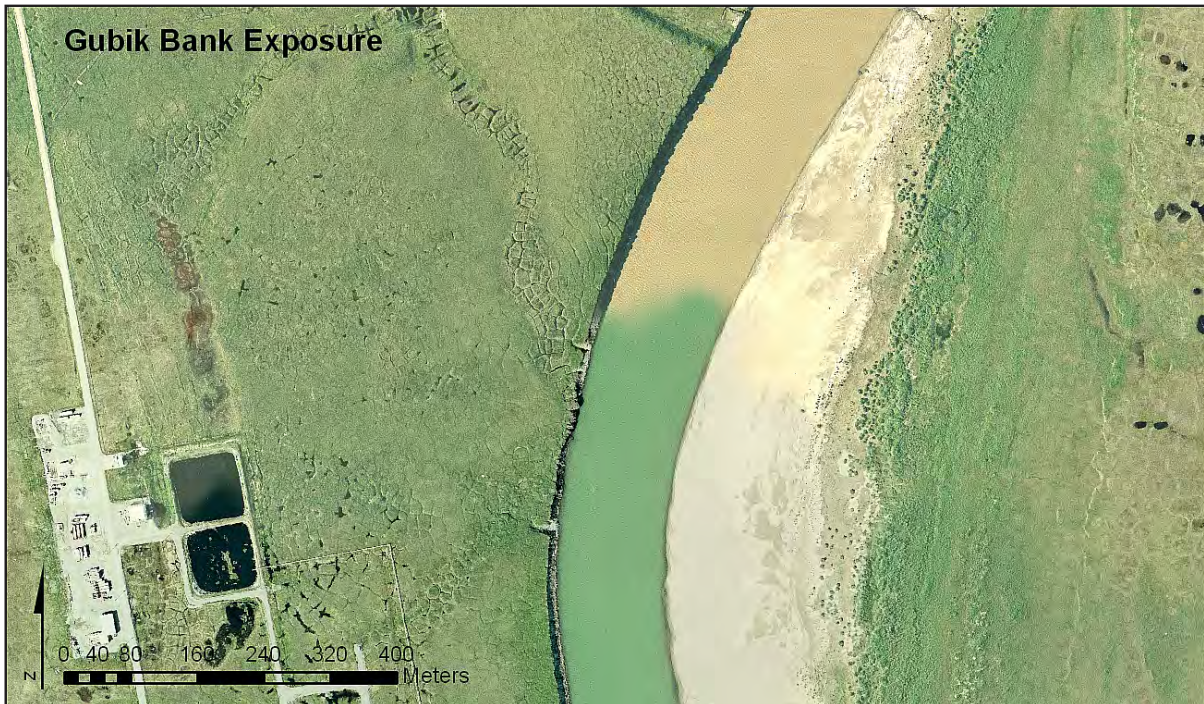


Figure 123. A 2004 airphoto of the riverbank below Nuiqsut that provides a large exposure of the coastal plain deposits associated with the Gubik Formation. Note location of Stops 5 and 6 on figure 109.



Figure 124. A thermo-erosional niche 8 m (26 ft) wide in the Gubik Formation (left) and the differential deposition of sediments in a niche (right). Note the melting ice wedge at upper left and the 3-m- (10-ft-) long rod in the niche (1966 photos by J. Walker).

increase. Frequently, the niche deepens sufficiently to cause block collapse, usually along ice wedges (fig. 125). Such ‘instantaneous’ action may result in a retreat of 6 m (20 ft) or more. During flooding most of the material that sloughed off the banks throughout the previous summer is transported downriver, exposing the permafrost-bound bank, which then begins to thaw and slough.

Between 1948 and 2004, the amount of bluff erosion at Nuiqsut ranged from only a few meters (10–15 ft) at the village site to more than 60 m (200 ft) at its northern end, which is equal to about one-half of the river width at that location (fig. 126).

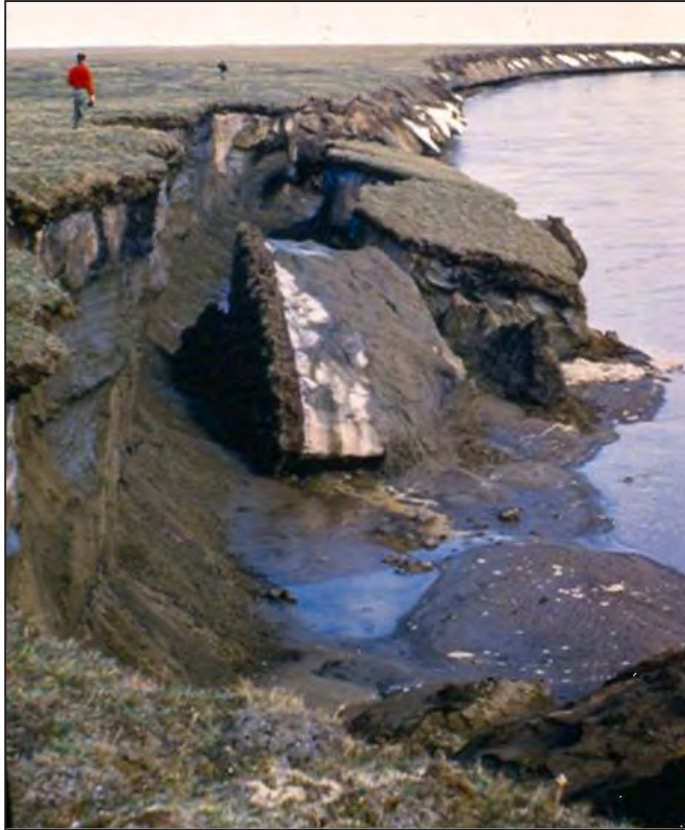
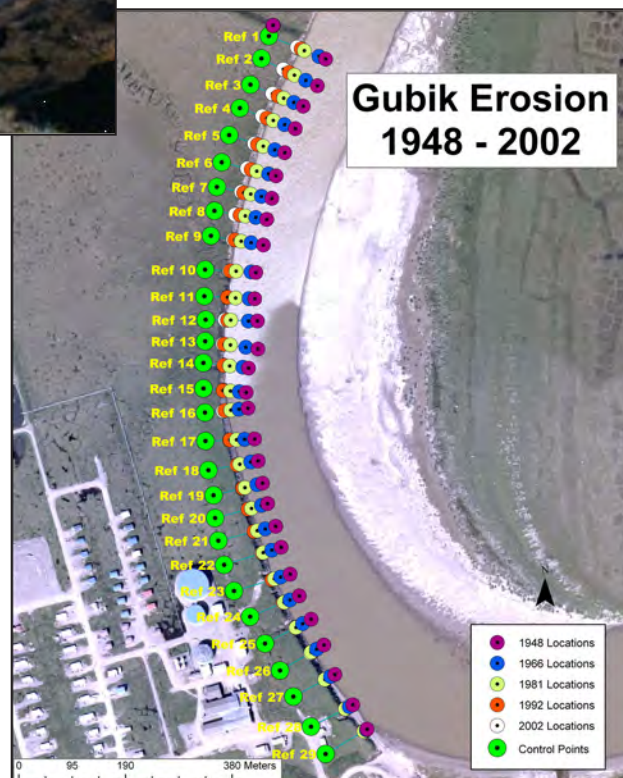


Figure 125. Blocks of permafrost in the Gubik often collapse along the weak lineaments of ice wedges (1962 photo by J. Walker).

Figure 126. Erosion of Gubik Formation at Nuiqsut 1948–2002 (courtesy J. Walker).



Because of the ice-rich nature of the sediments, the rate of retreat of both the wedges and the surrounding material (both organic and mineral matter) is about the same. Within the thermo-erosional niche, the ice-rich sediment thaws and drops to the base of the niche at a rate somewhat faster than does the meltwater from ice wedges. This results in the ice wedges forming ribs on the roof of the niche (fig. 124). Likewise, on the base, a small ridge and valley topography develops, reflecting differential sediment contents of the overlying materials. The temperature of the air also affects the rates of thawing of the exposed permafrost and the melting of the ice wedges. After floodwaters recede, most of the modification of the riverbanks is related to air temperature and gravity. In some instances the sloughing of the bank rapidly seals the niche, leaving a hidden cavity that is not exposed again until the next flood season.

The exposure at Nuiqsut reveals large ice wedges that have formed over a long period. Many of the wedges are 2–3 m (6.5–10 ft) across and have substantially deformed the soils adjacent to the ice wedges. Near riverbanks, surface water draining off the tundra becomes channelized along the degrading polygonal network of troughs above the wedges. Occasionally, the moving water can melt into the surface or side of the wedge ice, forming a tunnel. Freezing of the organic-rich water within the tunnel can form a distinctive tabular feature within the ice wedge (fig. 127).

The soil deposits adjacent to the wedges show enormous deformation caused by the growth of ice wedges, freezing and thawing of the permafrost table during syngenetic permafrost formation, and cryoturbation in the active layer (fig. 128). In this area, the Gubik Formation contains coastal plain deposits attributed to alluvial–marine origins (Carter and Galloway, 1985). The deposit is composed of slightly pebbly loamy sand, with clasts up to 10 cm (4 in) in size, and tends to be slightly saline. The deposit shows no apparent stratification, although near the surface there are large distorted inclusions of oxidized material that has been subducted deep into the profile, presumably during a large thaw event early in the Holocene. The upper portion of the deposit has inclusions of large masses of highly distorted peat. The deposit is covered by a thin blanket of peat. Oddly, the deposit lacks the distinctive stratification, shells, or plant macrofossils indicative of alluvial, marine, or eolian deposition. Larger stones from the formation erode and collect at the beach below the slope (fig. 129). Other stops on the delta will feature these deposition environments and help foster a discussion of the odd nature of these coastal plain deposits.

The point bar opposite the Nuiqsut bluff is advancing in a westward direction at about the same rate as the bluff is retreating. Deposition of sediment on parts of the bar, based on measurements of the thickness of sediment deposited on snow, is as much as 15 cm (6 in) during breakup. However, remnant snowmelt runoff and surface drainage across the bar carry much of the sediment back to the river after breakup. Frequently, small fan deltas develop along the edge of the river because of the cross-bar transport. As the point bar grows, a ridge and swale pattern develops, a type of topography that is reflected in the vegetation as well as relief.



Figure 127. An exposed ice wedge in the coastal plain deposits. The darker, thin horizontal layer of ice intruding into the left side of the ice wedge was formed by water that had thawed a tunnel in the ice and later froze in the cavity (photo by T. Jorgenson).

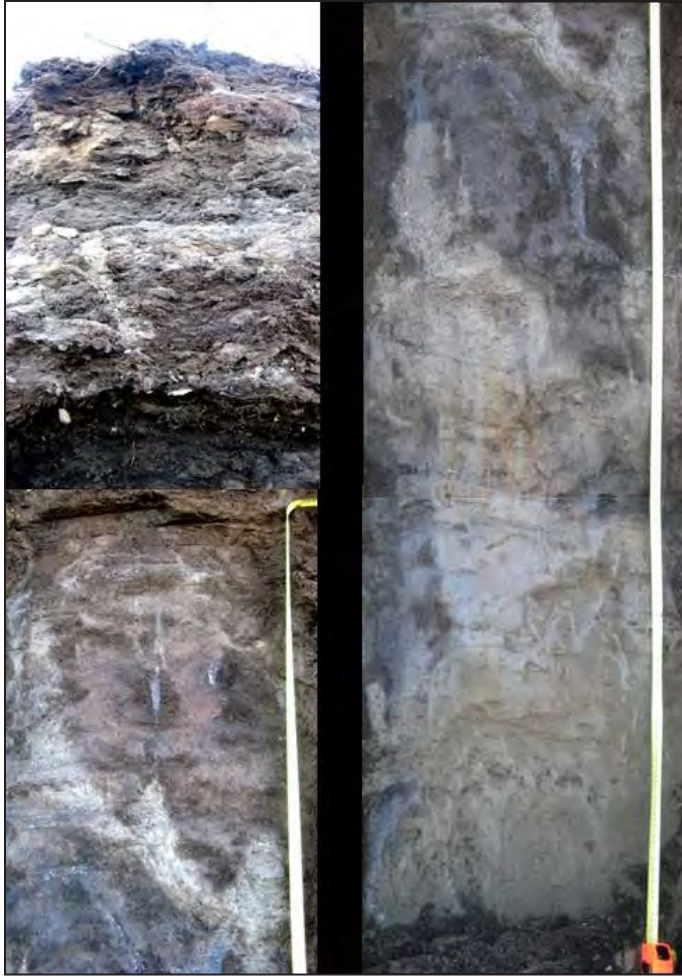


Figure 128. A 3-m- (10-ft-) high exposure of coastal plain deposits reveals the complex, disrupted stratigraphy of the interbedded peat and slightly pebbly loamy sands. Cryoturbated peat masses are frequently found at depths of 1–2 m (3.3–6.6 ft) (2007 photos by T. Jorgenson). Right photo is the lower section of photo at left.

Figure 129. Gravel and boulders on the beach at the base of an exposure of Gubik Formation (1970 photo by J. Walker).



STOP 6: DEGRADING ICE WEDGES

Deepening troughs and thermokarst pits that develop over thawing ice wedges are prevalent in the area (fig. 130). Many of those close to the village have been disturbed by human activity and the disturbance has contributed to the degradation, such as those on the riverbank near the fuel storage tanks (fig. 131). Thermokarst troughs and pits farther away, however, have been developing in response to recent climate warming. In some areas on the coastal plain west of Nuiqsut, extensive thawing of ice wedges has affected ~4 percent of the upland terrain (Jorgenson and others, 2006). Cottongrass tussocks grow and accumulate dead plant material over hundreds of years (fig. 132). The presence of dead tussocks in many of the pits provides good evidence that the degradation is not a response to normal climate fluctuations.

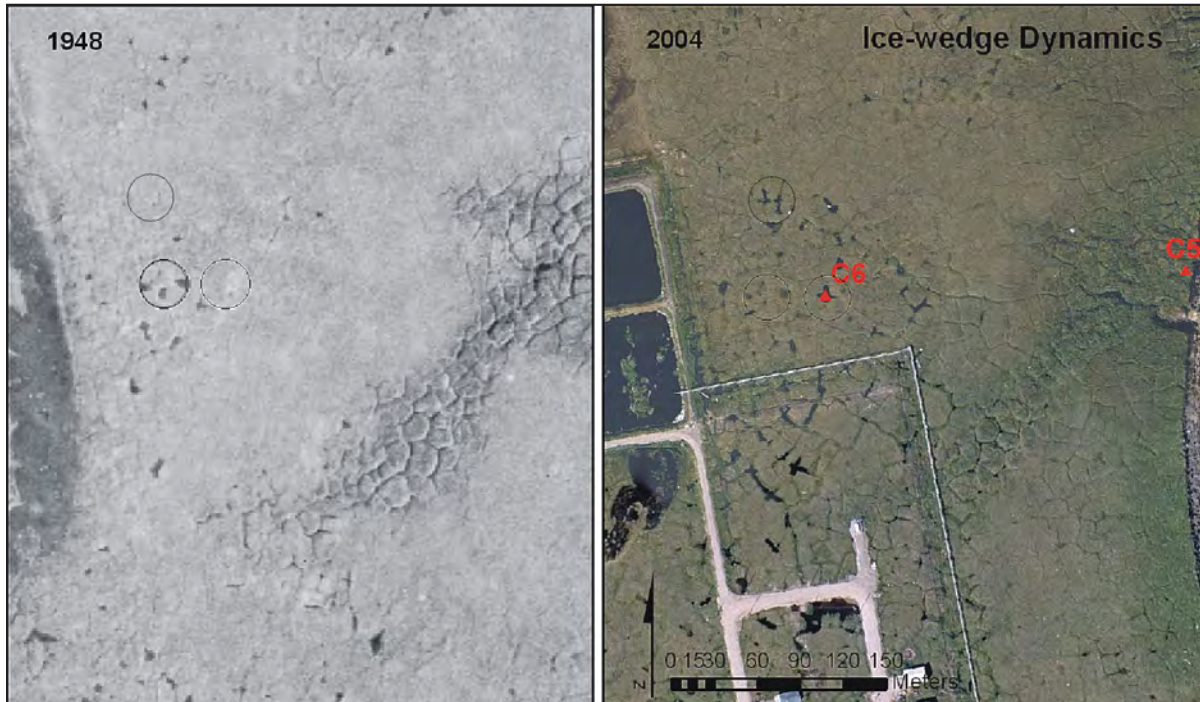


Figure 130. Comparison of 1948 and 2004 airphotos shows development of small waterbodies in the depressions formed by the thawing of ice wedges (Stop 6).



Figure 131. A dry trough (left) and gully (right) formed by the melting of ice wedges. Note the thermo-siphons around the fuel storage tank used to prevent permafrost thawing.



Figure 132. Cottongrass tussocks (*Eriophorum vaginatum*) on tundra surface (1981 photo by J. Walker).

STOP 7: PUTU CHANNEL

‘Putu,’ an Inupiat word that means ‘connection,’ is an appropriate name for the channel that connects the main channel of the Colville River with the Nechelik Channel (fig. 133). Within the past 50 years, Putu Channel has undergone major changes that have not only affected the discharge characteristics of the Nechelik but also its utilization by Nuiqsut boaters. Before the 1970s it was possible to use the channel throughout the summer and fall even during low stages in the river. The channel is one in which the flow reverses (fig. 134) with change in river stage. During low and normal stages, the water flows from east to west; during flood stage, flow is west to east.



Figure 133. A 2004 airphoto of the Putu Channel (Stop 7), which connects the Nechelik Channel (left) with the main east channel on the right.

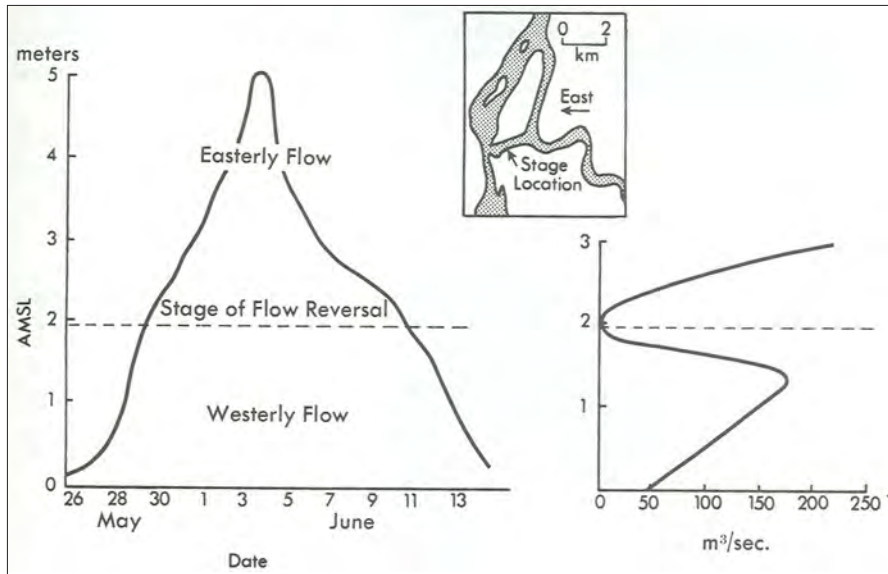


Figure 134. Diagram of flow reversal in Putu Channel (from Walker, 1983).

Because flow is eastward during breakup, much river ice that normally would flow down the Nechelik is returned to the main channel. During flow reversal large amounts of sediment are deposited in the channel. Thus, the channel has filled to such an extent that it is now impossible to traverse it at low water. As a result, attempts were made to deepen the main diversion channel by dredging. However, the location where the main channel diverges into the Nechelik is a locus for excessive deposition, much of it small gravel.

The Putu area contains excellent examples of one of the ways permafrost impacts drainage. An extensive dune system (among the highest in the delta) occurs on both sides of Putu channel. Within these systems small ponds have developed between dune bands because percolation through dune sand is impeded by permafrost. The ponds become perched, with permafrost acting as an aquiclude. It so happens three of these ponds (fig. 135) are situated close to the cabins of Camp Putu. This fortuitous location provided an ideal situation for the study of the development of the active layer in sand dunes under various types of vegetation (fig. 136). The outermost (southern) pond was selected for detailed surveys that were done as Sunday exercises during our seasons at the camp. (Incidentally, there was little objection to this Sunday exercise – partly because it was usually followed by a steak dinner.)

Putu pond, as we called it, is an example of an inter dune-band pond as is illustrated in the photograph. The crest of the pond's basin (2,600 m² [28,000 ft²]) varies between 10.2 and 13.7 m (33.5 and 44.9 ft) above sea level. The lowest part is some 6 m (20 ft) above the mud flat onto which overflow of meltwater drains (fig. 137). The



Figure 135. A 1972 airphoto of Putu ponds, which formed in swales between sand dunes. Note cabins of Camp Putu.

vegetation in the small basin includes thick mats of moss, grasses, flowering plants, and willows. The two most distinctive changes that occur seasonally within the basin are the development of the active layer and water-budget cycle. The rates of thaw of the permafrost within the basin vary greatly (fig. 138). For example, as shown by the diagram, the date the active layer had thawed to a depth of 20 cm ranged from May 12 under exposed sand to June 13 beneath the lake. The total seasonal thaw varied from less than 75 cm (29.5 in) under willow cover to nearly 170 cm (67 in) beneath the exposed sand surface.



Figure 136. Putu Pond showing vegetation types and a rare rainbow (photo by J. Walker).

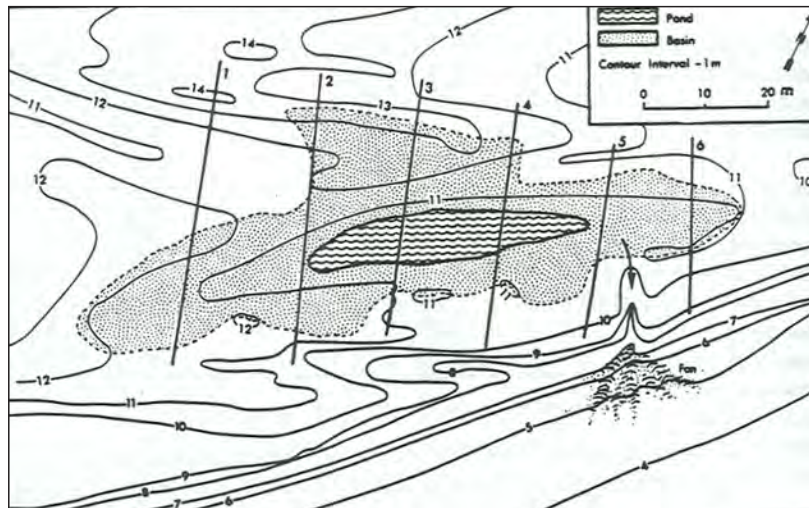


Figure 137. General map of Putu Pond in relation to the muddy riverbar on Putu Channel (Walker and Harris, 1976).

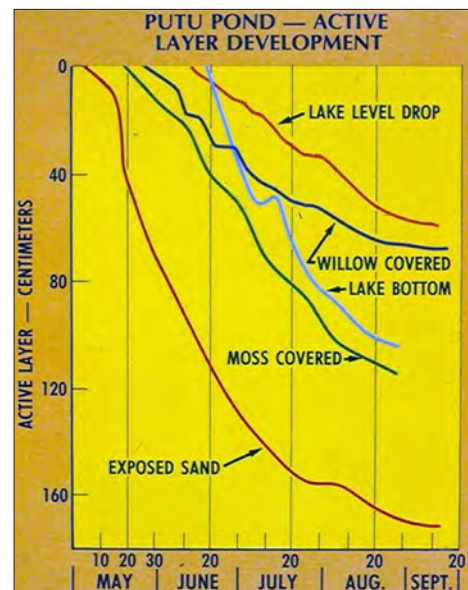


Figure 138. Active-layer development at Putu Pond under different surface conditions (Walker and Harris, 1976).

Incidentally, the sand dunes of the delta are ideal ground squirrel habitats (fig. 139). The squirrel dens during winter are partially protected from extremely low temperatures by snowdrifts. The snowdrifts can be quite thick; consequently, they are slow in melting and squirrels frequently burrow through them to get to the open air in spring.

Our view of Putu Channel is from one of the highest points in the delta. An extensive bar system can be seen to the southwest opposite the west end of Putu Channel. From here and for a long way downstream, the right bank is bordered by a series of gradually eroding dune bands interspersed with peat-filled swales (fig. 140), the majority of which trend at a slight angle to the channel. The peat and ice-wedge growth in the swales gradually reduces the local relief. This sand-dune system, which formed when the channel was northeast of its present position, is typical of the numerous dune systems in the delta. A shoreline bar has been migrating downstream toward the western edge of Putu Channel and now fronts the area of Stop 5.



Figure 139. Ground squirrels ('parka squirrels') are abundant on the sand dunes (1962 photo by J. Walker).

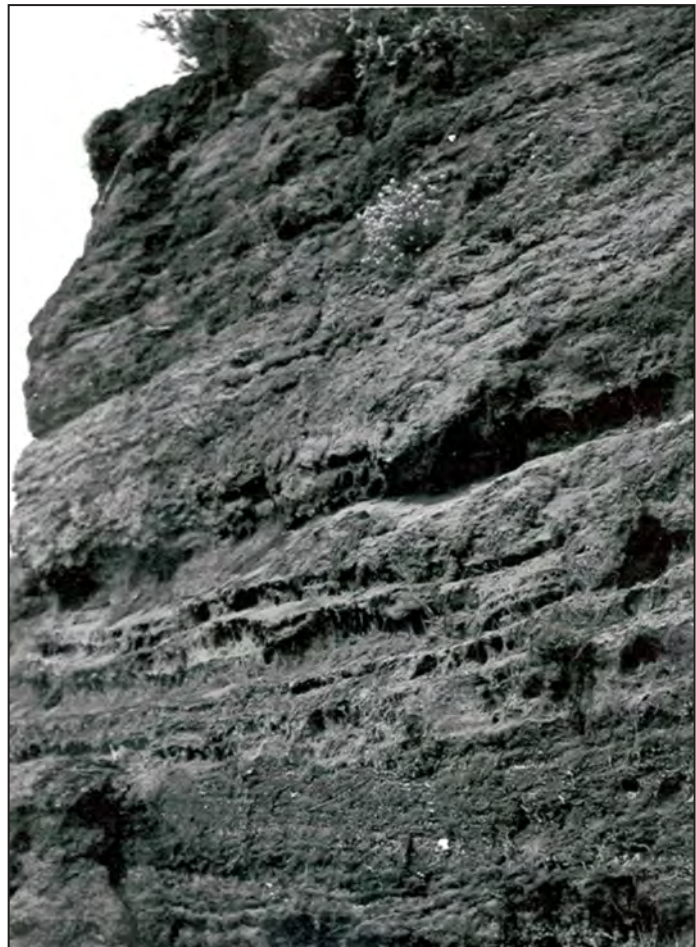


Figure 140. Interbedded peat and sand in an eolian sand deposit near west Putu Channel (1966 photo by J. Walker).

STOP 8: A TAPPED LAKE, AN ERODING PINGO AND THAW LAKES

As the Colville River migrates, it occasionally abandons portions of its channel, which become oxbow lakes. They can be quite long and relatively narrow but also deep. Later these lakes, as well as others in the delta, can be tapped by the migrating river. Stop 8 examines such an occurrence. Tapping and draining turned this former lake into a catchment basin where sediment can be trapped as flood waters back up into it (fig. 141). The shallowing of the lake by drainage and sediment input results in the lake's remaining water freezing to the bottom, which in turn results in the former talik freezing and becoming permafrost. Such a situation is ideal for the production of ice wedges and pingos (fig. 142). The pingo observed here has a typical crater at the top. It is now being eroded by the river, as are the deposits in the basin around it. Since it was tapped, erosion has reduced the width of the



Figure 141. A 1980 airphoto of a tapped lake that developed in an abandoned river channel (Stop 8). Small, circular lakes have formed in blowouts in the dunes.



Figure 142. Pingo formed in the middle of a tapped lake now being eroded by the Nechelik Channel.

former lake bed by about half. The relatively low lake bed also serves as a trapping area for river ice during breakup (fig. 143). Ice jams, which are frequent downstream from the pingo area, result in the backing of the flood water with its ice load as much as 1 km (0.6 mi) up the old channel, where the ice becomes stranded. Sand, gravel, and organic matter, such as peat shreds, grasses, and willow trees, that have been carried from upstream by the up-to-6-m- (up-to-20-ft-) thick river ice are deposited as the ice melts (fig. 144). Ice shove features are common along the sections of the riverbank that are overtopped by ice floes.

The basin is bordered on the north by a long, narrow dune ridge within which are two small ponds (fig. 141). These lakes were formed in a very different way than the perched ponds discussed at the Putu site. They are nearly circular and presumably are blowouts that may have developed from squirrel burrows that had attracted a hungry bear.



Figure 143. River ice 2 m (6.6 ft) thick deposited into a tapped lake by overbank flooding during spring breakup (1964 photo by J. Walker).



Figure 144. Ice floes 2 m (6.6 ft) thick with willow debris stranded at the pingo site (1964 photo by J. Walker).

STOP 9: PEAT BANKS, ICE WEDGES AND POLYGONS

The right bank (figs. 145 and 146) of the Nechelik Channel just downstream from the pingo is one of the most common types of riverbanks found in the Colville River Delta. Although somewhat more extensive along the right bank of the main channel, this Nechelik section is almost a textbook example of the type. They range up to 5 or 6 m (16–20 ft) in height and are usually quite smooth, especially after breakup flooding. Along their extent, ice wedges (fig. 147) are displayed at relatively regular intervals. These ice wedges, among the largest in the delta,

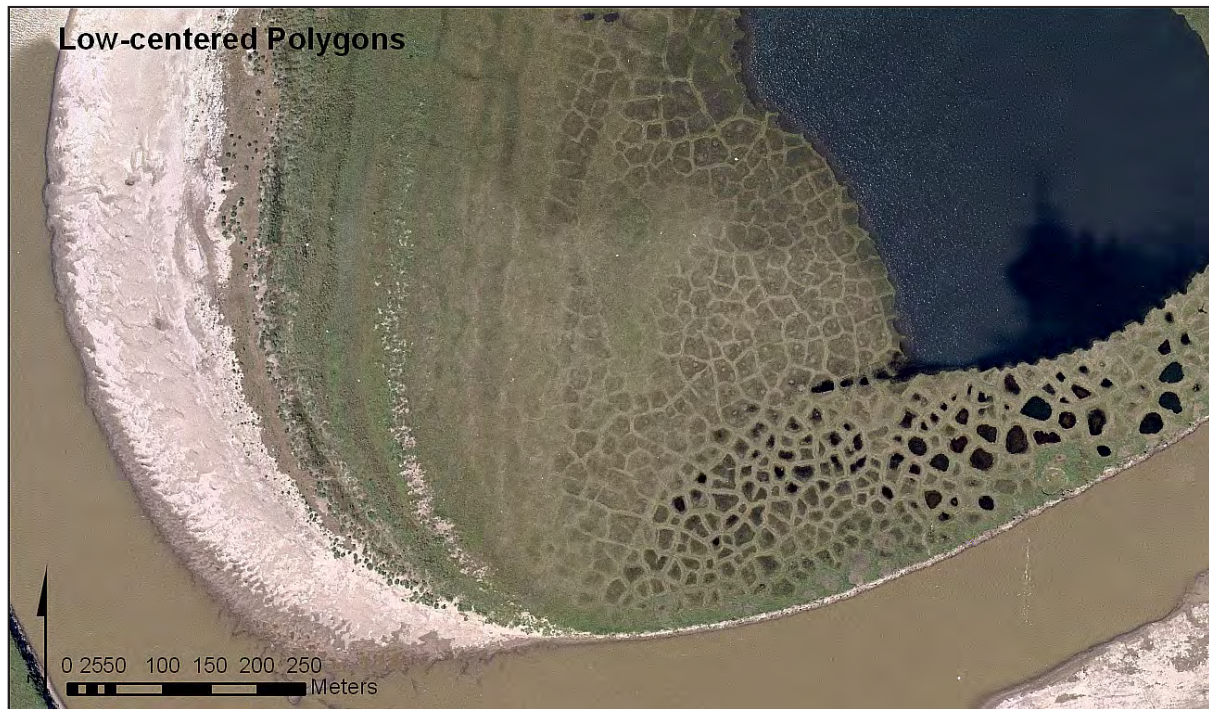


Figure 145. A 2004 airphoto of a large point bar near Nuiqsut showing the pattern of successional development from a barren riverbar (left) to an abandoned delta floodplain deposit with deep, low-centered polygons (right).



Figure 146. A 4-m- (13-ft-) high exposure of thick organic accumulations associated with an abandoned floodplain deposit along the Nechelik Channel (1970 photo by J. Walker).

have created a network that is quite conspicuous because the polygons have low centers with well developed troughs. These low-centered polygons, some 1 to 2 m (3–6.5 ft) deep, are distinctive landforms and are subject to draining as the riverbank retreats (fig. 148).

Erosion along this bank is typical of most peat-dominated banks in that the ice wedges recede at a faster rate than the peat that separates them. At the base of the wedges where undercutting has occurred, meltwater ponds usually develop and tundra mats drape over the upper edges. As summer progresses, parts of these peat ‘curtains’ fall into the ponds below. The ice wedges along the peat bank are wide enough so that some are exposed throughout the summer. Progressive melting of the ice wedges occurs along this section but not to the extent that it does along the main channel (fig. 149).



Figure 147. A 3-m- (9.8-ft-) wide ice wedge, which is a typical size for ice wedges in abandoned floodplain deposits, which develop over thousands of years (1970 photo by J. Walker).



Figure 148. A deep, low-centered polygon on an abandoned floodplain deposit after it was drained by development of gullies formed along melting ice wedges (1970 photo by J. Walker).

The Nechelik bank shows both the minimal notching that normally occurs in peat banks and the ice-scoured damage to the peat surface. Occasionally, however, undercutting of a peat block does occur, especially when it has a base of mineral matter (fig. 150). With erosion of peat banks, large quantities of peat (shreds and clumps) are contributed to the river. They become incorporated in the sediments that are found in the river. Although these peat banks rise to 5 m (17 ft) or more above normal river level, during flooding they are often overtopped. Driftwood (especially remnants of willow trees) is common, as are ice-shove features on the tundra surface.

To the north of this part of the Nechelik River is a large lake that is bordered by the same polygon field as the river. However, its erosional characteristics are quite different. It does not have the fluctuations in water level impacting its banks, such as those found in the river channel. However, it is affected by wind waves, which, because of the dominance of northeast winds in the snow/ice free period, impact the banks at about a 45-degree angle. The result is an irregular sawtooth-shaped bank (fig. 151). The character of the ice-wedge polygons (drained and undrained) are well defined.



Figure 149. The progressively melting ice wedges in ice-rich, abandoned flood-plain deposits lead to gully development (1981 photo by J. Walker).



Figure 150. Extreme undercutting of a peat/sand bank on the Nechelik Channel. A few hours after the picture was taken the block collapsed along the ice wedge that is visible in the picture (1981 photo by J. Walker)

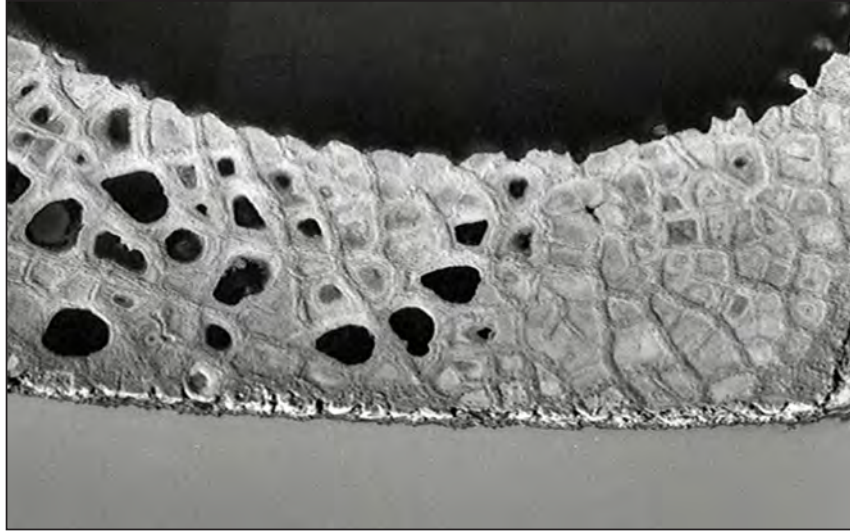


Figure 151. Airphoto illustrating the contrast between river (bottom) and lake (top) erosion of ice-wedge polygons (Stop 9). The deep, low-centered polygons are indicative of abandoned floodplain deposits.

STOP 10: A POINT BAR AND STABILIZED PORTION OF THE GUBIK FORMATION

From the north end of the Gubik Formation below Nuiqsut, a point bar extends downstream outlining a large meander (fig. 152). The bar's inner edge, which abuts an abandoned riverbank composed of the Gubik Formation (fig. 153), was at one time a deep portion of the Nechelik that trended perpendicular to the present river channel. The river eroded the formation at other locations that now form part of the floodplain. Since these sections were abandoned, the banks along the Gubik Formation have become stabilized and covered with vegetation. The major erosional factors that affect these stabilized banks are ground squirrels and, more recently, four-wheelers.



Figure 152. The first point bar downstream of Nuiqsut (Stop 10). The distance from the bluff cut into the Gubik Formation to the tip of point bar is 1 km (0.6 mi).

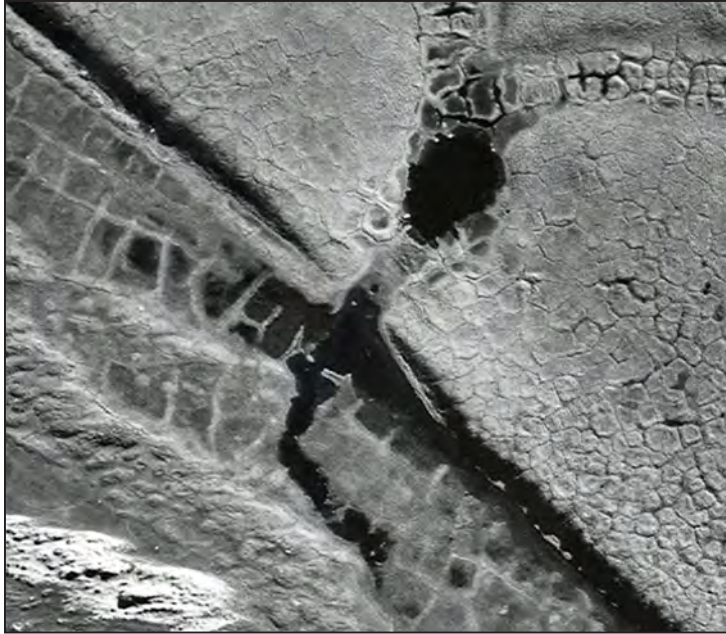


Figure 153. The bank transition from the ancient coastal plain of the Gubik Formation to the floodplain of the Colville River Delta. Note the contrast between the high density of high-centered polygons on the older surface and the low-density, low-centered polygons on the inactive floodplain. Both inactive and active sand dune bands appear in the lower left.

A section extending southwest from the river to the bluff on the Gubik Formation crosses many different types of surfaces (fig. 154). The first half (0.5 km [0.3 mi]) is composed of unvegetated sand. It is an area that is flooded each year and undergoes ice stranding and gouging during breakup and is an ideal source of sand for the prevailing northeast winds to mobilize.

The other half of the distance to the bluff along the Gubik Formation is composed of three dune bands of varying age. Those dunes nearest the present sand source are active with little vegetation but with some intra-dune ponds. The second set of bands is vegetated with few active portions. This series is composed of two to three separate bands, which merge at their upstream end, displaying a variety of ponds between bands. The downstream end of this series butts into the Gubik Formation. A third, shorter band of highly stabilized dunes lies inland of the second series.

Between the third dune band and the Gubik Formation is a relatively low area where the thalweg portion of the former channel flowed. It has a well-developed ice-wedge polygon system. These are large low-centered polygons that contrast with small, high-centered polygons that are present on the surface of the Gubik Formation. Across the second and third dune bands is a small drainage system that carries snow meltwater and presumably some ice-wedge meltwater (even if minimal) from the tundra surface.

Figure 154. North end of Nuiqsut Gubik Formation, showing the transition from the coastal plain deposits to a small dune ridge and on to an inactive delta floodplain deposit (1995 photo by J. Walker).



STOP 11: TAPPED LAKE AND LAKE DEGRADATION

Directly across from the point bar of Stop 10 is the remnant of a reversed L-shaped lake (fig. 155) that was tapped by the Nechelik and that now is more than half filled with sediment. The entrance to the lake lies between two peat banks at a sharp bend in a meander. The distance between the two peat banks is continually being enlarged through erosion. However, at that location the river is eroding even more rapidly into the river-side fill of the lake than it is into the more resistant peat banks. This focus of the channel's energy has also resulted in the transport of relatively coarse material over the bank at that location. Progressing inland from the bank, deposit grain size and quantity decreases. Sufficient time has not yet passed to have completely filled the former lake, but both ends of the L are now separate lakes, albeit shallow. Although the two remnants are shallow, their surface level has been affected by the buildup of the natural levee at the present entrance. Flowing across the stretch of lake bed that now forms the riverbank is a lake-drainage channel that carries snowmelt, ice meltwater, and river water that flowed into the basin during flooding. The walls of the drainage channel clearly show sediment banding that represents differential movement of varying sized particles during waxing and waning floodwaters. A traverse perpendicular to the Nechelik Channel extends from thick deposits with buried vegetation, to a zone where vegetation is growing up through finer textured sediments, to lush marsh grasses, and finally, lake water.

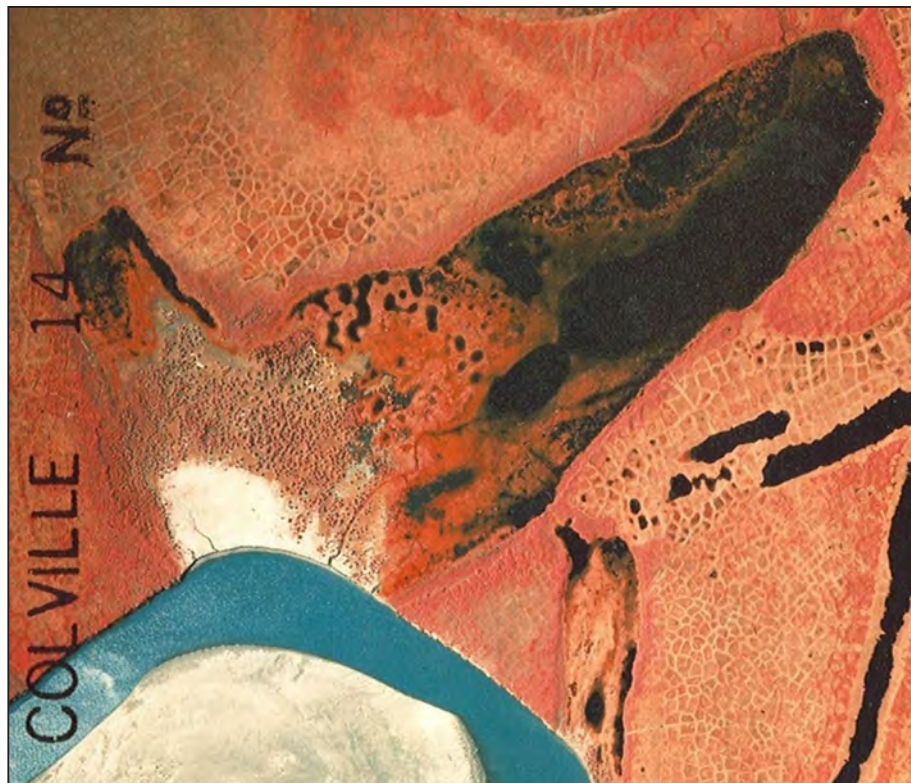


Figure 155. A 1992 airphoto of a tapped lake illustrating various degrees of fill (Stop 11).

STOP 12: FLOODPLAIN DEVELOPMENT

Flooding frequency, sedimentation, soil and permafrost characteristics, and vegetation all vary across the deltaic landscape in predictable patterns associated with channel migration (fig. 156). The toposequence at the stop originates on the barren riverbar and extends to the highest floodplain step, characterized as an abandoned floodplain cover deposit because of the lack of sediment accumulation in the thick surface peat (fig. 157). As sediment, organic matter, and ice raise the surface, sedimentation drops, organic accumulation increases, segregated ice aggrades in the permafrost, and vegetation growth slows in response to reduced nutrient input. The 3-m (10-ft) core obtained at the end of the transect had a radiocarbon age for the basal peat of 4.1 cal ka BP (Jorgenson and others, 1996).



Figure 156. A 2004 airphoto (Stop 12) showing a toposequence from the river to the highest floodplain step (Jorgenson and others, 1996).

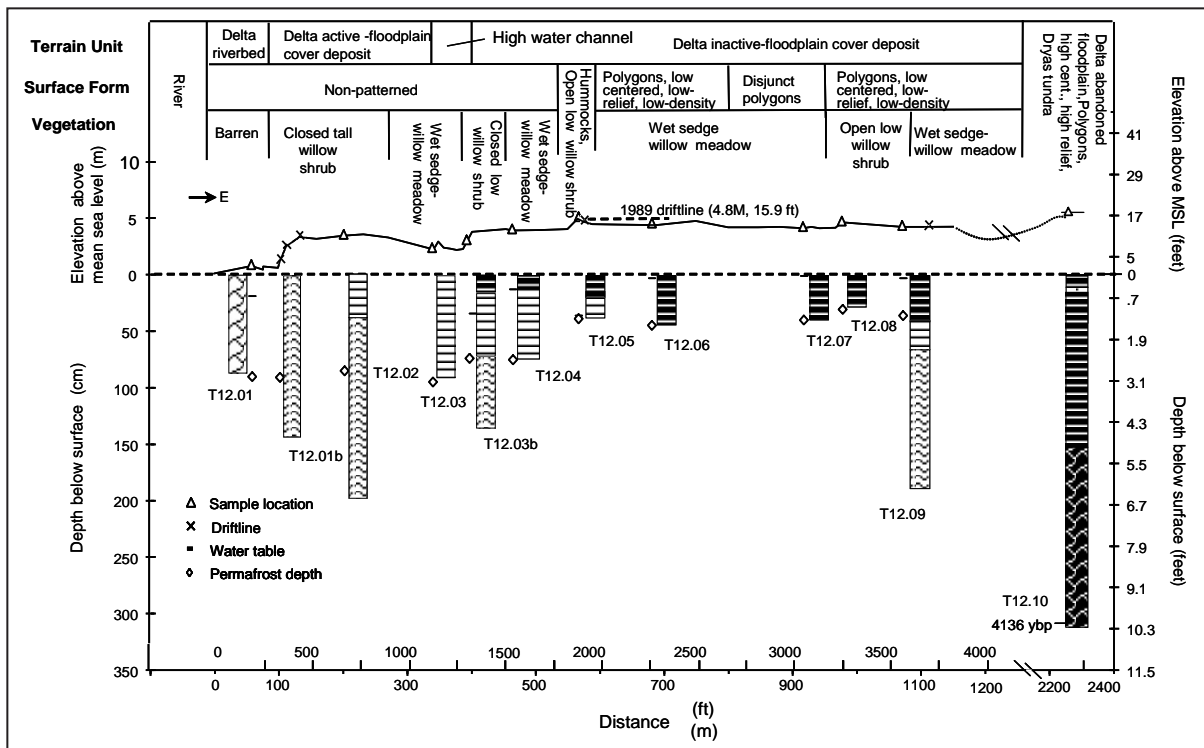


Figure 157. The toposequence across the floodplain illustrates changes in geomorphic units, soils, and vegetation as the delta develops over time (Jorgenson and others, 1997b).

STOP 13: DRILL SITE CD-4

Drill Site CD-4, formerly known as the Nanuq drill site, is one of two new drill sites recently added to the Alpine oil field (fig. 158). It is ~6.5 km (~4 mi) south of the Alpine Central Facility. Construction of CD-3 and CD-4 drill sites began in winter 2004–2005 and production started up for both drill sites in late summer 2006. To the north of Alpine, the Drill Site CD-3, also known as the Fjord well site, is the first roadless on-land drill site to be developed on the North Slope, and will only be accessible by air most of the year. The peak production rate is expected to exceed 3,000 bbls per day. Three long-reach horizontal wells are planned from CD-4 to develop the Nanuq–Kuparuk oil pool. Within the reservoir, these wellbores will be oriented parallel to each other and spaced 1,800 m (5,905 ft) apart. The oil will be processed through the existing Alpine facilities.

ConocoPhillips drilled the Nanuk No. 1 discovery well in 1996. The discovery was confirmed by the Nanuk No. 2 exploration well that was drilled during 2000. ConocoPhillips subsequently drilled three additional exploration wells to delineate the accumulation. Three-dimensional seismic and well data have been used to determine the geologic structure and reservoir distribution. The Nanuq–Kuparuk reservoir is the accumulation of hydrocarbons in an interval at 2,425–2,430 m (7,956–7,972 ft) that lies within the Cretaceous-aged Kuparuk River Formation. The Nanuq–Kuparuk reservoir is a thin, transgressive, shallow marine sandstone that lies atop the Lower Cretaceous Unconformity and is overlain by mudstone and shale assigned to the Kuparuk D interval, Kalubik Shale, HRZ, and basal Torok, in ascending order. Oil in place is estimated to be 21–36 million bbls and the recoverable portion of the oil is estimated to be 11–28 million bbl.

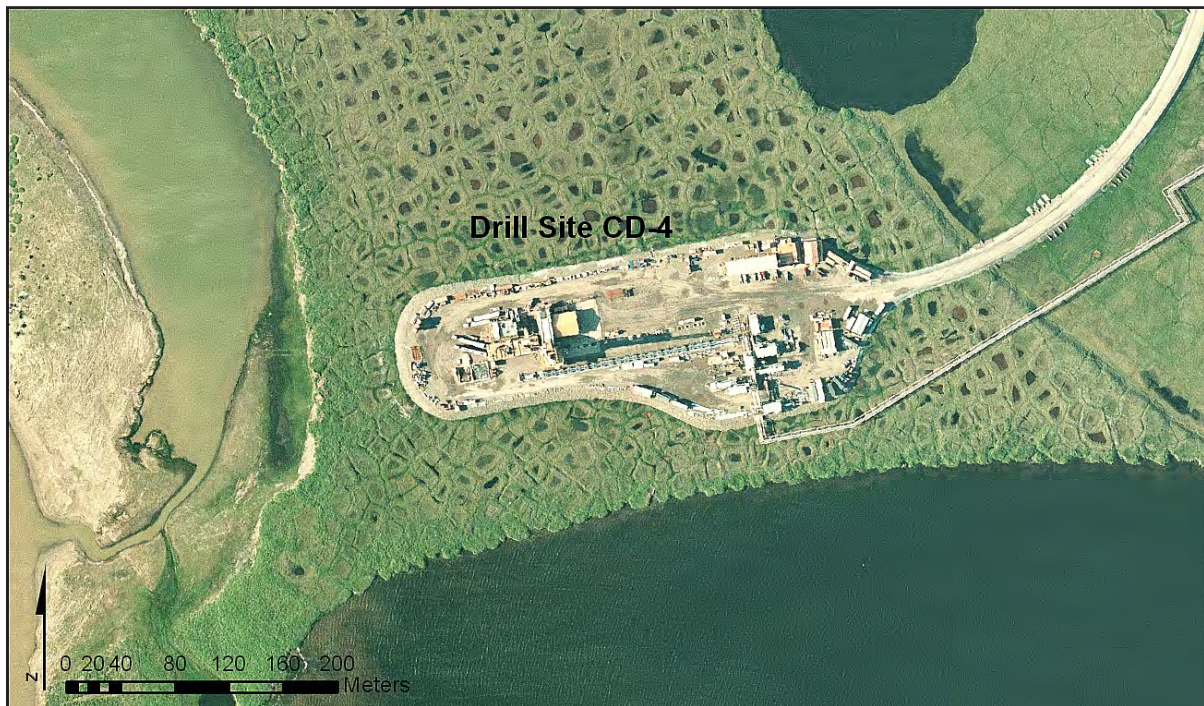


Figure 158. A 2004 airphoto showing the initial stages of construction of the CD-4 drill site (Stop 13), which was recently added to the two earlier drill sites at the Alpine oil field. New drill sites are highly compact with narrow well spacing, use far-reaching directional drilling, lack reserve pits, and are situated away from basins and drainage ways.

STOP 14. SLOUGH ENTRANCE, WILLOW VEGETATION, AND TURF-HOUSE SITE

Downstream from Stop12 the Nechelik butts into the Gubik Formation in a similar fashion to what it does at Nuiqsut (fig. 159). Its beach is different from that at Nuiqsut, however, in that it has exposed gravel and boulders. It is not uncommon to find mammoth tusks and teeth on the beach. The crest of the bluff has been (and may still be) a nesting location for eagles.

A short distance (1 km [0.6 mi]) north of the north end of the bluff is the entrance to a slough that meanders across delta fill until it reaches another exposure of the Gubik Formation and then flows north in a meandering fashion, butting up against the Gubik Formation in several places before wending its way back to the Nechelik.



Figure 159. A slough off the Nechelik Channel with two tapped lakes (Stop 14). Note the development of polygons in the lake basin on the right. Higher coastal plain deposits of the Gubik Formation are to the left.

The tundra surface north of the slough entrance is a relatively level plain with numerous ice-wedge polygons and low belts of sand dunes. A vast field of dwarf willow trees extends to the northwest. On the bluff above the slough entrance was a house site. One turf house was present during the 1980s, but may have been lost to erosion by now. The house was built on a low sand-dune ridge that extends inland from the riverbank. Turf blocks and corner logs were still in place during the 1980s.

The bank face illustrates a variety of deltaic environments and processes. The west bank of this section of the Nechelik is mainly peat, although dune sand and highly organic silt are interspersed with the peat. In some locations, dune sand overlies the peat. Wind scour and ground squirrel activity are evident and willow roots (some as long as 12 m [40 ft]) are visible because of bank retreat.

About halfway down the slough is a unique set of tapped lakes. The tapped lake on the east side possesses a varied set of polygons that apparently formed on the shallow portion of the lake and are now exposed except during flood. The entire area between the slough and the Nechelik Channel is a combination of abandoned migratory channels (some of which are quite conspicuous) and point bars with a few well-preserved sand dunes. Also present are numerous ice-wedge polygons, many of which are quite square and filled with water.

STOP 15: SAND DUNE AND TURF-HOUSE SITE

Some of the highest dunes along the Nechelik north of Nuiqsut are found 1 km (0.6 mi) south of the entrance to Nanuk Lake. It is a stabilized dune that is being eroded by the river so that it has a fresh, unvegetated slope facing west. It is high enough to trap so much snow during the winter that it often is the last in the delta to melt, even persisting well into July in some years (fig. 160).

Ice-wedge polygons have formed within the swales of this dune system. Some of these polygon fields are only one or two polygons wide within narrow swales. Linear lakes are also present in some of the swales.

This dune is the highest point in the area, thus frequently served as a camp site and observation post. The remains of turf houses that were constructed by reindeer herders during the early 1900s are still visible.



Figure 160. Sand dune near the entrance to Nanuk Lake with snowdrift lasting late in the season (1961 photo by J. Walker).

STOP 16: LAKE NANUK

Nanuk (Nanook) Lake or Polar Bear Lake (fig. 161) is a lake that was tapped only a few years before the first aerial photographs (1943) were made of the Colville River Delta. It is thus a good representative of the history of the changes that occur after the tapping of a major lake in an arctic delta. A cursory examination of the lake was made in 1961, an echo-sounding survey was done in 1962, and detailed surveys of the lake's entrance/exit have been made periodically since then. Thus, there is a fairly good record of the changes in Nanuk Lake during the past 50 years.



Figure 161. The drained-lake basin, or 'tapped lake', of the former Nanuk Lake (Stops 15 and 16).

After tapping, the two first occurrences were the draining of the lake and the creation of a scour hole where draining lake water meets the river. The scour hole, when first measured (1962), was more than 10 m (33 ft) deep. This scour hole persists (fig. 162) because during river flooding the lake fills and as the river stage lowers, lake drainage creates a whirlpool at the exit. The bank at the downstream end of the entrance is impacted by river flooding and ice jamming, subjecting it to severe erosion (fig. 163). The scour hole itself also migrates in a downstream direction. From the first airphotos in 1948 until 2004, the gap increased by 92 m (301 ft), averaging 1.6 m (52.5 ft) per year (fig. 164).

Once a lake is tapped, deposition proceeds rapidly. The coarser sediment is deposited just in from the entrance by inflowing water, forming a small lake delta. Finer (and lighter in the case of organic matter) materials are carried farther into the lake before deposition. Because the lake is essentially a stilling basin, deposition is heavy. With the largest amount of material being deposited soon after the floodwaters enter the lake, it does not take long before the lake is converted into two lakes with a sand/silt bar between (fig. 165). As the river stage lowers, lake drainage also creates an exit channel that frequently changes position as the lake fills.

Figure 162. Nanuk Lake entrance channel and scour hole (Roselle and Walker, 1966).

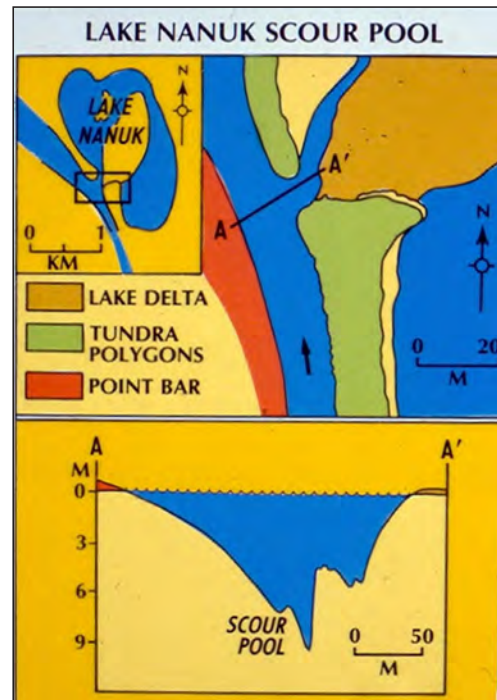


Figure 163. Nanuk Lake (center) during flooding in 1971. The large ice-covered lake (bottom) is Caribou Lake, which was tapped and drained in 1972 (photo by J. Walker).

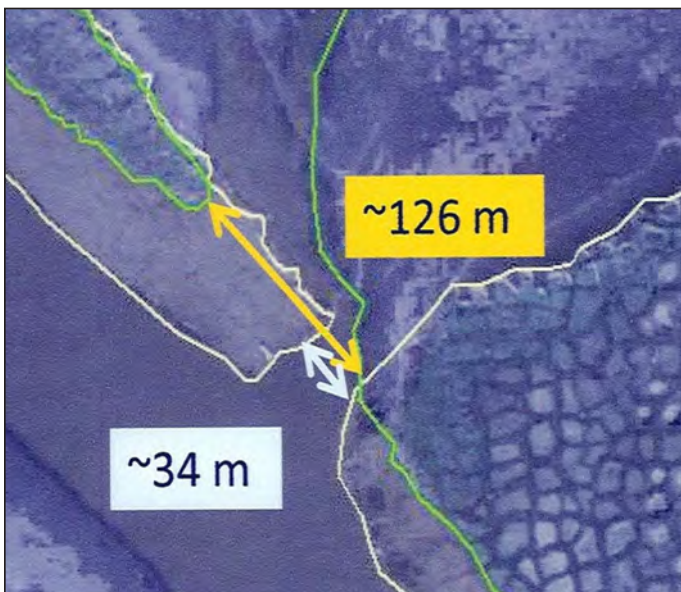


Figure 164. The expansion of the entrance/exit to Nanuk Lake between 1948 (white) and 2004 (green).

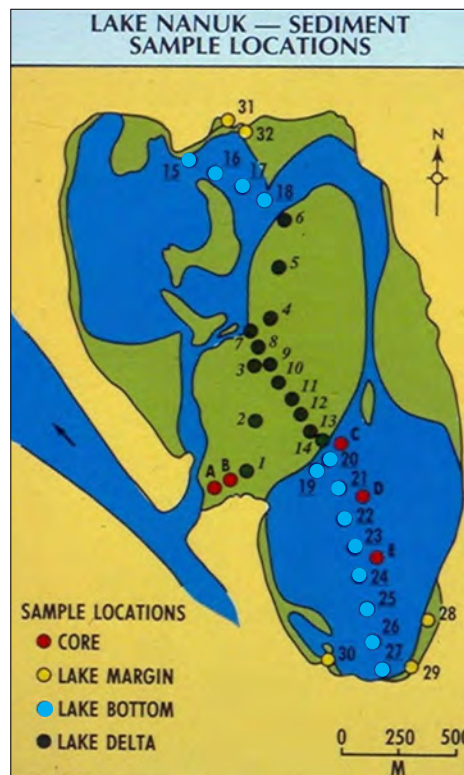


Figure 165. Nanuk Lake, illustrating the division into smaller lakes that results from heavy sediment deposition during flooding (Roselle and Walker, 1966).

Immediately after drainage little of the lake bottom was exposed even during low river stages, but over time the extent of exposed lake bottom increased rapidly due to accumulation of sediments in the basin. Thus, today (2007) most of the original lake area is now above river level at normal stage. After flooding, exposed sediments dry out rapidly and are subject to wind erosion and transport. With the prevailing northeast winds, dunes have formed on the tundra surface that separates the river from the lake. The bare sediments in the lake basin are frequently used by animals and birds of various types (fig. 166).

The entrance to the lake is another ideal location for a campsite. During a visit in 1970, erosion at the north end of the entrance exposed some artifacts that were about to fall into the river (fig. 167). Nearly the entire site had already disappeared because of the erosion of the north shoreline.

One additional element present at the lake’s exit is the oil boom that has been placed across the mouth for the purpose of preventing any oil that might be spilled into the lake from being carried out into the river (fig. 168).

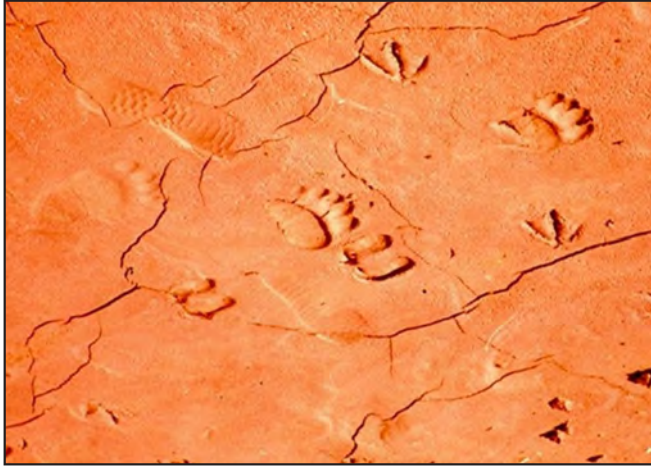


Figure 166. Lakebed with footprints of brown bear, caribou, geese, and Inupiat (with tennis shoes on) (1961 photo by J. Walker).



Figure 167. Artifacts being eroded into the river at Nanuk Lake entrance. Note caribou-horn digging tool, ulu, and bell (Russian trade item?) (1970 photo by J. Walker).



Figure 168. Drill Site CD-2 of the Alpine oil field initially completed in 2000 with an oil boom across mouth of Nanuk Lake (2006 photo by J. Walker).

STOP 17: LOW TUNDRA SURFACE

The tundra surface lowers in elevation as the front of the delta is approached (fig. 169). Peat is the common material and, as is true of the high peat banks elsewhere, erosion progresses more rapidly in the ice wedges than the material separating them (fig. 170). Although the area displays polygonal structures, they are not especially conspicuous. The ice wedges are as much as 45–50 m (148–164 ft) apart. Progressive ice-wedge melting is not as great as elsewhere in the delta because of the shearing of the peat between the wedges. The result is a bench that serves as a trap for driftwood. Flooding frequently overtops the bank, resulting in driftwood being carried as much as 100 m (330 ft) inland. Erosion rates along the left bank in this part of the delta average about 0.5 m (1.6 ft) per year, although the rates have decreased in the past 30 years (fig. 171).

This section of the river is frequently used for net fishing, and remnants of the camps are common (fig. 172). This section is also one of three sites recommended for construction of a year-round bridge that would service the expansion of the petroleum industry and Nuiqsut.



Figure 169. A 2004 airphoto of Drill Site CD-2 and the site of a proposed bridge crossing of the Nechelik Channel to provide access from Alpine to satellite fields in the NPRA (Stop 17).



Figure 170. Riverbank showing typical erosion (1971 photo by J. Walker).

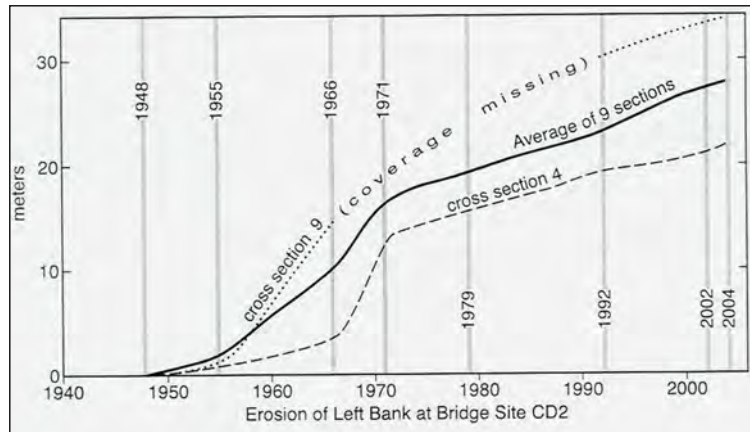


Figure 171. Erosion rates on the low tundra at the proposed bridge crossing (by J. Walker).



Figure 172. Low tundra with low-relief high-centered polygons (left) and high-relief, low-centered polygons (right) caused by ice-wedge expansion. Note fish camp site (2006 photo by J. Walker).

STOP 18: NIGLIK (THE WOODS' CAMP)

The Inupiat word for geese is 'niglik', which, when spoken rapidly ("niglik, niglik, niglik"), sounds like the call of geese. Niglik is one of the most famous locations along the north coast of Alaska (fig. 173), because this is the place where the Inupiat from Barrow met the people from the Anaktuvuk Pass area in the Brooks Range (and, by extension, from the Bering Sea region) for trade. On the tundra area just south of the Woods' Camp, remnants of campsites abounded until riverbank erosion destroyed them. During the past 50 years the bank has retreated by some 60 m (200 ft) (fig. 174) and, because the traders established their camps as close to the river edge as possible, it did not take much erosion to destroy all evidence of their material culture. Subsequent to the 1950s, relatively few remnants remained along the bank.

A 1979 report from the North Slope Borough notes that "Siberian goods, brought overland from the Sisualik trading site near present Kotzebue, continued their way into the Canadian Arctic from Niglik. Even after the arrival of commercial traders, the Niglik trade fairs continued, incorporating modern trade goods with traditional ones until the early decades of the century."

During the last half of the 20th century (fig. 175), this location served as the permanent home of the Woods (Kisik) family until they moved to Nuiqsut. The present-day members of the family (Abe, Joeb, Lydia, and their children and grandchildren) still own the location and utilize it at various times of the year. The family depended largely on caribou (fig. 176) and fish, both of which they stored in ice (permafrost) cellars (fig. 177). Of course, they dried fish as well (fig. 178). Until recently, driftwood collected along the river was the main fuel resource. Since the Woods family built their house and dug their ice cellars, riverbank erosion has taken its toll. Some of the cellars have been destroyed and the buildings moved.



Figure 173. A 2004 airphoto of the tidal flats at the mouth of the Nechelik Channel (right) (Stops 18 and 19).

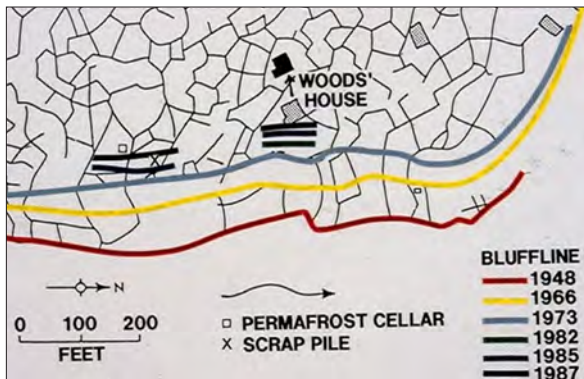


Figure 174. Erosion at the 'trade fair' area at Niglik, which later became the site of Woods' camp.



Figure 175. Niglik, or the Woods' camp, at the mouth of the Nechelik Channel (2006 photo by J. Walker).



Figure 176. Caribou in the river (1962 photo by J. Walker).

Figure 177. Permafrost cellars commonly used to keep fish and game frozen through the summer. The cellar at Niglik had a winch (left). The walls become covered with rime ice (right) (1970 photos by J. Walker).



Figure 178. Nannie Woods preparing white fish for drying (left) and hanging white fish ('pepsi') (1961 photos by J. Walker).

STOP 19: SAND BAR AND HARRISON BAY

From Niglik to where the Nechelik Channel joins Harrison Bay is about 5 km (3 mi) (fig. 179). The west side of the channel is an extensive sand bar that supports a variety of features including cross-channels, several sets of sand dunes (fig. 180), and extensive mudflats. To the southwest is one of the largest expanses of coastal wet meadows in northern Alaska (fig. 181), which are important habitats for brant and snow geese.

During breakup flooding, ice and organic debris become stranded on the flats (fig. 182). Much of the area, 15 km² (5.8 mi²) in size, also floods during high water from storm surges, which are quite common in fall when sea ice is farthest from the shore. During such surges, logs from the MacKenzie River occasionally become stranded on the sand bar (fig. 183).

Seaward of the Nechelik Channel are bars and flats in a shallow shelf area that stretches out many kilometers before depths of 2 m (7 ft) are reached. The sea ice (fig. 184), which lasts nine or more months of the year off shore, is bottom-fast during much of that period. Subsea permafrost is also present seaward of the delta.

Figure 179. Profile from Nechelik Channel to Harrison Bay across the Niglik sand bar (courtesy of J. Walker).

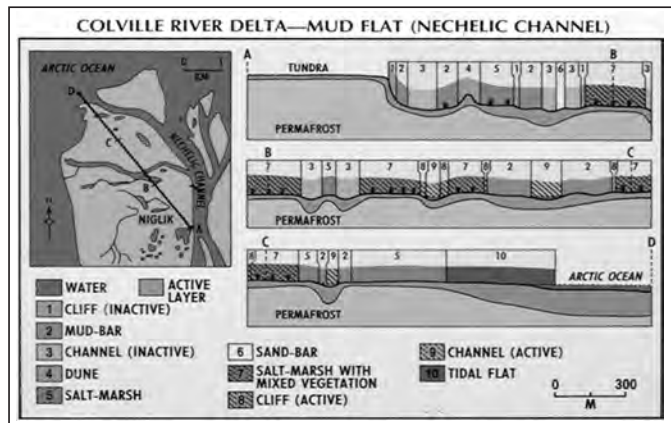


Figure 180. Low sand dune on mudflat vegetated with dune grass (1972 photo by J. Walker).



Figure 181 (below). Brackish coastal meadow with salt-tolerant sedges and grasses (left) and salt-killed tundra inundated by storm surges (right) (2003 photos by T. Jorgenson).

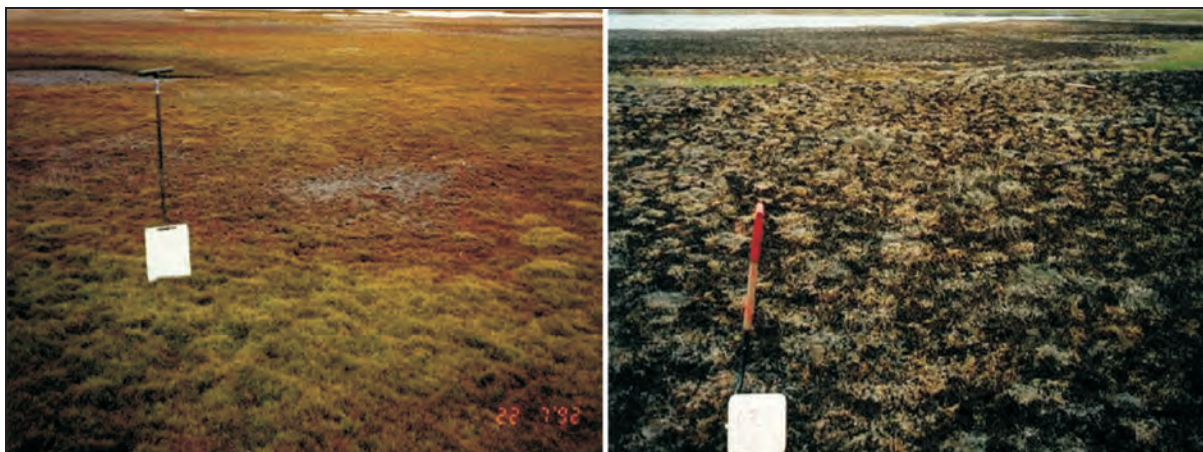




Figure 182. Detrital peat eroded up-river and trapped on a sand bar during waning floods. The peat fragments become buried in the sediments and are indicative of a specific depositional environment (1971 photo by J. Walker).

Figure 183. Large spruce logs, which originated from the boreal forest up the MacKenzie River, occasionally become stranded along the fringe of the delta (1961 photo by J. Walker).



Figure 184. Sea ice near the Colville River delta (1962 photo by J. Walker).

STOP 20: ALPINE OILFIELD

Discovered in 1994 and declared commercial in 1996, the Alpine oil field is the largest discovered in the U.S. since the mid 1980s. The initial exploration effort by ARCO Alaska, Inc., Anadarko Petroleum Co., and Union Texas Petroleum, used 970 km (600 mi) of modern 2D seismic data acquired from 1991 to 1994 (Gingrich and others, 2001). Several years of drilling in the area had resulted in successfully finding oil reservoirs, but none large enough to support a new production facility. Two final wells, ARCO Fiord #2 and Bergschrund #1, were drilled during the winter of 1993–94 to evaluate the potential of Cretaceous Kuparuk C sand and test a younger slope-fan prospect. Both of these plays proved unsuccessful, but the wells discovered oil in the ‘Alpine’ sand in the Upper Jurassic interval.

Development drilling began in 1998, and nine facilities modules were delivered to the North Slope via sealift in July 1999. Oil production from CD-1 began in November 2000 and from CD-2 in November 2001. The Alpine oil pool has now been penetrated by more than 100 wells, most of which are horizontal production and injection wells. Oil, gas, and water produced from the drill sites are carried via pipeline to Alpine’s CD-1 for processing. Sales quality crude is transported from CD-1 via the Alpine oil pipeline and Kuparuk pipeline to the Trans-Alaska Pipeline. Gas and Kuparuk-supplied seawater are delivered to the drill sites via pipelines from CD-1 for injection into the reservoirs. Originally projected to produce 80,000 bbls of oil per day, the Alpine oil pool production greatly exceeded expectations by producing an average of 115,000 bbls per day by 2005. The addition of the two satellite drill sites (CD-3 and CD-4) brought peak production to 135,000 bbls of oil per day in late 2007. Alpine is the first arctic oilfield built on the floodplain of a delta and has substantially reduced the footprint of modern oil development. Its facilities occupy only 39 ha (97 ac) at the surface, but it produces from about 10,118 ha or 101 km² (25,000 ac or 39 mi²) of reservoir (figs. 185 and 186).

A new oil pool, the Qannik accumulation, was discovered in 2006 during drilling at CD-2 to reach the Alpine accumulation, which is about 2,135 m (7,000 ft) deep. ConocoPhillips had seen the Qannik accumulation on logs and decided to test it in June 2006 and it achieved an average production of 1,200 bbls per day from a 7.6-m- (25-ft-) thick sandstone layer at the 1,220-m (4,000-ft) depth. Additional gravel was added to CD-2 during the winter of 2006–07 for development of Qannik and to allow for additional storage. The expansion made room for 18 Qannik wells. Facility construction and installation were completed in 2007 and development drilling began the spring of 2008. Production started in late 2008.



Figure 185. A 2006 airphoto of the Alpine oilfield in the central portion of the delta (Stop 20). The original two drill sites were completed in 2000 and the CD-4 drill site (off bottom) was completed in 2007.



Figure 186. An aerial view of the central production facility in the Alpine oilfield, showing the intense concentration of drilling and production facility on one pad.

STOP 21: COLVILLE PIPELINE CROSSING

A big technical and economic hurdle for the development of the Alpine oilfield was the need to build oil and gas pipelines across the Colville River, which is nearly 1.6 km (1 mi) wide (fig. 187). After evaluating various alternatives, including a suspension bridge and trenching, Alpine's owners decided on using horizontal directional drilling (HDD) technology to lay 1,372 m (4,500 ft) of pipeline 30 m (100 ft) below the river bottom. Although the HDD technology had been used all over the world, the Colville River crossing was its first application in permafrost.



Figure 187. A 2004 airphoto of the buried pipeline crossing on the east bank of the Colville River (Stop 21). Note the rows of thermo-siphons, pad where the hot-oil pipeline exits the permafrost, the high vertical loop used to control oil flow instead of a valve, and a red shed for oil spill response supplies.

A typical HDD installation begins with the boring of a small pilot hole along the desired profile. Drilling fluid is pumped to the drill motor through the drill stem and then returns to the entry point through the drilled annulus, carrying the cuttings in suspension with it. Once the pilot hole is complete, the hole is enlarged using a reamer. Depending on the outside diameter of the line to be installed, this procedure may require numerous passes with incrementally larger reamers. Reaming does not necessarily remove the cuttings produced during boring; rather, the cuttings are suspended in the drilling fluid circulated through the hole. Excess drilling fluid is pushed out of the bored hole, or into the surrounding soils, during the pullback process.

Although there was considerable uncertainty whether HDD would work in permafrost, preliminary studies and engineering models indicated the technology was feasible, despite the layer of gravel beneath the Colville riverbed and concerns about how the hot crude carried in the pipeline would affect permafrost surrounding the line (fig. 188). The work was begun in the winter of 1997 and was immediately beset with problems that raised tensions of the team trying the costly new technology in the Arctic (Jones, 2000). For starters, the ice road necessary to deliver equipment, supplies, and construction crews was delayed because of an unusually mild November and December that kept the ground too soft for tundra travel. The drilling crews then failed five times to bore a 1,372-m (4,500-ft) hole underneath the Colville River due to problems with the drilling mud. Drill mud is injected into the bore hole to keep the drill bit cool, to circulate out cuttings and, if necessary, to inject special chemicals if problems (such as a freeze-up) develop down the hole. Because of concerns about working in frozen ground that arose during work along portions of the borehole, the drilling team tried a special mixture that would lower the freezing point of the mud. But that mixture leached into the soils and melted the permafrost around the hole, causing the holes to collapse and the drill pipe to become stuck. Finally, crews started using a conventional mud mixture, without the special freeze-depressant chemicals. Success came just at the end of the spring 1998 season, as the first of four planned holes was finally bored out.

During the second construction season at Alpine, which ended in the spring of 1999, drillers reverted to a conventional mud system similar to that used in other parts of the world. As a result, the remaining three holes were completed in time with almost no problems. Crews were able to pull the four pipelines through the holes and hook up the system to carry crude oil from Alpine to Kuparuk, and on to the Trans-Alaska Pipeline (fig. 189). During both construction seasons, drillers lost some of the drilling mud in the bore holes, particularly in the thawed zone under the active river channel. Follow-up water monitoring was conducted to make sure the drilling fluids did not reach the surface.

To protect the stability of the permafrost, an array of thermo-siphons were installed where the hot oil pipeline emerges up through the permafrost (fig. 190). Thermal monitoring has revealed that ground temperatures and thawing have remained within design specifications. Although there has been substantial surface thawing of ice wedges above the pipe, this has not affected the stability of the pipe. Rehabilitation efforts have been undertaken to stabilize the surface. Bank erosion has continued to advance across the western bank of the HDD crossing toward the first set of thermo-siphons, but this was anticipated and a portion of the thermo-siphons were designed

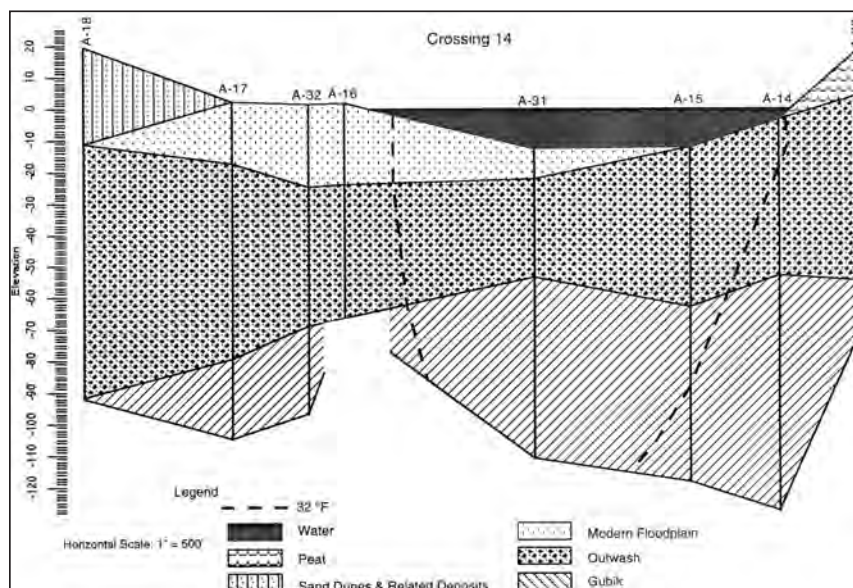


Figure 188. A cross-sectional profile of the buried pipeline crossing, showing surficial deposits and soil temperature isotherms (Miller and Phillips, 1996).

to be expendable. Also at the HDD crossing is an example of one of many large vertical loops that are designed to replace valves for controlling oil loss in case of a pipe failure. Both the HDD technology for tunneling pipelines under large rivers and the vertical loops are important design innovations made by the Alpine development.



Figure 189. Winter construction at the HDD project, showing the drilling of a pilot hole and later insertion of the welded pipe into the drill hole (2005 photos courtesy Michael Baker Jr., Inc.).

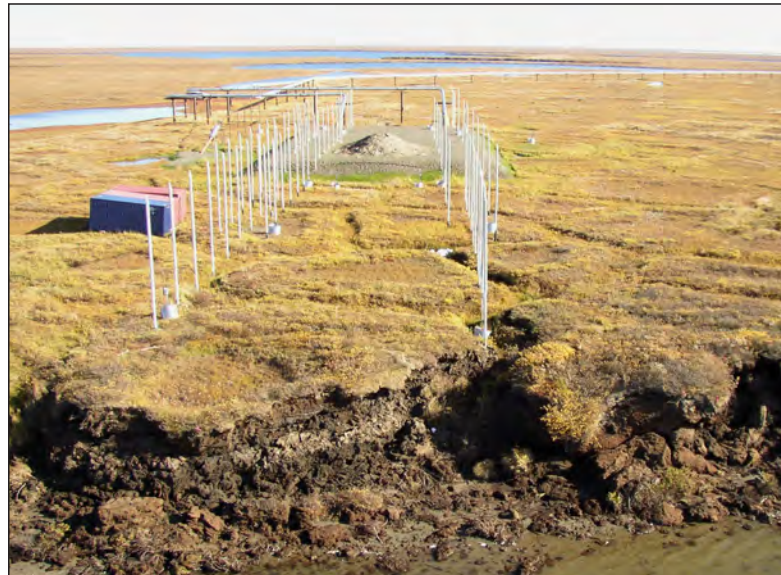


Figure 190. A 2005 aerial view of the HDD terminus on the east bank of the Colville River showing the vertical thermo-siphons and emergence of the pipelines from the Alpine oilfield.

STOP 22: COLVILLE MINE SITE

Gravel for building roads and pads is critical to development on permafrost; gravel for the Alpine development was obtained from a mine site on the delta floodplain near the head of the delta (figs. 191 and 192). The mine site, owned by the Arctic Slope Regional Corporation (ASRC), has provided gravel for both oilfield development and the village of Nuiqsut. Nuiqsut contractors originally received a permit from the U.S. Army Corps of Engineers in 1997, authorizing a 10-year phased development involving excavation of up to 3.8 million m³ (5 million yds³) of sand and gravel. During Phase 1 of initial construction at the Alpine Development, ~1.2 million m³ (~1.5 million yds³) were mined from a 13 ha (32 ac) area. Additional authorized phases to meet future sand and gravel needs include ~2.7 million m³ (~3.5 million yds³) from 32.4 ha (80 ac). The total permitted footprint for the ASRC mine site is 60.7 ha (150 ac).

Mining has been done during the winter to support winter road and pad construction. Blasting with dynamite was required to loosen the gravel, because of the permafrost. An ice bridge over the Colville River and ice roads across the floodplain were constructed to transport gravel to the Alpine oil field and to Nuiqsut. Equipment used during mining included large bulldozers, excavators and/or loaders, hauling trucks, drill rig/compressors, and road graders. Overburden at the site is ~7 m (~23 ft) thick and was stockpiled on ice pads during the winter for later backfilling of the pits.

A long-term mine reclamation plan was required by the permits (ABR, 2002). Upon closure of mining cells, the overburden material was to be placed back into the gravel pit. Landforms were to be constructed to increase habitat diversity, including shallow littoral zones, very shallow littoral zones, waterfowl nesting islands within the nesting lake, and artificial revegetation. New surface-water bodies created by the mine pit impoundments are to be left to recharge naturally through a stream or man-made channel during annual spring breakup floods. This process could be aided by placement of upwind soil berms to accumulate windblown snow in the water impoundments. Long-term monitoring is required to evaluate the success of the reclamation efforts.



Figure 191. A 2006 airphoto of the mine site on the east bank of the main channel (Stop 22), where gravel was excavated for the Alpine oilfield.



Figure 192. A 1999 aerial view of the second phase (foreground) of gravel mining at the mine site. Overburden from the second phase was placed in the pit from the first phase (background).

This page was intentionally left blank.

PART 5: TOUR OF BARROW

by Jerry Brown¹, Ken Hinkel², Torre Jorgenson³, Wendy Eisner², Anne Jensen⁴, Owen Mason⁵, and Leanne Lestak⁶

OVERVIEW

Barrow is the northern-most city in the United States, and is situated on a prominent peninsula jutting into the Arctic Ocean, bordered on the west by the Chukchi Sea and on the east by the Beaufort Sea (fig. 193). It is a meeting place of ocean currents, moving and destructive ice floes, age-old traditions of the Inupiat culture and western development, traditional environmental knowledge, and modern science. The present community of Barrow has grown to a population of approximately 4,500 people and is the largest Eskimo (Inupiat) community in Alaska.

The coastal climate is one of long, dry, cold winters and short, cool, foggy summers that are moderated by the close proximity of the ocean. Mean annual air temperature is -12°C (10.4°F) and annual precipitation is 125 mm (4.9 in), with about 40 percent falling in the short summer period. Snow cover is 20–40 cm (8–16 in) thick. Historical climatic records reveal that Barrow is experiencing the same warming trend that is occurring throughout much of the Arctic (fig. 194).

One is immediately struck by the flatness of the coastal plain, where elevations range from 3 to 5 m (10–16 ft) along Elson Lagoon on the east and rise to the southwest to higher than 10 m (33 ft). The 100-m (330-ft) bathymetric contour on the Chukchi side is some 8 km (5 mi) offshore in close proximity to the deep Barrow trench, while on the Beaufort side it is 140 km (88 mi) to the northwest because of the wide continental shelf. Permafrost underlies all land surfaces and is estimated to be 300 m (985 ft) thick at Barrow (Brewer, 1958a, b). The coastal plain is unglaciated and composed of near-shore marine, fluvial, alluvial and eolian deposits of mid- to late-Quaternary age (fig. 195). These deposits, termed the Gubik Formation, are >30 m (>100 ft) thick and subdivided into the Barrow and the Skull Cliff units (Black, 1964; O'Sullivan, 1961). Sellmann and Brown (1973) summarized the local stratigraphy of the Barrow region using additional results from their 1960s drilling

program and available subsurface information. The sediments are largely the product of a series of marine transgressions. The Barrow peninsula is dominated by wet, acidic soils. The average thickness of summer thaw or active layer is less than 40 cm (16 in).

Large, elliptical, oriented lakes cover up to 40 percent of the northern coastal plain (fig. 196). The remaining land surface comprises tundra-covered drained-lake basins and highly polygonized ground caused by gradual growth of ice wedges in the upper 2–4 m (7–13 ft) of the ground. Both the shallow lakes and the deeper lakes with underlying thaw bulbs (taliks) are effective agents of thermokarst as they thaw the excessive segregated ice and ice wedges along the banks and cause the ground to settle. The remaining, unaffected and elevated ice-rich land surfaces (or 'interfluves') have been referred to as remnants of the 'initial surfaces' (Hussey and Michelson, 1966; Eisner and others, 2005). Lake development, subsequent drainage, and aggradation of ground ice over time create a range of basin ages and surface characteristics across the landscape (Britton, 1957; Eisner and Peterson, 1998; Eisner and others, 2005) (fig. 197). The wet, saturated, nutrient-rich soils in the basins provide a good environment for plant growth and the accumulation of dead plant material in peat. This peat accumulation is strongly related to age of the basins (fig. 198). Because of the strong orientation of modern winds, and to some extensive winds in the distant past, the lakes also show strong orientation (Carson and Hussey, 1962) (fig. 199).

The coastal plain has a lower biodiversity as compared to the remainder of the Arctic Slope, consisting of 124 taxa of the 574 known vascular plant flora that occur on the Slope, 177 of the 410 mosses, and 49 of the 137 hepatics. Bird species number 28 and mammals 10 (Brown and others, 1980). Microtine rodents make up a substantial part of the mammal fauna.

¹Woods Hole Oceanographic Institution, Massachusetts 02543

²Department of Geography, University of Cincinnati, Mail Location 131, Cincinnati, Ohio 45221-0131

³ABR Inc., Environmental Research & Services, P.O. Box 80410, Fairbanks, Alaska 99708-0410; currently employed by Alaska Ecoscience, 2332 Cordes Way, Fairbanks, Alaska, 99709; ecoscience@alaska.net

⁴Ukpeagvik Inupiat Corporation, UIC Science, P.O. Box 577, Barrow, Alaska 99723

⁵GeoArch Alaska, P.O. Box 91554, Anchorage, Alaska 99509-1554

⁶University of Colorado–Boulder, INSTAAR, 450 UCB, Boulder, Colorado 80309-0450

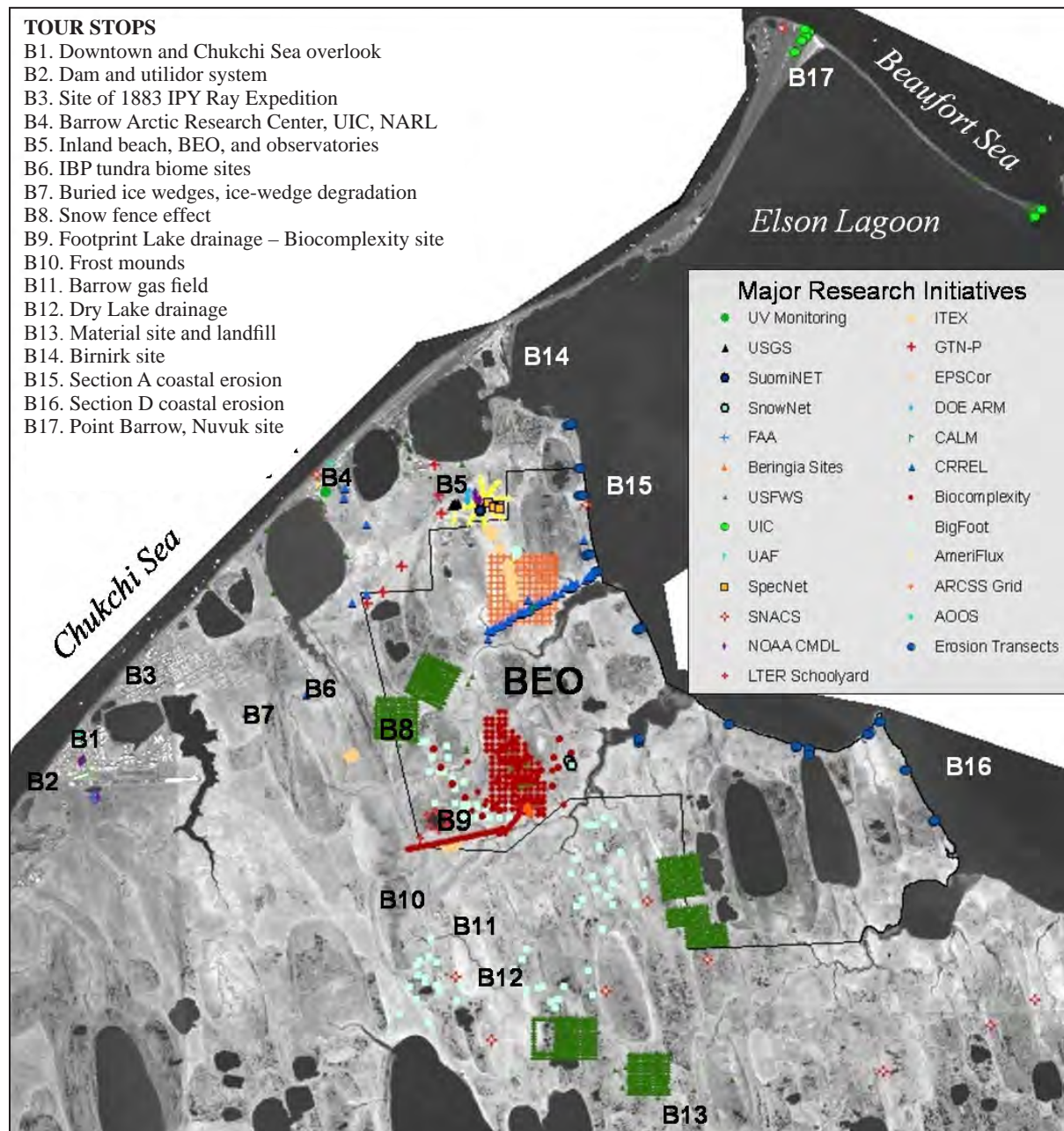


Figure 193. The Barrow landscape, Barrow Environmental Observatory (BEO; outlined in black), and tour stops. The 2002 Quickbird satellite image is a 0.7-m (2.3-ft) panchromatic satellite image from Digital Globe (Manley and others, 2006).

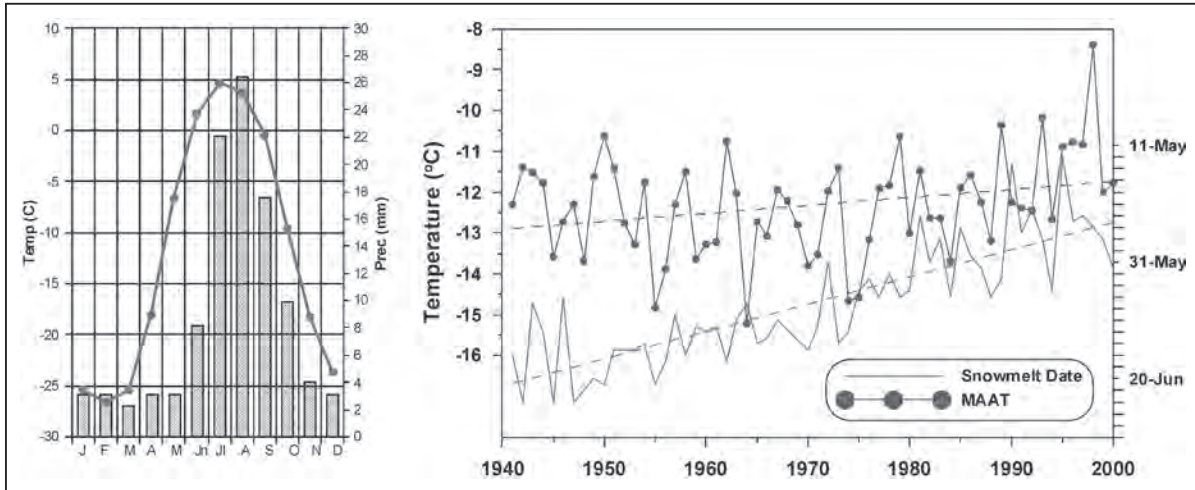


Figure 194. Mean monthly temperatures at Barrow (left) ranged from -27°C in February to 5°C in July. Climatic records since 1941 (right) reveal a $\sim 1^{\circ}\text{C}$ ($\sim 1.8^{\circ}\text{F}$) increase in mean annual air temperature (MAAT) and a ~ 25 -day advance in snowmelt date at Barrow (Hinkel and others, 2003b).

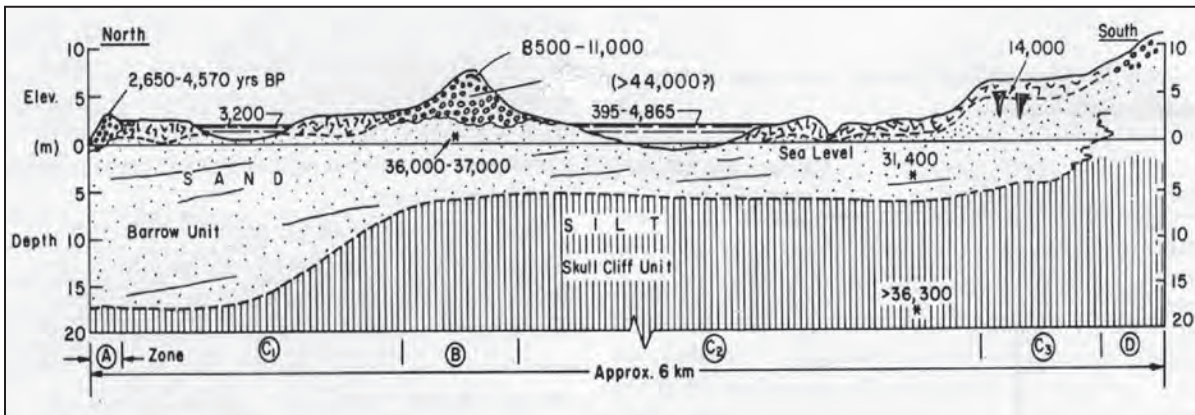
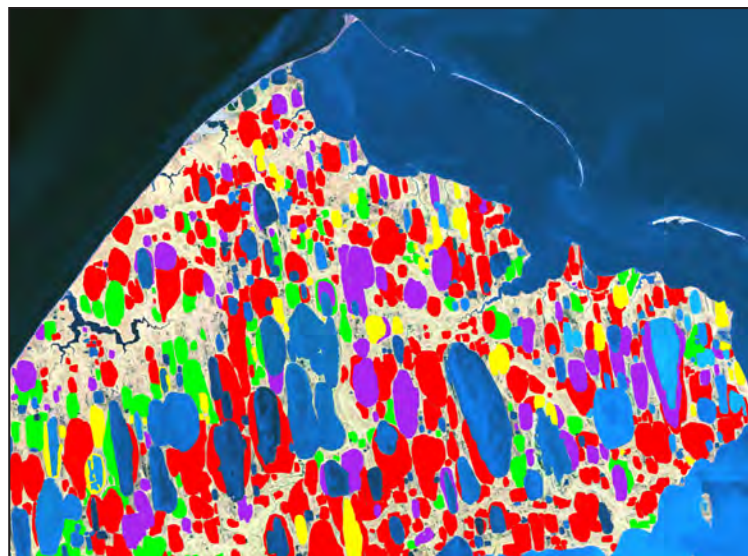


Figure 195. A stratigraphic section of the coastal landscape showing idealized stratigraphy and radiocarbon ages of various features (Sellmann and Brown, 1973).

Figure 196. Thaw lakes (blue) and drained-lake basins are dominant features of the coastal plain (Hinkel and others, 2003). Yellow areas represent young basins; purple areas represent medium-age basins; red areas represent old basins; and green areas represent ancient basins.



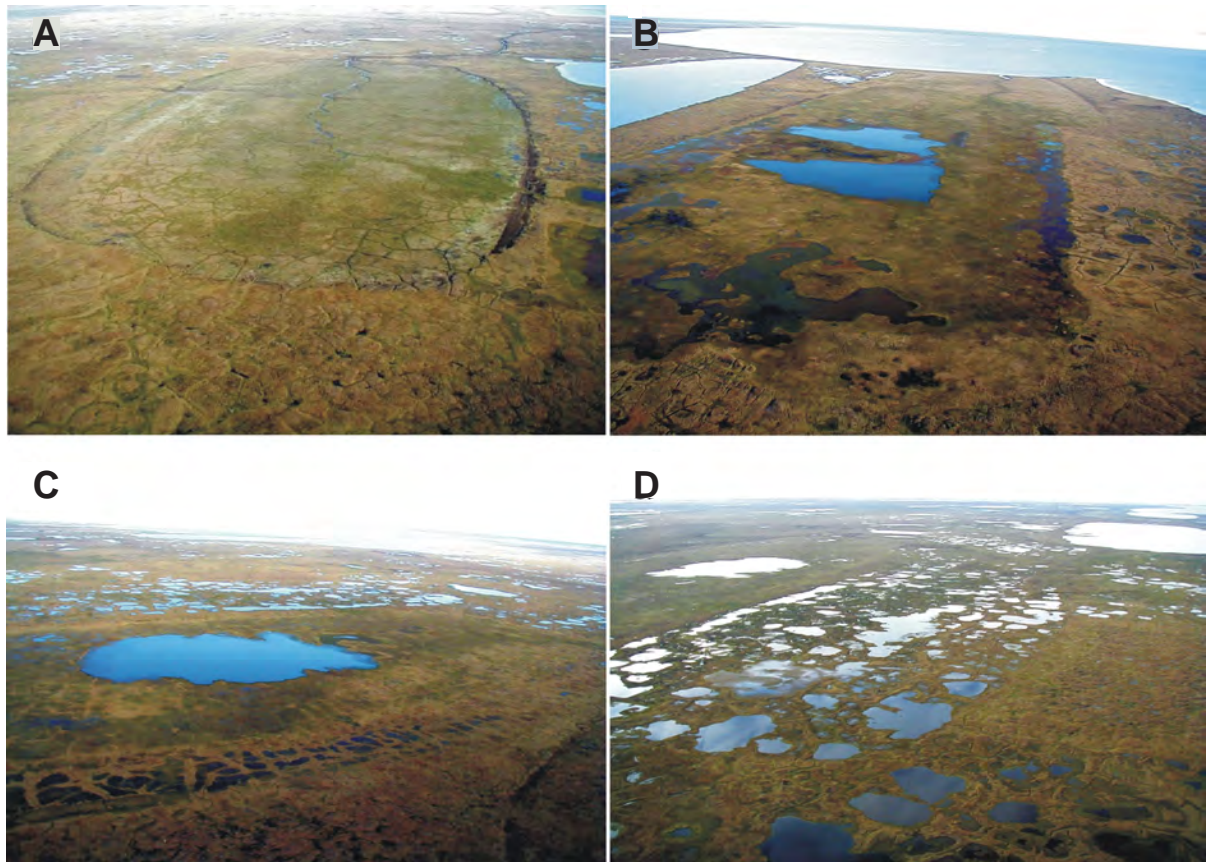


Figure 197. Aerial views of (A) young, (B) medium, (C) old, and (D) ancient drained-lake basins in various stages of development based on vegetation and surface patterns related to ice aggradation (photos by W. Eisner).

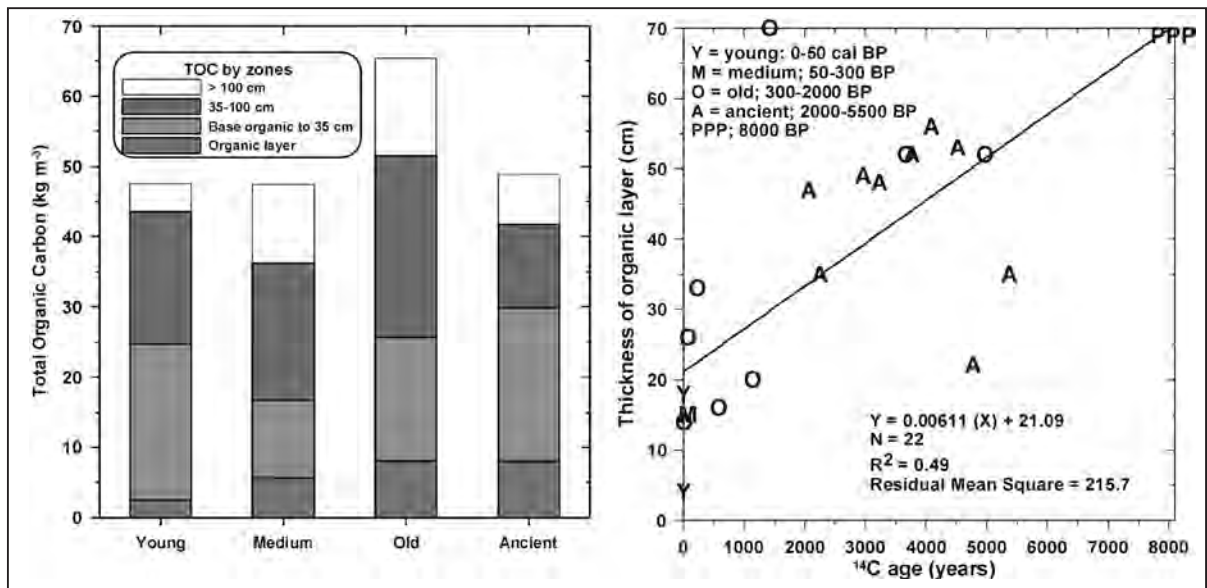


Figure 198. Differences in mean total organic carbon pools within the top 1 m (3.3 ft) among four different ages of drained-lake basins (Bockheim and others, 2004).

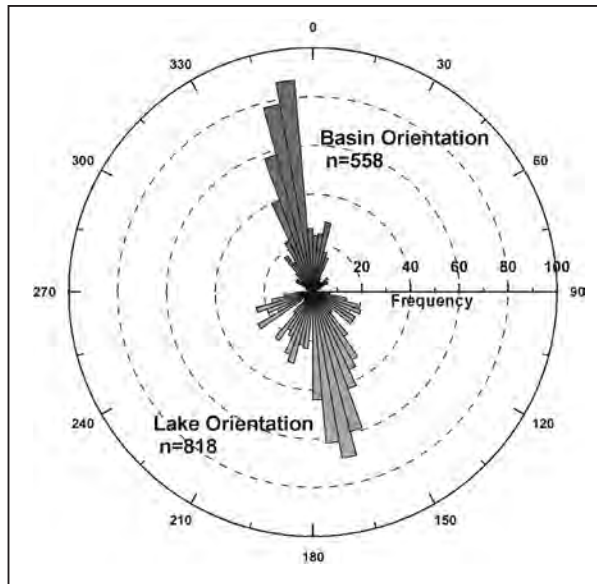


Figure 199. The drained-lake basins are predominantly oriented nearly north–south, while the lakes show more variation in orientation (Hinkel and others, 2003a).

STOP 1: DOWNTOWN BARROW

The high bluffs in downtown Barrow (near Arctic Pizza) provide a nice vantage point for looking northwest over the Chukchi Sea (fig. 200). While driving through Barrow, observe the many modern Borough and commercial buildings that are all built atop pilings embedded in the ice-rich permafrost. The causeway (dam) to Browerville was constructed to create a reservoir for freshwater retention of snow meltwaters (fig. 201).



Figure 200. Downtown Barrow fronting the Chukchi Sea (photo provided by J. Brown).



Figure 201. Aerial view south of Barrow along the Chukchi coast showing causeway built along the coast (left). Sea ice often pushes against the coast and can shove high ridges of sea ice along the shore (right) (photos provided by A. Mahoney).

STOP 2: CHANGES ALONG THE CHUKCHI COASTLINE

There has been increasing interest in processes affecting Arctic coastlines, including shoreline change, flooding, and sediment loading. Isolated coastal communities are more vulnerable as populations expand and climate changes. Analysis of high-resolution imagery with GIS and remote-sensing tools can help decision makers understand potential risks and better protect their populace. Recent comparative mapping (Manley and others, 2003; Lestak and others, 2004) of erosion along the coast shows substantial erosion in front of the city (fig. 202). More detailed studies of 32 km (20 mi) of the Chukchi coastline used a high-resolution (0.7 m) QuickBird satellite image, rectified aerial photography from seven time slices (1948, 1955, 1962, 1964, 1979, 1984, and 1997), and one-time GPS measurements (2001) (Lestak and others, 2008) (fig. 203). The long-term mean shoreline erosion rate is



Figure 202. Analysis of coastal erosion from 1948 to 1997 along a broader stretch of Chukchi coast revealed both erosion and depositional segments of the shoreline (Manley and others, 2003; Lestak and others, 2004). Shorelines from 1948 and 1997 are overlaid on 1948 (left) and 1997 (right) airphotos.

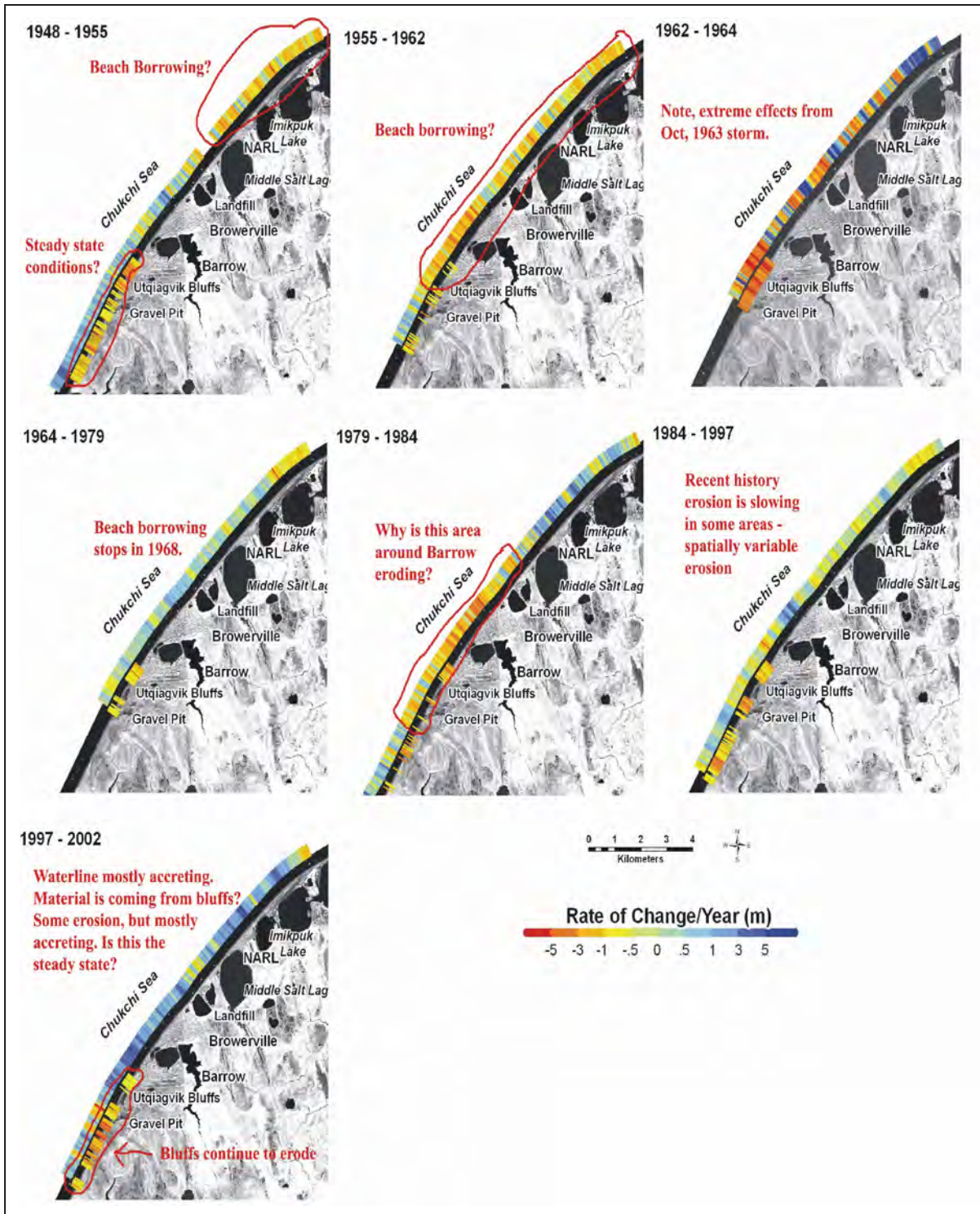


Figure 203. Coastal change for seven periods between 1948 and 2002. Offshore colors are waterline changes and onshore colors are bluff changes. Rate of change is yearly, red to light green is erosion, and green to dark blue is accretion (provided by L. Lestak).

-0.05 m (-2 in) per year. Inter-year mean change rates vary from -1.0 m (-3.3 ft) per year (erosion) to 1.41 m (4.6 ft) per year (accretion). Bluff-top long-term average erosion rates are -0.21 m (-8.3 in) per year. Direct impacts from storms include decrease of beach width, flooding, and loss of buildings and critical infrastructure in eroded areas. Onshore gravel mining and offshore dredging have contributed to erosion in the immediate region.

The October 1963 storm and storm surge are well documented, as are ice events that shove high ridges of ice onto the beach (fig. 201) (Walker, 1991; Hume and Schalk, 1967).

STOP 3: RAY EXPEDITION FOR THE FIRST INTERNATIONAL POLAR YEAR

The first International Polar Year (IPY) was an integrated circumpolar effort by 11 nations that had committed themselves to establishing 12 stations for the purpose of investigating the meteorology and earth magnetic field at high latitudes. Norway, Sweden, and Finland each planned to establish one station in their arctic territory (Taylor, 1981). Russia planned two along its coast and Holland planned to establish a station on the Siberian coast. The United States was to send an expedition to Point Barrow, Alaska, and another to Lady Franklin Bay on Ellesmere Island. The United States used the first IPY to establish a research station at its northernmost point, sending a party of men from the U.S. Signal Corps to Point Barrow in Alaska (figs. 204 and 205). Led by Lieutenant P. Henry

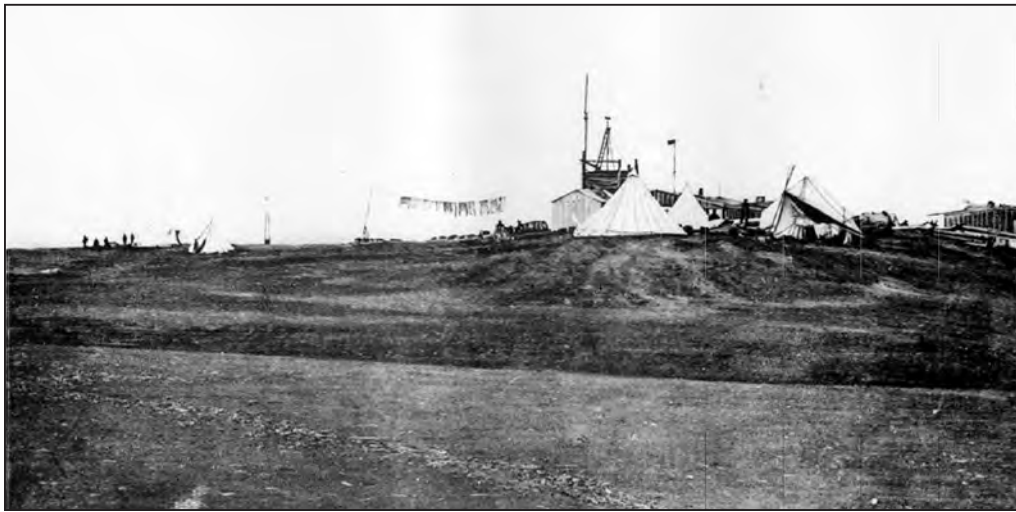


Figure 204. A view of the research station in 1883 (P. Ray, 1885).



Figure 205. The research station of the 1881–1883 Ray Expedition that collected the measurements for the first International Polar Year (P. Ray, 1885).

Ray, the expedition sailed from San Francisco on July 18, 1881, and returned October 7, 1883. The expedition is well documented with a major report (Ray 1885); materials from the personal journals of Sgt. Middleton Smith, a member of the expedition; the report written by John Murdoch, which contains his observations of the Inupiat people in the region; and photographs of the Inupiat community as well as of the U.S. Signal Corps buildings and people at Point Barrow. Permafrost temperatures were first measured at Barrow during the IPY Ray–Murdoch Expedition (1881–1883) in what eventually became a meat cellar near today’s Brower’s café.

STOP 4: BARROW RESEARCH FACILITIES

North along the coast road is Ukpeagvik Inupiat Corporation’s Naval Arctic Research Laboratory (UIC–NARL) and the location of the Barrow Arctic Science Consortium (BASC), a not-for-profit organization that provides logistical support for the many Federally-sponsored programs (figs. 206 and 207). The North Slope Borough’s Department of Wildlife Management is also based here; it conducts and coordinates research on marine and terrestrial living resources. The history of research at NARL starting in the 1940s is partially recorded in the 50th anniversary compendium (Brown, 2001; Norton, 2001).



Figure 206. Aerial view (~1970) of the Naval Arctic Research Laboratory camp (photo provided by J. Brown).



Figure 207. Aerial view in 1952 of the ARL–NARL (foreground) and airstrip on the gravel spit (background) (photo from M.E. Britton collection).

STOP 5: BARROW ENVIRONMENTAL OBSERVATORY AND EARLY RESEARCH

On the road past the freshwater Imikpuk Lake and the Distant Early Warning (DEW) Line facility are facilities and research areas where intensive monitoring is being conducted to assess environmental changes in the Arctic (fig. 208). The site is on Federal government lands owned by U.S. Geological Survey (USGS) and the National Oceanic and Atmospheric Administration (NOAA), with access by permission only. The USGS has maintained a magnetic observatory for more than 50 years (Townsend, 2001), while NOAA and the Department of Energy (DOE) maintain atmospheric observatories located to the east. Climate Monitoring & Diagnostics Laboratory (CMDL) is one of five worldwide sites that NOAA maintains to monitor air quality in pristine regions. It was established in 1974 and has a continuous record of trace gases collected from the clean air sector to the northeast. Immediately to the east is the Barrow Environmental Observatory (BEO), 3,022 ha (7,466 ac) of land that were permanently set aside for research in 1992 by the Ukpėagvik Iñupiat Corporation (UIC—the Barrow Village Corporation). The BASC manages the BEO for the UIC landowner. In 2003 the North Slope Borough Assembly designated the BEO as the first zoned Scientific Research District in the Borough.

Beyond the CMDL are a beach ridge and drained-lake basins where many pioneering research projects took place starting in the late 1940s. Black (1952) investigated the growth and fabrics of ice wedges, and excavated a series of trenches across the ridge; the trenches are still visible. Based on a recently obtained radiocarbon date (>46.9 RC ka BP, unpublished) from this inland beach ridge, which has a maximum elevation of 10 m (33 ft), the age of this last major transgression was reassigned to the Simpsonian transgression (70 ka BP by Brigham-Grette, pers. commun.). Ice-rafted boulders are reported on the low-relief tundra (MacCarthy, 1958), and presumably were deposited during this last major transgression. Koranda (1954) documented the vegetation across the raised beach ridge. Soil scientists from Rutgers University classified and described the soils, and measured the active layer thickness (figs. 209 and 210) (Drew and Tedrow, 1957, 1962; Drew and others, 1958). In 1957, a classic soil decomposition study was performed on sites representative of different moisture regimes (Douglas and Tedrow, 1959). In the 1960s, the U.S. Army Corps of Engineers Cold Regions Research and Engineering Laboratory (CRREL) initiated pedological, geological, hydrological, and vegetation projects on sites that are now within the



Figure 208. Aerial view of the northern section of the Barrow Environmental Observatory (BEO) and coastal plain landscape showing the prevalence of drained-lake basins and an ancient beach ridge (photo provided by J. Brown).

BEO (figs. 211 and 212) (Brown, 1969; Brown and others, 1968; Brown and Johnson, 1965). The 1960s active-layer measurements on some 20 plots (fig. 213) serve as comparative baseline for measurements that resumed in the early 1990s, and became the first site in the Circumpolar Active Layer Monitoring (CALM) network (Nelson and others, 2008). For the last decade (1998–2007), active-layer thickness (ALT) data, have remained close to the range of values from the 1960s. ALT values in the early 1990s were substantially less than in the 1960s and early 2000s. Maximum values were recorded in 1968, 1998, and 2004; these values coincide with the warmest summers. The 2003 minimum (29 cm [11 in]) was similar to 1993, but deeper than the shallowest thaws of 1991 and 1992 (24 cm [9 in]).



Figure 209. A soil trench excavated to expose a cross-section of frost boils (photo by J. Brown).

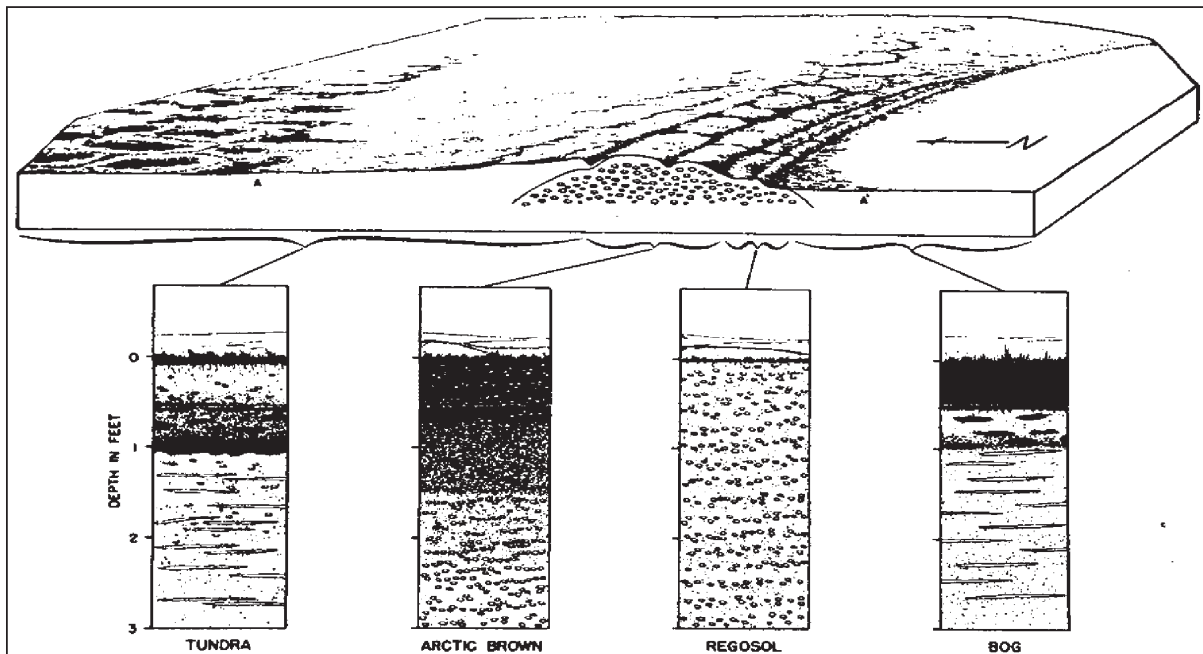


Figure 210. A cross-section of the coastal landscape showing the relationship of tundra soils to landscape position (Drew and others, 1958).

The BEO currently hosts a number of long-term observation projects as part of several international programs: active layer (CALM), permafrost temperatures (TSP), coastal erosion (ACD), and the International Tundra Experiment (ITEX); (Nelson and others, 2008; Aguirre and others, 2008; Hollister and others, 2006). The CALM site occupies a 1 x 1 km (0.6 x 0.6 mi) grid, where snow and active-layer depths have been measured since 1993 at 121 equally spaced (100 m [330 ft]) grid nodes. Many of the current projects are funded by the U.S. National Science Foundation (NSF), including a new observatory project on snow deposition and sublimation (Snow-Net). To the west, a short distance off the road, is one of the geothermal sites monitored during the 1950s by the USGS program. The site has been reoccupied under the IPY Thermal State of Permafrost project. Comparison of the 1950 annual profile with current measurements at the 14 m (46 ft) depth indicates about a 1.2°C (2.2°F) warming (fig. 214). This small increase over such a long period is consistent with a previous analysis of long-term permafrost temperature variations at Barrow for the period 1924–1997 (Nelson and others, 2008; Romanovsky and others, 2003; Yoshikawa and others, 2004).

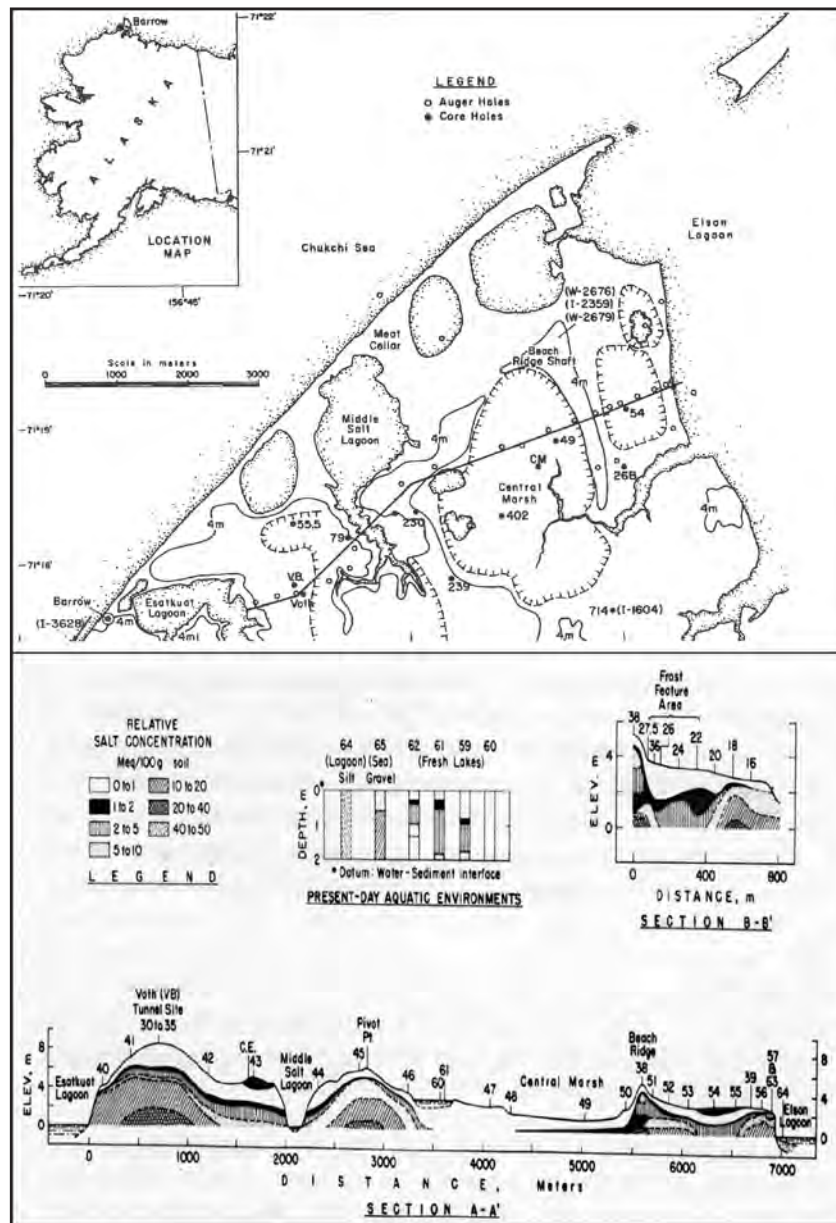


Figure 211. A cross-section of the coastal plain showing changes in topography and salt concentrations at depth (Brown, 1969).

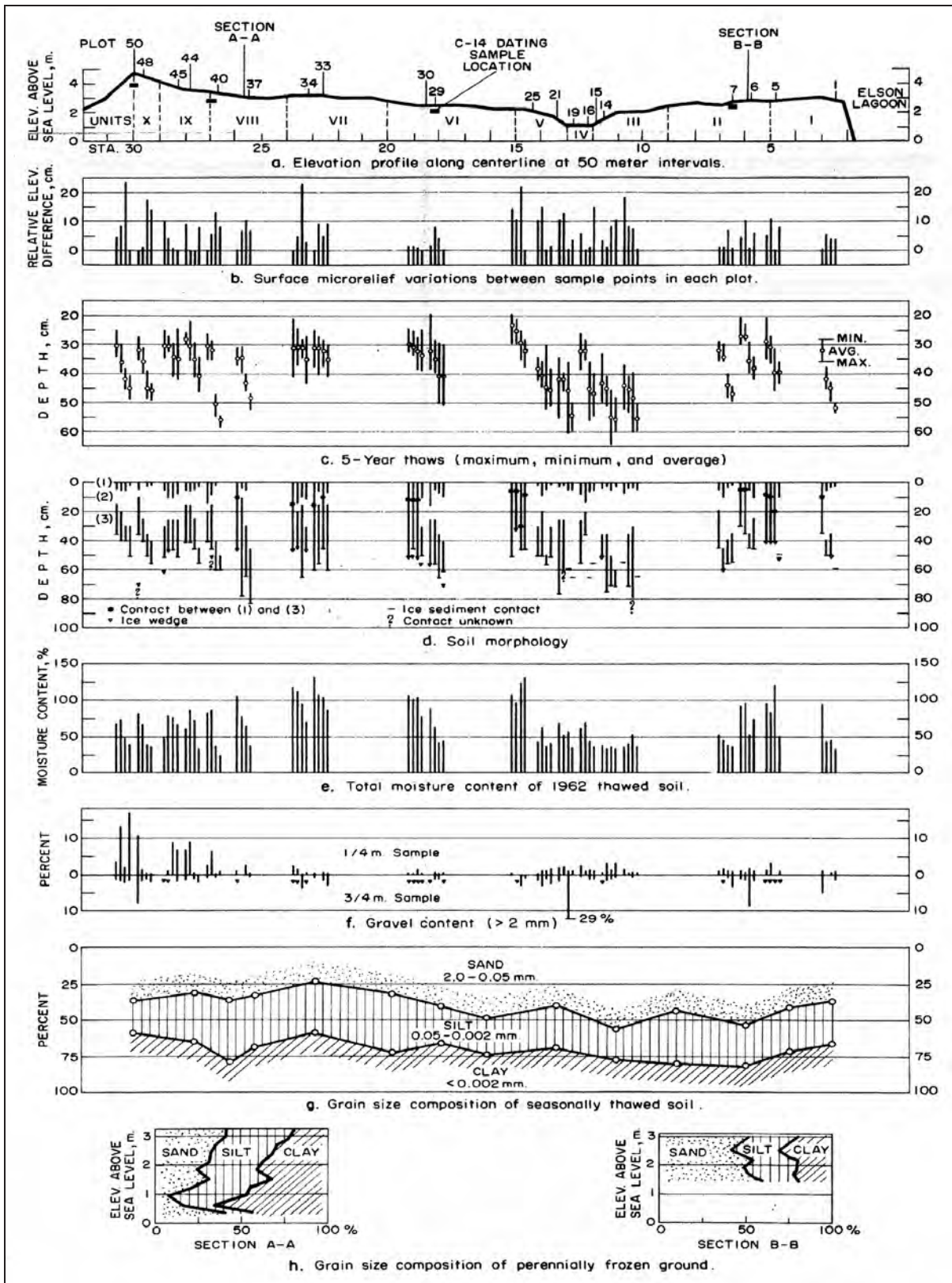


Figure 212. A toposequence across the coastal landscape, showing changes in micro-relief, thaw depths, soil morphology, moisture content, gravel content, and particle size distribution (from Brown and Johnson, 1965).

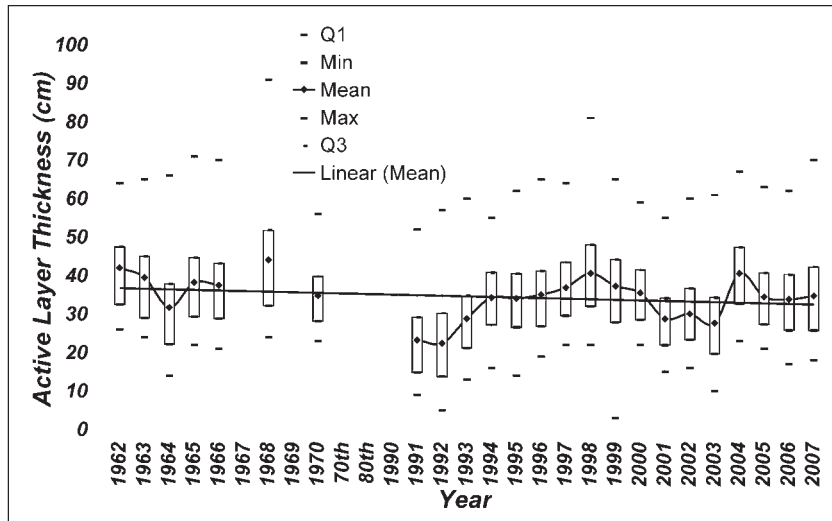


Figure 213. Mean thaw depths during the 1960s measured by CRREL compared to more recent thaw depths measured under the auspices of the Circumpolar Active Layer Monitoring (CALM) program (Nelson and others, 2008).

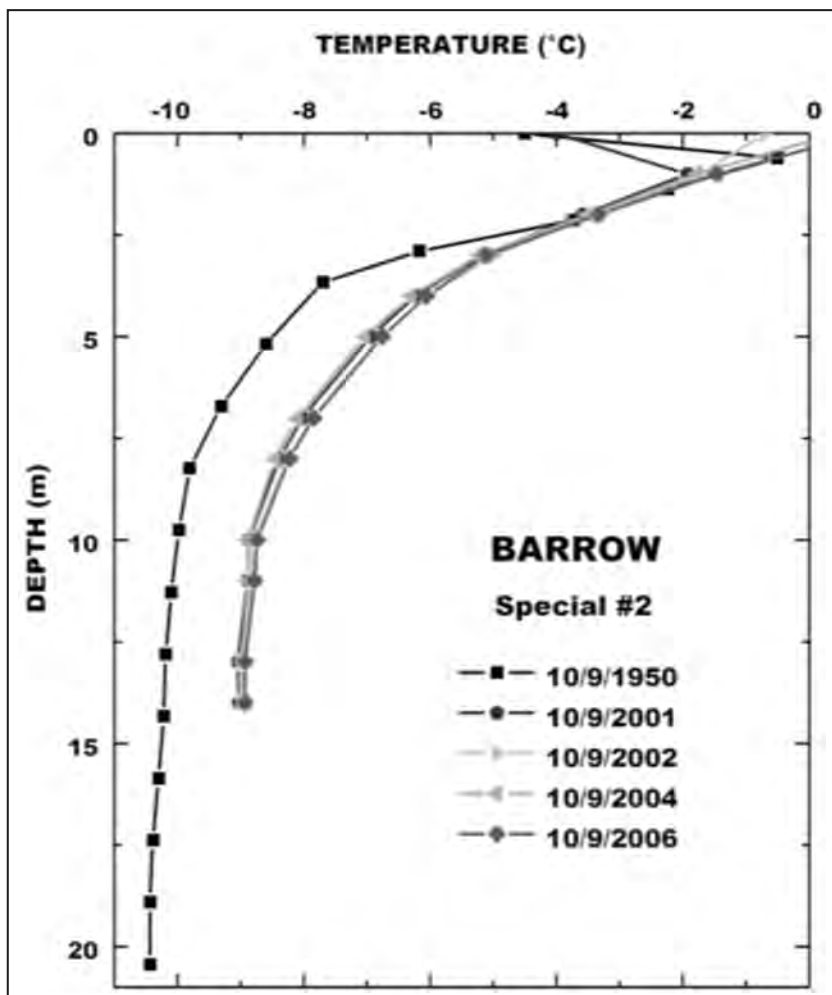


Figure 214. Annual permafrost temperatures for 1950s and 2000s at Special 2 site (Nelson and others, 2008).

STOP 6: INTERNATIONAL BIOLOGICAL PROGRAMME STUDIES

During the period 1969 to 1973, Barrow was an intensive site of a major international ecosystem program, the Tundra Biome Program of the International Biological Programme (IBP). Most of the study sites are located along Cake Eater Road (figs. 215 and 216). Three textbooks, several hundred papers, and more than 100 masters and doctoral dissertations resulted from these studies (Brown and others, 1980; Hobbie, 1980; Tieszen, 1978). Site 1, at the intersection of Cake Eater Road and Browerville subdivision, was used to study the responses of

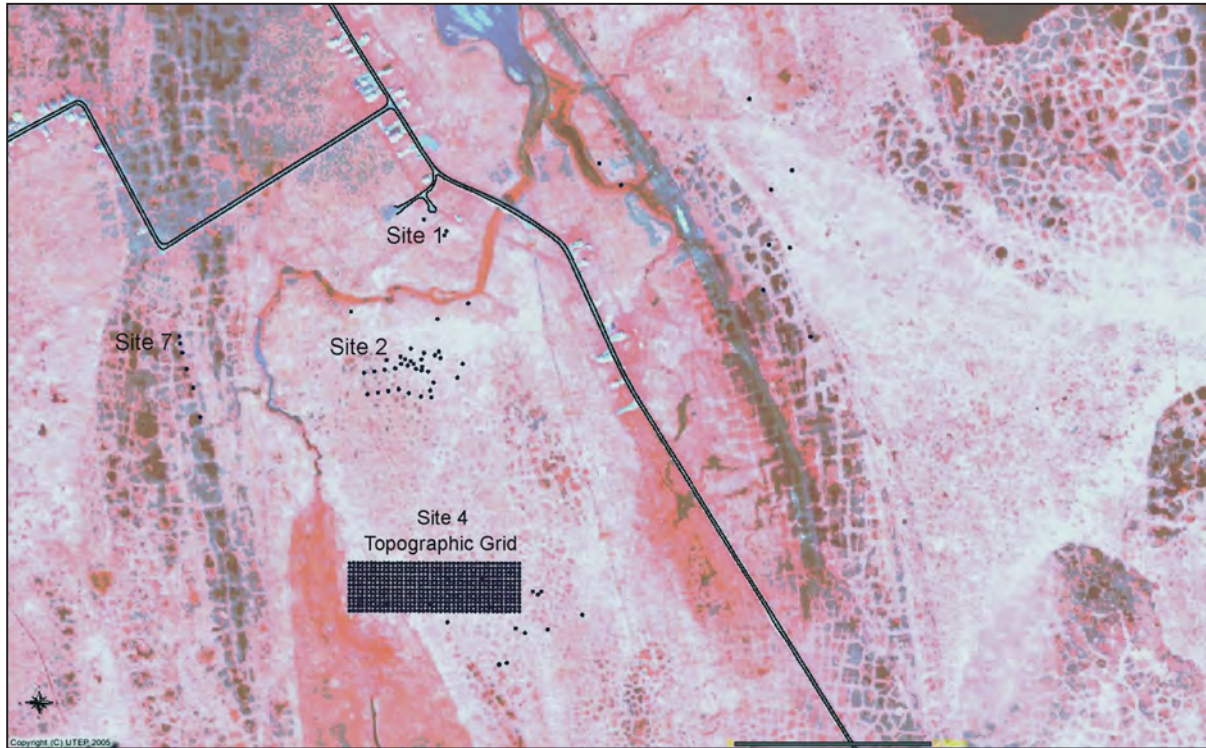


Figure 215. Map of the many study sites of the International Biome Programme. Base image is 2002 QuickBird satellite image (Manley and others, 2006).



Figure 216. Aerial oblique view of the main International Biome Programme Tundra Biome Sites in the early 1970s; pond sites and building are in mid foreground, sites 1 and 2 are in background along creek (photo provided by J. Brown; see Brown and others, 1980, and Hobbie, 1980).

tundra to surface disturbances. Site 2, across Footprint Creek and along the abandoned power line, was devoted to permanent plots to measure numerous ecosystem and micrometeorological parameters, including active layer and gas fluxes. Farther to the west along the powerline in an old drained-lake basin, a series of ponds were manipulated and studied (Hobbie, 1980). At Site 4, the influence of microtopography on tundra function and structure were investigated. Some of these sites have been revisited starting in the early 1990s to ascertain decadal changes in the tundra ecosystems.

Permanent plots established in 1973 for measuring vegetation and thaw depths were resurveyed in 2000 (fig. 217). A comparison of thaw depths in 1973 and 2000 show a strong relationship between the center of polygons and the polygonal troughs, and thaw depths in 2000 were much deeper in the polygon centers than in 1973 (fig. 218).

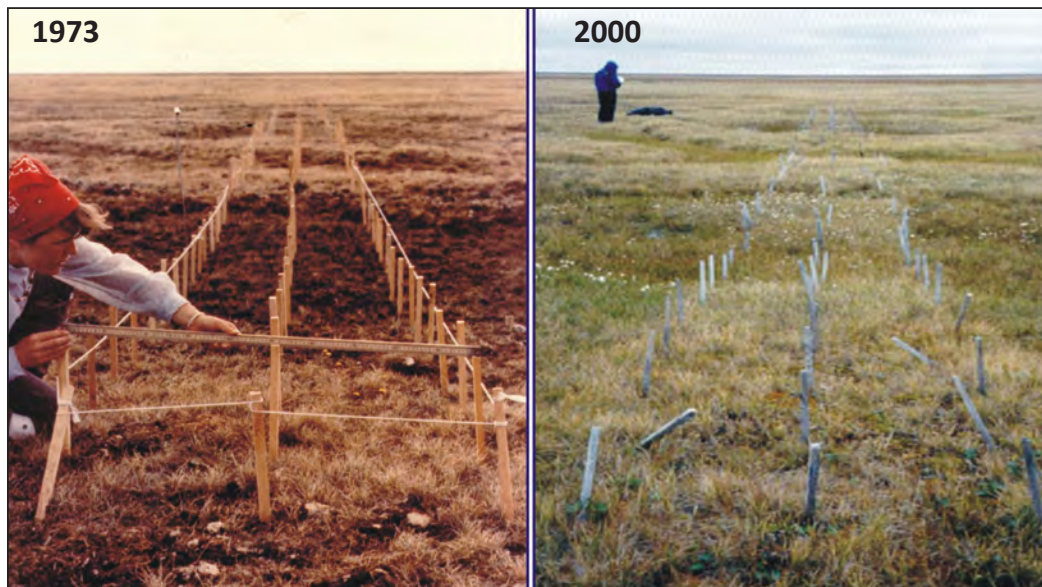


Figure 217. Tundra Biome Site 4 transect for measuring soil and vegetation characteristics established in 1973 and resurveyed in 2000 (photo by C. Tweedie).

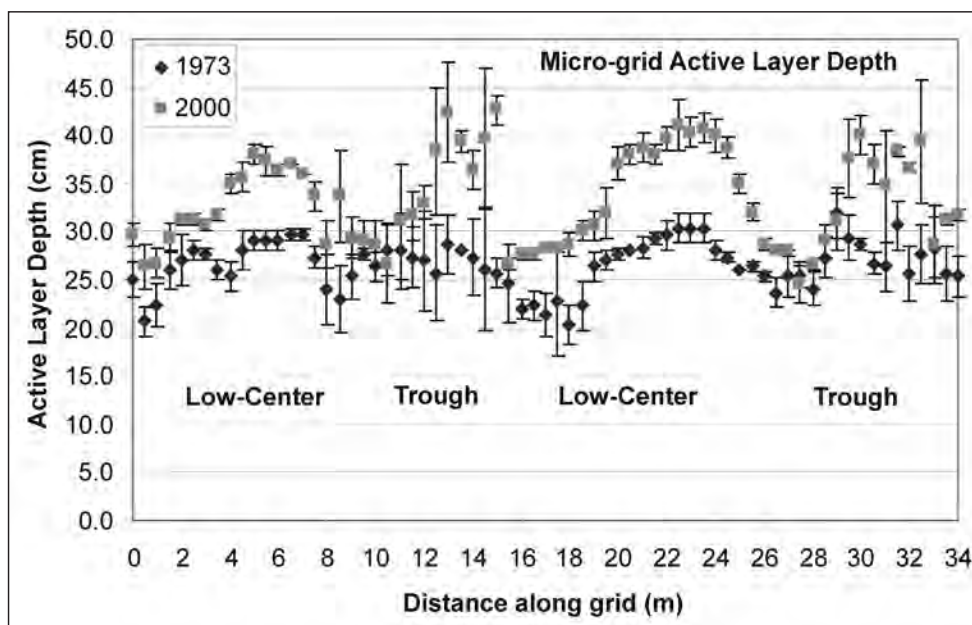


Figure 218. Comparison of thaw depths in 1973 and 2000 in relationship to microsites associated with low-centered polygons (provided by C. Tweedie).

The Tundra Biome sites are traversed by Footprint Creek, where the knick-point has eroded headward through ice-rich permafrost and a beaded-stream network has developed, and has been observed for many years. Lewellen (1972) reported on the early erosional events (fig. 219). The equilibrium of the stream was first disturbed in the 1940s when the water level in Middle Salt Lagoon was lowered each spring to avoid flooding of the Navy camp. Starting in 1950, the drainage area increased when Footprint Lake and Dry Lake to the south naturally drained through the creek (Britton, 1957). This increase in the magnitude of spring discharge has accelerated thermal erosion. The stream knick-point continues to erode southward, seeking a new equilibrium base level.

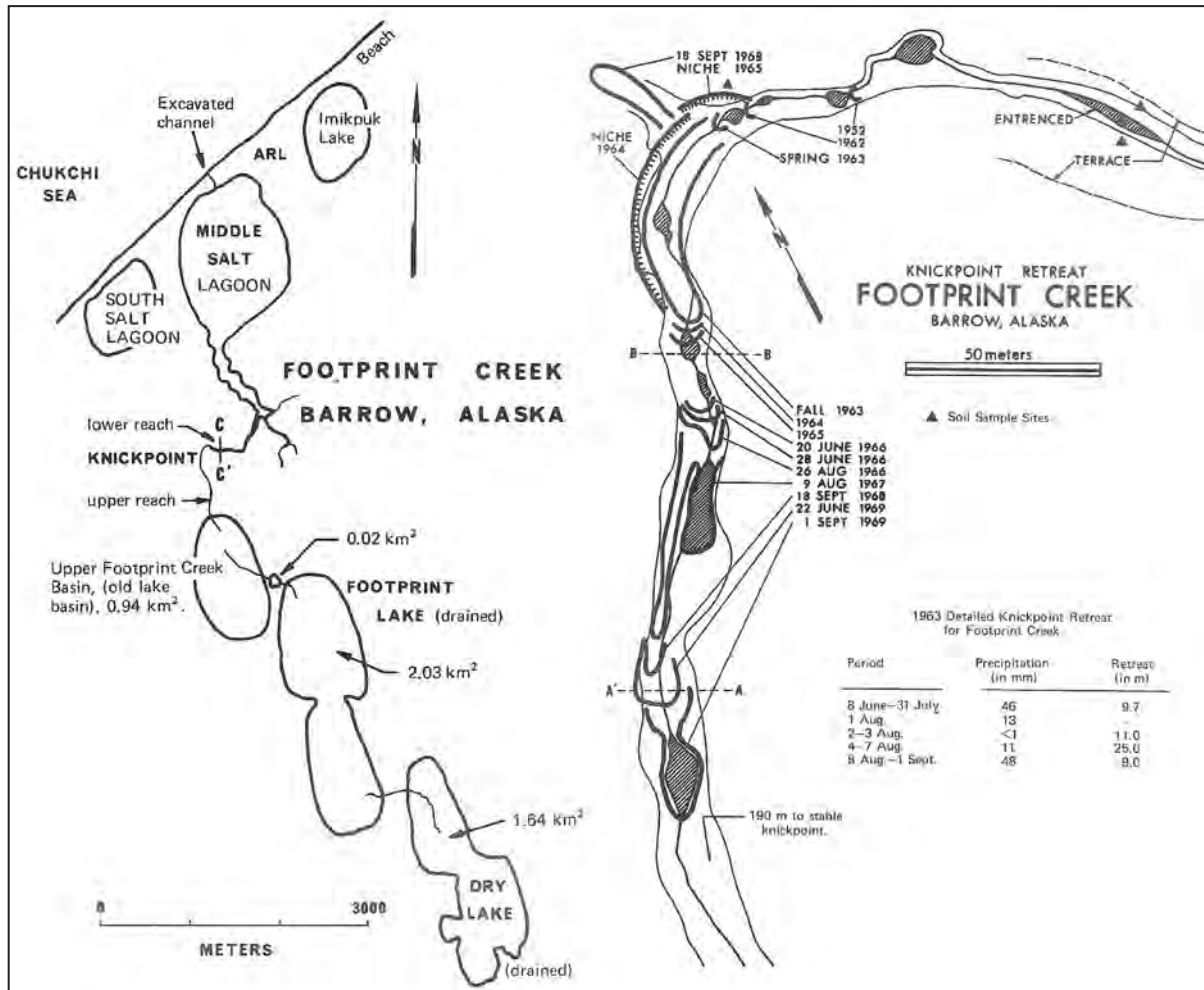


Figure 219. Map of the headwater erosion of knickpoints along Footprint Creek (Lewellen, 1972).

STOP 7: BURIED ICE WEDGES AND ICE-WEDGE DEGRADATION

Ice wedges, which form polygonal networks of wedge-shaped bodies of massive ice through repeated seasonal contraction and expansion of the ground, play an important role in surface stability (Lachenbruch, 1962) (fig. 220). During the early 1960s, within the framework of permafrost investigations conducted by CRREL, a buried ice-wedge complex at a depth of 3 m (10 ft) below the surface was hand excavated along a horizontal tunnel (9 m [30 ft] long and 2 m [7 ft] high) with the use of electric chain saws (fig. 221). The site is located at the end of the powerline on UIC land. Access to the tunnel requires a guide and permission from BASC, as well as a UIC land-use permit. The entire excavation intercepts a massive complex of vertically-foliated ice at the 3–6 m (10–20 ft) depth (fig. 222). A series of papers on the initial findings (Brown, 1963, 1965, 1967, 1969) included radiocarbon dating of buried organic matter recovered from the ice wedges, and chemical analyses of sediments and soil. Colinvaux (1964) provided paleoecological interpretations based on pollen recovered from the buried ice wedge (14 ± 0.5 RC ka BP) and adjacent frozen organic materials. Brines are found within several meters of the base of the tunnel



Figure 222. Views of the horizontal tunnel (left), pebbly sand loam at the east end of the tunnel (upper right), and extremely ice-rich segregated ice above the ice wedge (lower right) (photos by H. Meyer).

in close proximity to sea level and the adjacent Holocene lagoon now occupied by freshwater reservoirs (Faas, 1966). The deposits underlying the buried ice-wedge site belong to the Late Wisconsin part of the Barrow Unit of the Gubik Formation (Black, 1964).

The initial interpretation for the formation of this buried ice complex was that the pre-Holocene ice wedges developed under a colder and drier environment, followed by a deeper thaw at the onset of the Holocene with likely truncation of the tops of the now-buried wedges. With the onset of a cooler period, the existing or additional sediments refroze and smaller, secondary wedges formed (fig. 220). Finally, with development of the modern-day active layer, the current network of ice wedges and polygons were formed (Brown, 1967). As some of these ice wedges melted and troughs deepened, the characteristic landscape of high-centered polygons developed. Thermokarst pits developed where wedge melting was intensive. At this site, the thermal degradation process may have been accelerated by the draining of the sequence of lakes that occupy the area to the east (Sites 4 and 7). In addition, this upland area was subjected to intense vehicular traffic in the mid 1950s as part of the oil and gas exploration on the North Slope.

In 2004, access to underground excavation previously sealed by seepage of ground water into the access shaft was reopened. The site was resampled in 2004 and 2006 by a German team from the Alfred Wegener Institute in Potsdam. Since neither AMS C14 dating nor stable isotope techniques were readily available in the 1960s, the first step in these current investigations was to reconfirm and refine the age estimate of the site based on AMS dating. Isotope geochemistry reveals the intersection of two isotopically different ice wedges suggesting different phases of the regional climatic history during the period from 12.4 to 9.9 RC ka BP (Meyer and others, 2007). The Late Glacial Maximum age of the site is indicated by an AMS date of 21.7 RC ka BP (written commun., Lutz Schirrmeister) at the lateral contact of the wedge in the surrounding sediments. The surficial deposits above the ice wedge show a tremendous amount of aggradation of segregated ice during syngenetic permafrost development (fig. 223). As a result of these new studies, the depositional history of the site over the last 20,000 years is undergoing reinterpretation.

Adjacent to the tunnel, the surrounding ridge is undergoing extensive ice-wedge degradation (fig. 224). Ice wedges are particularly sensitive to degradation because they form just below the active layer and have little

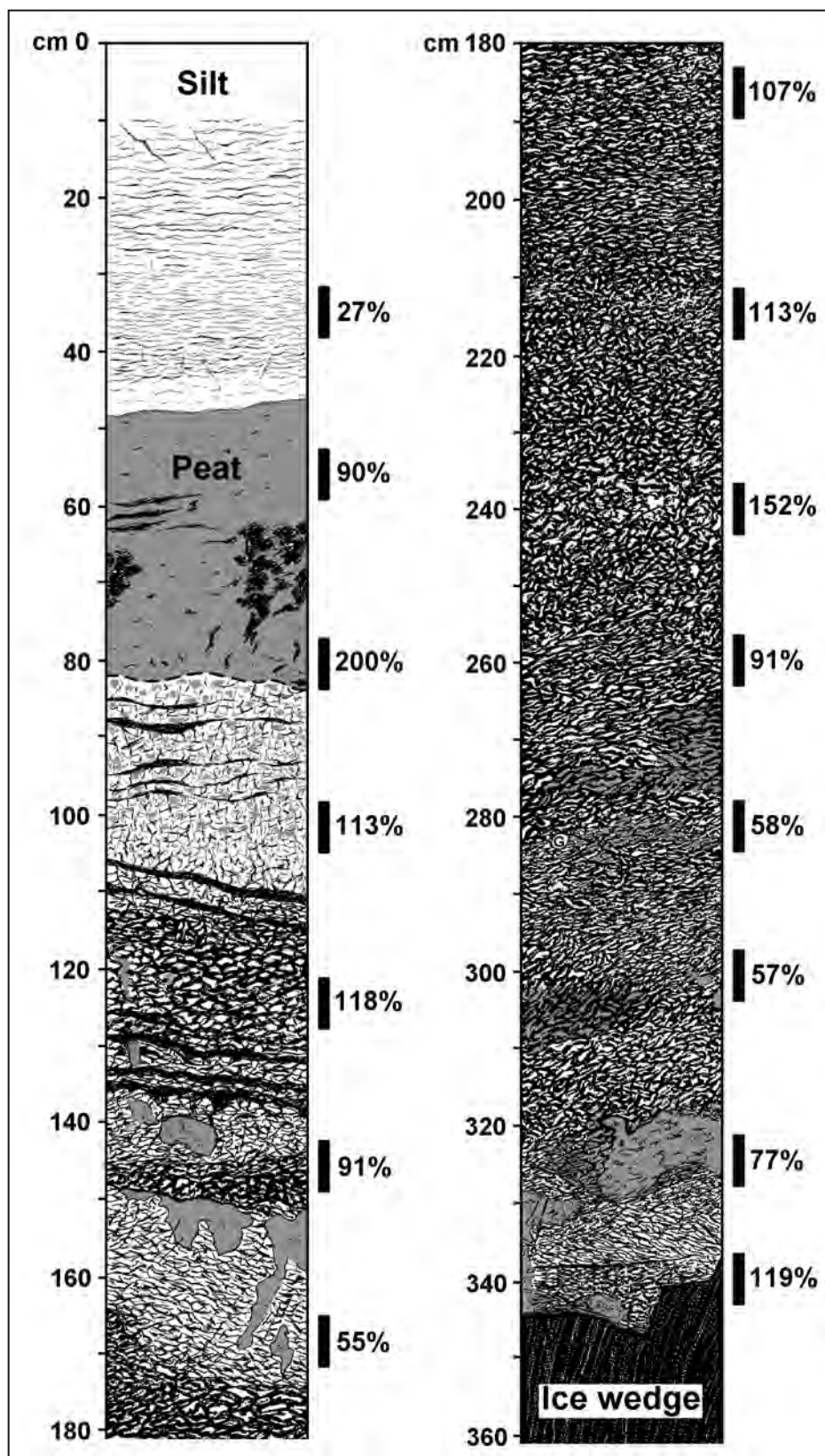


Figure 223. Permafrost stratigraphy illustrating ground-ice morphology and ice contents of the shaft to the buried ice-wedge tunnel. Ataxitic cryostructure dominates from 1.1 to 3.4 m; gravimetric moisture contents shown to right of profile (by M. Kanevskiy).

capacity to adjust to climate change by incorporating additional soil to the active layer (Jorgenson and others, 2006). A time-series of airphotos reveals that there were already extensive thermokarst pits across the terrain in 1955 and that numerous new thermokarst pits and troughs developed after 1979 (fig. 225). A close-up of one of the large ponds reveals substantial expansion and colonization by aquatic sedges over the time period (fig. 226).



Figure 224. The older terrain near the permafrost tunnel has very large ice wedges; degradation of the ice wedges is creating small ponds (photo in 2006 by E. Burger; also in Brown, 1967).

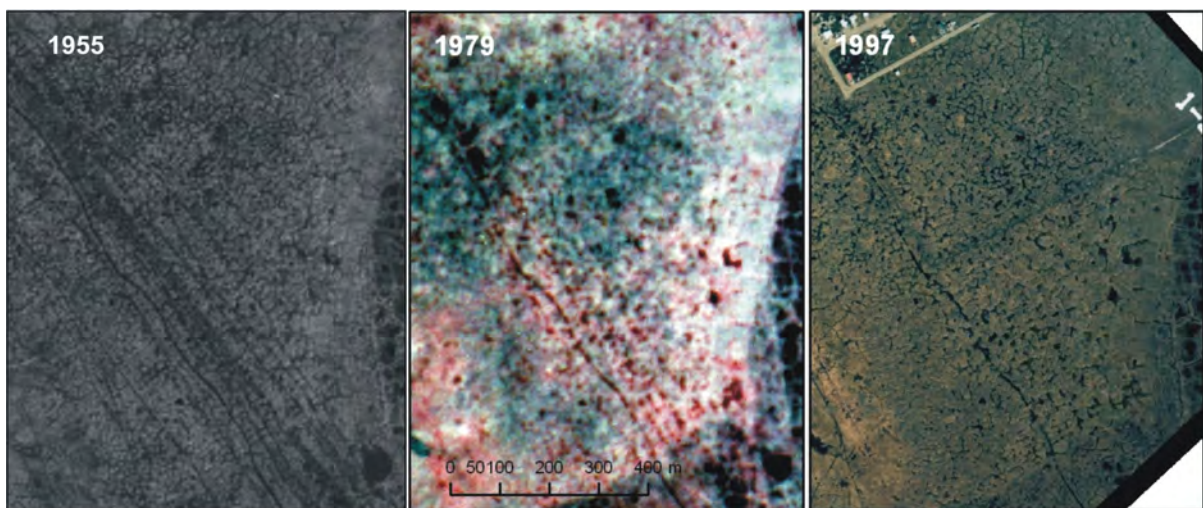


Figure 225. A time series of airphotos from 1955, 1979, and 1997 of the buried ice-wedge site, showing extensive degradation of ice wedges that has been increasing over time. Note the reduction in the number of visible trails and the thermokarst development along the main trail (by T. Jorgenson).

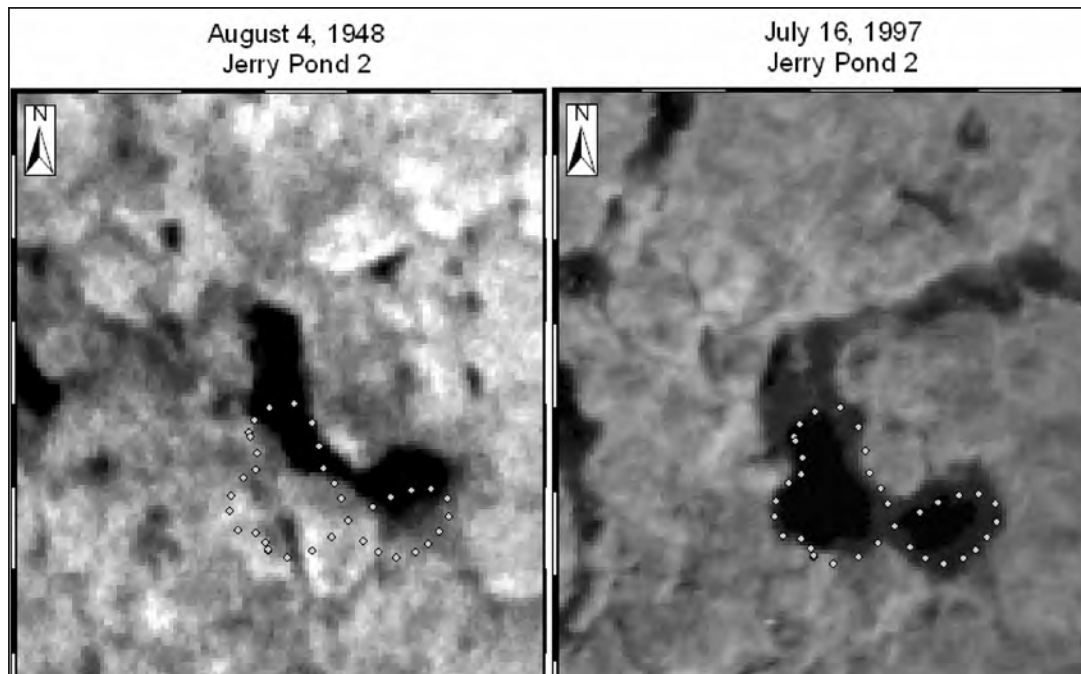


Figure 226. A close-up view of a pond that has been enlarged and subsequently colonized by aquatic sedges from 1948 to 1997. There is a slight error in the co-registration of the airphotos evident at this scale, but the outline shows the basic position and shape (photo by E. Burger).

STOP 8: CAKE EATER ROAD SNOW FENCE

The large snow fence at Cake Eater Road is one of several fences near Barrow that are designed to capture snow and reduce drifting in winter from strong easterly winds (fig. 227). Constructed in autumn 1997, the 2.2-km- (1.4-mi-) long fence is 4 m (13 ft) high. A large drift develops each winter on the downwind (road) side of the fence that is typically as high as the fence (fig. 228); a smaller drift (2 m [7 ft]) forms upwind. To monitor the thermal impact on ice-rich permafrost, nine monitoring sites were installed near the fence at this location in 1999 to measure near-surface soil temperature; three additional sites were located in the undisturbed tundra to the south and serve as a control. Maximum thaw and snow depth were measured annually, in August and April,

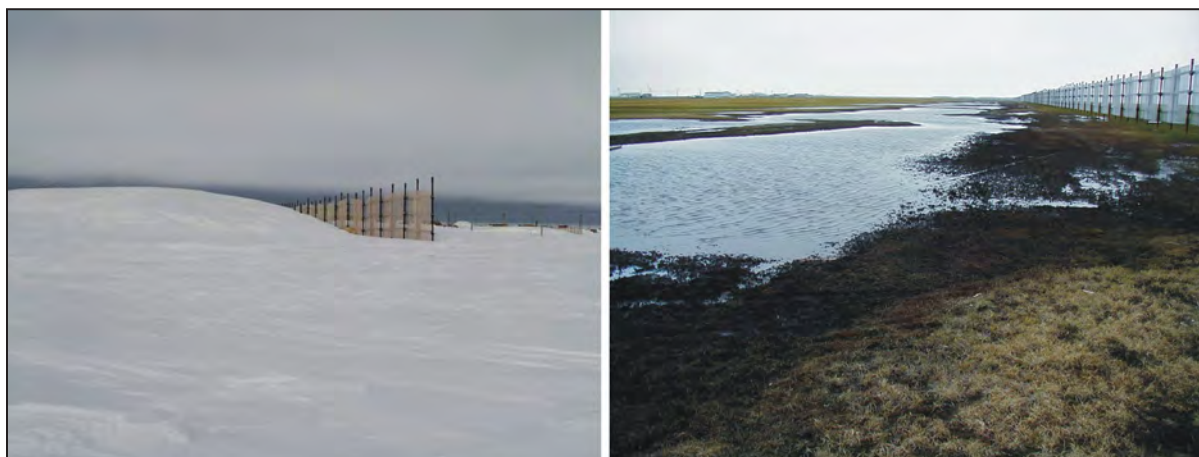


Figure 227. Snow fences used to reduce the amount of drifting snow that accumulates in Barrow (left). Melting of the high drifts creates large ponds during summer (right) (photos by K. Hinkel).

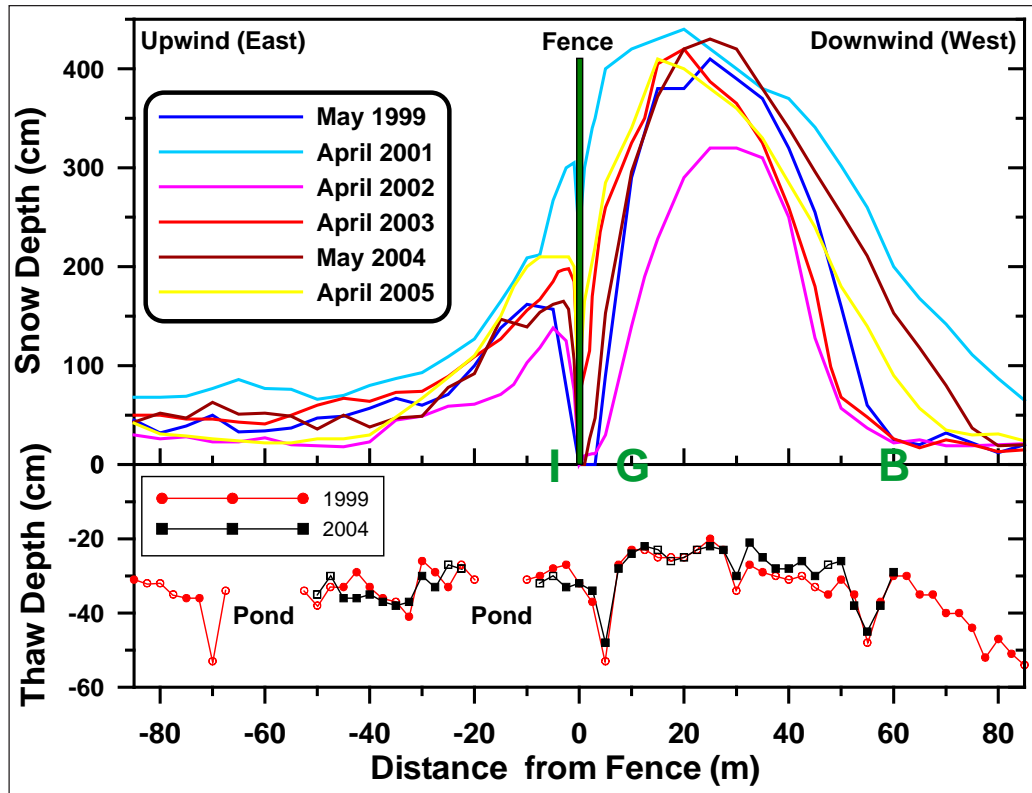


Figure 228. The 4-m- (13.1-ft-) high snow fence created snowdrifts ranging from 3.3 to 4.4 m (10.8–14.4 ft) high from 1999 to 2005 (top). Thaw depths under the drifts decreased slightly in response to the delayed snowmelt (bottom) (Hinkel and Hurd, 2006).

respectively. The results of a six-year study (Hinkel and Hurd, 2006) indicate that soil temperatures beneath the drift are 2–14°C (3.6–25.2°F) warmer than the control in winter due to the insulating effects of the snow (fig. 229). Since the drift persists 4–8 weeks after snow has disappeared from the undisturbed tundra, soil thaw is delayed and soil temperatures in summer are 2–3°C (3.6–5.4°F) cooler than the control. The mean soil temperature over the six-year period of record has warmed 2–5°C (3.6–9°F), and the uppermost permafrost has thawed. At this location, the ground surface has experienced 10–20 cm (4–8 in) of thaw subsidence and widespread thermokarst is apparent where snow meltwater ponds. Both direct soil warming and the indirect effects of ponding contribute to local permafrost destabilization.

A walk through the study area demonstrates that the vegetation beneath the drift has died in many places, and the organic mat is fragmented. Preexisting ponds have become larger and deeper over time, and new ponds have developed. This is apparent in the thermal records of some affected sites, and through measurements of ground-thaw depth and subsidence. These indirect effects appear to have enhanced thermokarst activity.

Ground subsidence, which allows water to impound in the resulting depressions, demonstrates large spatial variability across several scales (fig. 228). At this site, there is general subsidence near the fence where the drift is deepest. Most subsidence appears to be confined to the southern end of the fence where the terrain is flat and the drainage is poor. The middle and northern sections are well drained, lack ponding, and demonstrate no evidence of subsidence.

STOP 9: BIOCOMPLEXITY SITE AND MONITORING THE URBAN HEAT ISLAND

On the east side of the road is a pullout and entrance to the western side of the Barrow Environmental Observatory. The power line services a major NSF-funded research project that is manipulating and observing the changes in tundra gas fluxes resulting from flooding and water table fluctuation (Zona and others, 2007). Near the road are seasonally-deployed greenhouses that are used by Barrow high school students to study the effects of warming and nutrients on tundra vegetation and active layer.

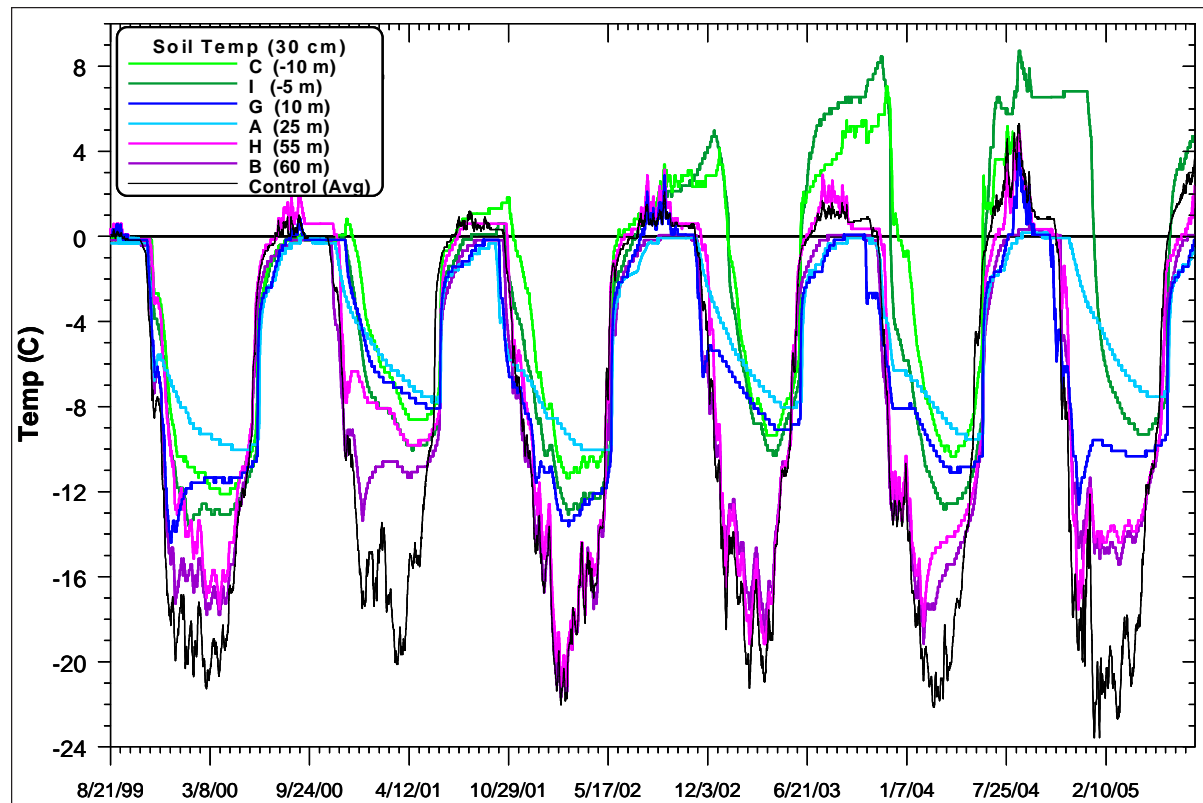


Figure 229. Soil temperatures at 30 cm (11.8 in) depth at varying distances from 10 m (33 ft) upwind to 60 m (200 ft) downwind of the snow fence collected from 1999 to 2005 reveal dramatic warming of surface soils under the large snow drifts (Hinkel and Hurd, 2006).

The biocomplexity project was funded in fall 2004 by NSF with the primary objective to understand the role of soil moisture in controlling ecosystem carbon balance. The four-year project focuses on a large-scale experimental flooding and draining manipulation on the Barrow Environmental Observatory and covers an area approximately 1,500 m long by 500 m wide (4,920 ft long by 1,640 ft wide). The scale of the experiment allows for a host of measurements to be made at different ecological scales. This is essential for understanding how small-scale processes affect larger scale phenomena and how large-scale phenomena feed back to control small-scale processes. A large-scale flooding and draining experiment forms a significant component of this project. The various sub-projects address methane flux, plant species interactions, fine-scale remote sensing, fine-scale chamber fluxes, large-scale ecosystem fluxes, and modeling. A major goal of the carbon flux measurements is to quantify ecosystem-level changes in carbon flux as a result of drying and flooding. Past results indicated that the Arctic tundra had changed from a sink to a source for carbon, in part attributed to long-term drying and warming. However, subsequent to these observations the system returned to a sink during the growing season (remaining a source on an annual basis when late fall, winter, and early spring contributions are included).

Near the road is an instrument mast that is part of the Barrow urban heat island study. Barrow is rather unusual in that nearly all of the fossil fuel needed to meet the heating, electrical, and personal needs of the ~4,600 residents is derived from local sources; only vehicle fuel is imported. In recent decades, as the population grew, a general increase of mean annual and mean winter air temperature has been recorded near the center of the town and a concurrent trend of progressively earlier snowmelt in the village has been documented. Satellite observations (Stone and others, 2002) and data from the nearby Climate Monitoring and Diagnostics Laboratory indicate a corresponding but much weaker snowmelt trend in the surrounding regions of relatively undisturbed tundra. Because the region is underlain by ice-rich permafrost, there is concern that early snowmelt will increase the thickness of the active layer and threaten the structural stability of roads, buildings, and pipelines. A four-year study (Hinkel and others, 2003b; Hinkel and others, 2008) demonstrated a strong urban heat island (UHI) during winter (fig. 230). Fifty-four data loggers were installed in the ~150 km² (~93 mi²) study area to monitor hourly air and soil temperature, and

daily spatial averages were calculated using the 6–7 warmest (urban) and coldest (rural) sites like the one nearby. During winter (December 2001–March 2002), the urban area averaged 2.2° C (4.0°F) warmer than the hinterland. The strength of the UHI increased as wind velocity decreased, reaching an average value of 3.2°C (5.8°F) under calm (<2 m/s [<4 mph]) conditions and maximum single-day magnitude of 6°C (10.8°F). UHI magnitude generally increased with decreasing air temperature in winter, reflecting the input of anthropogenic heat to maintain interior building temperatures. On a daily basis, the UHI reached its peak intensity in the late evening and early morning. There was a very strong positive relation between monthly UHI magnitude and natural gas production/use (fig. 231). Integrated over the period September–May, there was a 9 percent reduction in accumulated freezing–degree-days in the urban area. The evidence suggests that urbanization has contributed to early snowmelt in the village.

During summer, there is a strong maritime effect and a close correspondence between temperature distribution and wind regime (Hinkel and others, 2003b). Summer wind direction and velocity have a strong impact on mean daily air temperature and temperature range across the study area. Generally, winds from the northeastern and

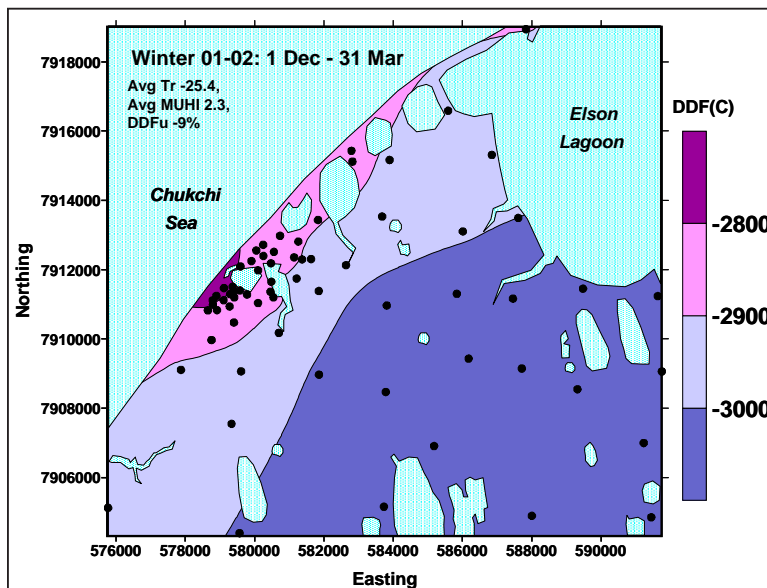


Figure 230. Heat of building and other human activity has contributed to a measurable (~2°C [$\sim 4^\circ\text{F}$]) warming of the city environment relative to the more distant areas in the Barrow region (Hinkel and Nelson, 2007). Tr = Temperature, MUHI = Monthly Urban Heat Island effect, DDF = Freezing Degree Days.

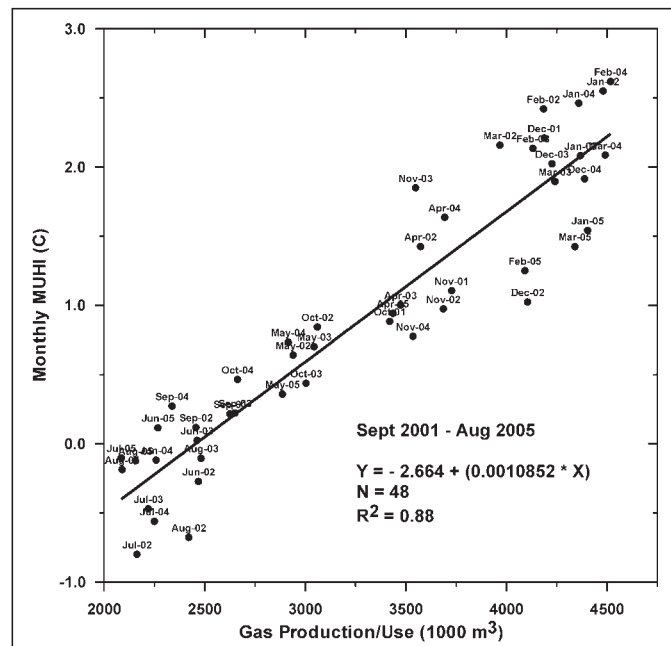


Figure 231. The increase in air temperatures in Barrow is closely related to the use of natural gas for heating (Hinkel and Nelson, 2007). MUHI = Monthly Urban Heat Island effect.

northwestern quadrants yield cold–cool temperatures due to the influence of open water or ice on onshore winds. Warmer conditions are associated with winds from the southwest and, especially, southeast quadrants. The maritime effect is pronounced along the windward coast while onshore breezes prevail, but is limited to a fairly narrow (several kilometer) littoral zone under normal wind velocity conditions. Strong winds prevent steep temperature gradients from developing across the study area. In contrast to the situation in winter, the effects of local urban infrastructure on air temperatures were relatively minor during summer.

STOP 10: FROST MOUNDS AT FOOTPRINT LAKE

The road parallels Footprint Lake which was drained in 1950 (fig. 232). Note the shallow depth of the old lake basin. A previous gravel road was located in the flat lake basin; it has since subsided into the permafrost and is covered by wet tundra vegetation.

Along the eastern shore of Footprint Lake there are numerous ice-cored frost mounds that have formed since it drained; most appear to have developed since the mid 1990s (fig. 233). A number of these mounds, ranging from 5 to 20 m (16–66 ft) across, have been cored since 1996. Standing about 40 cm (16 in) above the marsh surface, the thin surface layer of detritus contains plant stems and roots that are encased within the underlying ground ice. Dead plant parts, released by ablation of the mound surface, provide an effective thermal insulator and preserve

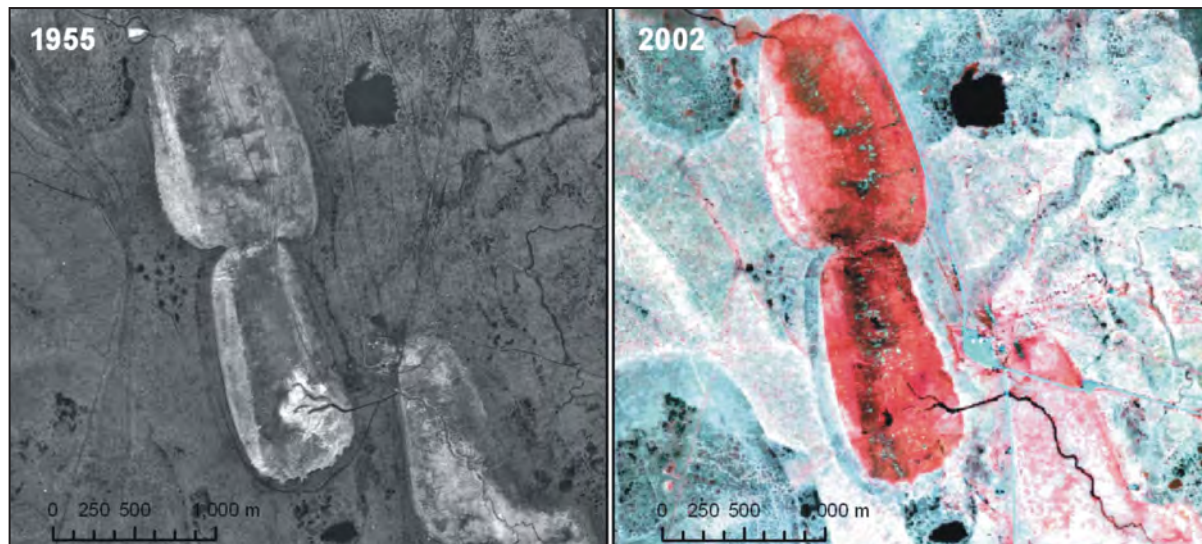


Figure 232. A 1955 airphoto and 2002 satellite image of Footprint and Dry lakes. To the east of Footprint Lake are the new road, the western edge of the BEO, and the site of an intensive biocomplexity study.

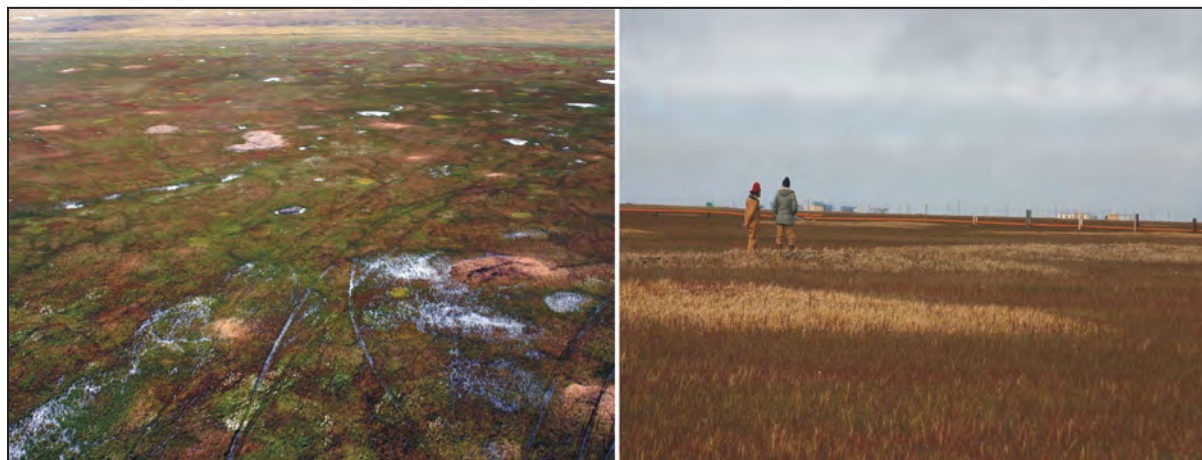


Figure 233. Frost mounds, small ice-cored mounds, are common in young drained-lake basins (2007 photos by K. Hinkel).

the features over summer. Pure ice is found deeper in the soil core (fig. 234) and provides evidence of lateral subsurface injection of water during closed-system freezeback of the active layer (Hinkel and others, 1996). The hydrostatic pressure is sufficient to generate large tension cracks that bisect the mounds. The spatial pattern of frost mounds appears nonrandom, as they are crudely aligned and concentrated on one side of the lake basin. The ice-cored mounds are continuous with the underlying permafrost. Development of wet and dry meadow tundra plant communities suggest that they are stable features, occupying a progressively larger proportion of the basin area over time.

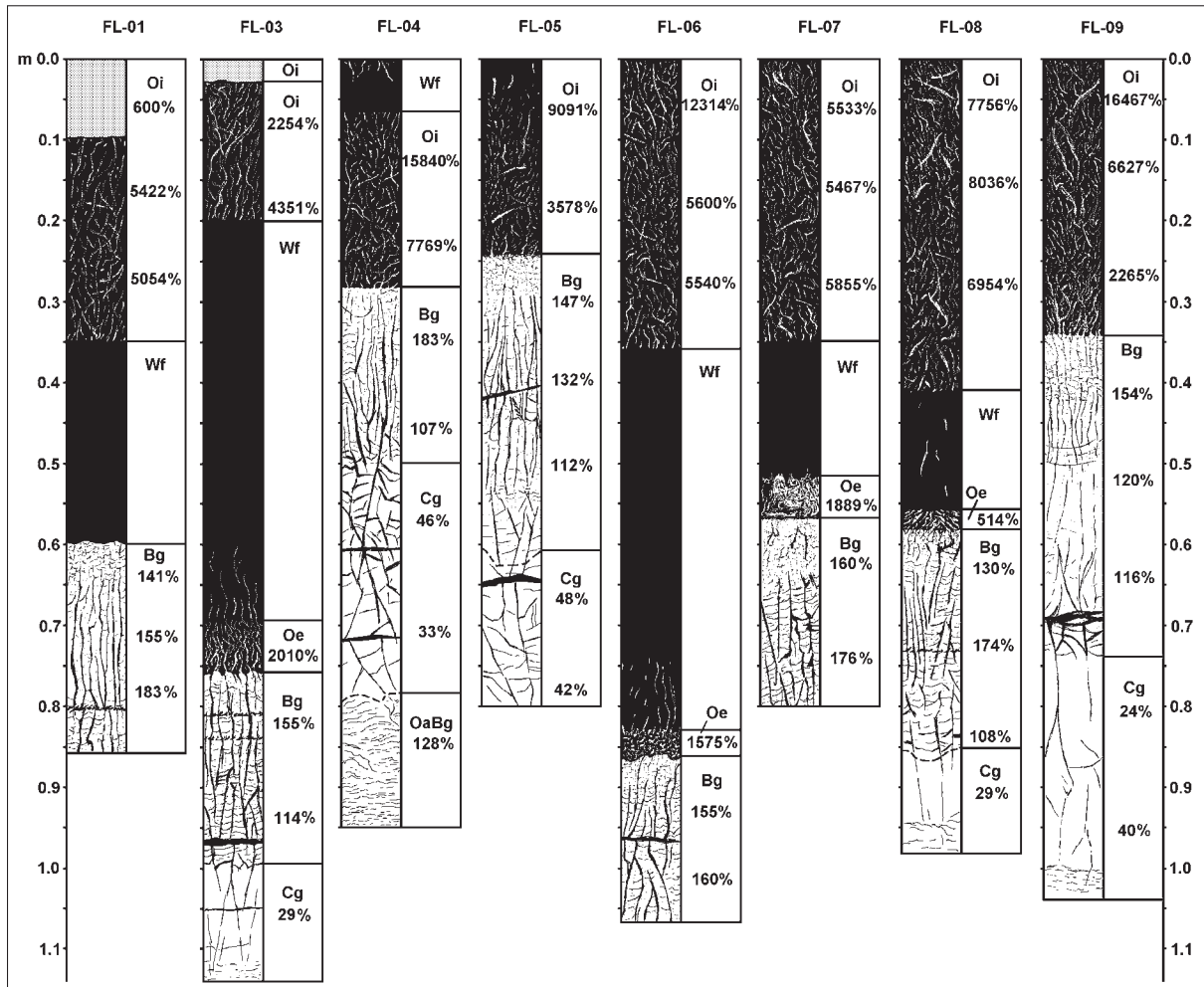


Figure 234. Soil stratigraphy of cores obtained from nine frost mounds, showing the relationship of thick surface organics, massive ice in the mound core, and the morphology of segregated ice below the massive ice (Munroe and others, 2007, illustration by M. Kanevskiy). Soil horizons are: Oi = Organic-fibric, Oe = Organic-hemic, Oa = Organic-sapric, Bg = B-gleyed, Cg = C-gleyed, WF = Water-frozen. Gravimetric water contents are percent dry weight.

STOP 11: BARROW GAS FIELDS

The South Barrow, East Barrow, and Ualiqpa (Walakpa) gas fields (fig. 235), the source of Barrow's heating and electrical energy, were developed by Navy and borough contractors over a period of 50 years (Glenn, 2002). The first exploration test well in the Barrow area, South Barrow No. 1, was drilled during the winter of 1948 after a series of shallow core test wells were completed. The South Barrow gas field was discovered with the drilling of the South Barrow No. 2 well in 1948. The No. 2 well, located 8 km (5 mi) inland from the Navy camp, was targeted in an early seismic exploration program. It was the first well drilled in the Naval Petroleum Reserve that was capable of significant oil or gas production. Following testing, plans were made to pipe the gas to the nearby

Navy camp (soon to become the Naval Arctic Research Lab or NARL). On July 29, 1949, South Barrow No. 2 began producing gas for the Navy camp. The 10-cm- (4-in-) diameter pipeline that transported the gas to the Navy camp was laid above ground on dunnage beams and 55-gallon drums. This pipeline was used by the Navy and, since, by UIC NARL and the DEW Line for almost 50 years (the line has recently been dismantled).

Over the next 10–20 years, more wells were drilled in the South Barrow field, and natural gas soon supplied government facilities in Barrow, such as the hospital, school, and weather station. Following a severe storm in 1963, Barrow residents petitioned for access to natural gas for home heating and electricity. This petition was approved with the support of NARL and the Bureau of Indian Affairs. By 1967, power generation and distribution pipes were being installed in Barrow. Demand for gas increased, and by 1974 eight additional wells were drilled in the South field.

The East Barrow gas field was discovered by the Navy in 1974 with the drilling of East Barrow No. 12. As with the South field discovery well, the No. 12 well was drilled over a seismically mapped target. The producing interval in the East Barrow No. 12, now known as the ‘Barrow Gas Sand,’ was nearly identical in age and properties to the producing interval in the South field.

The Department of Interior assumed control of exploration of the reserve from the Navy in 1976, and changed the name of the reserve to Naval Petroleum Reserve—Alaska (NPRO). The Interior-sponsored exploration of NPRO continued throughout the 1970s. By the end of the 1970s, more than 20 wells had been drilled in the Barrow area by the Navy, the Department of Interior, and their contractors. In 1980, with the drilling by Husky Oil of Walakpa No. 1, located about 19 km (12 mi) southwest of Barrow, a new potential gas accumulation was discovered. Follow-up drilling in 1981 of the Walakpa No. 2 well 8 km (5 mi) to the south of the discovery well continued to indicate the strong possibility of a large natural gas reservoir. In 1984, the North Slope Borough received ownership and operational responsibility of the producing intervals of the South and East fields as well as subsurface rights to the potentially productive ‘Walakpa Gas Sand’ interval in the Ualiqpaa area. Before any Ualiqpaa drilling had even occurred, a ‘shakedown well’ was drilled by the borough development team. The well, East Barrow No. 21, drilled during the winter of 1990, was located in the East field close to the gas field road system to minimize logistical problems. The well was successfully completed as a producer in the Barrow Gas Sand. It was the last well drilled in the East Barrow field. The well began production immediately, as town demand had grown and the additional volume was needed.

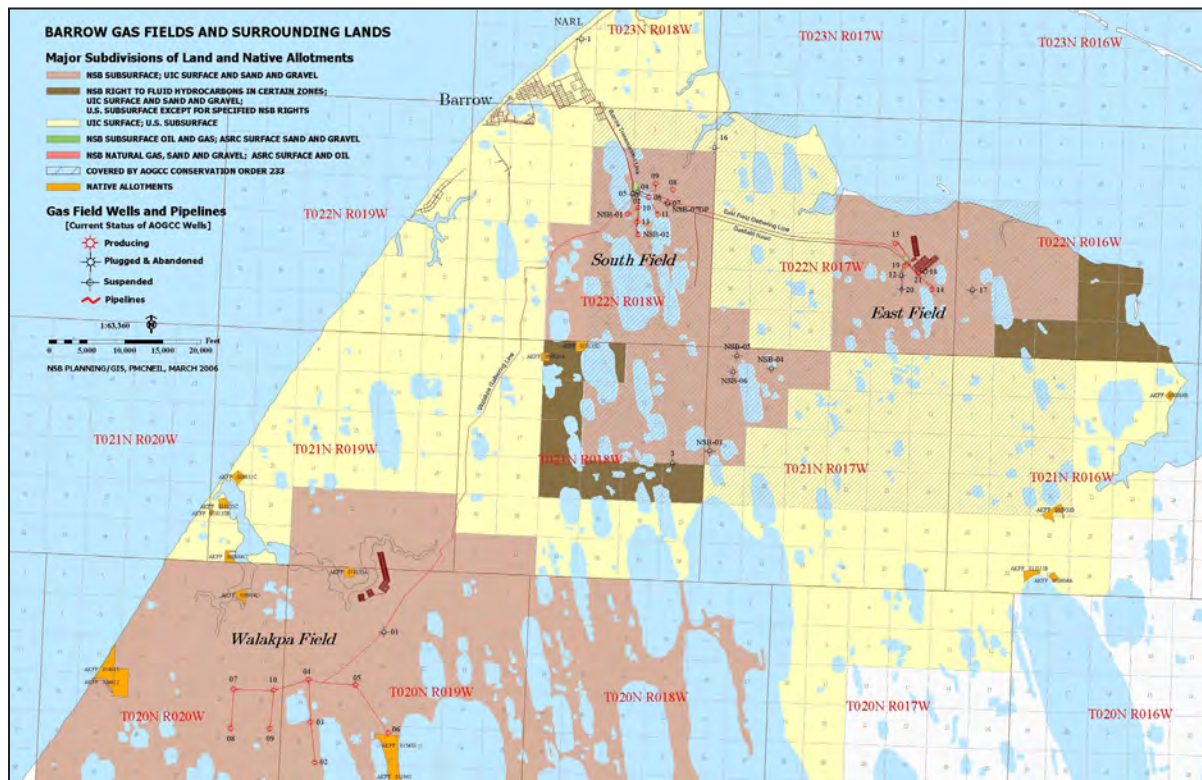


Figure 235. Map of Barrow gas fields.

By abandoning diesel and other fuels as a heating and electrical generation fuel source, Barrow is also a cleaner and safer town, less prone to environmental damage from fuel spills. Natural gas demand in the winter at Barrow can sometimes top 6 million cf/day, and the annual consumption for the community is almost 1.5 billion cf/yr. Locally-produced compressed natural gas has augmented imported gasoline as a fuel for cars and trucks in Barrow.

STOP 12: DRY LAKE DRAINAGE

Crossing the small bridge over the channel that drained Dry Lake in 1950, one observes the meltout of ice wedges that once existed beneath the shallow lake (fig. 232). Polygon patterns have developed on the lake bottom, indicating where ice wedges have melted after lake drainage. Interestingly, the shallow Footprint Lake basin did not show post-drainage evidence of these large ice wedges. At the far end of the road and to the west is Ikoravik Lake, the northernmost lake with a resident fish population. The lake is more than 3 m (10 ft) deep. Consequently, the lake does not freeze to the bottom during winter and a thaw bulb exists beneath the lake as it did at Imikpuk Lake (Fig. 219). The lake is connected to Dease Inlet through a series of drained-lake basins and beaded streams (Lewellen, 1972).

STOP 13: UIC MATERIAL SITE AND NSB SOLID WASTE DISPOSAL

The recently opened North Slope Borough waste disposal site is located south of the gas field road. The access road may be closed when not in operation. Also to the south is the UIC material pit that was developed in the late 1990s as a source of sand and gravel. These materials were deposited during an earlier marine transgression. A radiocarbon date on a log buried deep in the frozen sands produced an infinite date >45 RC ka BP (oral commun., David E. Putnam).

STOP 14: BIRNIRK ARCHAEOLOGICAL SITE

The abandoned Birnirk village site and a contemporary duck hunting camp are found along the summer beach road, which passes the old Air Force runway and continues to the boat launching site at Niksiuraq (fig. 236). Summer access beyond to Point Barrow requires off-road vehicles. The Birnirk site is a National Historic Landmark and the type site of the Birnirk culture. It appears to have been a sizable settlement at one time, but was later reduced to a small settlement with more intensive use as a seasonal duck hunting camp. Currently, it is still in use as a place to hunt ducks, although many users now commute rather than spend the night. Although there has been considerable excavation there, only the work carried out by James Ford in the 1930s has been published (Ford, 1959). Anne Jensen began additional excavations at Birnirk in 2008. A series of radiocarbon dates from the abandoned Birnirk at the base of the spit (fig. 236) led Hume and others to conclude that Birnirk was occupied at about 1500 AD and subsequently flooded by a rising sea level or a subsiding land surface. However, radiocarbon dates on a number of harpoon heads indicate occupation by 800–1000 AD, with the majority of the dates clustering around 1000–1200 AD (Morrison, 2001). The archaeological materials recovered through purchase suggest the possibility that the site was in use as early as 400 AD, based on artifact typology.

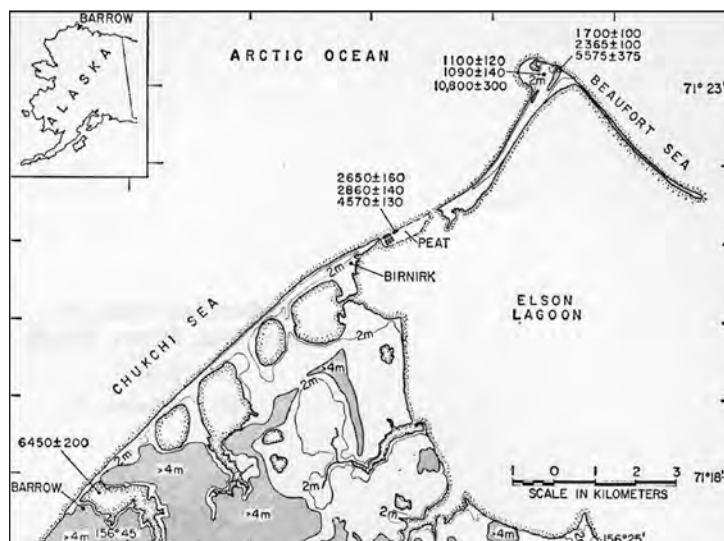


Figure 236. A map of the Barrow spit showing the location of the Birnirk village site, along with radiocarbon ages for numerous locations along the spit (Brown and Sellmann, 1966).

STOP 15: ELSON LAGOON NEAR BRANT POINT

The northernmost shoreline of Elson Lagoon is a major key site of the Arctic Coastal Dynamics (ACD) project (Rachold and others, 2005) and the shoreline has been subdivided into four segments for monitoring purposes (Brown and others, 2003) (fig. 237). The lagoon is bounded on the northeast by a series of low elevation barrier islands. Submerged bars lie at the mouth of most creeks draining from the BEO to Elson Lagoon and a shoal extends northwest from Tekegakrok Point, which marks the junction between Sections C and D of the coastal observatory. Fourteen transects perpendicular to the coast were established in 2002 along the 10.7-km- (6.6-mi-) long coast of the BEO. Several transects coincide with erosion sites first measured in the 1940s by MacCarthy (1953). The BEO coastline is divided into four segments with sections A, B, and D facing eastward and section C

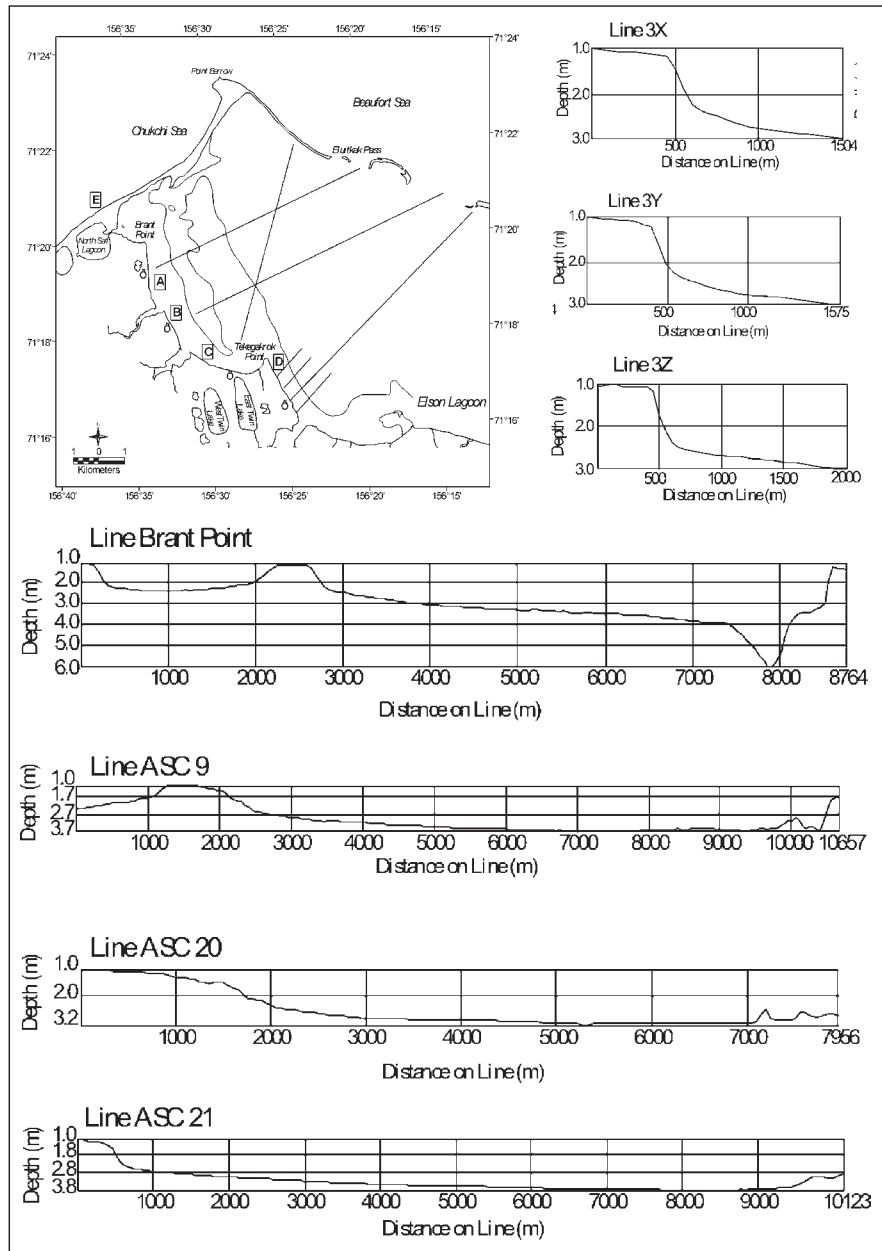


Figure 237. Map of monitoring segments A–D at the Elson Lagoon key site for the circumpolar Arctic Coastal Dynamics program (upper left) and bathymetric profiles of Elson Lagoon (Brown and others, 2003).

facing predominantly north (Brown and others, 2003). Water depth in Elson Lagoon ranges from 0.5 m to 3.5 m (1.6–11.5 ft). Winter ice cover on the lagoon freezes down to nearly 2 m (7 ft). Temperature measurements of lagoon sediments indicate that the sediments are frozen, which is possible because of the depressed freezing-point of hypersaline water below the ice (Lewellen, 1973) (figs. 238 and 239). The extent of permafrost beneath Elson Lagoon is not well known. It occurs close to the surface in shallow water (Lewellen, 1973). The exposed barrier islands are underlain by permafrost. As the island migrates over deeper water and the unfrozen lagoon sediments, permafrost forms. Where sea ice freezes to the bottom, permafrost persists close to the surface.

The shoreline of Elson Lagoon is rich in both organic matter and ice, but the soil characteristics vary by terrain type (Michaelson and others, 2008). The Section A site (ER-05) is within a portion of an old terrain surface. The soil profile from this site shows a thick surface-organic mat underlain by a middle horizon of highly disrupted organic masses within a slightly pebbly loamy sand (fig. 240). Below that the organic matter is lacking

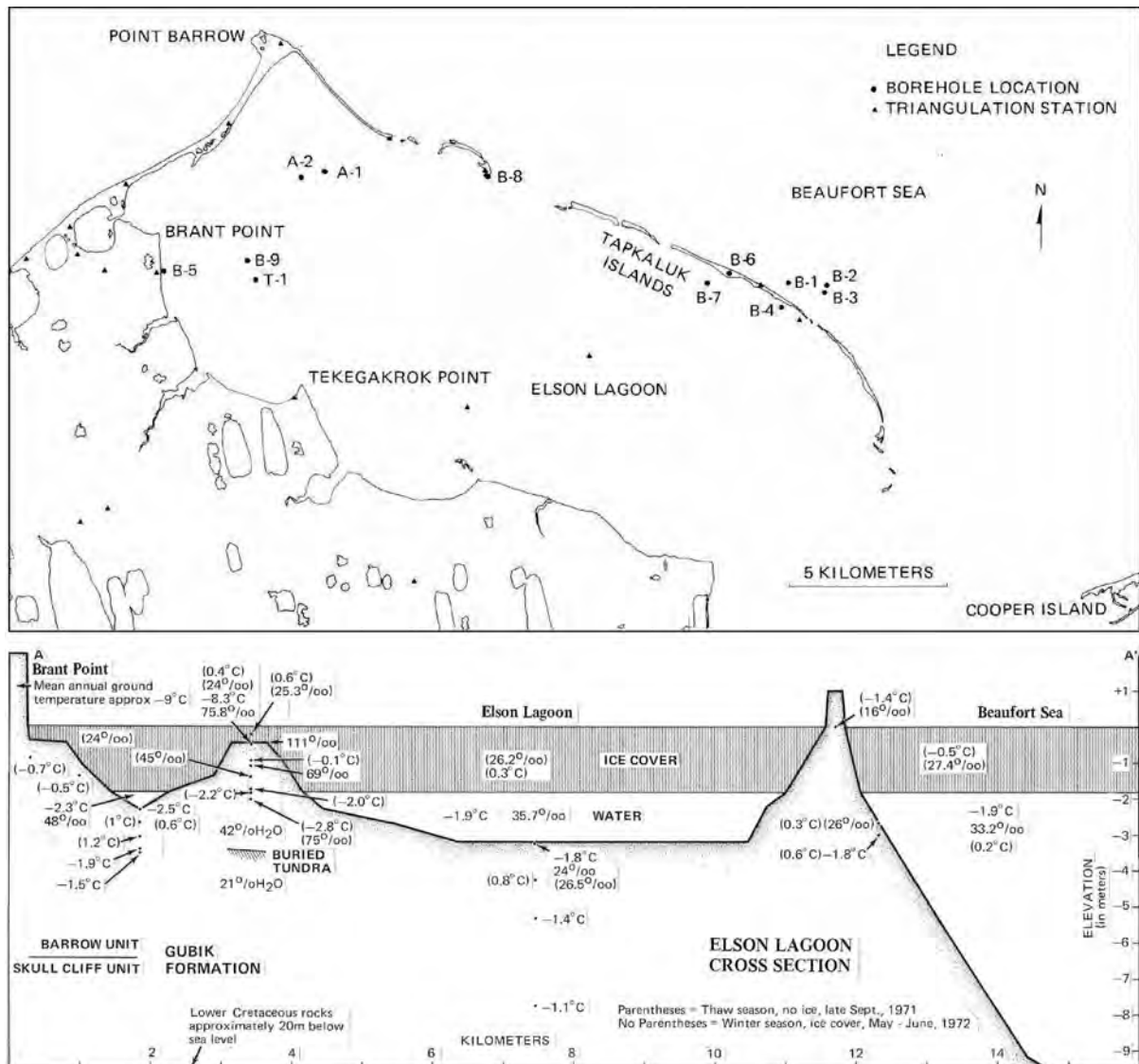


Figure 238. Cross-section of Elson Lagoon, illustrating water and soil temperatures and salinity (Lewellen, 1973).

Figure 239. Thermal profiles under Elson Lagoon (Lewellen, 1973).

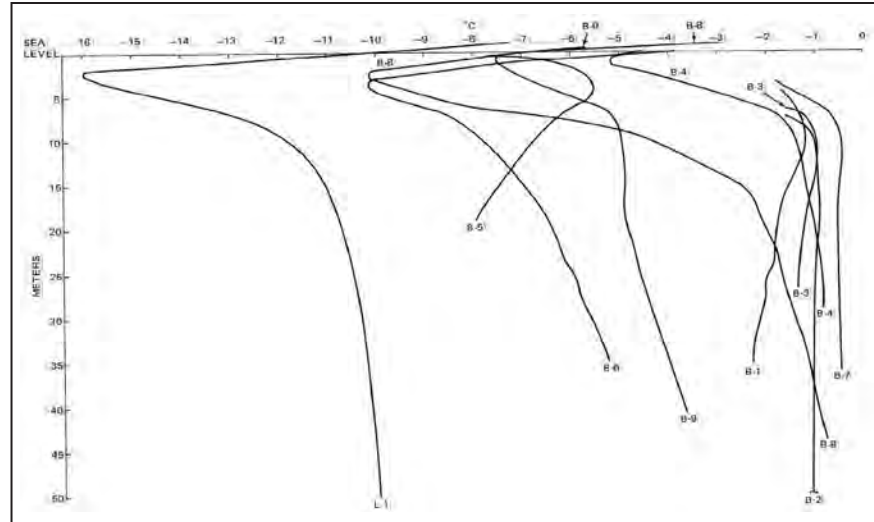


Figure 240. Views of soil exposures from an old, remnant surface (left, photo by T. Jorgenson) with highly deformed organic masses within a slightly pebbly, loamy sand; and an old, drained lake basin (right, photo by V. Tumskoy) with organic-rich limnic sediments.

STOP 16: ELSON LAGOON NEAR TEKEGAKROK POINT

Erosion along the ice-rich coastline of Elson Lagoon can be dramatic due to the occasional breaking off of blocks of ice-rich permafrost (fig. 241). Recently, annual measurements have been taken during late summer to quantify shoreline retreat (Brown and others, 2003). More recently, continuous, ground-based surveys using a Differential Global Positioning System (DGPS) were conducted along the entire length of the BEO coastline in 2003, 2006, and 2007 (Aguirre and others, 2008) (fig. 242). The mean annual erosion rate during the 4-year period was 2.3 m (7.5 ft) per year. A comparison of fall and summer erosion based on repeat DGPS surveys indicates similar amounts of erosion during fall 2006 (August 2006–June 2007, 8,120 m² [87,404 ft²]) and summer 2007 (June–August 2007, 7,934 m² [85,402 ft²]). The total area loss during the 4-year period was 9.8 ha (24.2 ac), with an average of 2.45 ha (6.05 ac) per year, which is almost twice the rate calculated for the period 1979–2000 (1.3 ha [3.21 ac]/yr) by previous studies (fig. 243).



Figure 241. Views of erosion along Elson Lagoon illustrating the abundance of ground ice (left) and the collapse of blocks along an ice wedge (right) (photos by Jim Bockheim).

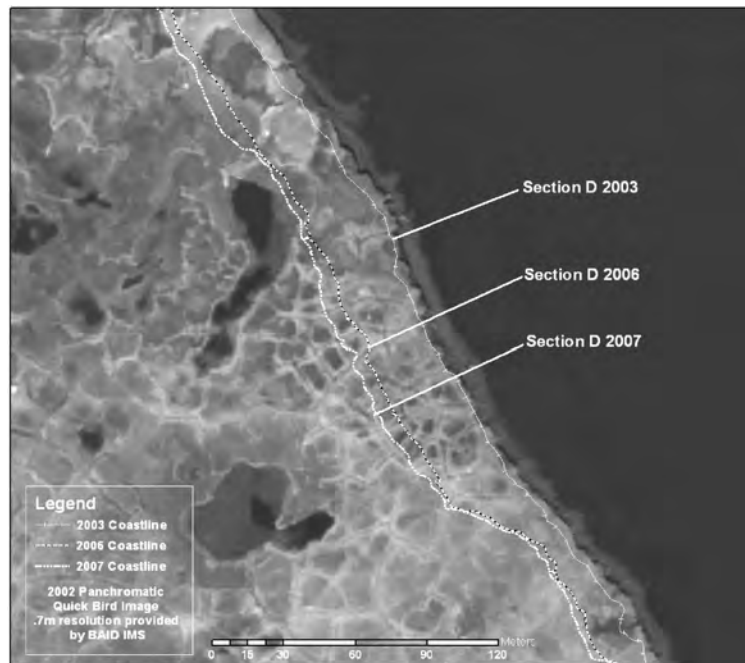
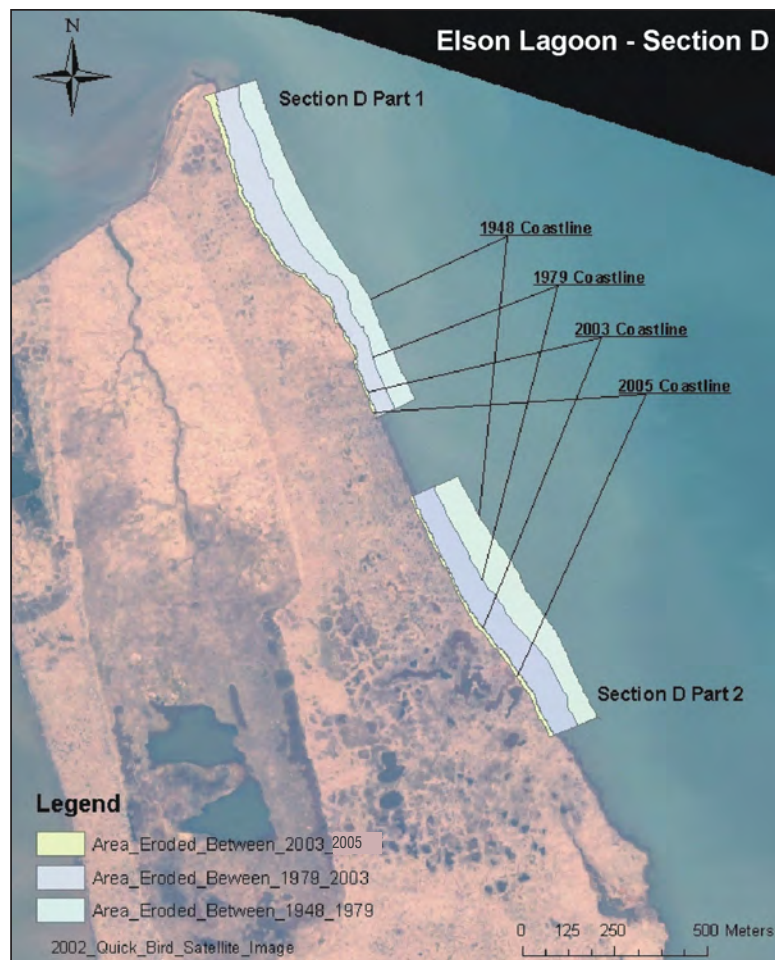


Figure 242. Changes in the coastline at Section D from 2003 to 2007 obtained by continuous ground survey along the top of the bluff with a differential GPS (based on Aguirre and others, 2008).

Figure 243. Changes in coastline along Section D from 1948 to 2005 (based on Serbin and others, 2004).



The soil at Section D (ASC-21) is from an old drained-lake basin. It also has a thick surface-organic mat, but is underlain by a thick sequence of extremely ice-rich, olive-brown, limnic sediments (fig. 240). The ice morphology is composed of beautiful ataxitic ice (suspended) structure in bands between horizontal ice layers.

STOP 17: BARROW SPIT AND THE NUVUK ARCHAEOLOGICAL SITE

Point Barrow is the northernmost tip of the United States. The gravel spit extends northward 8 km (5 mi) from the mainland and hooks to the southeast for 8 km (5 mi) to form Plover Point (fig. 236). Maximum elevation is ~5 m (16 ft) above sea level. The northeast section is an extension of the Barrow beach and is built by long shore drift of gravel and sands in the Chukchi Sea. The southeast section is built by long shore drift to the southeast.

The depositional history of the spit is known in outline and resembles that from other similar landforms across northern Alaska. Local elders report that the spit extended farther north prior to the 19th century. Péwé and Church (1962) also refer to earlier estimates that the shoreline at the Point had migrated southward more than 700 m (2,300 ft) since the early 1800s. Geologic data to establish its history derive from auger holes drilled in the 1960s (Péwé and Church, 1962), as well as stratigraphic observations in the 1960s (Hume, 1965) and from 2003 to 2007 (Mason, unpublished data). In the 1960s, Hume (1965) linked each gravel bed to eustatic sea-level rise, although present interpretations infer that the beds are storm deposits. Péwé and Church (1962) obtained radiocarbon dates of between 1.1 and 10.8 RC ka BP on wood fragments from the auger hole in the permafrost. Hume (1965) reported dates on three more pieces of driftwood between 1.7 and 5.6 RC ka BP (fig. 236). Stratigraphic observations by Mason (2003–07) and an additional seven dates on peat and driftwood confirm and extend the sequence established by the 1960s research. A consistent chronology emerges from the three sets of radiocarbon dates, if one excludes outlier samples in excess of 5.6 RC ka BP. The erosional face at the north margin of the Barrow spit reveals a complex sequence of storm beds that occasionally incorporated driftwood, some apparently ancient, and at least two laterally extensive (>20 m [>66 ft]) peat beds. The oldest peat formed during the first centuries AD atop gravel

ridges that are presently at mean high tide and are composed of coarse sand and granules. After AD 250, the spit underwent a drastic shift in deposition as intense storm surges, more than 3 m (10 ft) in elevation, constructed the first of two high composite ridges. Heightened storm intensities are also apparent in the larger clast sizes and the considerable thickness of individual beds. Storm intensities slackened around AD 1000–1100, the age of a large cemetery atop the ridge. A period of less intense storms followed, producing a low swale, followed by another period of strong storms that produced the second high ridge near Point Barrow. Storm deposits in the lower part of this ridge are dated by a limiting age ca. AD 1400 from an extensive organic horizon. In sum, the Point Barrow spit witnessed considerable expansion after AD 200, although its history prior to 200 BC remains undocumented and is complicated by the slightly lower sea level that prevailed at that time.

The peat deposits in the Point Barrow vicinity provide proxy records of eustatic sea-level rise. The Nuvuk peat, presently near high tide, reflects a rise in sea level of at least 50 cm (1.6 ft), an elevation similar to that from peat dated in the 1960s. The 1963 storm with its 3–4 m (10–13 ft) surge resulted in breaching of the spit in three places, exposing a thick peat deposit, extending to 1.5 m (4.9 ft) below sea level; its upper section dated between 2.7 and 4.6 RC ka BP (Brown and Sellmann, 1966). Botanical composition was of freshwater vegetation, mostly mosses, suggesting that this land area was inundated by a rising, late Holocene sea level. These data are similar to other sea level records in the Chukchi Sea (Mason and Jordan, 2002).

The first recorded visit of non-Natives to Point Barrow took place in 1826, when the expedition led by Captain Frederick Beechey of the Royal Navy, in command of the 15-gun sloop HMS Blossom, was exploring the coast. There they encountered the small Native village of Nuvuk, once North America's northernmost village. Next, Captain Rochfort Maguire in HMS Plover spent the winters of 1852 and 1853 in Elson Lagoon. During the first IPY expedition in 1982–1983, John Murdoch purchased a large collection of Inupiat cultural material from the residents of Nuvuk and Utkiaġvik (modern Barrow).

The Nuvuk village site (fig. 244) has been the subject of numerous archeological investigations because of its long history of settlement (Jensen, 2007). James Ford worked briefly at Nuvuk in 1932 and in 1953 and provided extensive description of artifacts of the Birnirk site. During 1951–1953, Wilbert Carter spent three seasons excavating sites at Birnirk and Nuvuk. His work at Nuvuk in 1953 identified 19 locations containing depressions or other



Figure 244. 1953 view of the bluff at the Nuvuk site at the tip of Point Barrow (photo from M.E. Britton collection).

indications of houses or meat caches. He found numerous harpoon heads at Nuvuk, which he attributed to Nuwuk or Kilimatavik types. In 1998, Anne Jensen excavated an eroding burial (designated Nuvuk-01) of an adult male with grave goods that was threatened with being lost by erosion (Jensen, 2007). The materials include a Sippo harpoon head, which is diagnostic of Early Thule culture that was much earlier than the Nuwuk types (fig. 245). The individual was skeletonized, with the cranium and long bones relatively well preserved, and had been interred with an animal hide. The evidence was too poorly preserved to determine if it had been sewn into garments.

Based on recent studies by Jensen (submitted) at Nuvuk, and accompanying radiocarbon dates, it appears that Nuvuk was occupied by the Inupiat continuously for at least the past 1,200 years. The village was relocated several times as coastal erosion threatened the dwellings. Nuvuk was abandoned during the first half of the last century. Jensen reports recent erosion of 53 m (174 ft) between the 2001 and 2006 field seasons. Currently, UIC scientists are continuing archeological work to resolve many of the questions related to human occupation of the spit and its recent changes.

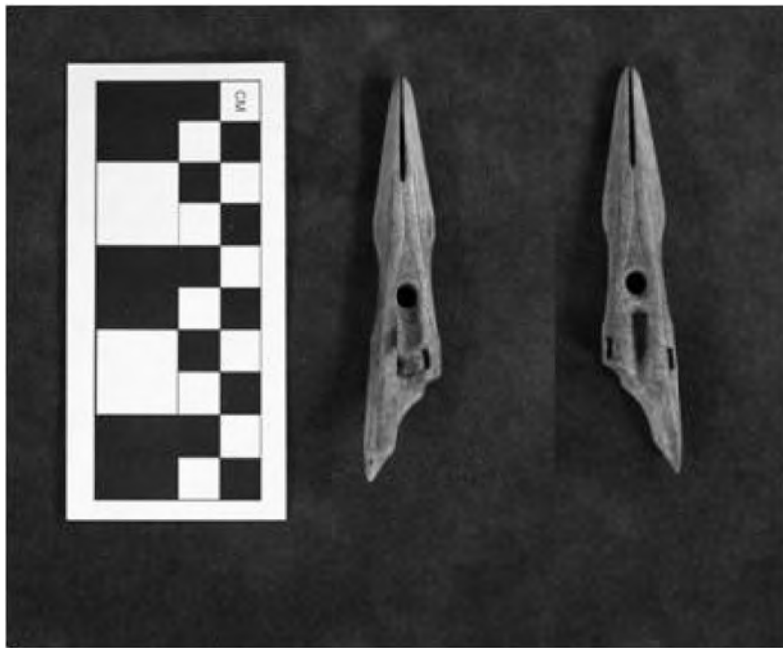


Figure 245. Two views of a harpoon head excavated from the Nuvuk site. The harpoon has two vestigial barbs, an incised triangle above the line hole, and incised lines running from the base of the blade slot to the base of the harpoon head (photo by A. Jensen).

ACKNOWLEDGMENTS

This guidebook was a collaborative effort among many individuals and we thank those that helped with reviews, including Richard Glenn, David Payer, John Payne, Chuck Racine, Richard Reger, and Rupert Tart. Field logistical support was generously provided by ConocoPhillips Alaska for the tour of the Kuparuk and Prudhoe Bay oilfields. We appreciate the partial support from the U.S. National Science Foundation associated with our ongoing projects in northern Alaska, including OPP-0436165, ARC-0454985, and EPSCoR 0701898. In Barrow, field logistics are currently provided by the Barrow Arctic Science Consortium (BASC) in support of numerous National Science Foundation projects. Access to the Ukpeagvik Inupiat Corporation (UIC) land is by permit. Bart Ahsogeak, Director, UIC Real Estate, provided assistance in re-opening the buried ice-wedge tunnel shaft and the construction and installation of the

new insulated portal. We also acknowledge the former Naval Arctic Research Laboratory and its directors (ARL and NARL) for logistical support of the many projects starting in the 1940s and continuing through the 1970s, and to the Cold Regions Research and Engineering Laboratory (CRREL) for its sponsorship of the Frozen Ground Project led by Jerry Brown. Scientific research was supported by grants to individuals. The Barrow photographs from the M.E. Britton collection were scanned by Ben Jones, USGS. De Anne Stevens, Joni Robinson, and Paula Davis with the Alaska Division of Geological & Geophysical Surveys helped with editing and production of the guidebook. Any opinions, findings, conclusions, or recommendations expressed in this material are those of the authors and do not necessarily reflect the views of the NSF.

REFERENCES

- ABR Inc., Environmental Research & Services, 2002, Rehabilitation of the Colville gravel mine: Unpublished report prepared by ABR Inc., Environmental Research & Services, Fairbanks, AK, for Tom Mortensen Associates, Anchorage, AK, 17 p.
- ABR Inc., Environmental Research & Services, and BP, 2007, Rehabilitation report for the GC 2 oil transit line release, Western Operating Area, Prudoe Bay Oilfield, Alaska: Unpublished report by ABR Inc., Environmental Research & Services, Fairbanks, AK, and BP Environmental Studies Group, Anchorage, AK, 45 p.
- Acevedo, W., Walker, D., Gaydos, L., and Wray, J., 1982, Vegetation and land cover, Arctic National Wildlife Refuge coastal plain, Alaska: U.S. Geological Survey Miscellaneous Investigations Map I-1443, 8 p., 1 sheet, scale 1:250,000.
- ACIA, 2005, Arctic Climate Impact Assessment: Cambridge University Press, 1,042 p., 200 plates.
- Aguirre, A., Tweedie, C.E., Brown, J., and Gaylord, A., 2008, Erosion of the Barrow Environmental Observatory Coastline 2003–2007, Northern Alaska, in Proceedings, Ninth International Conference on Permafrost, in press.
- Ahmoagak, G.N., 2004, Testimony on erosion in the North Slope Borough, Alaska: Washington, DC, U.S. Senate Committee on Appropriations, <http://appropriations.senate.gov/text/hearmarkups/record.cfm?id=223525> ed
- Ahrens, R.J., Bockheim, J.G., and Ping, C-L., 2004, The Gelisol order in soil taxonomy, in Kimble, J.M., ed., Cryosols, permafrost-affected soils: New York, Springer-Verlag, p. 627–636.
- Alaska Department of Environmental Conservation (ADEC), 1985, Information sheet for reserve pit discharge general permit: Alaska Department of Environmental Conservation, Juneau, AK.
- Alyeska Pipeline Service Company (APSC), 2008, Pipeline Facts: Fairbanks, AK. <http://www.alyeska-pipe.com/pipelinefacts.html>.
- Are, F.E., 1988, Thermal abrasion of sea coasts: *Polar Geography and Geology*, v. 12, p. 1–57.
- Arnborg, L., Walker, H.J., and Peipo, J., 1966, Water discharge in the Colville River, 1962: *Geografiska Annaler*, v. 48A, p. 195–210.
- Atkinson, D.E., 2005, Observed storminess patterns and trends in the circum-arctic coastal regime: *Geo-Marine Letters*, v. 25, p. 98–109.
- Auerbach, N.A., Walker, M.D., and Walker, D.A., 1997, Effects of roadside disturbance on substrate and vegetation properties in arctic tundra: *Ecological Applications*, v. 7, p. 218–235.
- Bailey, A., 2006, BP; Learning from oil spill lessons: *Petroleum News*, v. 11, no. 20.
- Barnes, P.W., Rawlinson, S.E., and Reimnitz, E., 1988, Coastal geomorphology of arctic Alaska; Arctic coastal processes and slope protection design: American Society of Civil Engineers, TCCR Practice Report, p. 3–30.
- Barnes, P.W., Reimnitz, E., Smith, G., and Melchior, J., 1977, Bathymetric and shoreline changes, northwestern Prudhoe Bay, Alaska: U.S. Geological Survey Open-File Report 77-167, 15 p.
- Bergman, R.D., Howard, R.L., Abraham, K.F., and Weller, M.W., 1977, Waterbirds and their wetland resources in relation to oil development at Storkersen Point, Alaska: Washington, D.C., U.S. Fish & Wildlife Service Publication 129, 38 p.
- Billings, W.D., and Peterson, K.M., 1980, Vegetational change and ice-wedge polygons through the thaw lake cycle in Arctic Alaska: *Arctic and Alpine Research*, v. 12, p. 413–432.
- Bird, K.J., and Houseknecht, D.W., 1998, Arctic National Wildlife Refuge, 1002 Area, Petroleum Assessment, Including Economic Analysis: U.S. Geological Survey Fact Sheet 028-01, 6 p.
- 2002a, U.S. Geological Survey 2002 petroleum resource assessment of the National Petroleum Reserve in Alaska (NPR); Play maps and technically recoverable resource estimates: U.S. Geological Survey Open-File Report 02-207, 18 p.
- 2002b, U.S. Geological Survey 2002 petroleum resource assessment of the National Petroleum Reserve in Alaska (NPR). U.S. Geological Survey Fact Sheet 045-02, 6 p.
- 2006, Sizing up oil on Alaska's North Slope: *Geotimes*, November 2006, v. 51, no. 11, p. 24–27.
- Bishop, S.C., Kidd, J.G., Cater, T.C., and Max, K.N., 2000, Land rehabilitation studies in the Kuparuk oilfield, Alaska, 1999: Anchorage, AK, Annual report prepared for ARCO Alaska, Inc., 38 p.
- 2001, Land rehabilitation studies in the Kuparuk oilfield, Alaska, 2000: Unpublished report prepared by ABR Inc., Environmental Research & Services, Fairbanks, AK, for ARCO Alaska, Inc., Anchorage, AK, 40 p.
- Black, R.F., 1952, Growth of ice-wedge polygons in permafrost near Barrow, Alaska: *Geological Society of America Bulletin*, v. 63, no. 12, p. 1,235–1,236.
- 1964, Gubik Formation of Quaternary age in northern Alaska. U.S. Geological Survey Professional Paper 302-C, p. 59–91.

- Black, R.F., 1976, Features indicative of permafrost: *Annual Review of Earth and Planetary Sciences*, v. 4, p. 75–94.
- 1983, Three superposed systems of ice wedges at McLeod Point, northern Alaska, may span most of the Wisconsin stage and Holocene, *in Proceedings, Fourth International Permafrost Conference: Washington, D.C., National Academy Press*, p. 68–73.
- Black, R.F., and Barksdale, W.L., 1949, Oriented lakes of northern Alaska: *Journal of Geology*, v. 57, p. 105–118.
- Bliss, L.C., and Cantlon, J.E., 1957, Succession on river alluvium in northern Alaska: *American Midland Naturalist*, v. 58, p. 452–469.
- Bockheim, J.G., and Hinkel, K.M., 2007, The importance of deep organic carbon in permafrost-affected soils of Arctic Alaska: *Soil Science Society of America Journal*, v. 71, p. 1,889–1,892.
- Bockheim, J.G., Everett, L.R., Hinkel, K.M., Nelson, F.E., and Brown, J., 1999, Soil organic carbon storage and distribution in arctic tundra, Barrow, Alaska: *Soil Science Society of America Journal*, v. 63, p. 934–940.
- Bockheim, J.G., Hinkel, K.M., Eisner, W.R., and Dai, X.Y., 2004, Carbon pools and accumulation rates in an age-series of soils in drained thaw-lake basins, arctic Alaska: *Soil Science Society of America*, v. 68, p. 697–704.
- Bockheim, J.G., Hinkel, K.M., and Nelson, F.E., 2003, Predicting carbon storage in tundra soils of arctic Alaska: *Soil Science Society of America Journal*, v. 67, p. 948–950.
- Bockheim, J.G., Walker, D.A., Everett, L.R., Nelson, F.E., and Shiklomanov, N.I. 1998, Soils and cryoturbation in moist nonacidic and acidic tundra in the Kuparuk River Basin, Arctic Alaska, USA: *Arctic and Alpine Research*, v. 30, p. 166–174.
- Brewer, M.C., 1958a, The thermal regime of an arctic lake: *Transactions, American Geophysical Union*, v. 39, no. 2, p. 278–284.
- 1958b, Some results of geothermal investigations of permafrost in northern Alaska. *American Geophysical Union*, v. 39, p. 19–26
- Brigham, J.K., 1983, Correlation of late Cenozoic marine transgressions of the Arctic Coastal Plain with those in western Alaska and northeastern Russia: *U.S. Geological Survey Circular 911*, p. 47–52.
- Britton, M.E., 1957, Vegetation of the Arctic tundra, *in Hanson, H.P., ed., Arctic Biology*, Corvallis, OR, Oregon State University Press, p. 26–61.
- Brower, Jr., W.A., Baldwin, R.G., Williams, C.N., Wise, Jr., J.L., and Leslie, L.D., 1988, Climatic atlas of the Outer Continental Shelf waters and coastal regions of Alaska; Volume 1, Gulf of Alaska: Anchorage, AK, University of Alaska Anchorage Arctic Environmental Information and Data Center, 530 p.
- Brown, J., 1963, Ice-wedge chemistry and related frozen ground processes, Barrow, Alaska: *Proceedings, Permafrost International Conference (Purdue University)*, NAS-NRC, Publication 1287, p. 94–98.
- 1965, Radiocarbon dating, Barrow, Alaska: *Arctic*, v. 18, no. 1, p. 36–47.
- 1967, Tundra soils formed over ice wedges, northern Alaska: *Proceedings – Soil Science Society of America*, v. 31, no. 5, p. 686–691.
- 1968, An estimation of the volume of ground ice, coastal plain, northern Alaska: Hanover, NH, U.S. Army Cold Regions Research and Engineering Laboratory (CRREL) Technical Note, 22 p.
- 1969, Soil properties developed on the complex tundra relief of northern Alaska: *Biuletyn Peryglacjalny*, v. 18, p. 155–67.
- 2001, NARL-based terrestrial bioenvironmental research including the U.S. IBP Tundra Biome program, 1957–1997, *in Norton, D.W., ed., Fifty more years below zero; Tributes and meditation for the Naval Arctic Research Laboratory’s first half century at Barrow, Alaska*: Fairbanks, AK, University of Alaska Fairbanks, p. 191–200.
- Brown, J. and Berg, R., eds., 1980, *Environmental Engineering Investigations along the Yukon River—Prudhoe Bay Haul Road, Alaska*: U.S. Army Cold Regions Research and Engineering Laboratory Report 80-19.
- Brown, J., and Grave, N.A., 1979, Physical and thermal disturbance and protection of permafrost: Hanover, NH, U.S. Army Cold Regions Research and Engineering Laboratory, Special Report 79-5, 42 p.
- Brown, J., and Johnson, P.L., 1965, Pedo-ecological investigation, Barrow, Alaska: Hanover, NH, U.S. Army Cold Regions Research and Engineering Laboratory, Technical Report 159, 46 p.
- Brown, J., and Sellmann, P.V., 1966, Radiocarbon dating of coastal peat, Barrow, Alaska: *Science*, v. 153, p. 299–300.
- Brown, J., Dingman, S.L., and Lewellen, R.L., 1968, Hydrology of a drainage basin on the Alaskan coastal plain: Hanover, NH, U.S. Army Cold Regions Research and Engineering Laboratory Research Report 240, 18 p.
- Brown, J., Ferrians, O.J., Heginbottom, J.A., Jr., and Melnikov, E.S., 1997, Circum-Arctic map of permafrost and ground-ice conditions: U.S. Geological Survey Circum-Pacific Map 45, 1 sheet.

- Brown, J., Hinkel, K.M., and Nelson, F.E., 2000, The circumpolar active layer monitoring (CALM) program: research designs and initial results: *Polar Geography*, v. 24, p. 165–258.
- Brown, J., Jorgenson, M.T., Smith, O.P., and Lee, W., 2003, Long-term rates of erosion and carbon input, Elson Lagoon, Barrow, Alaska, *in* Phillips, M., Springman, S.M., and Arenson, eds., ICOP 2003 Permafrost: Proceedings of the 8th International Conference on Permafrost: Netherlands, A.A. Balkema Publishers, p. 101–106.
- Brown, J., Miller, P.C., Tieszen L.L., and Bunnell, F.L., eds., 1980, An arctic ecosystem; The coastal tundra at Barrow, Alaska: Stroudsburg, PA, Dowden Hutchinson & Ross, p. 1–29.
- Bureau of Land Management (BLM), 2003, Final Environmental Impact Statement, renewal of the federal grant for the Trans-Alaska Pipeline System right-of-way, volume 1: Executive Summary: Anchorage, AK, U.S. Department of Interior, BLM/AK/PT-03/005+2880+990, 70 p.
- 2004, Alpine satellite development plan: Final environmental impact statement: Anchorage, AK, U.S. Department of Interior, 1,650+ p.
- Cabot, E.C., 1947, The northern Alaskan coastal plain interpreted from aerial photographs: *Geographical Review*, v. 37, p. 639–648.
- Cameron, R.D., Lenart, E., Reed D.J., Whitten, K.R., and Smith, W.T., 1995, Abundance and movements of caribou in the oilfield complex near Prudhoe Bay, Alaska: *Rangifer*, v. 15, p. 3–7.
- Cannon, P.J. and Mortensen, T.W., 1982, Flood hazard potential of five selected arctic rivers, Arctic coastal plain; Report prepared for North Slope Borough Coastal Management Program, by Mineral Industries Research Lab, University of Alaska, Fairbanks, Alaska, 56 p.
- Cantlon, J.E., 1961, Plant cover in relation to macro-, meso- and micro-relief: Washington, DC, Arctic Institute of North America, Final Report of subcontracts ONR 208–212, 128 p.
- Carson, C.E., 1968, Radiocarbon dating of lacustrine strands in arctic Alaska: *Arctic*, v. 21, p. 12–26.
- Carson, C.E., and Hussey, K., 1962, The oriented lakes of arctic Alaska: *Journal of Geology*, v. 70, p. 417–439.
- Carter, L.D., 1981, A Pleistocene sand sea on the Alaskan Arctic coastal plain: *Science*, v. 211, p. 381–383.
- 1988, Loess and deep thermokarst basins in arctic Alaska, *in* Senneset, K., ed., Proceedings of the Fifth International Conference on Permafrost, Trondheim, Norway: Norway, Tapir Publishers, v. 1, p. 706–711.
- Carter, L.D. and Galloway, J.P., 1979, Arctic Coastal Plain pingos in National Petroleum Reserve in Alaska, *in* Johnson, K.M., and Williams, J.R., eds., The U.S. Geological Survey in Alaska; Accomplishments during 1978: U. S. Geological Survey Circular 804-B, p. B33–B35.
- 1982, Terraces of the Colville River Delta region, Alaska, *in* The United States Geological Survey in Alaska: Accomplishments during 1980: U.S. Geological Survey Circular 884, p. 49–52.
- 1985, Engineering-geologic maps of northern Alaska, Harrison Bay quadrangle: U.S. Geological Survey Open File Report, 85-256, 47 p.
- Carter, L.D., and Robinson, S.W., 1981, Minimum age of beach deposits north of Teshekpuk Lake, Arctic coastal plain, *in* Albert, N.R.D., and Hudson, T., eds. The United States Geological Survey in Alaska: Accomplishments during 1979: U.S. Geological Survey Circular 823-B, p. B8–B9.
- Carter, L.D., Brigham-Grette, J.K., and Hopkins, D.M., 1986, Late Cenozoic marine transgressions of the Alaskan Arctic coastal plain, *in* Heginbottom, J.A., and Vincent, J.S., eds., Correlation of Quaternary deposits and events around the margin of the Beaufort Sea; Contributions from a joint Canadian–American workshop, April 1984: Geological Survey of Canada Open File Report 1237, p. 21–26.
- Carter, L.D., Forester, R.M., and Nelson, R.E., 1984, Mid Wisconsin through early Holocene changes in seasonal climate in northern Alaska: American Quaternary Association Eighth Biennial Meeting, Boulder, University of Colorado, Program with Abstracts, p. 20–22.
- Carter, L.D., Heginbottom, J.A., and Woo, M., 1987, Arctic Lowlands, *in* Geomorphic Systems of North America, Centennial Special, v. 2: Boulder, CO, U.S. Geological Society of America, p. 583–628.
- Carter, L.D., Repenning, C.A., Marinovich, L.N., Hazel, J.E., Hopkins, D.M., McDougall, K., and Naeser, C.W., 1977, Gubik and pre-Gubik Cenozoic deposits along the Colville River near Ocean Point, North Slope, Alaska, *in* Blean, K.M., ed., The United States Geological Survey in Alaska: Accomplishments during 1976: U.S. Geological Survey Circular 751-B, p. B12–B14.
- Cater, T.C., 2007, Use of tundra sod with live vegetation to restore wetlands after oil spills on the North Slope of Alaska: Anchorage, AK, Arctic Science Conference, Arctic Division AAAS.

- Cater, T.C., and Jorgenson, M.T., 1993, Land rehabilitation studies in the Kuparuk oil field, Alaska, 1992: Annual report prepared for ARCO Alaska Inc. and Kuparuk River Unit, by Alaska Biological Research, Fairbanks, AK, 38 p.
- 1994, Land rehabilitation studies in the Kuparuk oil field, Alaska, 1993: Annual report prepared for ARCO Alaska, Inc. and Kuparuk River Unit, by Alaska Biological Research, Fairbanks, AK, 39 p.
- 2001, Long-term ecological monitoring of tundra affected by a crude oil spill near Drill Site 2U, Kuparuk oilfield, 2000: Final report prepared for Phillips Alaska, Inc., Anchorage, AK, by ABR Inc., Environmental Research & Services, Fairbanks, AK, 82 p.
- Circumpolar Arctic Vegetation Mapping Team (CAVM), 2003, Circumpolar Arctic Vegetation Map, *in* Conservation of Arctic Flora and Fauna (CAFF) Map No. 1: Anchorage, AK, U.S. Fish & Wildlife Service, 1 sheet, scale 1:7,500,000.
- Clow, G.D., and Urban, F.E., 2002, Largest permafrost warming in northern Alaska during the 1990s determined from GTN-P borehole temperature measurements: EOS, Transactions, American Geophysical Union, v. 83, no. 47 p. F258.
- Côté, M.M., and Burn, C.R., 2002, The oriented lakes of Tuktoyaktuk Peninsula, western Arctic coast, Canada; A GIS-based analysis: Permafrost and Periglacial Processes, v. 13, p. 61–70.
- Colinvaux, P.A., 1964, Origin of ice ages; Pollen evidence from Arctic Alaska: Science, v. 145, p. 707–708.
- Curotolo, J.A., and Murphy, S.M., 1986, The effects of pipelines, roads, and traffic on movements of caribou, Rangifer tarandus: Canadian Field Naturalist, v. 100, p. 218–224.
- Davis, N., 2001, Permafrost; A guide to frozen ground in transition: Fairbanks, AK, University of Alaska Press, 351 p.
- Dinter, D.A., 1985, Quaternary sedimentation of the Alaskan Beaufort shelf; Influence of regional tectonics, fluctuating sea levels, and glacial sediment sources: Tectonophysics, v. 114, p. 133–161.
- Dinter, D.A., Carter, L.D., and Brigham-Grette, J., 1990, Late Cenozoic geologic evolution of the Alaskan North Slope and adjacent continental shelves, *in* Grantz, A., Johnson, L., and Sweeney, J.F., eds., The Geology of North America, Volume L, The Arctic Ocean Region: Boulder, CO, Geological Society of America, Decade of North American Geology (DNAG), p. 459–490.
- Divoky, G.J., 1984, The pelagic and nearshore birds of the Alaskan Beaufort Sea; Biomass and trophics, *in* Barnes, P.W., Schell, D.M., and Reimnitz, E., eds., The Alaskan Beaufort Sea; Ecosystems and environments: New York, Academic Press, p. 417–437.
- Douglas, L.A., and Tedrow, J.C.F., 1959, Organic matter decomposition rates *in* arctic soils: Soil Science, v. 88, p. 305–312.
- Drew, J.V., and Tedrow, J.C.F., 1957, Pedology of an Arctic brown profile Point Barrow, Alaska: Soil Science Society of America Journal, v. 21, no. 3, p. 336–339.
- 1962, Arctic soil classification and patterned ground: Arctic, v. 15, p. 109–116.
- Drew, J.V., Tedrow, J.C.F., Shanks, R.E. and Koranda, J.J., 1958, Rate and depth of thaw in Arctic soils: EOS, Transactions, American Geophysical Union, v. 39, no. 4, p. 697–701.
- Ducks Unlimited, 1998, National Petroleum Reserve—Alaska earth cover classification: Rancho Cordova, CA, Final Report prepared for U.S. Bureau of Land Management, Anchorage, AK, by Ducks Unlimited, Inc., 81 p.
- Dunton, K.H., Reimnitz, E., and Schonberg, S., 1982, An Arctic kelp community in the Alaskan Beaufort Sea: Arctic, v. 35, p. 465–484.
- Eisner, W.R., and Peterson, K.M., 1998, Pollen, fungal, and algae as age indicator of drained lake basins near Barrow, Alaska, *in* Lewkowicz, A.G., and Allard, M., eds., Proceedings, Seventh International Permafrost Conference: Yellowknife, Collection Nordicana, v. 57, p. 245–250.
- Eisner, W.R., Bockheim, J.G., Hinkel, K.M., Brown, T.A., Nelson, F. E., Peterson, K.M., and Jones, B.M., 2005, Paleoenvironmental analyses of an organic deposit from an erosional landscape remnant, Arctic Coastal Plain of Alaska: Palaeogeography, Palaeoclimatology, and Palaeoecology, v. 217, p. 187–204.
- Emers, M., and Jorgenson, J.C., 1997, Effects of winter seismic exploration on tundra vegetation and the soil thermal regime on the Arctic National Wildlife Refuge, Alaska, *in* Crawford, R.M.M., ed., Disturbance and Recovery in Arctic Lands, An Ecological Perspective: Dordrecht, Netherlands, Kluwer Academic Publishers, p. 443–456.
- Everett, K.R., 1975, Soil and landform associations at Prudhoe Bay, Alaska; A soils map of the Tundra Biome area, *in* Brown, J., ed., Ecological investigations of the Tundra Biome in the Prudhoe Bay region, Alaska: Fairbanks, AK, University of Alaska Fairbanks Special Report 2, p. 53–59.
- 1980, Distribution and properties of road dust along the northern portion of the Haul Road, *in* Brown, J., and Berg, R.L., eds., Environmental engineering and ecological baseline investigations along the Yukon

- River–Prudhoe Bay Haul Road: Hanover, NH, U.S. Army Cold Regions Research and Engineering Laboratory Report 80-19, p. 101–128.
- Everett, K.R., and Brown, J., 1982, Some recent trends in the physical and chemical characterization and mapping of tundra soils, *Arctic Slope of Alaska: Soil Science*, v. 133, p. 264–280.
- Everett, K.R., and Parkinson, R.J., 1977, Soil and landform associations, Prudhoe Bay area, Alaska: *Arctic and Alpine Research*, v. 9, p. 1–19.
- Everett, K.R., Vassiljevskaya, V.P., Brown, J., and Walker, B.D., 1981, Tundra and analogous soils, in Bliss, L.C., Heal, O.W., and Moore, J.J., eds., *Tundra Ecosystems; a Comparative Analysis*: Cambridge, UK, Cambridge University Press, p. 139–179.
- Faas, R.W., 1966, Paleocology of an arctic estuary: *Arctic*, v. 19, no. 4, p. 343–348.
- Felix, N.A., and Reynolds, M.K., 1989, The effects of winter seismic trails on tundra vegetation in northeastern Alaska: *Arctic and Alpine Research*, v. 21, p. 188–202.
- Ferrians, O.J., Jr., 1988, Pingos in Alaska; A review, in *Proceedings of the 5th International Conference on Permafrost*: Trondheim, Tapir Publishers, p. 734–739.
- Ferrians, O.J., Jr., Kachadorian, R., and Greene, G.W., 1969, Permafrost and related engineering problems in Alaska: U.S. Geological Survey Professional Paper 678, 37 p.
- Fetterer, F., and Knowles, K., 2004, Sea ice index monitors polar ice extent: *Eos, Transactions of the American Geophysical Union*, v. 85, p. 163.
- Forbes, B.C., and McKendrick, J.D., 2004, Polar tundra, in Perrow, M.R., and Davy, A.J., eds., *Handbook of Ecological Restoration*: Cambridge, UK, Cambridge University Press, v. 2, p. 354–374.
- Ford, J.A., 1959, Eskimo prehistory in the vicinity of Point Barrow, Alaska: *Anthropological Papers of the American Museum of Natural History*, v. 47, p. 1.
- Frohn, R.C., Hinkel, K.M., and Eisner, W.R., 2005, Satellite remote sensing classification of thaw lakes and drained thaw lake basins on the North Slope of Alaska: *Remote Sensing of Environment*, v. 97, p. 116–126.
- Garrity, C.P., Houseknecht, D.W., Bird, K.J., Potter, C.J., Moore, T.E., Nelson, P.H. and Schenk, C.J., 2005, U.S. Geological Survey 2005 Oil and Gas Resource Assessment of the Central North Slope, Alaska—Play Maps and Results: U.S. Geological Survey Open-File Report 2005-1182, 25 p.
- Gilder, M.A., and Cronin, M.A., 2000, North Slope oil field development, in Truett, J.C., and Johnson, S.R., eds., *The natural history of an Arctic oilfield*: New York, Academic Press, p. 15–34.
- Gilliam, J.J., and Lent, P.C., 1982, Caribou/waterbird impact analysis workshop, in *Proceedings of the National Petroleum Reserve in Alaska (NPR-A)*: Anchorage, AK, Alaska State Office, U.S. Bureau of Land Management, 29 p.
- Gingrich, D., Knock, D., and Masters, R., 2001, Geophysical interpretation methods applied at Alpine oil field, North Slope, Alaska: *The Leading Edge*, July, p. 730–738.
- Glenn, Richard, 2002, America's farthest north producing gas fields; A narrative of the USGS and its early hydrocarbon exploration efforts near Barrow, Alaska: Washington, DC, presented at the USGS Congressional briefing, "Science, Society, Solutions," September 20, 2002, Capitol Hill.
- Gold, L.W., and Lachenbruch, A.H., 1973, Thermal conditions in permafrost: A review of the North American literature, in *North American Contribution, Second International Conference on Permafrost Proceedings*: Washington, D.C., National Academy of Sciences, p. 3–23.
- Gryc, George, ed., 1988, *Geology and exploration of the National Petroleum Reserve in Alaska, 1974–1982*: U.S. Geological Survey Professional Paper 1399, 940 p.
- Hanson, H.C., 1953, Vegetation types in northwestern Alaska and comparisons with communities in other arctic regions: *Ecology*, v. 34, no. 1, p. 111–140.
- Harper, J.R., 1978, Coastal erosion rates along the Chukchi Sea coast near Barrow, Alaska: *Arctic*, v. 31, p. 428–433.
- Hemming, C.R., 1988, Aquatic habitat evaluation of flooded North Slope gravel mine sites, 1986–1987: Juneau, AK, Alaska Department of Fish & Game Technical Report 88-1, 69 p.
- 1995, Fisheries enhancement investigations in the Prudhoe Bay and Kuparuk River oilfields, 1993: Juneau, AK, Alaska Department Fish & Game Technical Report 95-3, 62 p.
- Henry, R.F., and Heaps, N.S., 1976, Storm surges in the southern Beaufort Sea: *Journal of the Fisheries Research Board of Canada*, v. 33, p. 2,362–2,376.
- Hinkel, K.M., and Hurd, J.K., Jr., 2006, Permafrost destabilization and thermokarst following snow fence installation, Barrow, Alaska, USA: *Arctic, Antarctic and Alpine Research*, v. 38, no. 4, p. 530–539.

- Hinkel, K.M., and Nelson, F.E., 2003, Spatial and temporal patterns of active layer thickness at Circumpolar Active Layer Monitoring (CALM) sites in northern Alaska, 1995–2000: *Journal of Geophysical Research – Atmospheres*, v. 108, no. D2, 13 p.
- Hinkel, K.M., and Nelson, F.E., 2007, Anthropogenic heat island at Barrow, Alaska, during winter; 2001–2005: *Journal of Geophysical Research–Atmospheres*, v. 112, p. D06118, doi:10.1029/2006JD007837.
- Hinkel, K.M., Eisner, W.E., Bockheim, J.G., Nelson, F.E., Peterson, K.M., and Xiaoyan, D., 2003a, Spatial extent, age, and carbon stocks in drained thaw lake basins on the Barrow Peninsula: *Arctic Antarctic Alpine Research*, v. 35, no. 3 p. 291–300.
- Hinkel, K.M., Frohn, R.C., Nelson, F.E., Eisner, W.R., and Beck, R.A., 2005, Morphometric and spatial analysis of thaw lakes and drained thaw lake basins in the western Arctic Coastal Plain, Alaska: *Permafrost and Periglacial Processes*, v. 16, no. 4, p. 327–341.
- Hinkel, K.M., Klene, A.E., and Nelson, F.E., 2008, Spatial and interannual patterns of winter N-factors near Barrow, Alaska: *Proceedings, Ninth International Conference on Permafrost*, in press.
- Hinkel, K.M., Nelson, F.E., Klene, A.E., and Bell, J.H., 2003b, The urban heat island in winter at Barrow, Alaska: *International Journal of Climatology*, v. 23, p. 1,889–1,905.
- Hinkel, K.M., Peterson, K.M., Eisner, W.R., Nelson, F.E., Turner, K.M., Miller, L.L., and Outcalt, S.I., 1996, Formation of injection frost mounds over winter 1995–96 at Barrow, Alaska: *Polar Geography*, v. 20, no. 4, p. 235–248.
- Hinzman, L.D., Robinson, D.W., and Kane, D.L., 1998, A biogeochemical survey of an arctic coastal wetland: The 7th International Permafrost Conference: *Collection Nordicana*, v. 57, p. 459–464.
- Hobbie, J.E., ed., 1980, *Limnology of tundra ponds*: Stroudsburg, PA, Dowden, Hutchinson & Ross. 491 p.
- 1984, *The ecology of tundra ponds of the Arctic coastal plain; A community profile*: Washington, DC, U.S. Fish & Wildlife Service FWS/OBS-83/25. 52 p.
- Hollister, R.D., Webber, P.J., Nelson, F.E., and Tweedie, C.E., 2006, Soil thaw and temperature response to air warming varies by plant community; Results from an open-top chamber experiment in northern Alaska: *Arctic, Antarctic, and Alpine Research*, v. 38, no. 2, p. 206–215.
- Holowaychuk, N., Petro, J., Finney, H.R., Farnham, R.S., and Gersper, P.L., 1966, Soils of Ogotoruk Creek watershed, *in* Wilimovsky, N.J., and Wolfe, J.N., eds., *Environment of the Cape Thompson region, Alaska*: U.S. Atomic Energy Commission, Oak Ridge, Tennessee. p. 221–273.
- Hopkins, D.M., 1949, Thaw lakes and thaw sinks in the Imuruk Lake area, Seward Peninsula, Alaska: *Journal of Geology*, v. 57, p. 119–131.
- 1967, Quaternary marine transgressions in Alaska, *in* Hopkins, D.M., ed., *The Bering land bridge*: Stanford, CA, Stanford University Press, p. 47–90.
- 1982, Aspects of the paleogeography of Beringia during the late Pleistocene, *in* Hopkins, D.M., Matthews, J.V., Jr., Schweger, C.E., and Yount, S.B., eds., *Paleoecology of Beringia*: New York, Academic Press, p. 3–28.
- Hopkins, D.M., and Hartz, R.W., 1978, Coastal morphology, coastal erosion, and barrier islands of the Beaufort Sea, Alaska: U.S. Geological Survey Open-File Report 78-1063, 54 p.
- Hume, J.D., 1965, Sea-level changes during the last 2000 years at Point Barrow, Alaska: *Science*, v. 150, no. 3700, p. 1,165–1,166.
- Hume, J.D., and Schalk, M., 1967, Shoreline processes near Barrow, Alaska; A comparison of the normal and the catastrophic: *Arctic*, v. 20, p. 86–103.
- Hussey, K.M., and Michelson, R.W., 1966, Tundra relief features near Point Barrow, Alaska: *Arctic* v. 19, p. 162–184.
- Jensen, A.M., 2007, Nuvuk Burial 1; An early Thule hunter of high status: *Alaska Journal of Anthropology* v. 5, no. 1, p. 117–120.
- in press, Nuvuk, Point Barrow, Alaska: Implications for Neoeskimo Prehistory: Submitted to *Festschrift for HC Gulløv*.
- Johnson, A.W., Viereck, L.A., Johnson, R.E., and Melchior, H., 1966, Vegetation and flora, *in* Wilimovsky, N.J., and Wolfe, J.N., eds., *Environment of the Cape Thompson region, Alaska*: Oak Ridge, TN, U.S. Atomic Energy Commission, Division of Technical Information, Report PNE-481, p. 277–354.
- Johnson, L.A., 1981, Revegetation and selected terrain disturbances along the Trans-Alaska Pipeline, 1975–1979: Hanover, NH, U.S. Army Cold Regions Research and Engineering Laboratory, CRREL Report 81-12, 115 p.
- Johnston, G.H., ed., 1981, *Permafrost, Engineering design and construction*: Toronto, John Wiley, 404 p.
- Jones, P., 2000, Engineering demands at the Colville River: *Alaska Business Monthly*, February 2000.

- Jorgenson, J.C., Joria, P.E., McCabe, T.R., Reitz, B.E., Reynolds, M.K., Emers, M., and Willms, M.A., 1994, User's guide for the land-cover map of the coastal plain of the Arctic National Wildlife Refuge: Anchorage, AK, U.S. Fish & Wildlife Service, 46 p., 1 sheet, scale 1:500,000.
- Jorgenson, M.T., 1988, Rehabilitation studies in the Kuparuk Oilfield, Alaska, 1987: Annual Report prepared for ARCO Alaska, Inc., Anchorage, by Alaska Biological Research, Inc., Fairbanks, 90 p.
- 1997, Patterns and rates of, and factors affecting, natural recovery on land disturbed by oil development in Arctic Alaska, *in* Disturbance and recovery in arctic lands; An ecological perspective: Dordrecht, Netherlands, Kluwer Academic Publishers, NATO ASI Series 2 Environment, v. 25, p. 421–442.
- Jorgenson, M.T., and Brown, J., 2005, Classification of the Alaskan Beaufort Sea coast and estimation of carbon and sediment inputs from coastal erosion: *Geo-marine Letters*, v. 25, p. 69–80.
- Jorgenson, M.T., and Cater, T.C., 1992, Land rehabilitation studies in the Kuparuk oilfield, Alaska, 1991: Unpublished report prepared for ARCO Alaska by Alaska Biological Research, Inc., Fairbanks, AK.
- 1996, Minimizing ecological damage during cleanup of terrestrial and wetland oil spills, in Storage tanks; Advances in environmental control technology: Houston, TX, Gulf Publishing, p. 257–293.
- Jorgenson, M.T., and Heiner M., 2003, Ecosystems of northern Alaska: Anchorage, AK, The Nature Conservancy, unpublished map.
- Jorgenson, M.T., and Joyce, M.R., 1994, Six strategies for rehabilitating land disturbed by oil development in Arctic Alaska: *Arctic*, v. 47, p. 374–390.
- Jorgenson, M.T., and Shur, Y., 2007, Evolution of lakes and basins in northern Alaska and discussion of the thaw lake cycle, *in* Zhang, Tingjun, Nelson, F.E., and Gruber, Stephan, eds., Permafrost and seasonally frozen ground under a changing climate: *Journal of Geophysical Research*, v. 112, no. F2.
- Jorgenson, M.T., Aldrich, J.W., Kidd, J.G., and Smith, M.D., 1993, Geomorphology and hydrology of the Colville River Delta, Alaska, 1992: Final Report prepared for ARCO Alaska, Inc., Anchorage, by Alaska Biological Research, Inc., and Arctic Hydrologic Consultants, Fairbanks, 79 p.
- Jorgenson, M.T., Aldrich, J.W., Pullman, E., Ray, S., Smith, M.D., and Shur, Y., 1996, Geomorphology and hydrology of the Colville River Delta, Alaska, 1995: Final report prepared for ARCO Alaska, Inc., Anchorage, by ABR Inc., Environmental Research & Services, and Shannon and Wilson, Inc., Fairbanks.
- Jorgenson, M.T., Cater, T.C., and Jacobs, L.L., 1992a, Wetland creation and revegetation on an overburden stockpile in arctic Alaska, *in* Bandopadhyay, S. and Nelson, M., eds., Proceedings of the Second International Symposium on Mining in the Arctic, Fairbanks, AK, p. 265–275
- Jorgenson, M.T., Cater, T.C., and Jacobs, L.L., 1992a, Wetland creation and revegetation on an overburden stockpile at Mine Site D, Kuparuk Oilfield, 1991: Annual report prepared for ARCO Alaska, Inc., Anchorage, by Alaska Biological Research, Inc., Fairbanks.
- Jorgenson, M.T., Cater, T.C., Joyce, M., and Ronzio, S., 1992b, Cleanup and bioremediation of a crude-oil spill at Prudhoe Bay, Alaska, *in* Proceedings of the Fifteenth Arctic and Marine Oil Spill Program Technical Seminar, Edmonton, Alberta: Ottawa, Ontario, Canada, Environment Canada, p. 715–722.
- Jorgenson, M.T., Cater, T.C., Kidd, J.G., Jacobs, L.L., and Joyce, M.R., 1995, Techniques for rehabilitating lands disturbed by oil development in the Arctic, *in* Proceedings, High Altitude Revegetation Workshop No. 11: Ft. Collins, CO, Colorado State University, Information Series no. 80. p. 146–169.
- Jorgenson, M.T., Kidd, J.G., Cater, T.C., and Bishop, S.C., 2003d, Long-term evaluation of methods for rehabilitating lands disturbed by industrial development in the Arctic, *in* Rasmussen, O., and Koroleva, N.E., eds., Methodologies in evaluation of socioeconomic and environmental consequences of mining and energy production in the Arctic and Sub-Arctic: Dordrecht, The Netherlands, Kluwer Academic Publishers, NATO Science Series, Earth and Environmental Sciences, v. IV, p. 173–190.
- Jorgenson, M.T., Krizan, L.W., and Joyce, M.R., 1991, Bioremediation and tundra restoration after an oil spill in the Kuparuk Oilfield, Alaska, 1990, *in* Proceedings of the 14th Annual Arctic and Marine Oil Spill Technical Program, Vancouver, BC: Ottawa, Ontario, Environment Canada, p. 149–154.
- Jorgenson, M.T., Lawhead, B.E., and Johnson, C.B., 1997a, Integrated studies of geomorphology, landscape ecology, and wildlife for environmental impact analysis of a proposed oil development in Arctic Alaska, *in* Zubeck, H.K., Woolard, C.R., White, D.M., and Vinson, T.S., eds., ISCORD '97, Proceedings of the Fifth International Symposium on Cold Region Development, Anchorage, Alaska, American Society of Civil Engineers, International Association of Cold Regions Development Studies, and U.S. Army Cold Regions Research and Engineering Laboratory, p. 365–368.

- Jorgenson, M.T., Macander, M., Jorgenson, J.C., Ping, C.P., and Harden, J., 2003a, Ground ice and carbon characteristics of eroding coastal permafrost at Beaufort lagoon, northern Alaska, *in* Phillips, M., Springman, S.M., and Arenson, L.U., eds., *Permafrost; Proceedings of the Eighth International Permafrost Conference: Lisse, the Netherlands*, A.A. Balkema Publishers, p. 495–501.
- Jorgenson, M.T., and Osterkamp, T.E., 2005, Response of boreal ecosystems to varying modes of permafrost degradation: *Canadian Journal of Forest Research*, v. 35, p. 2,100–2,111.
- Jorgenson, M.T., Pullman, E.R., and Shur, Y.L., 2004, Geomorphology of the northeast planning area of the National Petroleum Reserve–Alaska, 2003: Third Annual Report prepared for ConocoPhillips Alaska, Inc., Anchorage, AK, by ABR Inc., Environmental Research & Services, Fairbanks, AK, 40 p.
- Jorgenson, M.T., Pullman, E.R., Zimmer, T., Shur, Y., Stickney, A.A., and Li, S., 1997b, Geomorphology and hydrology of the Colville River Delta, Alaska, 1996: Fifth Annual Report prepared for ARCO Alaska, Inc., Anchorage, AK, by ABR Inc., Environmental Research & Services, Fairbanks, AK, 148 p.
- Jorgenson, M.T., Roth, J.E., Emers, M., Schlentner, S., and Mitchell, J., 2003b, Assessment of ecological impacts associated with seismic exploration near the Colville Delta [abs.], *in* Alaska Conference on Reducing the Effects of Oil and Gas Exploration and Production on Alaska’s North Slope; Issues, Practices, and Technologies: Idaho National Engineering and Environmental Laboratory, U.S. Department of Energy, p. 7.
- Jorgenson, M.T., Roth, J.E., Emers, M., Schlentner, S., Swanson, D.K., Pullman, E., Mitchell, J., and Stickney, A.A., 2003c, An ecological land survey for the northeast planning area of the National Petroleum Reserve–Alaska, 2002: Final Report prepared for ConocoPhillips, Anchorage, AK, by ABR Inc., Environmental Research & Services, Fairbanks, AK, 128 p.
- Jorgenson, M.T., Roth, J.E., Pullman, E.R., Burgess, R.M., Reynolds, M.K., Stickney, A.A., Smith, M.D., and Zimmer, T., 1997c, An ecological land survey for the Colville River Delta, Alaska, 1996: Final report prepared for ARCO Alaska, Inc., Anchorage, AK, by ABR Inc., Environmental Research & Services, Fairbanks, AK, 160 p.
- Jorgenson, M.T., Shur, Y.L., and Pullman, E.R., 2006, Abrupt increase in permafrost degradation in Arctic Alaska: *Geophysical Research Letters*, v. 33, no. 2, 4 p.
- Jorgenson, M.T., Shur, Y., and Walker, H.J., 1998, Factors affecting evolution of a permafrost dominated landscape on the Colville River Delta, northern Alaska, *in* Lewkowicz, A.G., and Allard, M., eds., *Proceedings of the Seventh International Permafrost Conference: Sainte-Foy, Quebec, Universite Laval, Collection Nordicana*, no. 57, p. 523–530.
- Kane, D.L., and Reeburgh, W.S., 1998, Introduction to special section: Land–Air–Ice Interactions (LAI) Flux Study: *Journal of Geophysical Research*, v. 103, no. D22, p. 28,913–28,915.
- Kane, D.L., Hinzman, L.D., McNamara, J.P., Zhang, Z., and Benson, C.S., 2000, An overview of a nested watershed study in Arctic Alaska: *Nordic Hydrology*, v. 4, no. 5, p. 245–266.
- Kane, D.L., Hinzman, L.D., Woo, M., and Everett, K.R., 1992, Arctic hydrology and climate change, *in* Arctic ecosystems in a changing climate: San Diego, CA, Academic Press, Inc., p. 35–58.
- Kanevskiy, M., Fortier, D., Shur, Y., Bray, M., and Jorgenson, T., 2008, Detailed cryostratigraphic studies of syngenetic permafrost in the winze of the CRREL permafrost tunnel, Fox, Alaska, *in* Kane, D.L., ed., *Proceedings of Ninth International Conference on Permafrost*, University of Alaska, Fairbanks, AK, in press.
- Kaufman, D.S., Farmer, G.L., Miller, G.H., Carter, L.D., and Brigham-Grette, J.K., 1990, Strontium isotopic dating of upper Cenozoic marine deposits, northwestern Alaska, *in* Gosnell, L.B., and Poore, R.Z., eds., *Pliocene climates—scenario for global warming: U.S. Geological Survey Open-File Report 90-64*, p. 17–21.
- Keyes, D.E., 1977, Ice and snow construction; workpads, roads, airfields, and bridges, *in* Proceedings of the Second International Symposium on Cold Regions Engineering, August 12–14, 1976, Fairbanks, AK, p. 369–382.
- Kidd, J.G., 1990, The effect of thaw-lake development on the deposition and preservation of plant macrofossils; A comparison with the local vegetation: Fairbanks, Alaska, University of Alaska Fairbanks, M.S. thesis, 48 p.
- Kidd, J.G., Streever, B., and Jorgenson, M.T., 2006, Site characteristics and plant community development following partial gravel removal in an Arctic Oilfield. *Arctic, Antarctic, and Alpine Research*, v. 38, p. 384–393.
- Kidd, J.G., Streever, B., Joyce, M.R., and Fanter, L.H., 2004, Wetland restoration of an exploratory well on Alaska’s North Slope; A learning experience: *Ecological Restoration*, v. 22, p. 30–38.
- Kimble, J.M., 2004, *Cryosols, permafrost-affected soils*: New York, Springer-Verlag, 726 p.
- Klinger, L.F., Walker, D.A., and Weber, P.J., 1983, The effects of gravel roads on Alaskan arctic coastal plain tundra, *in* Permafrost Fourth International Conference Proceedings, University of Alaska Fairbanks: Washington, DC, National Academy Press, p. 628–633.

- Kokelj, S.V., Burn, C.R., and Tarnocai, C., 2007, The structure and dynamics of earth hummocks in the subarctic forest near Inuvik, Northwest Territories, Canada: *Arctic, Antarctic, and Alpine Research*, v. 39, p. 99–109.
- Komarkova, V., and Webber, P.J., 1980, Two low arctic vegetation maps near Atkasook, Alaska: *Arctic and Alpine Research*, v. 12, p. 447–472.
- Koranda, J.J., 1954, A phytosociological study of an uplifted beach ridge near Point Barrow, Alaska: East Lansing, MI, Michigan State College, M.S. Thesis, 132 p.
- Kowalik, Z., 1984, Storm surges in the Beaufort and Chukchi seas: *Journal of Geophysical Research*, v. 89, p. 10,570–10,578.
- Kreig, R.A., and Reger, R.D., 1982, Air-photo analysis and summary of landform soil properties along the route of the Trans-Alaska Pipeline System: Alaska Division of Geological & Geophysical Surveys Geologic Report 66, 149 p.
- Lachenbruch, A.H., 1962, Mechanics of thermal contraction cracks and ice-wedge polygons in permafrost: *Geological Society of America Special Paper* 70, 69 p.
- Lachenbruch, A.H., and Marshall, B.V., 1986, Changing climate; Geothermal evidence from permafrost in the Alaskan Arctic: *Science*, v. 234 p. 689–696.
- Lachenbruch, A.H., Brewer, M.C., Greene, G.W., and Marshall, B.V., 1962, Temperatures in permafrost; Temperature—Its Measurements and Control in Science and Industry, vol. 3, Part 1, Reinhold Publishing Corp., New York, p. 791–803.
- Lachenbruch, A.H., Cladouhos, T.T., and Saltus, R.W., 1988, Permafrost temperature and the changing climate, *in* Senneset, K., ed., *Proceedings from the Fifth International Conference on Permafrost*: Trondheim, Norway, Tapir Publishers, v. 3, p. 9–17.
- Lachenbruch, A.H., Sass, J.H., Marshall, B.V., and Moses, T.H., Jr., 1982, Permafrost, heat flow, and the geothermal regime at Prudhoe Bay, Alaska: *Journal of Geophysical Research*, v. 87, p. 9,301–9,316.
- Leffingwell, E. de K., 1915, Ground-ice wedges, the dominant form of ground-ice on the north coast of Alaska: *Journal of Geology*, v. 23, p. 635–654.
- Leffingwell, E. de K., 1919, The Canning River region of northern Alaska: U.S. Geological Survey Professional Paper 109, 251 p.
- Lestak, L.R., Manley, W.F., Maslanik, J.A., 2004, Photogrammetric analysis of coastal erosion along the Chukchi coast at Barrow, Alaska: *Reports on Polar and Marine Research*, v. 482, p. 38–40.
- Lestak, L.R., Manley, W.F., Sturtevant, P.M., Maslanik, J.A., Tweedie, C.E., and Brown, J., 2007, High-resolution rectified aerial photography for collaborative research of environmental change at Barrow, Alaska, USA: Boulder, CO, National Snow and Ice Data Center, DVD.
- Lestak, L.R., Manley, W.F., Sturtevant, P.M., and Maslanik, J.A., 2008, Photogrammetric analysis of coastal erosion along the Chukchi coast at Barrow, Alaska: Unpublished data.
- Lewellen, R.I., 1972, Studies on fluvial environments, arctic plain province, northern Alaska: Unpublished report, volumes I and 11, 282 p.
- 1973, The occurrence and characteristics of nearshore permafrost, northern Alaska., *in* *Permafrost*, Second International Conference: Washington, DC, National Academy of Sciences, p. 131–135.
- 1977, A study of Beaufort Sea coastal erosion, northern Alaska; Environmental assessment of the Alaskan Continental Shelf, annual reports of principal investigators for the year ending March 1977: U.S. National Oceanic and Atmospheric Administration, v. 15. p. 491–527.
- Livingstone, D.A. 1954, On the orientation of lake basins: *American Journal of Science*, v. 252, p. 547–554.
- Lynch, A.H., Cassano, E.N., Cassano, J.J., and Lestak, L.R., 2003, Case studies of high wind events in Barrow, Alaska; Climatological context and development processes: *Monthly Weather Review*, v. 131, p. 719–732.
- Lynch, A.H., Curry, J.A., Brunner, R.D., and Maslanik, J.A., 2004, Toward an integrated assessment of the impacts of extreme wind events on Barrow, Alaska: *Bulletin of the American Meteorological Society*, v. 85, no. 2, p. 209–221.
- Mackay, J.R., 1973, The growth of pingos, western arctic coast, Canada: *Canadian Journal of Earth Science*, v. 10, no. 6, p. 979–1,004.
- 1994, Pingos and pingo ice of the western Arctic coast, Canada: *Terra*, v. 106, p. 1–11.
- 1997, A full-scale field experiment (1978–1995) on the growth of permafrost by means of lake drainage, western Arctic coast; A discussion of the method and some results: *Canadian Journal of Earth Sciences*, v. 34, no. 1, p. 17–33.
- MacCarthy, G.R., 1953, Recent changes in the shoreline near Point Barrow Alaska: *Arctic*, v. 6, no. 1, p. 44–51.

- MacCarthy, G.R., 1958, Glacial boulders on the arctic coast of Alaska: *Arctic*, v. 11, no. 2, p. 70–85.
- Manley, W.F., Lestak, L.R., and Maslanik, J.A., 2003, Photogrammetric analysis of coastal erosion along the Chukchi coast at Barrow, Alaska: *Ber. Polarforsch. Meeresforsch.*, no. 443, p. 66–68.
- Manley, W.F., Lestak, L.R., Tweedie, C.E., and Maslanik, J.A., 2006, High-resolution QuickBird imagery and related GIS layers for Barrow, Alaska: Boulder, CO, National Snow and Ice Data Center, DVD.
- Marion, G.M., Hastings, S.J., Oberauer, S.F., and Oechel, W.C., 1989, Soil–plant element relationships in a tundra ecosystem: *Holarctic Ecology*, v. 12, p. 296–303.
- Mason, O.K., and Jordan, J.W., 2001, Minimal late Holocene sea level rise in the Chukchi Sea: Arctic insensitivity to global change?: *Global and Planetary Change*, v. 32, p. 13–23.
- McGuire, A.D., Chapin, F.S., III, Walsh, J.E., and Wirth, C., 2006, Integrated regional changes in arctic climate feedbacks; Implications for the global climate system: *Annual Review of Environment and Resources*, v. 31, p. 61–91.
- McKendrick, J.D., 1990, *Arctophila* revegetation feasibility study: Fairbanks, Alaska, University of Alaska Fairbanks, 1988 annual report by Alaska Agricultural and Forestry Experiment Station, 63 p.
- 1997, Long-term tundra recovery in northern Alaska, *in* Crawford, R.M.M., ed., *Disturbance and recovery in Arctic lands, an ecological perspective*: Dordrecht, Netherlands, Kluwer Academic Publishers, p. 503–518.
- 2000, Vegetative responses to disturbance, *in* Truett, J.C., and Johnson, S.R., eds., *The natural history of an Arctic oilfield*: New York, Academic Press, p. 35–56.
- McNamara, J.P., Kane, D.L., and Hinzman, L.D., 1997, An analysis of streamflow hydrology in the Kuparuk River basin, Arctic Alaska; A nested watershed approach: *Journal of Hydrology*, v. 206, p. 39–57.
- Mendez, J., Hinzman, L.D., and Kane, D.L., 1998, Evapotranspiration from a wetland complex on the Arctic coastal plain of Alaska: *Nordic Hydrology*, v. 29, p. 303–330.
- Meyer, Hanno, Brown, Jerry, Schirrmeyer, Lutz, Yoshikawa, Kenji, Andreev, Andrei, Wagner, Dirk, and Hubberten, Hans-W., 2007, Late glacial and Holocene environmental history of a buried ice-wedge system, Barrow, Alaska: *Quaternary International*, v. 281, p. 167–168.
- Meyers, C.R., 1985, *Vegetation of the Beaufort Sea coast, Alaska; Community composition, distribution, and tidal influences*: Fairbanks, AK, University of Alaska Fairbanks M.S. Thesis, 206 p.
- Michael Baker Jr. Inc., 2000, 2000 Colville River Delta spring breakup and hydrologic assessment: Unpublished Report prepared for Phillips Alaska, Inc., Anchorage.
- 2007, 2007 Colville River Delta lakes recharge monitoring and analysis; Final report prepared for ConocoPhillips, Inc., Anchorage, AK, by Michael Baker Jr. Inc., Anchorage, AK, 110919-MJB-RPT-001, 163 p.
- Michaelson, G.J., Ping, C.-L., and Kimble, J.M., 1996, Carbon storage and distribution in tundra soils of arctic Alaska, U.S.A: *Arctic and Alpine Research*, v. 28, p. 414–424.
- Michaelson, G.J., Ping, C.-L., Kling, G.W., and Hobbie, J.E., 1998, The character and bioactivity of dissolved organic matter at thaw and in the spring runoff waters of the arctic tundra, North Slope, Alaska: *Journal of Geophysical Research*, v. 103, p. 28,939–28,946.
- Michaelson, G.J., Ping, C.-L., Lynn, L.A., Jorgenson, M.T., and Dou, F., 2008, Properties of eroding coastline soils along Elson Lagoon, Barrow, Alaska, *in* Kane, D.L., ed., *Proceedings of Ninth International Conference on Permafrost*, University of Alaska, Fairbanks, AK.
- Miller, D.L., and Phillips W.T., 1996, Geotechnical exploration, Alpine Development Project, Colville River, Alaska; Final report prepared for ARCO Alaska, Inc., Anchorage, by Duane Miller and Associates, Anchorage, 36 p.
- Mitchell, W.W., McKendrick, J.D., Wooding, F.J., and Barzee, M.A., 1974, Agronomists on the banks of the Sagavaniktok: *Agroborealis*, v. 6, p. 33–35.
- Moitoret, C.S., Walker, T.R., and Martin, P.D., 1996, Predevelopment surveys of nesting birds at two sites in the Kuparuk Oilfield, Alaska, 1988–1992: U.S. Fish & Wildlife Service, Technical Report NAES-TR-96-02.
- Moore, N., and Wright, S.J., 1991, Studies on the techniques for revegetation with *Arctophila fulva*: Unpublished Final Report prepared for ARCO Alaska, Inc., Anchorage, AK, by Plant Materials Center, Alaska Department of Natural Resources, Palmer, AK.
- Moore, T.E., Wallace, W.K., Bird, K.J., Karl, S.M., Mull, C.G., and Dillon, J.T., 1994, Geology of northern Alaska, *in* Plafker, G., and Berg, H.C., eds., *The Geology of Alaska*: Denver, CO, Geological Society of America, *The Geology of North America*, v. G-1, p. 49–140.
- Moulton, L.L., 1996, Lakes sampled for fish in and near the Colville River Delta, Alaska: Unpublished report prepared for ARCO Alaska, Inc., Anchorage, AK 99510, by MJM Research, Bainbridge Island, WA, 3 p.

- Moulton, L.L., and George, J.C., 2000, Freshwater fishes in the arctic oil-field region and coastal plain of Alaska, *in* Truett, J.C. and Johnson, S.R., eds., *The natural history of an Arctic Oil Field*: New York, Academic Press, p. 328–348.
- Muller, F., 1959, Observations on pingos: *Meddelelser on Gronland*, v. 153, 127 p.
- Muller, S.V., Racoviteanu, A.E., and Walker, D.A., 1999, Landsat MSS-derived land-cover map of northern Alaska; Extrapolation methods and a comparison with photo-interpreted and AVHRR-derived maps: *International Journal of Remote Sensing*, v. 20, p. 2,921–2,946.
- Munroe, J.S., Doolittle, J.A., Kanevskiy, M.Z., Hinkel, K.M., Jones, B.M., Shur, Y., Nelson, F.E., and Kimble, J.M., 2007, Application of ground-penetrating radar imagery for three-dimensional visualization of ice-wedge networks and frost boils in ice-rich permafrost, Barrow, Alaska: *Permafrost and Periglacial Processes*, v. 18, no. 4, p. 309–321.
- Murray, D.F., 1978, Vegetation, floristics, and phytogeography of northern Alaska, *in* Tieszen, L.L., ed., *Vegetation and production ecology of an Alaskan Arctic tundra*: New York, Springer-Verlag, p. 16–36.
- Naidu, A.S., and Mowatt, T.C., 1975, Depositional environments and sediment characteristics of the Colville and adjacent deltas, northern arctic Alaska, *in* Broussard, M.L.S., ed., *Delta models for exploration*: Houston Geological Society, p. 283–309.
- Naidu, A.S., Finney, B.P., and Baskaran, M., 1999, 210Pb- and 137Cs-based sediment accumulation rates in inner shelves and coastal lakes of subarctic and arctic Alaska: A synthesis: *GeoResearch Forum*, v. 5, p. 185–196.
- Naidu, A.S., Mowatt, T.C., Rawlinson, S.E., and Weiss, H.V., 1984, Sediment characteristics of the lagoons of the Alaska Beaufort Sea coast and evolution of Simpson Lagoon, *in* Barnes, P.W., Schell, D.M., and Reimnitz, E., eds., *The Alaska Beaufort Sea; Ecosystems and Environments*: Orlando, FL, Academic Press, p. 275–292.
- National Research Council (NRC), 2003, *Cumulative environmental effects of oil and gas activities on Alaska's North Slope*: Washington, DC, National Academy Press, 288 p.
- National Snow and Ice Data Center (NSIDC), 2005, *Sea ice*: Boulder, CO, University of Colorado, Boulder, National Snow and Ice Data Center (NSIDC) <http://nsidc.org/seaice>.
- Natural Resource Conservation Service (NRCS), 2003, *Keys to Soil Taxonomy*, Ninth Edition: Washington, D.C., U.S. Department of Agriculture, 332 p.
- Neiland, B.J., and Hok, J.R., 1975, Vegetation survey of the Prudhoe Bay region, *in* Brown J., ed., *Ecological investigations of the tundra biome in the Prudhoe Bay region, Alaska*: Fairbanks, AK, University of Alaska Fairbanks, Biological Papers of the University of Alaska, Special Report Number 2, 215 p.
- Nelson, F.E., Shiklomanov, N.I., Streletskiy, D.A., Romanovsky V.E., Yoshikawa, K., Hinkel, K.M., and Brown, J., 2008, A permafrost observatory at Barrow, Alaska; Long-term observations of active-layer thickness and permafrost temperature: *Proceedings of the Ninth International Conference on Permafrost*, in press.
- NOAA-OCSEAP, 1983, Sale 87—Harrison Bay synthesis: Juneau, AK, U.S. Department Commerce.
- Norton, D.W., 2001, Fifty more years below zero; Tributes and meditations for the Naval Arctic Research Laboratory's first half century at Barrow, Alaska: Calgary, Alberta, The Arctic Institute of North America, 576 p.
- Nuka Research and Planning Group (NRPG), 2004, *Alaska spill response tactics manual project*: Anchorage, AK, Nuka Research and Planning Group, LLC.
- Oechel, W.C., Hastings, S.J., Vourlitis, G., Jenkins, M., Riechers, G., and Grulke, N., 1993, Recent change of arctic tundra ecosystems from a net carbon dioxide sink to a source: *Nature*, v. 361, p. 520–523.
- Osterkamp, T.E., 2003, A thermal history of permafrost in Alaska, *in* Phillips, M., Springman, S.M., and Arenson, L.U., eds., *Proceedings of the Eighth International Conference on Permafrost*, July 21–25, 2003, Zurich, Switzerland: Netherlands, A.A. Balkema Publishers, v. 2, p. 863–867.
- 2005, The recent warming of permafrost in Alaska: *Global and Planetary Change*, v. 49, p. 187–202.
- 2007, Characteristics of the recent warming of permafrost in Alaska, *in* Zhang, Tingjun, Nelson, F.E., and Gruber, Stephan, eds., *Permafrost and seasonally frozen ground under a changing climate*: *Journal of Geophysical Research*, v. 112, issue F2, doi:10.1029/2006JF000578.
- Osterkamp, T.E., and Jorgenson, J.C., 2005, Warming of permafrost in the Arctic National Wildlife Refuge: *Permafrost and Periglacial Processes*, v. 16, p. 1–5.
- Osterkamp, T.E., and Romanovsky, V.E., 1996, Characteristics of changing permafrost temperatures in the Alaskan Arctic, USA: *Arctic and Alpine Research*, v. 28, p. 267–273.
- O'Sullivan, J.B., 1961, *Quaternary geology of the arctic coastal plain, northern Alaska*: Iowa State University, Ph.D. Thesis, 191 p.

- Oswood, M.W., Everett, K.R., and Schell, D.M., 1989. Some physical and chemical characteristics of an arctic beaded stream: *Holarctic Ecology*, v. 12, no. 3, p. 290–295.
- Ott, A.G., 1993a, An evaluation of the effectiveness of rehabilitation at selected streams in North Slope oilfields: Juneau, AK, Alaska Department Fish and Game, Technical Report 93-5, 61 p.
- 1993b, North Slope oil and gas cross drainage report: Juneau, AK, Alaska Department Fish and Game, Technical Report 93-5, 72 p.
- Papineau, J., 2004, Anatomy of high wind events along the Alaska's North Slope: Anchorage, AK, National Weather Service, 10 p., http://pafc.arh.noaa.gov/papers/brw_winds1.pdf
- Peterson, K.M., and Billings, W.D., 1978, Geomorphic processes and vegetation change along the Meade River sand bluffs, northern Alaska: *Arctic*, v. 31, p. 7–23.
- Peterson, K.M., and Billings, W.D., 1980, Tundra vegetational patterns and succession in relation to microtopography near Atkasook, Alaska: *Arctic Alpine Research*, v. 12, p. 473–482.
- Peterson, R.A., and Krantz, W.B., 2003, A mechanism for differential frost heave and its implications for patterned ground formation: *Journal of Glaciology*, v. 49, p. 69–80.
- Péwé, T.L., 1966, Ice wedges in Alaska; classification, distribution, and climatic significance, *in* Proceedings, Permafrost, International Conference: Washington, DC, National Academy of Sciences, p. 76–81.
- Péwé, T.L., 1975, Quaternary geology of Alaska: U.S. Geological Survey Professional Paper, 836, 145 p.
- Péwé, T.L., and Church, R.E., 1962, Age of the spit at Barrow, Alaska: *Geological Society of America Bulletin*, v. 73, no. 10, p. 1,287–1,291.
- Ping, C.-L., Bockheim, J.G., Kimble, J.M., Michaelson, G.J., and Walker, D.A., 1998, Characteristics of cryogenic soils along a latitudinal transect in Arctic Alaska: *Journal of Geophysical Research*, v. 103, no. D22, p. 28,917–28,928.
- Ping, C.-L., Lynn, L.A., Michaelson, G.J., Jorgenson, M.T., Shur, L.S., and Kanevskiy, M., 2008, Classification of Arctic tundra soils along the Beaufort Sea coast, Alaska, *in* Kane, D.L., ed., Proceedings of Ninth International Conference on Permafrost: University of Alaska, Fairbanks, AK, in press.
- Ping, C.-L., Michaelson, G.J., and Cherkinsky, A., 1997, Characterization of soil organic matter by stable isotopes and radiocarbon ages of selected soil in arctic Alaska, *in* Drozd, J., Gonet, S.S., Senesi, N., and Weber, J., eds., *The role of humic substances in the ecosystem and in environmental protection*: Wroclaw, Poland, Polish Society of Humic Substances, p. 475–480.
- Ping, C.-L., Michaelson, G.J., Kimble, J.M., and Everet, L.R., 2002, Organic carbon stores in Alaska soils, *in* Kimble, J.M., Lal, R., and Follett, R.F., eds., *Agricultural practices and policies for carbon sequestration in soil*: Boca Raton, LA, Lewis Publishers, p. 485–494.
- Polyak, L., Edwards, M.H., Coakley, B.J., and Jakobsson, M., 2001, Ice shelves in the Pleistocene Arctic Ocean inferred from glaciogenic deep-sea bedforms: *Nature*, v. 410, p. 453–457.
- Popov, A.I., 1967, Permafrost related features in soil crust (cryolithology) (in Russian): Moscow State University Press, 303 p.
- Porsild, A.E., 1938, Earth mounds in unglaciated Arctic northwestern America: *Geographical Review*, v. 28, no. 1, p. 46–58.
- Pullman, E.R., Jorgenson, M.T., and Shur, Y., 2007, Thaw settlement in soils of the Arctic coastal plain, Alaska: *Arctic, Antarctic, and Alpine Research*, v. 39, p. 468–476.
- Rachold, V., Are, F.E., Atkinson, D.E., Cherkashov, G., and Solomon, S.M., 2005, Arctic Coastal Dynamics (ACD); An introduction: *Geo-Marine Letters*, v. 25, p. 63–68.
- Racine, C.H., 1981, Tundra fire effects on soils and three plant communities along a hill-slope gradient in the Seward Peninsula, Alaska: *Arctic*, v. 34, p. 71–84.
- Racine, C.H., Jandt, R., Meyers, C., and Dennis, J., 2004, Tundra fire and vegetation change along a hillslope on the Seward Peninsula, Alaska, U.S.A.: *Arctic, Antarctic, and Alpine Research*, v. 36, no. 1, p. 1–10.
- Rawlinson, S.E. ed., 1983, Guidebook to permafrost and related features, Prudhoe Bay, Alaska: Guidebook 5, Fourth International Conference on Permafrost, Alaska Division of Geological & Geophysical Surveys Guidebook 1, 177 p.
- 1993, Surficial geology and morphology of the Alaskan Central Arctic Coastal Plain: Alaska Division of Geological & Geophysical Surveys Report of Investigations 93-1, 172 p.
- Ray, P.H., ed., 1885, Report of the the International polar expedition to Point Barrow, Alaska: Washington, DC, U.S. Government Printing Office, 695 p.

- Raynolds, M.K., Walker, D.A., and Maier, H.A., 2006, Alaska arctic tundra vegetation map, scale 1:4,000,000: Anchorage, AK, U.S. Fish and Wildlife Center, Conservation of Arctic Flora and Fauna (CAFF) map no. 2.
- Reed, J.C., and Sater, J.E., eds., 1974, The coast and shelf of the Beaufort Sea [Symposium on Beaufort Sea coast and shelf research, San Francisco, CA, January 7–9, 1974]: Arlington, VA, Arctic Institute of North America, 750 p.
- Reimnitz, E., and Barnes, P.W., 1974, Sea ice as a geologic agent on the Beaufort Sea shelf of Alaska, *in* Reed, J.C., and Sater, J.E., eds., The coast and shelf of the Beaufort Sea, Symposium on Beaufort Sea cost and shelf research, San Francisco, CA, January 7–9, 1974: Arlington, VA, The Arctic Institute of North America, p. 301–353.
- Reimnitz, E., and Maurer, D.K., 1979, Effects of storm surges on the Beaufort Sea coast, northern Alaska: *Arctic*, v. 32, p. 329–344.
- Reimnitz, E., and Wolf, S.C., 1998, Are North Slope surface alluvial fans pre-Holocene relicts?: U.S. Geological Survey Professional Paper 1605, 9 p.
- Reimnitz, E., Graves, S.M., and Barnes, P.W., 1985, Beaufort Sea coastal erosion, sediment flux, shoreline evolution, and the erosional shelf profile: U.S. Geological Survey Open-File Report 85-380, 66 p.
- 1988, Beaufort Sea coastal erosion, sediment flux, shoreline evolution, and the erosional shelf profile: U.S. Geological Survey Miscellaneous Geologic Investigations Map I-1182-G.
- Repenning, C.A., 1983, New evidence for the age of the Gubik Formation: Alaskan North Slope: *Quaternary Research*, v. 19, p. 356–372.
- Ritchie, W., and Walker, H.J., 1974, Riverbank forms of the Colville River Delta, *in* Reed, J.C., and Sater, J.E., eds., The coast and shelf of the Beaufort Sea: Washington, DC, Arctic Institute of North America, p. 545–566.
- Rodeick, C.A., 1979, The origin, distribution, and depositional history of gravel deposits on the Beaufort Sea continental shelf, Alaska: U.S. Geological Survey Open-File Report 79-234, 87 p.
- Romanovsky, V.E., and Osterkamp, T.E., 1997, Thawing of the active layer on the coastal plain of the Alaskan Arctic: *Permafrost and Periglacial Processes*, v. 8, no. 1, p. 1–22.
- Romanovsky, V.E., Burgess, M., Smith, S., Yoshikawa, K., and Brown, J., 2002, Permafrost temperature records: Indicator of climate change: *Eos Transactions*, v. 83, no. 50, p. 593–594.
- Romanovsky, V.E., Sergueev, D.O., and Osterkamp, T.E., 2003, Temporal variations in the active layer and near-surface permafrost temperatures at the long-term observatories in northern Alaska, *in* Phillips, M., Springman, S.M., and Arenson, L.U., eds., Proceedings of 8th International Conference on Permafrost: Netherlands, A.A. Balkema Publishers, p. 989–994.
- Roselle, D., and Walker, H., 1966, Erosional and depositional history of two lakes in arctic Alaska: Heidelberg, Germany, *Heidelberger Geographische Arbeiten*, v. 104, p. 413–426.
- Roth, J.E., Loomis, P.F., Emers, M., Stickney, A.A., and Lentz, W., 2007, An ecological land survey in the central Kuparuk study area, 2006: Final Report prepared for ConocoPhillips Alaska, Inc., Anchorage, AK, by ABR Inc., Environmental Research & Services, Fairbanks, AK, 44 p.
- Rothe, T.C., Markon, C.J., Hawkins, L.L., and Koehl, P.S., 1983, Waterbird populations and habitat analyses of the Colville River Delta, Alaska, 1981 summary report: Anchorage, AK, U.S. Fish and Wildlife Service, Special Studies Progress Report, 67 p.
- Schindler, J.F., 2001, Naval Petroleum Reserve No. 4 and the beginnings of the Arctic Research Laboratory (ARL), *in* Norton, D.W., ed. Fifty More Years Below Zero: Winnipeg, Manitoba, Arctic Institute of North America, p. 29–32.
- Schrader, F.C., 1904, A reconnaissance in northern Alaska across the Rocky Mountains, along the Koyukuk, John, Anaktuvuk and Colville rivers and the Arctic coast to Cape Lisburne in 1901: U.S. Geological Survey Professional Paper 20, 139 p.
- Sellmann, P.V., and Brown, J., 1973, Stratigraphy and diagenesis of perennially frozen sediments in the Barrow, Alaska, region, *in* Permafrost: The North American contribution to the Second International Conference; Washington, DC, National Academy of Sciences, p. 171–181.
- Sellman, P.V., Brown, J., Lewellen, R.I., McKim, H., and Merry, C., 1975, The classification and geomorphic implications of thaw lakes on the Arctic coastal plain, Alaska: Hanover, NH, Cold Regions Research and Engineering Laboratory, Research Report 344, 21 p.
- Serbin, S., Graves, A., Zaks, D., Brown, J., Tweedie, C.E., 2004, The utility of survey grade differential global positioning systems (DGPS) technology for monitoring coastal erosion; Arctic Coastal Dynamics—Report of the 4th International Workshop: *Berichte zur Polar-und Meeresforschung*, v. 482, p. 29–30.
- Serreze, M.C., Holland, M.M., and Stroeve, J., 2007, Perspectives on the Arctic's shrinking sea-ice cover: *Science* v. 315, p. 1,533–1,536.

- Serreze, M.C., Mas, J., Amol, A., Scambos, T.A., Fetterer, F., Stroeve, J., Knowles, K., Fowler, C., Drobot, S., Barry, R.G., and Haran, T.M., 2003, A record minimum arctic sea ice extent and area in 2002: *Geophysical Research Letters*, v. 30, p. 1,110 doi:10.1029/2002GL016406.
- Shannon and Wilson, Inc., 1996, 1996 Colville River Delta spring breakup and hydrologic assessment, North Slope, Alaska: Unpublished report prepared for Michael Baker Jr., Inc., Anchorage, 16 p.
- 1997, Colville River Delta two-dimensional surface water model: Annual Report prepared for Michael Baker, Jr., Inc. and ARCO Alaska, Inc., Anchorage, AK, by Shannon and Wilson, Inc., Fairbanks, AK.
- Short, A.D., 1973, Beach dynamics and nearshore morphology of the Alaskan Arctic coast: Baton Rouge, LA, Louisiana State University, Unpublished Ph.D. dissertation, 140 p.
- Shumskiy, P.A., and Vturin, B.I., 1963, Underground ice, *in* Proceedings, Permafrost International Conference: Washington, D.C., National Academy of Sciences, p. 108–113.
- Shur, Y.L., and Jorgenson, M.T., 1998, Cryostructure development on the floodplain of the Colville River Delta, northern Alaska, *in* Lewkowicz, A.G., and Allard, M., eds., Proceedings of Seventh International Conference on Permafrost: Sainte-Foy, Quebec, Universite Laval, Collection Nordicana, v. 57, p. 993–1,000.
- Shur, Y.L., and Jorgenson, M.T., 2007, Patterns of permafrost formation and degradation in relation to climate and ecosystems: *Permafrost and Periglacial Processes*, v. 18, p. 7–19.
- Shur, Y.L., French, H.M., Bray, M.T., and Anderson, D.A. 2004. Syngenetic permafrost growth: cryostructure observations from the CRREL Tunnel near Fairbanks, Alaska: *Permafrost and Periglacial Processes*, v. 15, p. 339–347.
- Shur, Y.L., Jorgenson, M.T., Kanevskiy, M.Z., 2008, Formation of frost boils and earth hummocks, *in* Ninth International Conference on Permafrost (in press).
- Shur, Y.L., Vasiliev, A., Kanevsky, M., Maximov, V., Pokrovsky, S., and Zaikanov, V., 2002, Shore erosion in Russian Arctic, *in* Merrill, K.S., ed., Cold regions engineering; cold regions impacts on transportation and infrastructure: Reston, VA, American Society of Civil Engineers, Proceedings of the International Symposium on Cold Regions Engineering, v. 11, p. 736–747.
- Solomon, S., 2005, Storminess in the western Arctic; Extending the historical record using Hudson's Bay Company records: Ottawa, Canada, Environment Canada.
- Spatt, P.D., and Miller, M.C., 1981, Growth conditions and vitality of Sphagnum in a tundra community along the Alaska Pipeline Haul Road: *Arctic*, v. 34, p. 48–54.
- Spetzman, L.A., 1959, Vegetation of the Arctic Slope of Alaska: U.S. Geological Survey Professional Paper 302B, p. 19–58.
- Stone, R.S., Dutton, E.G., Harris, J.M., and Longenecker, D., 2002, Earlier spring snowmelt in northern Alaska as an indicator of climate change: *Journal of Geophysical Research*, v. 107, no. D10, p. 49, doi:10.1029/2000JD000286.
- Stow, D.A., Hope, A., McGuire, D., Verbyla, D., Gamon, J., Huemmerich, F., Houston, S., Racine, C., Sturm, M., Tape, K., Hinzman, L., Yoshikawa, K., Tweedie, C., Noyle, B., Silapaswan, C., Douglas, D.C., Griffith, B., Jia G., Epstein, H., Walker, D., Daeschner, S., Petersen, A., Zhou, L., and Myneni, R.B., 2004, Remote sensing of vegetation and land-cover change in Arctic tundra ecosystems: *Remote Sensing of Environment*, v. 89, no. 3, p. 281–308.
- Streletskiy, D.A., Shiklomanov, N.I., and Nelson, F.E., 2008, 13 Years of observations at Alaskan CALM sites; Long-term active layer and ground surface temperature trends, *in* Kane, D.L., ed., Proceedings of Ninth International Conference on Permafrost: Fairbanks, Alaska, University of Alaska Fairbanks, in press.
- Stroeve, J., Holland, M.M., Meier, W., Scambos, T., and Serreze, M.C., 2007, Arctic sea ice decline; Faster than forecast: *Geophysical Research Letters*, 34, L09501, doi:10.1029/2007GL029703.
- Sturtevant, P.M., Lestak, L.R., Manley, W.F., and Maslanik, J.A., 2005, Coastal erosion along the Chukchi coast due to an extreme storm event at Barrow, Alaska: *Reports on Polar and Marine Research*, v. 506, p. 114–118.
- Sumgin, M.I., 1927, Permafrost in USSR: Vladivostok, Far-East Geophysical Observatory, 372 p.
- Sutton, J.T., Hermanutz, L., and Jacobs, J.D., 2007, Are frost boils important for the recruitment of arctic-alpine plants?: *Arctic, Antarctic, and Alpine Research*, v. 38, no. 2, p. 263–272.
- Taylor, R.J., 1981, Shoreline vegetation of the arctic Alaska coast: *Arctic*, v. 34, p. 37–42.
- Tedrow, J.C.F., 1973, Soils of the polar region of North America: *Biuletyn Peryglacjalny*, v. 23, p. 157–165.
- Tedrow, J.C.F., and Cantlon, J.E., 1958, Concepts of soil formation and classification in arctic regions: *Arctic*, v. 11, p. 166–179.
- Tedrow, J.C.F., Drew, J.V., Hill, D.E., and Douglas, L.A., 1958, Major genetic soils of the Arctic Slope of Alaska: *Journal of Soil Science*, v. 9, p. 33–45.

- Tieszen, L.L., 1978, Vegetation and production ecology of an Alaskan Arctic tundra: Springer-Verlag, Ecological Series 29, 686 p.
- Townsend, J., 2001, Fifty years of monitoring geophysical data at Barrow, Alaska, *in* Norton, D.W., ed., Fifty More Years Below Zero; Tributes and Meditation for the Naval Arctic Research Laboratory's First Half Century at Barrow, Alaska: Fairbanks, Alaska, University of Alaska Fairbanks, p. 61–64.
- Troy, D.M., 2000, Shorebirds, *in* Truett, J.C., and Johnson, S.R., eds., The natural history of an Arctic oil field: New York, Academic Press, p. 277–303.
- Truett, J.C., and Johnson, S.R., eds., 2000, The natural history of an Arctic oil field: New York, Academic Press, 400 p.
- Truett, J.C., Miller, M.E., and Kertell, K., 1997, Effects of arctic Alaska oil development on brant and snow geese: *Arctic*, v. 50, no. 2, p. 138–146.
- University of Alaska, 1972, Baseline study of the Alaska arctic aquatic environment: College, AK, Institute of Marine Science, Report R72-3, 275 p.
- U.S. Fish and Wildlife Service, 1993, Polar bear mauls man at arctic coastal radar site: News Release 1, December 1993, <http://www.fws.gov/news/NewsReleases/>.
- U.S. Geological Survey (USGS), 1978, Water resources data for Alaska, water year 1977: Anchorage, AK, Water Resources Division, Water Data Report AK-77-1, 439 p.
- Walker, D.A., 1985, The vegetation and environmental gradients of the Prudhoe Bay region, Alaska: Hanover, NH, U.S. Army Cold Regions Research and Engineering Laboratory, CRREL Report 85-14, 239 p.
- Walker, D.A., and Acevedo, W., 1987, Vegetation and a Landsat-derived land cover map of the Beechey Point Quadrangle, Arctic coastal plain, Alaska: Hanover, NH, U.S. Army Cold Regions Research and Engineering Laboratory, CRREL Report 87-5, 63 p.
- Walker, D.A., and Everett, K.R., 1987, Road dust and its environmental impact on Alaska taiga and tundra: *Arctic and Alpine Research*, v. 19, p. 479–489.
- 1991, Loess ecosystems of northern Alaska—regional gradient and toposequence at Prudhoe Bay: *Ecological Monographs*, v. 61, p. 437–464.
- Walker, D.A., and Walker, M.D., 1991, History and pattern of disturbance in Alaskan arctic terrestrial ecosystems: a hierarchical approach to analyzing landscape change: *Journal of Applied Ecology*, v. 28, p. 244–276.
- Walker, D.A., and Webber, P.J., 1979, Relationships of soil acidity and air temperature to the wind and vegetation at Prudhoe Bay, Alaska: *Arctic*, v. 32, p. 224–236.
- Walker, D.A., Auerbach, N.A., Bockheim, J.G., Chapin, F.S., III, Eugster, W., King, J.Y., McFadden, J.P., Michaelson, G.J., Nelson, F.E., Oechel, W.C., Ping, C.L., Reeburg, W.S., Regli, S., Shiklomanov, N.I., and Vourlitis, G.L., 1998, Energy and trace-gas fluxes across a soil pH boundary in the Arctic: *Nature*, v. 394, p. 469–472.
- Walker, D.A., Cate, D., Brown, J., and Racine, C., 1987, Disturbance and recovery of arctic Alaskan tundra terrain; A review of recent investigations: Hanover, NH, U.S. Army Cold Regions Research and Engineering Laboratory, CRREL Report 87-11, 63 p.
- Walker, D.A., Epstein, H.E., Gould, W.A., Kelley, A.M., Kade, A.N., Knudson, J.A., Krantz, W.B., Michaelson, G., Peterson, R.A., Ping, C.-L., Reynolds, M.K., Romanovsky, V.E., and Shur, Y., 2004, Frost-boil ecosystems; Complex interactions between landforms, soils, vegetation and climate: *Permafrost and Periglacial Processes*, v. 15, no. 2, p. 171–188.
- Walker, D.A., Epstein, H.E., Jia, G.J., Balsler, A. Copass, C., Edwards, E.J., Hollingsworth W.A., Gould, J., Knudson, J., Maier, H.A., Moody, A., and Reynolds, M.K., 2003, Phytomass, LAI, and NDVI in northern Alaska; Relationships to summer warmth, soil pH, plant functional types and extrapolation to the circumpolar Arctic: *Journal of Geophysical Research*, v. 108, D8169, doi:10.1029/2001JD000986.
- Walker, D.A., Everett, K.R., Webber, P.J., and Brown, J., 1980, Geobotanical atlas of the Prudhoe Bay region, Alaska: Hanover, NH, U.S. Army Corps of Engineers Cold Regions Research and Engineering Laboratory Report 80-14, 69 p.
- Walker, D.A., Gould, W.A., Meier, H.A., and Reynolds, M.K., 2002, The circumpolar arctic vegetation map: *International Journal of Remote Sensing*, v. 23, p. 2,552–2,570.
- Walker, D.A., Reynolds, M.K., Daniëls, F.J.A., Einarsson, E., Elvebakk, A., Gould, W.A., Katenin, A.E., Kholod, S.S., Markon, C.J., Melnikov, E.S., Moskalenko, N.G., Talbot, S.S., and Yurtsev, B.A., 2005, The circumpolar Arctic vegetation map: *Journal of Vegetation Science*, v. 16, no. 3, p. 267–282.
- Walker, D.A., Walker, M.D., Everett, K.R., and Webber, P.J., 1985, Pingos of the Prudhoe Bay region, Alaska: *Arctic and Alpine Research*, v. 17, p. 321–336.

- Walker, D.A., Webber, P.J., Binnian, E.F., Everett, K.R., Lederer, N.D., Nordstrand, E.A., and Walker, M.D., 1987, Cumulative impacts of oil fields on northern Alaskan landscapes: *Science*, v. 238, p. 757–761.
- Walker, H.J., 1973, Morphology of the North Slope, *in* Britton, M.E., ed., *Alaskan Arctic Tundra*: Washington, D.C., The Arctic Institute of North America, p. 49–92.
- Walker, H.J., 1974, The Colville River and the Beaufort Sea; Some interactions, *in* Reed, J.C., and Sater, J.E., eds., *The coast and shelf of the Beaufort Sea*: Washington, DC, Arctic Institute of North America, p. 513–540.
- 1976, Depositional environments in the Colville River Delta, *in* Miller, T.P., ed., *Recent and ancient sedimentary environments in Alaska*, Proceedings, Alaska Geological Society Symposium: Anchorage, AK, Alaska Geological Society, p. C1–C22.
- 1978, Lake tapping in the Colville River Delta, *in* Proceedings of the Third International Conference on Permafrost: Ottawa, National Research Council of Canada, p. 233–238.
- Walker, H.J., 1983, Colville River Delta, Alaska, guidebook to permafrost and related features: Alaska Division of Geological & Geophysical Surveys Guidebook 2 for Fourth International Conference on Permafrost, 34 p.
- 1991, Bluff erosion at Barrow and Wainwright, Arctic Alaska: *Zeitschrift für Geomorphologie*, v. 3, no. 81, p. 53–61.
- 1994, Environmental impact of river dredging in arctic Alaska: *Arctic*, v. 47, p. 176–183.
- Walker, H.J., and Arnborg, L., 1966, Permafrost and ice-wedge effect on riverbank erosion, *in* Proceedings, Permafrost, International Conference: Lafayette, IN, National Academy of Sciences, p. 164–171.
- Walker, H.J., and Harris, M., 1976, Perched ponds: An arctic variety: *Arctic*, v. 29, p. 223–238.
- Walker, H.J., and Morgan, H.M., 1964, Unusual weather and river bank erosion in the delta of the Colville River, Alaska: *Arctic*, v. 17, p. 41–47.
- Washburn, A.L., 1973, *Periglacial Processes and Environments*: London, England, Edward Arnold, 320 p.
- Webber, P.J., 1978, Spatial and temporal variation in the vegetation and its production, Barrow, Alaska, *in* *Vegetation and production ecology of an Alaskan Arctic tundra*: New York, Springer-Verlag, p. 35–112.
- Webber, P.J., and Walker, D.A., 1975, Vegetation and landscape analysis at Prudhoe Bay, Alaska, a vegetation map of the tundra biome study area, *in* Brown J., ed., *Ecological investigations of the tundra biome in the Prudhoe Bay region, Alaska*: Fairbanks, AK, University of Alaska Fairbanks, Special Report 2, p. 80–91.
- West, J.J., and Plug, L.J., 2008, Time-dependent morphology of thaw lakes and taliks in deep and shallow ground ice: *Journal of Geophysical Research*, v. 113, doi:10.1029/2006JF000696.
- Wiggins, I.L., and Thomas, J.H., 1962, *A flora of the Alaska Arctic Slope*: Toronto, Ontario, Canada, University of Toronto Press, 425 p.
- Williams, J.R., Yeend, W.E., Carter, L.D., and Hamilton, T.D., 1977, Preliminary surficial deposits map, National Petroleum Reserve, Alaska: U.S. Geological Survey Open-File Report 77-868, 2 sheets, scale 1:500,000.
- Wiseman, W.J., Jr., Coleman, J.M., Gregory, A., Hsu, S.A., Short, A.D., Suhayda, J.N., Walters C.D., Jr., and Wright, L.D., 1973, *Alaskan Arctic coastal processes and morphology*: Baton Rouge, LA, State University of Louisiana Coastal Studies Institute, Technical Report 149, 171 p.
- Woodward, D.F., Snyder-Conn, E., Riley, R.G., and Garland, T.R., 1988, Drilling fluids and the arctic tundra of Alaska; Assessing contamination of wetlands habitat and the toxicity to aquatic invertebrates and fish: *Archives of Environmental Contamination and Toxicology*, v. 17, p. 683–697.
- Wright, J.F., Duchesne, C., and Côté, M.M., 2003, Regional-scale permafrost mapping using the TTOP ground temperature model, *in* Phillips, M., Springman, S.M., and Arenson, L.U., eds. *Proceedings of the Eighth International Conference on Permafrost*. Lisse, The Netherlands, A.A. Balkema Publishers, p. 1241–1246.
- Yokel, D., Brumbaugh, R., Huebner, D., and Ver Hoef, J., 2003, Impacts of seismic trails, camp-move trails and ice roads on tundra vegetation in the northeast National Petroleum Reserve—Alaska [Abs.], *in* Yokel, D., ed., *Draft proceedings of workshop on the impacts of winter exploration activities on tundra soils and vegetation of Alaska's North Slope*: Fairbanks, AK, U.S. Bureau of Land Management, p. 13.
- Yoshikawa, K., Romanovsky, V., Duxbury, N., Brown, J., and Tsapin, A., 2004, The use of geophysical methods to discriminate between brine layers and freshwater taliks in permafrost regions: *Journal of Glaciology and Geocryology*, v. 26, p. 301–309.
- Zona, D., Walter, O.C., Kochendorfer, J., Salyuk, A.N., Hastings, S., Paw, U.K., and Harazono, Y., 2007, CH₄ and CO₂ fluxes from the arctic tundra during the Biocomplexity Manipulation Experiment: American Geophysical Union, Fall Meeting 2007, abstract #GC11B-02.



STATE OF ALASKA

Sean Parnell, *Governor*
Daniel S. Sullivan, *Commissioner, Department of Natural Resources*
Robert F. Swenson, *State Geologist and Director*